INFORMATION TO USERS

This manuscript has been reproduced from the microfilm master. UMI films the text directly from the original or copy submitted. Thus, some thesis and dissertation copies are in typewriter face, while others may be from any type of computer printer.

The quality of this reproduction is dependent upon the quality of the copy submitted. Broken or indistinct print, colored or poor quality illustrations and photographs, print bleedthrough, substandard margins, and improper alignment can adversely affect reproduction.

In the unlikely event that the author did not send UMI a complete manuscript and there are missing pages, these will be noted. Also, if unauthorized copyright material had to be removed, a note will indicate the deletion.

Oversize materials (e.g., maps, drawings, charts) are reproduced by sectioning the original, beginning at the upper left-hand corner and continuing from left to right in equal sections with small overlaps.

Photographs included in the original manuscript have been reproduced xerographically in this copy. Higher quality 6" x 9" black and white photographic prints are available for any photographs or illustrations appearing in this copy for an additional charge. Contact UMI directly to order.

ProQuest Information and Learning
300 North Zeeb Road, Ann Arbor, MI 48106-1346 USA
800-521-0600

INTEGRATING COMPUTATIONAL CHEMISTRY AND MASS SPECTROMETRY :

A Study of Isomerization Reactions of Oxygen-Containing Ions in the Gas Phase.

By

Lorne Montgomery Fell, B.Sc., M.Sc.

A Thesis Submitted to the School of Graduate Studies

in Partial Fulfilment of the Requirements for the Degree

Doctor of Philosophy

McMaster University

for my parents,
for Samantha,
for me.

INTEGRATING COMPUTATIONAL CHEMISTRY AND MASS SPECTROMETRY :

A Study of Isomerization Reactions of Oxygen-Containing Ions in the Gas Phase.

DOCTOR OF PHILOSOPHY (1999)
(Chemistry)

McMASTER UNIVERSITY
Hamilton, Ontario

TITLE: **INTEGRATING COMPUTATIONAL CHEMISTRY AND MASS SPECTROMETRY** : A Study of Isomerization Reactions of Oxygen-Containing Ions in the Gas Phase.

AUTHOR: Lorne Montgomery Fell

SUPERVISOR: Professor Johan K. Terlouw

NUMBER OF PAGES: xv, 192

ABSTRACT

The unimolecular chemistry of several organic radical cations has been studied with ab initio molecular orbital calculations and tandem mass spectrometric experiments. The computational chemistry involves Hartree-Fock (HF), density functional (DFT), Moeller-Plesset perturbation, (MP) and coupled cluster (CC) theories. The tandem mass spectrometry experiments involves metastable ion (MI), collision induced dissociative ionization (CID), and neutralization-reionization mass spectrometry (NRMS) in conjunction with isotopic labeling using ^{2}H, ^{13}C and ^{18}O isotopes.

The chemistry has been interpreted by consideration of several fascinating intermediates in the gas-phase which include hydrogen-bridged radical cations, distonic ions and ion-dipole complexes. Two new hydrogen-bridged radical cations have been identified by experiments and were characterized by calculations.

The unimolecular chemistry of ionized 1,2-propanediol was re-examined with these methods. It was found that a considerable simplification of a previous mechanistic proposal could be brought about by invoking two different mechanistic concepts, a 1,2-*proton* shift catalyzed by a dipole and charge (electron) transfer taking place in ion-dipole complexes. This new mechanistic proposal was compared to a more conventional alternative which involves hydrogen *atom* shifts in distonic ions for both 1,2-propanediol and its lower homologue 1,2-ethanediol. It was found that a surprisingly large barrier exists for a 1,4-H atom shift in these stable distonic ions. Other low energy dissociation processes in ionized 1,2-propanediol (involving the loss of $CH_3^{\bullet}$, H_2O, H_2O + $CH_3^{\bullet}$, H_2O + CH_4) were interpreted by Bohme's 'methyl cation shuttle' mechanism taking place in ion-dipole complexes.

Tandem mass spectrometry experiments confirmed previous indirect evidence that commercially available oxalacetic acid, $HOOCCH_2C(=O)COOH$ (OAA) samples do not have the structure of the acid but rather that of its (Z)-enol, hydroxyfumaric acid, HOOCC(H)=C(OH)COOH. It was further established that : (i) the samples contained a minor impurity assigned as a dehydration product of 4-hydroxy-4-methyl-2-ketoglutaric acid; (ii) careful evaporation of OAA yielded mass spectra characteristic of the (Z)-enol form; partial ketonization of the neutral (Z)-enol takes place and these species are either

ionized intact or decarboxylate giving a mixture of α-hydroxyacrylic acid and its keto isomer, pyruvic acid and (iii) no (E)-enol, hydroxymaleic acid isomer exists at any point, in contrast to previous proposals.

A related α-keto-acid, β-hydroxypyruvic acid, (HPA) $HOCH_2C(=O)COOH$ does not enolize similar to OAA but instead retains its keto structure. The ion chemistry of this species is quite interesting since decarbonylation takes place producing two distinct species depending on the internal energy content of the ion. In the high energy regime (ions generated in the source of the mass spectrometer) decarbonylation yields a hydrogen-bridged radical cation, $CH_2{=}O{\bullet\bullet\bullet}H{\bullet\bullet\bullet}O{=}C\text{-}OH^{\bullet+}$. The long-lived, low internal energy (metastable) ions enolize prior to loss of C=O yielding an ion-dipole complex of ionized hydroxyketene and water, $HOC(H){=}C{=}O^{\bullet+}/H_2O$. The high energy hydrogen-bridged radical cations also show an intriguing rearrangement ion, $CH_2OH_2^{\bullet+}$, resulting from a decarboxylation process. This reaction likely occurs via communication with ionized glycolic acid and the hydrogen-bridged radical cation $CH_2OH_2^{\bullet+}{\bullet\bullet\bullet}O{=}C{=}O$.

The methyl ester of β-hydroxypyruvic acid, $HOCH_2C(=O)COOCH_3$, behaves analogously: upon decarbonylation the high and low internal energy ions are $CH_2{=}O{\bullet\bullet\bullet}H{\bullet\bullet\bullet}O{=}C\text{-}OCH_3^{\bullet+}$ and $HOC(H){=}C{=}O^{\bullet+}/CH_3OH$ respectively. The hydrogen-bridged radical cation formed in the high internal energy process shows an intriguing rearrangement as well. This ion rearranges extensively before dissociation into protonated methylformate, $CH_3OC(H)OH^+$ and the formyl radical, $HC{=}O^{\bullet}$. This rearrangement occurs via sequential transfers of a proton, electron and another proton within ion-dipole complexes in the gas-phase, akin to that proposed for the diols mentioned above.

In the EI mass spectrum of HPA an ion at m/z 59 is observed which was confirmed to have the expected structure $HOCH_2{-}C^+{=}O$. We found the calculated dissociation energy of ionized HPA into $HOCH_2{-}C^+{=}O$ and $HOCO^{\bullet}$ to be rather different from that derived from an earlier experimental and theoretical study. This observation led us to re-examine the enthalpies of formation for the m/z 59 $C_2H_3O_2^+$ system of ions, which includes the methoxycarbonyl ion $CH_3{-}O{-}C^+{=}O$, with high level G2 ab initio calculations. A variety of calculated reactions and reconsideration of previous and new experimental measurements resulted in an upwards revisal, by 9 kcal/mol, of the ΔH_f assigned to these ions.

PREFACE

This thesis describes the results obtained by the author during four years of research in gas-phase ion chemistry. This field is ideally suited for investigations of theoretical and experimental nature since both computational chemistry and mass spectrometry readily examine isolated molecules and ions. Experiment and theory working in concert can eliminate several *a priori* reasonable mechanistic proposals for the rearrangement of radical cations. Such investigations necessitate the collaboration of both experimentalists and theoretical chemists and the collaborative contributions of all co-authors of the papers resulting from this work is appreciated. The assistance of Prof. Dr Paul J.A. Ruttink and Dr Peter C. Burgers deserves special mention, both have provided keen insight to the ion chemistry problems discussed in this thesis.

The permission of Elsevier Science, NRC Research Press and ACS Publication Division to reproduce data and text which has been previously published is appreciated.

LIST OF PUBLICATIONS

11. P.J.A. Ruttink, P.C. Burgers, L.M. Fell, J.K. Terlouw, Further insight into the gas-phase ion chemistry of the hydrogen-bridged radical cation $[CH_2{=}O{\bullet\bullet\bullet}H{\bullet\bullet\bullet}O{=}C\text{-}OH]^{\bullet+}$: a theoretical study, *Can. J. Chem.*, in preparation.

10. D.J.Lavorato, L.M. Fell, J.K. Terlouw, G.A. McGibbon, S. Sen and H. Schwarz, Identifying ylide ions and methyl migrations in the gas phase: The decarbonylation reactions of simple ionized N-heterocycles, *Int. J. Mass Spectrom.*, accepted.

9. P.J.A Ruttink, P.C. Burgers, L.M. Fell and J.K. Terlouw, The dissociation chemistry of the hydrogen-bridged radical cation $[CH_2{=}O{\bullet\bullet\bullet}H{\bullet\bullet\bullet}O{=}C\text{-}OCH_3]^{\bullet+}$: another example of proton transport catalysis with electron transfer, *Int. J. Mass Spectrom.*, accepted.

8. P.J.A Ruttink, P.C. Burgers, L.M. Fell and J.K. Terlouw, G2 Theory and Experiment in Concert: The enthalpy of formation of CH_3OCO^+ and its isomers, *J. Phys. Chem. A*, **103** (1999) 1426-1431.

7. P.J.A Ruttink, P.C. Burgers, L.M. Fell and J.K. Terlouw, The dissociation of ionized 1,2-ethanediol and 1,2-propanediol: proton transport catalysis with electron transfer, *J. Phys. Chem. A*, **102** (1998) 2976-2980.

6. L.M. Fell, P.C. Burgers, P.J.A. Ruttink and J.K. Terlouw, The decarbonylation of ionized β-hydroxypyruvic acid : The hydrogen-bridged radical cation $[CH_2{=}O{\bullet\bullet\bullet}H{\bullet\bullet\bullet}O{=}C\text{-}OH]^{\bullet+}$ studied by experiment and theory, *Can. J. Chem.*, **76** (1998) 335-349.

5. L.M. Fell, J.T. Francis, J.L. Holmes and J.K. Terlouw, The intriguing behavior of (ionized) oxalacetic acid investigated by tandem mass spectrometry, *Int. J. Mass Spectrom. Ion Processes*, **165/166** (1997) 179-194.

4. P.C. Burgers, L.M. Fell, A. Milliet, M. Rempp, P.J.A. Ruttink and J.K. Terlouw, The dissociation of low energy 1,2-propanediol ions: an intriguing mechanism revisited, *Int. J. Mass Spectrom. Ion Processes*, **167/168** (1997) 291-308.

3. A.D.O. Bawagan, L.M. Fell, J. Logan, Time-resolved structures of electrical discharges in gases: experiment and stochastic model, *Can. J. Chem.*, **76** (1998) 1-9.

2. L.M. Fell, H.F. Shurvell, Complex formation between 2-propanone and chloroform Part 2: Infrared and Raman Spectroscopic Study of Binary Mixtures of 2-propanone and chloroform., *Can. J. Appl. Spectrosc.* **41** (1996) 96-102.

1. L.M. Fell, H.F. Shurvell, Complex formation between 2-propanone and chloroform Part 1: Literature, *Can. J. Appl. Spectrosc.* **41** (1996) 90-95.

ACKNOWLEDGEMENTS

First of all I would like to thank my supervisor, Professor Johan K. Terlouw. His perseverance, patience and guidance are truly appreciated and our sometimes heated discussions taught me a great deal about chemistry and computers. I feel our partnership was quite successful and rewarding.

I am also indebted to Professor J.L. Holmes for providing appearance energy measurements from the late Dr F.P. Lossing's collection and his involvement in the project described in Chapter 4.

Professors A.P. Hitchcock and N.H. Werstiuk were willing to serve as supervisory committee members. Their expert advice and readiness to answer my sometimes unorthodox questions has been of great help.

Greatly valued are the stimulating professional and personal interactions with past and present members of the research group and the McMaster Regional Center for Mass Spectrometry: Dr James T. Francis, Dr Richard W. Smith, Faj Ramelan, Dave "Catz" Lavorato, Leah Allan, M. Anna Trikoupis, Lisa Heydorn, Sue Ackloo and Dr Dennis Suh. Invaluable technical advice which got me up to speed on the mass spectrometer and the various computer systems came from external group member Dr A.A. "Sander" Mommers, and Mike "Geek at Large" Mallot.

Support and encouragement from my family has been instrumental to bring this venture to a successful end. Especially to James and Valerie Fell, my parents, and Samantha, my fiancée and best friend : thank you for your love and support.

TABLE OF CONTENTS

LIST OF FIGURES

LIST OF ABBREVIATIONS

2ffr/3ffr	= second/third field free region
6-31G*	= basis set indicating 6 functions for core electrons and split (3,1) valence functions
AE	= appearance energy
B3LYP	= a DFT method
CBS-X	= Complete Basis Set calculation
cc-pVDZ	= correlation-consistent polarization valence double zeta (basis set)
CCSD(T)	= coupled cluster singles doubles and triples calculation
CI	= Configuration Interaction
CID (CA)	= Collision Induced Dissociation (Collision Activation) Mass spectra
dbc	= direct bond cleavage
DFT	= Density Functional Theory
EI	= electron ionization
G2	= Gaussian-2 theory
HBRC	= hydrogen-bridged radical cation
HF	= Hartree-Fock theory
HPA	= β-hydroxypyruvic acid
IE_{adia}	= adiabatic ionization energy
IE_{vert}	= vertical ionization energy
m*	= metastably generated ion
MI	= Metastable Ion Mass Spectra
MO	= molecular orbtial
MP2	= second order Møller-Plesset Perturbation theory
MS	= mass spectrometer or mass spectrometry
NRMS	= Neutralization-Reionization Mass Spectra
OAA	= oxalacetic acid
PA	= proton affinity
QCISD(T)	= Quadratic Configuration Interaction, singles doubles and triples calculation
SCF	= Self Consistent field theory
ZPVE	= Zero point vibrational energy

CHAPTER 1

INTRODUCTION

More than ten years ago, a paper entitled "Theory and Experiment in Concert: the $CH_3OC{=}O^+$ Ion and its Isomers" appeared in the Journal of the American Chemical Society [1]. This paper, although not the first of its kind, was typical of a broadening area of combined research in gas-phase ion chemistry. This combined approach, that is the use of theory and experiment in a synergistic way, is very persuasive and has often led to novel solutions to the problems of gas-phase ion chemistry. The identification of the structure of a gas-phase ion and the mechanism by which it is generated are of primary interest in gas-phase ion chemistry. Computational chemistry derives ion structure readily as well as the pathway between isomers, the relative energies of these species and their corresponding ionic dissociation levels. Mass spectrometry gives insight into connectivity (structure), the rates of dissociation and ion energetics. The mechanism and structure of gas-phase ions can then be derived from these complementary techniques. We may also attempt to generalize and look for trends in the mechanisms and structures of related species, as chemists have typically done throughout this century.

This powerful combination of theory and experiment began in the early 1980s as computer power expanded and computational chemistry programs became generally available. The advent of *ab initio* molecular orbital theory [2], and successful implementations on computer programs such as Gaussian and GAMESS [3], to name only two of the several available computational chemistry programs, have given chemists powerful alternative tools. The calculation of energy differences between isomers, thermochemical quantities and relative energies of dissociation levels has become commonplace in the chemical community. This is particularly relevant to the interpretation of mass spectra since it is these parameters which characterize an ion's structure and its dissociations.

These types of combined investigations are presented in this thesis. In Chapters 2, 3, 5 and 6 we have examined low internal energy organic radical cations and characterized their structure and we have proposed mechanisms for the formation of these structures based on information from both theory and experiment. Chapters 4 and 7 have

slightly different emphases, one strongly experimental in nature, the other with a computational emphasis. In Chapter 4 we study the behaviour of an interesting organic acid in both the high and low energy regimes from an experimental point of view, whereas in Chapter 7, a largely theoretical study on the enthalpy of formation of the ion mentioned at the outset, $CH_3OC{=}O^+$, is presented.

In order to provide a suitable background to understand the studies contained in this thesis the following background material and introductions will be presented :

(a) the techniques used in tandem mass spectrometry to elucidate ion structure and reactivity

(b) some general principles and practices of gas-phase ion chemistry

(c) the use of quantum (computational) chemistry to aid in the understanding and interpretation of (a) and (b).

The description of ion structure determination, ion reactivity and dissociation pathways follows those given in standard resources in the literature [4], as does the use of quantum chemistry as an aid to interpretation of mass spectrometric experiments [5]. The standard ideas of gas-phase ion chemistry are also derived from key sources [6]. As stated in the Preface, the focus of the work presented in this thesis is of a computational nature and hence this aspect will be emphasized in this introduction.

TANDEM MASS SPECTROMETRY AND ITS USE FOR THE DETERMINATION OF ION STRUCTURE AND REACTIVITY

Our introduction to tandem mass spectrometry will follow classic reviews from the literature [4] and standard texts [7]. Mass spectrometry (MS) is a fundamental technique that has its roots in the studies of early physics. It is based on methods which separate a beam of charged particles based on the individual mass to charge (m/z) ratios by magnetic field analyzers (B) or alternatively separation based on different translational energies of the ions by electrostatic field analyzers (E). Tandem mass spectrometry involves successive applications of these two analyzers yielding multiple separations of an ion beam: MS/MS/MS. For the most part this technique has been used to identify unknown samples and determine their exact composition by combinations of

fingerprinting and exact mass measurement [8]. MS has been used to characterize the gas-phase chemistry of some truly remarkable species. This chemistry is remarkable since many novel species and mechanisms have been invoked to describe "strange" dissociation patterns.

We will limit ourselves to the chemistry of singly charged positive ions. There are two broad classes of such ions, those containing an even number of electrons (all electrons are paired) and those containing an odd number of electrons (one or more unpaired electrons). Most organic molecules contain an even number of electrons and so removal of an electron by electron impact ionization (EI) yields a radical cation, $M^{\bullet +}$, as the molecular ion. The dissociation of the molecular ion can occur in two ways, via direct bond cleavage (dbc) to produce an even electron cation and a radical or via a rearrangement to an ionized molecule and a stable neutral molecule.

There are two ways in which MS can be used to determine an ion's structure and reactivity (1) by measurement of ion enthalpies and transition state energies for fragmentation and (2) by the detailed examination of unimolecular and collision induced fragmentation processes of ions. None of these methods can suffice to determine the structure and reactivity of an ion on its own, but when combined the methods provide a powerful tool for these investigations.

To understand the scope and limitations of mass spectrometry for structure elucidation and reactivity, one must be somewhat familiar with the theory of unimolecular ion decompositions and Quasi-Equilibrium Theory (QET) [9]. The fast process (~ femtosec) of ionization (by removal of an electron) of neutral molecules by fast moving electrons (70 eV) produces molecular ions with a range of internal energies (0 – 20 eV, ~100 kcal/mol) whose average deposited internal energy is 2-3 eV (40-60 kcal/mol). Ionic dissociations from these species exhibit a broad range of behaviour due to this wide energy deposition by the electrons and as noted above both rearrangements and dbc reactions may occur. Ions usually spend on the order of microseconds (10^{-6} sec) in the ion source and along the flight path before being detected. This time frame allows for the redistribution of internal energy from the ionization event. QET states that internal energy will be equally distributed throughout an ionized molecule between all available degrees of freedom. The distribution of internal energies is expressed as, P(E), which is

the probability of a molecular ion to have an energy, E. The probability of decomposition or isomerization is expressed as k, the rate constant, which will also change with an ion's internal energy, k(E). The relationship between E, k(E) and P(E) is elegantly summarized in a Wahrhaftig diagram, see Fig. 1-1, for a molecular ion $M^{\bullet+}$ undergoing two competing dissociation reactions, a rearrangement $M^{\bullet+} \rightarrow AD^{\bullet+}$ and a direct bond cleavage reaction $M^{\bullet+} \rightarrow AB^{+}$. Such a diagram provides an ideal basis through which to discuss the appearance of a typical mass spectrum.

Figure 1-1. Wahrhaftig Diagram, describing the relationship between P(E) and k(E) for incipient molecular ions, $M^{\bullet+}$ dissociating via a rearrangement and a direct bond cleavage reaction.

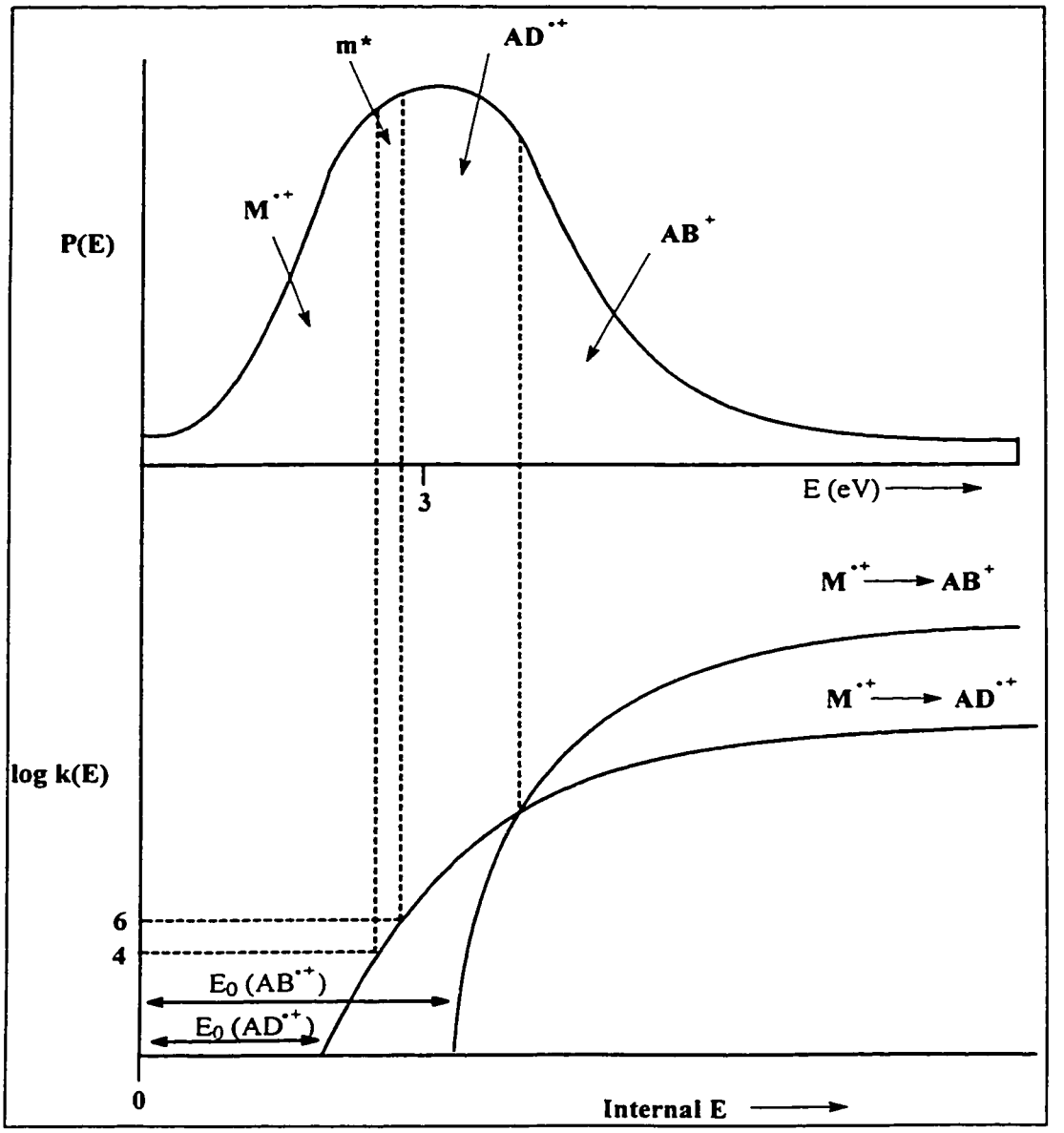

In the upper half of this figure is the distribution of internal energies, P(E) vs. E, where the arrows refer to the relative amounts (areas under the curve) of the various types of ions. In the lower half of this figure, the relationship between log k(E) vs. E is given, which shows that ions with low internal energy have very small decomposition rates and therefore appear as intact molecular ions, $M^{\bullet+}$, in the mass spectrum. At rate constants greater than 10^6 s^{-1} (log k ~ 6) decomposition occurs in the ion source which gives rise to the other peaks in typical electron impact (EI) mass spectra.

The curve for the rearrangement reaction $M^{\bullet+} \rightarrow AD^{\bullet+}$ shows the minimum energy for the production of this ion at log k = 6 which is greater than the reaction critical energy $E_0(AD^{\bullet+})$. At high internal energies the rate constant for the production of AB^+ becomes much greater than that for $AD^{\bullet+}$ and so the production of AB^+ is favoured over that of $AD^{\bullet+}$ even though $AD^{\bullet+}$ has a more favourable enthalpy requirement. The reaction of lowest critical energy does not always lead to the most abundant ion. The production of ions in a mass spectrum depends on both the P(E) and k(E) relationships and can be very complex. Note further that the abundance of the individual ions indicated in Fig. 1-1 are initial values : those ions which have sufficient internal energy will decompose subsequently via their own P(E) and k(E) functions.

This indicates that mass spectra can contain many peaks, all of which can be derived from many competing reactions of both primary and consecutive types. Metastable ions, labeled m* in Fig. 1-1, are quite interesting species since they correspond to fairly low internal energy ions and are typically involved in rearrangement reactions. These processes are of particular interest in this thesis (*vide infra*).

Ion Thermochemistry

Ion thermochemistry plays a very important role in the identification of ion structures as it allows for the discrimination of experimental data. The important thermochemical quantities are summarized in Figure 1-2 below. The fundamental measurements of ionization energy (IE) and appearance energy (AE) are key experiments for the thermochemistry of gas-phase ions. The ionization energy is the energy required to remove an electron from a molecule and the appearance energy is the minimum energy

required to produce a product ion from the ground state neutral molecule. Another key measurement is that of proton affinity (PA) which is the energy required to protonate a neutral molecule. These experimental values can be used to calculate heats (enthalpies) of formation, ΔH_f, for many ions, which can in turn verify an assignment of a particular ion structure. Heats of formation of the ions may be derived according to the following equations.

$$\Delta H_f(M^{+\bullet}) = IE(M) + \Delta H_f(M)$$

$$\Delta H_f(A^+ \text{ or } A^{+\bullet}) = AE(A^+ \text{ or } A^{+\bullet}) - \Delta H_f(B) + \Delta H_f(M)$$

$$\Delta H_f(MH^+) = PA(M) + \Delta H_f(M) + \Delta H_f(H^+)$$

Figure 1-2. An Energy Diagram describing the dissociation chemistry of a neutral molecule ABCD and its ionic counterpart.

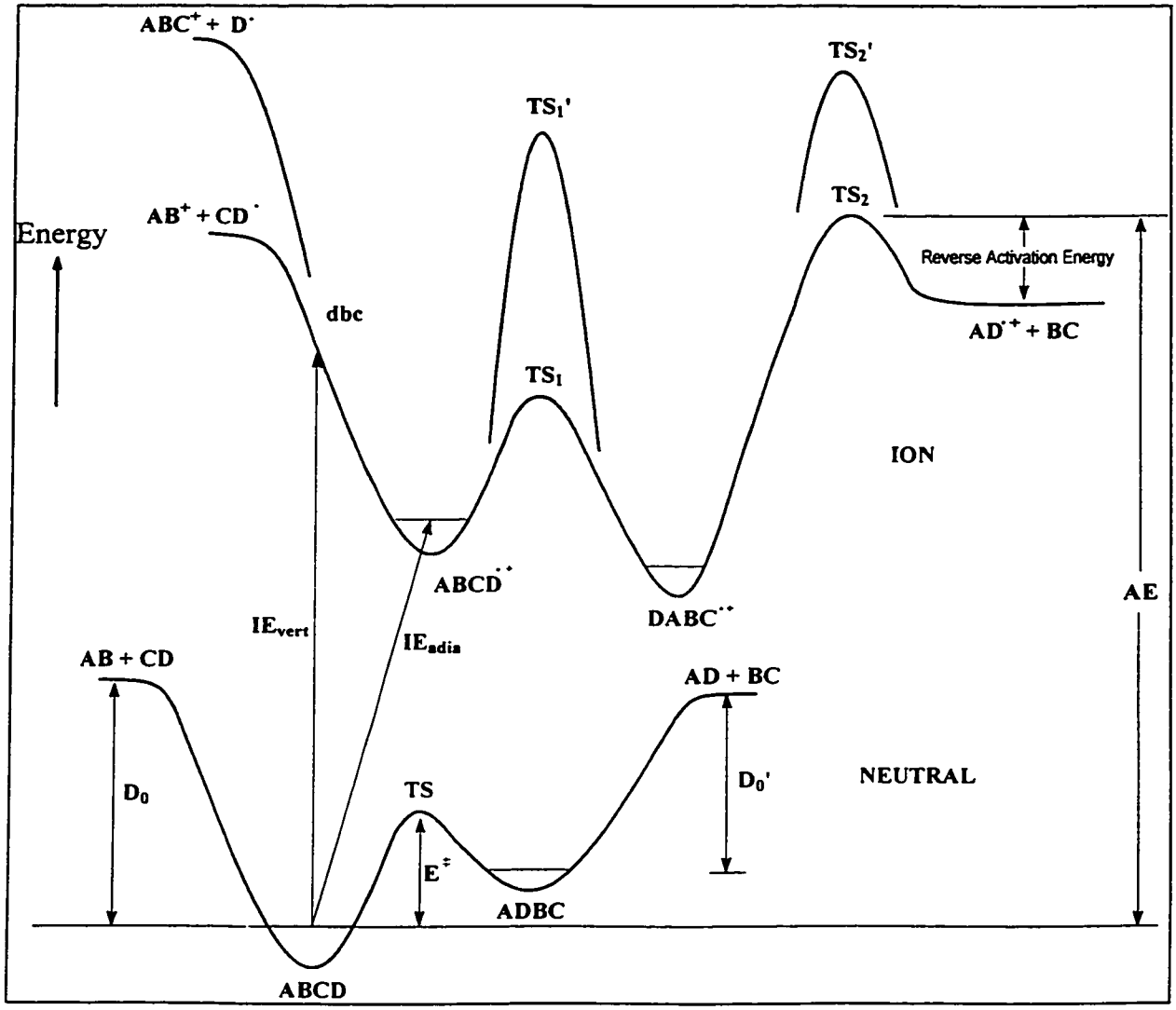

This figure also shows the various processes which can be involved in gas-phase ion chemistry. The lower energy surface, labeled NEUTRAL, shows us that starting from a stable neutral molecule, ABCD may isomerize via TS into ADBC if imparted with sufficient energy, E^*, the activation energy. These isomeric neutral molecules may also dissociate into various species such as, AB + CD or AD + BC, with dissociation energies D_0 or D_0'. If dissociation occurs into the component atoms, this energy is termed the atomization energy. Although isomerization of a neutral molecule could occur in the source of a mass spectrometer, this does not normally occur. The neutral molecule may be ionized to reach the upper energy surface, labeled ION. Vertical ionization, IE_{vert}, is a process where the electron is removed without any change in geometry and adiabatic ionization energy, IE_{adia}, is the difference between the neutral and the lowest ro-vibrational level of the ion. IE_{adia} is typically measured in photoionization spectroscopy and derived from photoelectron spectroscopy whose values are used to derive an ion's ΔH_f [10]. Once ionized the ion may undergo several isomerizations and dissociations as mentioned in the previous section. If isomerization does not occur then the ion $ABCD^{\bullet+}$ may dissociate via two competing dbc routes into $ABC^+ + D^\bullet$ or $AB^+ + CD^\bullet$ and typically the dissociation with lower enthalpy requirement will be the favoured pathway unless kinetic reasons are a substantial factor. On the other hand, $ABCD^{\bullet+}$ can isomerize to $DABC^{\bullet+}$ via TS_1 when the barrier for conversion lies below the two dissociation levels. The dissociation pathway will again tend to favour the lower enthalpy pathway and the dissociations observed will be indicative of that of the isomerized structure. i.e. formation of AB^+, ABC^+ and $AD^{\bullet+}$. If the barrier to isomerization is higher than the dissociation levels, i.e. TS_1', then the molecule will not isomerize. Typically, isomerization occurs to a lower energy structure, in this example $DABC^{\bullet+}$, if these species dissociate via a rearrangement reaction as portrayed in Fig. 1-2, this process will have a barrier, labeled TS_2 in the Figure. This barrier would raise the AE value for the formation of $AD^{\bullet+}$ and hence the derived heat of formation on such species represent an upper limit.

Not included in this diagram is the so-called "kinetic shift" which is the amount of energy in excess of E_0, see Fig. 1-1, required to generate the ion with a rate constant in the microsecond (10^{-6}) timeframe [4]. AE measurements refer to threshold energy of reactions with a minimum rate constant of 10^{-4} seconds, therefore the kinetic shift

increases the measured AE of an ion. It is derived from the fact that ions are produced by dependence on the rate of formation and therefore not just the minimum energetic threshold is required to detect an ion. This value can be minimized by careful experimentation and comparison to well established AE values. A "competitive shift" is another source of increase in the measured AE. In this situation a particular fragmentation may become thermodynamically possible, but it is not observed because the precursor ion is fragmenting by a more favourable competing pathway that has become possible at or below the AE of the ion of interest. The heat of formation, ΔH_f, derived is then an upper limit. This section has summarized the thermochemistry and some of the dissociation processes which are relevant to the dissociation chemistry of gas-phase ions. The next section goes into more depth on the experimental aspects of these dissociations.

Ion dissociation characteristics: Collision-induced and unimolecular reactions

The dissociations of an ion can characterize its structure and its reactivity. There are two different classes of ionic dissociations: unimolecular and collision-induced, they are differentiated based on the internal energy ranges sampled by each technique. Both of these techniques can be quite structurally characteristic in their own right but it is the combination of the two techniques which is the most unambiguous for structure determination. *Structure* in this section is not defined as bond lengths, angles as in the upcoming computational chemistry section but merely by atom connectivity.

Metastable Peaks

Metastable (m*) ions, are ions which for kinetic reasons have not dissociated in the source but actually dissociate on the way to the detector in a mass spectrometer. They are referred to as "low energy" ions as is indicated by the associated internal energies shown in Fig. 1-1. "High energy" ions are ions generated in the ion source and are shown on the right hand side of Fig.1-1. A Metastable Ion (MI) spectrum typically contains fewer peaks than does either a normal EI mass spectrum or a collision-induced mass spectrum. If a fragment ion is uniquely and solely generated from a precursor ion then the MI spectrum will be characteristic of that ion, provided no isomerization takes place before dissociation. Although the range of internal energies is small for m* ions, they still

have relatively high internal energies that are typically above the threshold for formation of an ion and rearrangements can occur before dissociation. Therefore the metastable ion represents the structure of the rearranged isomer and not that of the original precursor molecule. MI peak shapes are not always of a standard Gaussian shape. They can be of composite shape (two overlaid peaks with different kinetic energy releases) and this usually indicates that two different transition states are involved in the process. In the case where there is a barrier to the metastable dissociation the extra energy required to overcome this barrier is released in the form of kinetic energy to the products. Thus the kinetic energy released (KER) results in a broadening of the m* peak. This quantity has been examined in detail [11], but for our purposes we will define it as the difference in the width at half heights of the metastable peak and the main beam (the beam from which the m* ion is generated), the symbol for these values is $T_{0.5}$. These values are typically on the order of 10 meV and as a rule of thumb, $T_{0.5} < 18$ meV [4] implies that neither a large kinetic shift nor a reverse energy barrier exists. The measurement of the AE of a m* peak (see Fig. 1-2) is an estimation of the barrier height of a process. In combination with KER data and other energetic information the number of possible reaction mechanisms is greatly reduced. These measurements place an upper energy constraint on any mechanism proposed for a process.

Collision Induced Processes

A significant portion of the ions generated in the ion source have energies below the transition states for isomerization and dissociation levels and therefore will retain their original structure. These ions can then be induced to decompose by collision with an inert gas (typically He or O_2). This process yields the structure characteristic Collision-Induced Dissociation (CID also referred to as Collisional Activation, CA) mass spectrum. The increase in internal energy from collisions allows the ions to fragment rapidly and thus CID spectra are more structurally diagnostic than MI spectra. Another useful collision induced experiment is Neutralization-Reionization Mass Spectrometry (NRMS) which is indicative of an ion's reactivity [12]. NRMS involves a multiple collision experiment where ions are neutralized in a first collision cell and subsequently reionized in a second collision cell. This technique gives an immediate indication of the nature of

the selected ion by the observation of a survivor ion. A survivor ion, as the name implies, survives the NR process and is indicative of whether or not the selected ion has a stable neutral counterpart. This technique has been often referred to as a laboratory in itself, in that it can generate elusive neutral molecules such as carbenes or nitrenes and study their dissociation chemistry [12]. Finally, these surviving ions can be selectively transmitted to another collision cell to generate a NR/CA mass spectrum. All of these techniques combine to present a detailed description of the structure and reactivity of a gas-phase radical cation.

The tandem mass spectrometer used throughout the studies in this thesis, the ZAB-R, has three sectors and is of reversed geometry : BE_1E_2 (B = magnetic sector, E = electric sector) [13]. Metastable ion spectra are obtained by scanning the first electric sector while holding the magnetic sector fixed, thereby obtaining a spectrum of the low energy dissociations of the selected ion in the second field free region. The second field free region (2ffr, between B and E_1) is equipped with two collision gas cells, which are used to perform the CID and NR mass spectrometry by scanning E_1 and fixing B. The third field free region (3ffr, between E_1 and E_2) also contains a collision cell and by scanning E_2, spectra resulting from multiple collision experiments can be obtained such as MI/CA, NR/CA, CA/CA.

In this section the experimental aspects of tandem MS have been presented. In the next section the structural and mechanistic findings derived from these experiments will be introduced. These findings are rooted in the accumulation of many years of research by gas-phase ion chemists.

Some General Principles and Practices of Gas-Phase Ion Chemistry

This section will present a short sketch of the structures and the mechanistic concepts which are invoked by gas-phase ion chemists to interpret mass spectrometric results. It should be noted at this stage that a wide variety of experiments can be performed for a given collection of atoms. Taking the $C_2H_4O_2^{\bullet+}$ system of ions as an example, some of the isomeric ions including $CH_3COOH^{\bullet+}$ and $HCOOCH_3^{\bullet+}$ can be generated by direct ionization of their stable neutral counterparts, acetic acid and

methylformate respectively. Other isomers, including the ionized enol $CH_2=C(OH)_2^{\bullet+}$ and the ion-dipole complex $CH_2=C=O^{\bullet+}/H_2O$ can only be obtained by dissociative ionization of (carefully selected) larger precursor molecules. Labelling of specific H,C and O atoms in the various precursor molecules with the stable ^2H, ^{13}C and ^{18}O isotopes provides a time-honoured strategy to obtain useful structural and mechanistic information. This yields information on the dominant features of an ion's potential energy surface which can be quite complex. Early researchers had to begin with the smallest molecules and perform a building up process where each structure's chemistry was identified and used to investigate larger species.

The residence time of the ions generated in the ion source of a tandem mass spectrometer is typically 1 μs. Such a time-frame allows a vast number of vibrations and rotations to occur, which in turn enables many rearrangements to proceed. Gas-phase ion chemists realized fairly early that the presence of certain peaks in mass spectra could only be interpreted by multiple bond cleavages and multiple bond formation prior to dissociation. For example, when ionized 1,2-ethanediol [14] dissociates a peak is observed at m/z 32, which can only have the elemental composition $[C,H_4,O]^{\bullet+}$. Initially it seemed obvious that m/z 32 represents ionized methanol, $CH_3OH^{\bullet+}$, but analysis of its CID mass spectrum indicated that this structure was better represented as $^{\bullet}CH_2OH_2^+$ [15]. This is our first example of a novel class of ions, the now well-characterized and commonly proposed *distonic* ions. A distonic ion is characterized by the separation of the formal charge and the radical site by one or more atoms (α-distonic or ylid, β-, γ-, ions). At this point we have also introduced a ubiquitous rearrangement in gas-phase ion chemistry, the shift of a hydrogen (H) atom, in this case a 1,4-H shift :

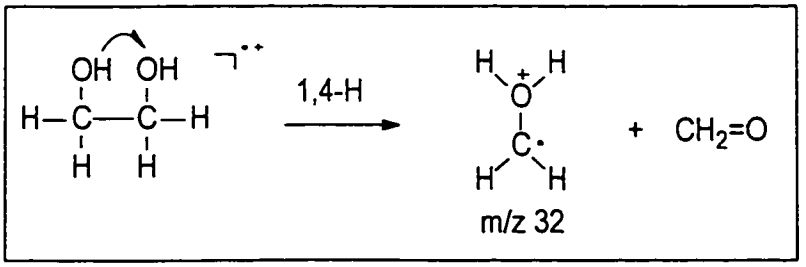

Such shifts can be suppressed by deuterium labeling which slows the rate of transfer and produces an *isotope effect*. Other transfers or shifts are less frequently

witnessed in mass spectra but have been observed, for instance methyl cation shifts, CH_3^+ [16].

The distonic ion has been invoked often to explain classic H rearrangements. One of the most attractive features of distonic ions is that they are often more stable than their counterparts of conventional structure. The ylid ion, $CH_2OH_2^{\bullet+}$ was touted as a "triumph of theory" since ab initio calculations predicted this species to be stable in the gas-phase before it was experimentally identified [5].

The next class of intermediates are ion-dipole complexes, also referred to in the literature as ion-molecule or ion-neutral complexes. As the name implies, these species consist of two moieties bound together by an electrostatic interaction of a point charge (in one part of the complex) and a permanent electric dipole (on the other). Formally these species can derive stability from attractive forces other than ion-induced dipole interactions (i.e. higher order interactions) but we will limit ourselves to the term ion-dipole complexes. Such a complex can be either an odd electron: [radical cation - neutral molecule] complex or an even electron [cation - neutral radical] complex, i.e. $M^{\bullet+}\bullet\bullet\bullet R$ or $M^{+}\bullet\bullet\bullet R^{\bullet}$, respectively. These species derive most of their stabilization energy, SE, relative to the infinitely separated ion and dipole, from ion-dipole interactions as expressed in the equation:

$$SE\,(kcal/mol) = \frac{68.8\mu\cos\theta}{r^2}$$

where 68.8 is a conversion factor, μ is the dipole moment in Debye, θ the angle between the direction of the dipole and the center of positive charge and r is the distance between the centers of the charge and the dipole. This SE is critical since it allows a complex to rearrange prior to dissociation.

Hydrogen-bridged radical cations (HBRC) can be considered as a subset of ion-dipole complexes. Many O•••H•••O bridged radical cations can best be described as H-bridged ion-dipole complexes of the type $[M\bullet\bullet\bullet H\text{-}R]^{\bullet+}$ or $[M\text{-}H\bullet\bullet\bullet R]^{\bullet+}$ (M = molecule, R = radical), where stability is derived from hydrogen bonding and attractive ion-permanent dipole interactions. Numerous HBRC species have been proposed as intermediates in reaction mechanisms, such as N•••H•••O, O•••H•••O and C•••H•••O bridged ions.

Although the proton bridge provides some stabilization, its main function is to direct the course of isomerization by allowing facile proton transfer.

Their even electron counterparts, proton-bound molecular pairs, can conveniently be generated in ion/molecule experiments and an empirical relationship for their SE was derived which can also be applied to HBRCs. The equation relates the SE to the difference in proton affinities at the two H binding sites and for oxygen containing ions [17] :

$$SE = 30.4 - 0.3\,\Delta PA \quad \text{(kcal/mol)}$$

The SE derived from this equation has been quite successful in reproducing SE values from calculations [18]. Although not an easy task, several stable HBRC have been experimentally identified: the vinylalcohol/water ion $CH_2{=}C(H)O{\bullet\bullet\bullet}H{\bullet\bullet\bullet}OH_2^{\bullet+}$ [19a] and the carbonic acid isomer $HO{\bullet\bullet\bullet}H{\bullet\bullet\bullet}O{=}C{=}O^{\bullet+}$ [19b] to name only two.

A concept related to the ion-dipole complex is the Charge Transfer (CT) complex. The formulation of this concept arose from the need to explain some specific double hydrogen transfers. In our example, ionized 1,2-ethanediol also produces an ion at m/z 33, which can only be protonated methanol, $CH_3OH_2^+$. One can expect the first H transfer to occur akin to that shown in the Scheme above but with a concomitant C–C cleavage to produce a HBRC. The second H transfer could be envisaged as a 1,5-H transfer from the formaldehyde moiety to the $CH_2OH_2^{\bullet+}$ but this was found to be an energetically unfavourable pathway and also incompatible with an isotopic labelling experiment:

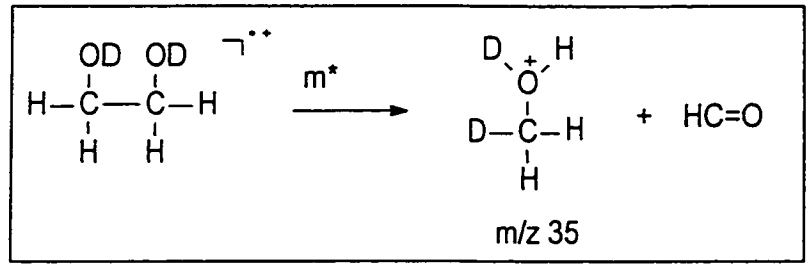

This surprising O–D to C–D conversion was explained using another mechanistic concept, the 1,2-H shift catalyzed by a base molecule. This concept, also referred to as proton-transport catalysis [20], utilizes the presence of a base molecule to reduce the energy barrier required to perform a 1,2-H shift. The unassisted 1,2-H shift in $CH_2OH_2^{\bullet+}$ → $CH_3OH^{\bullet+}$ requires about 25 kcal/mol whereas the assisted shift has a negligible barrier,

~ 1 kcal/mol (see *Applications of model chemistries* below). In the case of ionized 1,2-ethanediol, a formaldehyde catalyzed 1,2-H shift was envisaged:

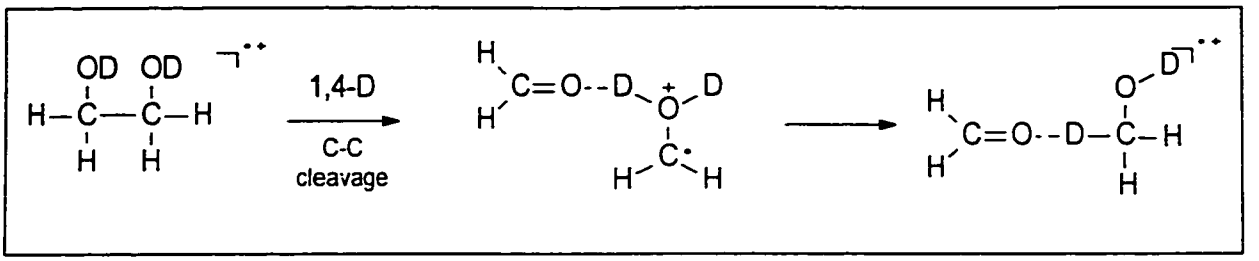

The CT complex becomes necessary at this stage, since in order to transfer the second H from the final ion in this Scheme (the C•••H•••O bridged ion), the formaldehyde would have to rotate and orient its H atoms towards the $CH_3OH^{\bullet+}$ moiety but in doing so all ion-dipole stabilization energy would be lost and the components of the complex would fly apart. Therefore it was proposed that a charge transfer occurs where $CH_2{=}O{\bullet\bullet\bullet}CH_3OH^{\bullet+}$ becomes $CH_2{=}O^{\bullet+}{\bullet\bullet\bullet}O(H)CH_3$. Note that the CH_3OH moiety has been turned around such that ion-dipole interaction is maintained. If one examines the geometry of the derived CT structure [14], one observes that the dipole of each neutral moiety points in the direction of the other ionized part of the complex and hence no matter where the charge resides, ion-dipole interaction is maintained in a CT complex. The CT complex is not a stable species but an actual Minimum Energy Crossing Point between two surfaces, one surface corresponding to $A{\bullet\bullet\bullet}B^{\bullet+}$ and the other to $A^{\bullet+}{\bullet\bullet\bullet}B$. As one might expect this was not an easily formulated concept but theoretical chemistry provided the answer [14,21]. It has been found that when the two moieties have substantial dipole moments and similar ionization energies the charge transfer complex occurs below the energetic threshold for dissociation. Minimum Energy Crossing Points have been found to be low in relative energy for crossings between singlet and triplet states of the phenyl cation [23] and other species in the gas-phase [23]. This is an example of two-state reactivity, where it is proposed that the transition probability between the surfaces is of the same fundamental importance as are transition states, entropic requirements and barrier heights in the classical single state reactivity model [23].

These two concepts, dipole-catalyzed proton shift and charge transfer have been applied to the ionic rearrangement reaction mechanisms of several organic radical cations, such as 1,2-ethandiol [14] and its sulphur-substituted analogues [24], acetol [25], and

lactamide [26]. It is interesting to note the relevance of these different mechanistic proposals. Morton recognized fairly early that many gas-phase ion chemistry experiments could be compared directly to solvolysis in solution [6], particularly reactions involving asymmetric proton-bound molecular pairs. The ionized vinyl alcohol/water ion-dipole complex has been proposed to be a key intermediate in the enzyme catalyzed dehydration of 1,2-ethanediol [27].

THE APPLICATION OF QUANTUM CHEMISTRY TO GAS-PHASE ION CHEMISTRY

Thus far we have overlooked the contribution of computational chemistry to the chemistry of gas-phase ions. It is now time to remedy this situation. At one time, Coulson [28] stated:

> *"... that calculating the dissociation energy of a heavy molecule (with Molecular Orbital Theory) is like weighing the captain of a ship by determining the displacement of his ship when he is, or is not, on aboard!"*

This view was shared by many chemists and persisted until recently when powerful computers became available which do allow calculations at a sufficient level of accuracy. In addition to the calculation of dissociation energies, computational chemistry can contribute in most areas of gas-phase ion chemistry. For example, many ions and radicals do not have well-established experimental ΔH_f values. These quantities are fundamental to the interpretation of ionic dissociation reactions in mass spectrometry. Computational thermochemistry can aid this shortcoming greatly by the calculation of ΔH_f values and this area has recently been reviewed [29]. We can also find the corresponding equilibrium structures and transition states on potential energy surfaces (PES). We can calculate vibrational frequencies for both sets of stationary points which can be used to characterize minima (all frequencies are real) and transition states (one imaginary frequency). These quantities can also be used to determine isotope effects, temperature dependencies of heats (enthalpies) of reactions and reaction rates via transition state theories [5].

This section deals with important aspects of modern computational chemistry and how it can be applied to gas-phase ion chemistry. Computational Chemistry, in its barest form, is the application of the methods of theoretical chemistry to real chemical problems.

It has developed on its own by the continuing advancement of computer hardware and software and is now distinct from theoretical chemistry [30]. The applicability of computational chemistry is rapidly expanding, particularly in the industrial (pharmaceutical) sector [30a]. Applications in statistical mechanics, the modeling of biomolecules and ligand design have spurred this interest [30b]. In this thesis we are interested in the question: What can computational chemistry/quantum chemistry tell us about the chemistry of gas-phase ions? The basic theory and tenets of quantum chemistry are described in many excellent textbooks [31] and so will not be described here. We are interested in the application of computational chemistry to the study of dissociation of ions in the gas phase and will briefly deal with questions as to how the calculations are performed by the computational chemistry programs and how they can be applied to gas-phase ion chemistry. Quantum chemistry is ideally suited for the study of (ionic) reaction mechanisms in the gas-phase. Essentially, the absence of a solvent reduces the demand on the computations significantly. This allows larger systems to be investigated or alternatively investigations of smaller systems using a fairly high level of theory.

The steadily increasing ability of computers to perform complex and laborious calculations at extremely high speeds makes it now possible to obtain solutions to the Schrödinger equation for systems of chemical interest. Recent advances in computer hardware and developments in efficient mathematical algorithms have also contributed to the now widespread use of quantum computational chemistry. This usage of "chemistry by computer" has become so prevalent that theoretical results are usually presented in conjunction with experimental results and agreement between the two approaches is truly compelling.

The calculations are largely based upon ab initio molecular orbital theory [2], a mathematical procedure that uses no experimental information other than fundamental physical constants to calculate the total energies. There are other related theories which are used to calculate energies but these will not be introduced here, see [32] and the density functional theory discussion below. The calculations can be used to predict properties of primary interest to chemists, such as the structure of ionized molecules and the mechanisms of reactions in which they are involved. The calculations can be applied to reactive (and therefore transient) gas-phase ions as easily as to their more stable neutral

counterparts, they play a particularly useful role in cases where appropriate experiments are not easily performed.

There are several basic calculations to consider before introducing some of the finer details of computational chemistry. First and foremost is the optimization of structure within a certain method yielding a stationary point of the potential energy surface (PES). This occurs by the calculation of the force constants between atoms, using the direction of these forces to change the relationship of the atoms and minimizing these forces to some specified limit, yields an equilibrium geometry. This calculation is called a *geometry optimization*. A test to verify the stability of the resulting structure involves a more accurate calculation of the force constants, called a *frequency calculation*. This calculation generates the vibrational frequencies and these are used to differentiate between minima (all frequencies real) and transition states. A transition state (TS) is characterized by one imaginary vibrational frequency, that is an energy maximum in one direction (the reaction co-ordinate) whereas in all other directions it is a minimum. This transition state structure can be characterized further by performing another computation, which follows the reaction coordinate of the imaginary frequency and thereby connects the transition state to minima. Typically, the method used to perform the geometry optimization and the frequency calculation does not yield relative energies of "chemical" accuracy and a higher level theoretical method is necessary (*vide infra*). The following sections introduce the various methods of computational chemistry and for the simplest method illustrate how a calculation is performed by the program.

Electronic Structure Theory

Basic Quantum Chemistry involves approximated solutions to the time independent, non-relativistic Schrödinger equation $H \Psi = E \Psi$. Given a wavefunction Ψ and the Hamiltonian H, the total energy E may be calculated from this equation. This type of calculation can be performed since the Schrödinger equation can be reduced to an eigenvalue problem and hence solved by standard mathematical methods. The Hamiltonian, H, is the quantum mechanical equivalent of an equation of motion, and it describes all the forces acting within a system. Exact solutions of the Schrödinger equation are not possible except for the smallest of systems (H_2^+). Therefore, one must

use approximations to solve this equation. The various methods and basis sets used in theoretical chemistry, for example HF/6-31G* (method/basis set), involve different choices for solving the Schrödinger equation and different choices for approximations to the wavefunction. The solution to the Schrödinger equation, in whichever formalism desired, is found to yield the electronic energy of a system. All equations in this section will use atomic units, which greatly simplify the equations of quantum chemistry. In atomic units, the energy quantity is the hartree = e/a_0 (= 627.5095 kcal/mol) where e is the charge on an electron and a_0 is the unit of length, the Bohr radius $a_0 = h^2/4\pi m_e e^2 = 0.529$ Å (where h is Planck's constant and m_e is the mass of an electron).

The so-called Born-Oppenheimer approximation leads to separation of nuclear and electron motions (here the lower case **r** denotes coordinates of the electron and upper case **R** denotes nuclear coordinates and both are vector quantities) and then the kinetic energy of the nuclei can be separated from that of the electrons.

$$H^{elec} = T^{elec}(\mathbf{r}) + T^{nuclear}(\mathbf{R}) + V^{nuclear-elec}(\mathbf{R},\mathbf{r}) + V^{elec}(\mathbf{r}) + V^{nuclear}(\mathbf{R})$$

Where T and V represent kinetic and potential energies. The full Hamiltonian:

$$H^{elec} = -\frac{1}{2}\sum_{i}^{elec}\nabla^2 - \sum_{i}^{elec}\sum_{I}^{nuclear}\left(\frac{Z_I}{|\mathbf{R}_I - \mathbf{r}_i|}\right) + \sum_{i}^{elec}\sum_{j<i}^{elec}\left(\frac{1}{|\mathbf{r}_i - \mathbf{r}_j|}\right) + \sum_{I}^{nucl}\sum_{J<I}^{nucl}\left(\frac{1}{|\mathbf{R}_I - \mathbf{R}_J|}\right)$$

Therefore the Schrödinger equation becomes:

$$H^{elec}\psi^{elec}(\mathbf{r},\mathbf{R}) = E^{effective}(\mathbf{R})\psi^{elec}(\mathbf{r},\mathbf{R})$$

The solution of this equation yields the total energy of a system for a set of fixed nuclei : a so-called single point calculation.

Orbitals

The key approximation in quantum chemistry is the orbital approximation. An orbital is a mathematical construct where the position of an electron is treated as a probability distribution in real space. This is performed for each electron in a molecule (or pair of electrons *vide infra*). Solutions to the Schrödinger equation typically begin with an approximation of the wavefunctions, ϕ as:

$$\phi_u = \sum_{u=1}^{N} c_{ui}\chi_u$$

where the sum is over the total number of electrons N, c_{ui} are the molecular orbital expansion coefficients and basis functions χ_u are typically Gaussian-type probability functions. Orbitals are usually defined as spin orbitals, $\chi(x)$, since the wavefunction describing a region of space can be separated into spatial and spin components (where by convention $\alpha(\omega)$ denotes spin up and $\beta(\omega)$ denotes spin down,).

$$\chi(x) = \begin{cases} \psi(\mathbf{r}) & \alpha(\omega) \\ \psi(\mathbf{r}) & \beta(\omega) \end{cases}$$

The constraints (indistinguishabililty of electrons, normalization and antisymmetry) on the wavefunction for the whole system leads to the Slater determinant:

$$\Psi(x_1, x_2 \ldots x_n) = (N!)^{\frac{1}{2}} \begin{vmatrix} \chi_i(x_1) & \chi_j(x_1) & .... & \chi_k(x_1) \\ \chi_i(x_2) & .... & .... & .... \\ .... & .... & .... & .... \\ \chi_i(x_N) & \chi_j(x_N) & .... & \chi_k(x_N) \end{vmatrix}$$

for a proper description of the wavefunction. This description is simplified by the ket notation of Dirac [33],

$$\Psi(x_1, x_2, \ldots, x_N) = \left| \chi_i(x_1)\chi_j(x_2) \ldots \chi_k(x_N) \right\rangle$$

and even further simplified to:

$$\left| \Psi_0 \right\rangle = \left| \chi_1 \chi_2 \cdots \chi_N \right\rangle$$

which symbolizes the ground state wavefunction. The variational principle states that the best wavefunction is the one that gives the lowest possible expectation value to the energy:

$$E_0 = \langle \Psi_0 | H | \Psi_0 \rangle$$

where the flexibility is in the choice of the (coefficients of) the spin orbitals describing the wavefunction.

The Hartree-Fock (HF) approximation is the next key approximation in molecular orbital (MO) theory. The essence of this approximation is that the many particle (electron) wavefunction, Ψ, can be replaced by a series of individual one electron problems, where electron-electron repulsion in an average way.

$$f(i)\chi(x_i) = \varepsilon\, \chi(x_i)$$

where *f(i)* is the Fock operator, an effective one electron operator:

$$f(i) = -\frac{1}{2}\nabla_i^2 - \sum_{A=1}^{N}\frac{Z_A}{r_{iA}} + v^{HF}(i)$$

where $v^{HF}(i)$ is the average potential experienced by electron *i*. Note that the wavefunction has been replaced by spin orbitals. The self-consistent field (SCF) procedure is then carried out to optimize the spin orbital coefficients until v^{HF} no longer changes. This solution yields a new set of spin orbitals $\{\chi_k\}$ with a corresponding set of energies $\{\varepsilon_k\}$ which defines the HF ground state wavefunction in its entirety and is the best variational approximation of a ground state wavefunction in single determinant form. In practice, the HF equation is solved by using a finite set of spatial basis functions $\{\phi_\mu(\mathbf{r}) \mid \mu=1,2...k\}$. The spatial part of the spin orbitals can then be expanded in terms of the known set of functions for both α and β spin functions and both substituted into the HF eigenvalue equation above for two sets of equations. This is the so-called *open shell* formalism since each electron is treated individually (also called Unrestricted Hartree-Fock, UHF). Another formalism is the *closed shell* model where pairs of electrons are described by the molecular orbitals (also called Restricted Hartree-Fock, RHF). Alternatively, a formalism labeled *restricted open shell* (ROHF) may also be used for unpaired electrons [5]. In order to obtain a proper description of dissociation (bond breaking) in gas-phase ion chemistry one needs to use an unrestricted or restricted-open shell method.

Therefore, for a basis set of k spatial functions, $\{\phi_\mu(\mathbf{r})\}$, leads to a set of 2k spin orbitals which have N occupied spin orbitals $\{\chi_a\}$ and 2k-N unoccupied (virtual) orbitals $\{\chi_r\}$. A single Slater determinant formed from $\{\chi_a\}$ is the variational HF ground state and is typically represented by Ψ_0 or $|\Psi_0\rangle$. The use of larger and more extensive sets of basis functions gives greater flexibility in the spin orbitals and lowers the calculated energy, E_0. If an infinite basis set were used the so-called Hartree-Fock limit would be reached and E_0 would be the lowest energy for that state.

Electron Correlation

The HF procedure is clearly only one of many determinants that can be formed from the 2k spin orbitals. An easy way to describe the other determinants is to state how they differ from the reference HF ground state. That is, by stating which occupied spin orbitals have been replaced by virtual ones, and generating excited state determinants such as single or double excitations (*abc* denotes occupied orbitals and *rst* denotes unoccupied) ,

$$\left|\Psi_a^r\right\rangle = \left|\chi_1\chi_2\cdots\chi_r\chi_b\cdots\chi_N\right\rangle$$

$$\left|\Psi_{ab}^{rs}\right\rangle = \left|\chi_1\chi_2\cdots\chi_r\chi_s\cdots\chi_N\right\rangle$$

The exact wavefunction can be expressed as a combination of ground and excited state configurations:

$$\left\{\left|\Psi_i\right\rangle\right\} = \left\{\left|\Psi_0\right\rangle, \left|\Psi_a^r\right\rangle, \left|\Psi_{ab}^{rs}\right\rangle, \left|\Psi_{abc}^{rst}\right\rangle, \ldots\right\}$$

Using these different configurations of spin orbitals is sensibly called *configuration interaction* (CI). Its incorporation into the computational scheme lowers the total energy of a system since it introduces non-dynamical correlation energy into the computational scheme above. *Electron correlation* (E_{corr}) is a fundamental concept in quantum chemistry, it is defined as,

$$E_{corr} = \varepsilon_0 - E_0$$

where ε_0 is the lowest configuration interaction energy. There are two different types of correlation energy: dynamical and non-dynamical. Non-dynamical correlation occurs when excited states contribute to the total energy of the system and dynamical correlation occurs when a pair of electrons interact [29] to lower the energy of the system. In all but the smallest systems, the incorporation of the entire set of excitations, called *Full CI*, is impossible because of the large number of determinants. If this feat (Full CI) were possible an exact non-relativistic energy would be calculated for a given basis set. Typically, the CI expansion is truncated at some reasonable order, the largest of which is usually quadruple excitations (S, SD, SDT, SDTQCI for singles CI, singles-doubles... CI). The main drawback of this type of calculation is that size consistency is not maintained (*vide infra*), but size correction schemes have been developed to compensate for this error [34]. There exist many different approaches for the incorporation of electron

correlation into ab initio calculations. It must be re-enforced at this stage that incorporation of electron correlation is necessary to obtain accurate relative energies and proper descriptions of PES. The following paragraphs will briefly touch on some of the more popular methods and will introduce the reader to abbreviations used in subsequent chapters.

Two common approaches which incorporate electron correlation at a moderate level are many body perturbation theory (as described by Møller - Plesset, MP [35]) and density functional theory (DFT). Perturbation theory expresses electron correlation as a perturbation of the Hamiltonian. If this perturbation is terminated at the second (third or fourth) stage of the perturbation series, it is referred to as MP2 (MP3 or MP4). It has been found that lower orders of perturbation converge the correlation energy slowly [29].

Density functional theory (DFT) uses a fundamentally different method to calculate the energy of a system. Hohenberg and Kohn showed that the ground-state energy of a many electron system is uniquely determined by its electron density [36]. The basic idea is to replace the complicated *n*-electron wave function and associated Schrö dinger equation with the electron density $\rho(r)$ and its associated computational scheme [37]. Although the dependence of the energy on the density is not fully understood, good empirical approximations have been developed and are now in widespread usage [37]. Most popular of the DFT methods is the so-called B3LYP method which is a hybrid of Becke's three parameter exchange functional [38a], B3, and Lee, Yang and Parr's correlation functional [38b], LYP. This method is only slightly more computationally demanding than simple HF methods and has enjoyed widespread use [29,36].

The methods MP2 and B3LYP have been found to reproduce experimental (neutral) geometries very well but are inadequate for the accurate computation of thermochemical quantities at moderate basis set size and thus other methods are required.

The coupled-cluster approximation is the method of choice for many quantum chemical applications [39]. A main drawback of CI methods is that they are not size consistent, but coupled cluster and its sister methods remedy this shortcoming. Coupled-cluster is a technique steadily increasing in prominence for the treatment of electron correlation and has been shown to be adequate for accurate calculations of

thermochemical quantities [39b]. The coupled cluster method starts from an exponential form of the wavefunction:

$$\Psi = \exp(T)\Psi_0$$

where T (= $T_1 + T_2 + T_3 + \ldots$) is an excitation operator and the subscript refers to the number of excited electrons. The energy of a system is then derived from the equation:

$$E = \langle \Psi_0 | H \exp(T) | \Psi_0 \rangle$$

This method provides an elegant and efficient way to include effects of higher excitations while remaining size extensive. When single and double excitations are included in the treatment this method is referred to as CCSD. A method related to coupled cluster theories was introduced by Pople and termed Quadratic Configuration Interaction, QCI [40]. The CISD equations were modified in QCI to include terms which are quadratic in the expansion coefficients and a non-iterative (iterations refer to SCF procedure above) treatment of triple excitations, hence the abbrevation QCISD(T). This latter method for non-iterative triples incorporation has also been applied to coupled cluster methods, CCSD(T). The last two methods QCISD(T) and CCSD(T) are usually chosen for the accurate calculation of thermochemical quantities [29, 39].

Ab initio calculations are restricted in two ways: (i) truncation of the size of basis set used and (ii) the amount of electron correlation included in the calculation of total energy. Ideally, we would like to use a very high level of electron correlation in conjunction with a very large basis set to come close to the exact solution of the Schrödinger equation. The computational expense of performing such high level (treatment of electron correlation) methods and large basis set calculations scales dramatically with the size of system and we must limit either the size of system or the level of calculation. The largest sources of error in ab initio molecular orbital calculations are the level of theory (amount of electron correlation) and the size of basis set.

Population Analysis

Another important result from the ab initio calculations is the description of the location of the charge (and radical) in the equilibrium structures obtained based on the analysis of population of electrons in the spin orbitals. These types of analyses are

performed in most calculations and the default method is that proposed by Mulliken [2]. It is well known that little faith can be conveyed on the magnitude of the charges derived from this arbitrary scheme, but more importantly for gas-phase ion chemistry, the general location of the bulk of the positive charge density through this method is in agreement with more rigorous theories based on charge densities, such as Atoms in Molecules [41]. Further, from the spin orbitals we can average the spin densities for the α and β spins and for species with unpaired electrons take the difference between these two densities and find out where the unpaired electron resides in the molecule.

Lastly, there exists a check for the UHF formalism which checks the wavefunction for *spin contamination*. Formally, this corresponds to the expectation value of the square of the spin operator [5b], $\langle S^2 \rangle$, and for a lone unpaired electron the exact value is 0.75. This value indicates the extent of interference of an excited state into the reference HF ground state. Typically, the range of $\langle S^2 \rangle = 0.75 + 10$ % is considered acceptable, no significant interference is observed and energy values generated therefrom are reliable.

Model Chemistries

Now that the various types of calculations (single point, vibrational frequencies, geometry optimizations) and methods (HF, MP2, B3LYP and CCSD(T)) have been introduced, the discussion must turn to the application of these methods to gas-phase ion chemistry and some of the advantages (and disadvantages) of using the various methods. In order to investigate a system of atoms a "model chemistry" must be defined [5]. A theoretical model chemistry is a computational procedure which is uniformly applicable to the system and whose effectiveness may be assessed by comparison to experimental data. A model chemistry should be: (i) size extensive; (ii) generally applicable to a wide selection of gas-phase ion chemistry problems; (iii) efficient and cost effective; (iv) applicable to excited states and open shells and (v) able to dissociate an ionized molecule correctly into its fragments. A model chemistry is described by:

Single Point method / basis set large // PES characterization method / basis set small

Typically, a structure is optimized and the vibrational frequencies are analyzed at a lower theoretical level with a smaller basis set than that used to calculate its total energy (single point). This approximation is performed since geometries of stable neutral molecules are

know to be accurately described by these lower level calculations. The single point energy is typically performed at as high a level of theory and as large a basis set as is practical given the available computing resources. Many model chemistries are summarized in ref 5b. All are meant to predict the thermochemical quantities described by Fig. 1-2 in section 1.2 of this introduction. In gas-phase ion chemistry we are primarily interested in the following thermochemical quantities: ΔH_f (ion), IE, PA or AE which means the calculation of numerous different thermochemical quantities.

All energies calculated with a single point calculation refer to total electronic energy at zero degrees Kelvin (0 K). For comparisons to experimental data we must perform a conversion from potential energy (E_0) into enthalpy (H) and free energy (G):

$$E = E_0 + E_{vib} + E_{rot} + E_{trans}$$

$$H = E + RT$$

$$G = H - TS$$

where E_{vib}, E_{rot} and E_{trans} refer to translational, rotational and vibrational energies (the latter at T = 0 K is also known as the zero-point vibrational energy: ZPVE) T is temperature, R is the gas constant and S is entropy. These values are made available by the frequency calculation and/or from experiment. Most experimental values are listed in various compendia and web sources [42]. There have also been numerous alternative computational schemes which reproduce thermochemical data. Most of these methods do not require the computational might of computers and are reviewed in ref 30. A notable scheme is the additivity scheme of Benson [43].

The most accurate and popular of the *ab intio* computational methods are labeled G2 and CBS-Q [44]. Both of these methods are composite methods which rely on a series of approximations and empirical corrections to achieve highly accurate results. G2 was proposed in 1991 by Pople et al. and stands for Gaussian-2 theory [44a]. The G2 composite method approximates a highly correlated level of theory with a large basis set, QCISD(T)/6-311+G(3df,2p)//MP2(full)/6-31G(d), by a series of additivity assumptions on increasing size of basis set and varying levels of theory. CBS-Q stands for Complete Basis Set Quadratic Configuration Interaction and was proposed in 1994 by Petersson and co-workers [44b]. The CBS set of composite methods (CBS-4, CBS-Q and CBS-APNO) are based on the approximation that the largest error in *ab initio* calculations comes from

the truncation of the basis set and uses the asymptotic convergence of pair natural orbital orbitals to extrapolate to the complete basis set limit. Both of these methods are quoted to produce mean deviations from experiment around chemical accuracy, ~ 2 kcal/mol.

Since these methods were introduced, there has been a rapid expansion in computational-composite-method thermochemistry. A number of revised computational schemes have since been published, such as G2(MP2), G2(MP2,SVP) and G2MCC which indicates the rapid growth of this field in the past several years [45]. Very recently (Jan 1999) a new method, entitled G3, and its corresponding G3(MP2) has been introduced by Pople et al. [46], both methods increase the accuracy and speed of the G2 method. Also very recent, there was a new CBS method introduced, CBS-RAD, designed primarily for radicals which may be a good method for radical cations as well [47].

Applications of model chemistries to gas-phase ion chemistry

There have been many applications of model chemistries to gas-phase ion chemistry. This section will briefly present some of the composite methods used and their successes and failures. These methods have been applied to both even electron and odd electron species. The mass spectrometry community has been progressively involved with calculating both ionic and neutral species using composite and standard computational methods, notably the groups of Schwarz [48a], Tureček [48b], Hammerum [48c], Bouchoux [48d] and Terlouw [48e] have contributed. Primarily, composite methods have been used to derive the thermochemical quantities such as ΔH_f, IE and PA. Composite methods themselves have not been used often to study the reaction mechanisms of gas-phase ion chemistry. This is mainly due to the motivation behind these methods : the reproduction and prediction of thermochemistry of stable neutral molecules. The few composite studies that exist have been limited to fairly small organic systems [48d,51]. Radom and co-workers have presented several detailed studies of proton affinities by calculation with Gaussian methods [49]. Radom was also one of the first to apply G2 theory to organic radical cations [50]. This group has also recently presented several computational papers dealing with "Ion-Transport Catalysis" (*vide supra*) which characterize the ability of a spectator molecule to catalyze an isomerization with a composite method [51].

Although the G2 type methods have been outstandingly successful for a variety of compounds there are a few cases where this method does not perform well. For instance, it was found to behave very poorly for the calculation of ΔH_f in some species [54]. This failing was recently attributed to the lack of an experimental spin-orbit correction and the G3 method incorporates this correction [46].

The computational expense of G2 is also limiting: the size of species examinable is typically six first row heavy atoms. At the size and complexity of a six heavy atom system, the G2 method becomes cumbersome and the rewards for use are somewhat uncertain. As an example, the G2 method was applied to a series of ionic dissociations for the $C_3H_6O_3^{\bullet+}$ system discussed in Chapter 6. The results are presented in Table 2-1 and are compared to their well established experimental values. This comparison of G2 to experiment shows that the differences are close to the estimated deviation of the computational procedure (so-called chemical accuracy ~1-2 kcal/mol) but the ordering of the dissociation levels is wrong.

Table 1-1. G2 total energies, relative energies and experimental relative energies for the dissociation of the $C_3H_6O_3^{\bullet+}$ system.

Species	G2(298K)	ΔE_{rel} (298K) G2	ΔE_{rel} 298K expt [42]
CH_2=O + $CH_3OC(H)$=$O^{\bullet+}$	-342.66009	34.6	35
CH_2=O + $CH_3OCOH^{\bullet+}$	-342.67184	27.2	29
CH_2OH^+ + CH_3OC=$O^{\bullet}$	-342.67025	28.2	25
$CH_2OH^{\bullet}$ + CH_3OC=O^+	-342.67462	25.5	22
HC=$O^{\bullet}$ + $CH_3OC(H)OH^+$	-342.71522	0.0	0

Another drawback to the study of gas-phase ion chemistry with composite methods involves the determination of barrier heights. These methods were not designed to investigate transitions states and often the surface is explored with a fairly low level of theory which may be inappropriate for radical cations. A solution to this problem has been recently proposed and is termed the IRCMax method [55]. This method is reported to reduce errors in geometries and classical barrier heights quite dramatically. These

reasons, *inter alia*, led us to investigate the various ionized systems presented in this thesis with a variety of model chemistries.

The outlook for the use of computational chemistry to study ion structures and reaction mechanisms in gas-phase ion chemistry is quite good. The rapidly increasing computational and algorithmic power will undoubtedly lead to the use of computational chemistry as the principal tool in the interpretation and understanding of the bewildering array of rearrangement reactions of ionized molecules.

References:

1. M.C. Blanchette, J.L. Holmes, C.E.C.A. Hop, F.P. Lossing, R. Postma, P.J.A. Ruttink and J.K. Terlouw, J. Am. Chem. Soc., 108 (1986) 7589.
2. W.J. Hehre, L. Radom, P.v.R. Schleyera and J.A. Pople, Ab Initio Molecular Orbital Theory, John Wiley & Sons, New York, 1986.
3. (a) M.F. Guest, J. Kendrick. GAMESS Users Manual, SERC Daresbury Laboratory, computational chemistryP/86/1, 1986 ; M. Dupuis, D. Spangler and J. Wendolowski. NRcomputational chemistry Software Catalog, Vol. 1, Program No. QG01 (GAMESS), 1980 ; M.F. Guest, R.J. Harrison, J.H. van Lenthe and L.C.H. van Corler, Theor. Chim. Acta ,71 (1987) 117. (b) Gaussian 94, Revision B.3, M. J. Frisch, G.W. Trucks, H.B. Schlegel, P.M.W. Gill, B.G. Johnson, M.A. Robb, J.R. Cheeseman, T.A. Keith, G.A. Peterson, J.A. Montgomery, K. Raghavachari, M.A. Al-Laham, V.G. Zakrevski, J.V. Ortiz, J.B. Foresman, C.Y. Peng, P.Y. Ayala, W. Chen, M.W. Wong, J.L. Andres, E.S. Replogle, R. Gomperts, R.L. Martin, D.J. Fox, J.S. Binkley, D.J. de Frees, J. Baker, J.P. Stewart, M. Head-Gordon, C. Gonzales and J.A. Pople, Gaussian Inc., Pittsburgh PA, 1995.
4. Holmes, J.L. Org. Mass Spectrom., 20 (1985) 169.
5. (a) L. Radom, Org. Mass Spectrom. 26 (1991) 359. (b) L. Radom, Int. J. Mass Spectrom. Ion Processes, 118/119 (1992) 339. (b) J.B.Foresman and A. Frisch, Exploring Chemistry with Electronic Structure Methods, Gaussian Inc: Pittsburgh, 1996 and references cited therein. (c) A. Szabo and N.S. Ostlund, Modern Quantum Chemistry: Introduction to Advanced Electronic Structure Theory, Dover Publications, New York, 1989.
6. (a) P.C. Burgers and J.K. Terlouw, in M.E. Rose (Ed.) Specialist Periodical Reports : Mass Spectrometry, The Royal Society of Chemistry, London, 1989, Vol. 10, Chapter 2. (b) J.S. Splitter in J.S. Splitter and F. Turecek (Ed.) Applications of Mass Spectrometry to Organic Stereochemistry, VCH, Weinheim, 1994, Chapter 3. (a) D.J. McAdoo and T.H. Morton, Acc. Chem. Res., 26 (1993) 295. (b) P. Longevialle, Mass Spectrom. Rev., 11 (1992) 157. (c) R.D. Bowen, Acc. Chem. Res., 24 (1991) 364. (d) S. Hammerum in K.R. Jennings (Ed.) Fundamentals of Gas Phase Ion Chemistry, pp. 379-390. (e) D.J. McAdoo , Mass Spec. Rev., 7 (1988) 363. (f) T.H. Morton, Tetrahedron, 38 (1982) 3195. (g) R.D. Bowen, Org. Mass Spectrom., 28 (1993) 1577. (h) N. Heinrich and H. Schwarz, in J.P. Maier (Ed.) Ion and Cluster Ion Spectroscopy and Structure, Elsevier, Amsterdam, 1989 , p. 329.
7. (a) F.W. McLafferty and F. Tureček, Interpretation of Mass Spectra, University Science Books, California, 1993. (b) M.E. Rose and R.A.W. Johnstone Mass Spectrometry for Chemists and Biochemists New York, Cambridge University Press, 1982 (c) F.W. McLafferty, Tandem Mass Spectrometry, New York Wiley, 1983. (d) J.R. Chapman, Practical Organic Mass Spectrometry, New York, Wiley, 1985 (e) K. Levsen, Fundamental Aspects of Organic Mass Spectrometry, New York, Verlag Chemie, 1978.
8. M.T. Bowers, A.G. Marshall and F.W. McLafferty, J. Phys. Chem. 100 (1996) 12897.
9. R.G. Cooks, J.H. Beynon, R.M. Caprioli and R.G. Lester, Metastable Ions, Elsevier, Amsterdam, 1973.
10. K. Kimura et al., Handbook of HeI photoelectron spectra of fundamental organic molecules : New York : Halsted Press, 1981.

11. J.L. Holmes and J.K. Terlouw, Org. Mass. Spectrom. 15 (1980) 383.
12. C.A. Shalley, G. Hornung, D. Schroder and H. Schwarz, Chem. Soc. Rev. 27 (1998) 91. (b) C.A. Shalley, G. Hornung, D. Schroder and H. Schwarz, Int. J. Mass Spectrom. Ion Proc., 172 (1998) 181. (c) K. Levsen and H. schwarz, Angew. Chem. Int. Ed. Engl., 15 (1976) 509 (d) C. Wesdemiotis and F.W. McLafferty, Chem. Rev. 87 (1987) 485. (e) F.W. McLafferty, Science, 247 (1990) 925 (f) J.K. Terlouw and H. Schwarz, Angew. Chem. Int. Ed. Engl., 26 (1987) 805.(g) F.W. McLafferty, Int. J. Mass Spectrom. Ion Proc., 118/119 (1992) 221 (h) G.I. Gellene and R.F. Porter, Acc. Chem. Res. 16 (1983) 200.(i) N. Goldberg and H. Schwarz, Acc. Chem. Res., 27 (1994) 347.
13. H.F. van Garderen, P.J.A. Ruttink, P.C. Burgers, G.A. McGibbon and J.K. Terlouw, Int. J. Mass Spectrom. Ion Processes, 121 (1992) 159.
14. P.J.A. Ruttink and P.C.Burgers, Org. Mass Spectrom. , 28 (1993) 1087.
15. J.L. Homes, F.P. Lossing, J.K. Terlouw, and P.C. Burgers, J. Am. Chem. Soc.104 (1982) 2931.
16. V. Baranov, S. Petrie and D.K. Bohme, J. Am. Chem. Soc., 118 (1996) 4500.
17. M. Meot-Ner (Mautner). J. Am. Chem. Soc. 106, 1257 (1984).
18. M. George, C.A. Kingsmill, D. Suh, J.K. Terlouw and J.L. Holmes, J. Am. Chem. Soc. 116 (1994) 7807.
19. (a) J.K. Terlouw, W. Heerma, P.C. Burgers and J.L. Holmes. Can. J. Chem. 62, 289 (1984) ; (b) R. Postma, P.J.A. Ruttink, F.B. van Duijneveldt, J.K. Terlouw and J.L. Holmes. Can. J. Chem. **63**, 2798 (1985) ; (c) R. Postma, S.P. van Helden, J.H. van Lenthe, P.J.A. Ruttink, J.K. Terlouw and J.L. Holmes. Org. Mass Spectrom. **23**, 503 (1988) (d) D. Sülzle, J.K. Terlouw and H. Schwarz. Angew. Chem. Int. Ed. Engl. **29**, 404 (1990).
20. D.K. Bohme, Int. J. Mass Spectrom. Ion Processes, 115 (1992) 95.
21. N. Koga and K. Morokuma, Chem. Phys. Lett., 119 (1985) 371.
22. J.N. Harvey, M. Aschi, H. Schwarz and W. Koch, Theor. Chem. Acc., 99 (1998) 95.
23. D.A. Plattner, Angew. Chem. Int. Ed. Engl. 38 (1999) 82.
24. O. Sekiguchi, T.Kosaka, T. Kinoshita and S. Tajima, Int. J. Mass Spectrom. Ion Processes, 145 (1995) 25.
25. P.J.A. Ruttink, P.C. Burgers and J.K. Terlouw, Can. J. Chem., 74 (1996) 1078
26. H. Friedrichs, G.A. McGibbon and H. Schwarz, Int. J. Mass Spectrom. Ion Processes, 1524 (1996) 217.
27. P. George, J.P. Glusker and C.W. Bock. J. Am. Chem. Soc., 117 (1995) 10131.
28. C.A. Coulson, Valence, 2nd ed. Oxford University Press, 1961, p.91
29. K.K. Irikura and D.J. Frurip (Ed.), Computational Thermochemistry, American Chemical Society, Washington, D.C., 1998
30. (a) J.H. Drieger, Chem. Eng. News, 30, May 12, 1997. (b) G.H. Grant and W.G. Richards, Computational Chemistry, Oxford 1996.
31. (a) T.H. Dunning Jr and P.J. Hay, in H.F. Schaeffer III (Ed.) Modern Theoretical Chemistry, Vol.3, Methods of Electronic Structure Theory, Plenum Press, New York, 1977, pp.1-28. (b) I.N. Levine, Quantum Chemistry, 3rd Ed., Allyn and Bacon, Massachusetts, 1983. (c) D.A. McQuarrie, Quantum Chemistry, University Science Books, California, 1983.
32. R. McWeeny and B.T. Sutcliffe, Methods of Molecular Quantum Mechanics, Academic Press, London, 1969.
33. P.A.M. Dirac, The Principles of Quantum Mechanics, University Press, Oxford, 1947.
34. (a) V.R. Saunders and J.H. van Lenthe, Mol. Phys. 48 (1983) 923 (b) J.A. Pople, R. Seeger and R. Krishnan, Int. J. Quantum Chem., 11 (1977) 149.
35. C. Møller and M.S. Plesset, Phys. Rev., 46 (1934) 618.
36. (a) P. Hohenberg and W. Kohn, Phys. Rev., 136 (1964) B 864. (b) W. Kohn and L.J. Sham, Phys. Rev., 140 (1965) A 1133.
37. For lead references see: (a) W. Kohn, A.D. Becke and R.G. Parr, J. Phys. Chem. 100 (1996) 12974 (b) K.B. Lipkowitz and D.B. Boyd ed., Reviews in Computational Chemistry, Vol. 7, VCH Publishers, New York, 1996 (c) R.G. Parr, W. Yang, Density Functional Theory of Atoms and Molecules, Oxford University Press, New York, 1989.
38. (a) A.D. Becke, J. Chem. Phys., 98 (1993) 5648. (b) C. Lee, W. Yang and R.G. Parr, Phys. Rev. B, 37 (1988) 785. (c) B. Meihlich, A. Savin, H. Stoll and H. Preuss, Chem. Phys. Lett., 157 (1989) 200.

39. (a) R.J. Bartlett, Ann. Rev. Phys. Chem., 32 (1981) 359 (b) T.J. Lee and G.E. Scuseria in Quantum Mechanical Electronic Structure Calculations with Chemical Accuracy, S.R. Langhoff (Ed.), Kluwer Academic Publishers, 1995, p.47.
40. (a) J.A. Pople, M. Head-Gordon and K. Raghavachari, J. Chem. Phys., 87 (1987) 5968 (b) J. Paldus, J. Čižek and B. Jeziorski, J. Chem. Phys. 90 (1989) 4356 (c) J.A. Pople, M. Head-Gordon and K. Raghavachari, J. Chem. Phys., 90 (1989) 4635 (d) J. Paldus, J. Čižek and B. Jeziorski, J. Chem. Phys. 93 (1990) 1485.
41. R.F.W. Bader, Atoms in Molecules, Pergamon Press, Toronto, 1996.
42. (a) K.K. Irikura and D.J. Frurip (Ed.), Computational Thermochemistry, American Chemical Society, Washington, D.C., 1998 Appendix A (b) S. Lias, J.E. Bartmess, J.F. Liebman, J.L. Holmes, R.D. Levin and W.G. Mallard. J. Phys. Chem. Ref. Data, 17 (1988) Supplement 1. (c) Holmes, J.L.; Lossing, F.P.; Mayer, P.M. J. Am. Chem. Soc. 1991, 113, 9723. (d) Simões, J.A.M.; Greenberg, A.; Liebman, J.F., Ed. Energetics of Organic Free Radicals; Blackie Academic & Professional, New York, 1996.
43. S.W. Benson, Chem. Rev., 93 (1993) 2419.
44. (a) L.A. Curtiss, K. Raghavachari and J.A. Pople. J. Chem. Phys. 98 (1993) 1293; (b) J.W. Ochterski, G.A. Petersson and J.A. Montgomery Jr., J. Chem. Phys. 104 (1996) 2598 and references cited therein.
45. (a) B.J. Smith and L. Radom, J. Phys. Chem., 99 (1995) 6468 (b) A.M. Mebel, K. Morokuma and M.C. Lin, J. Chem. Phys., 103 (1995) 7414 (c) C.W. Bauschlicher and H. Partridge, J. Chem. Phys., 103 (1995) 1788 (d) L.A. Curtiss, K. Paghavachari and J.A. Pople, J. Chem. Phys., 103 (1995) 4192.
46. (a) L.A. Curtiss, K. Raghavachari, P.C. Redfern, V. Rassolov and J.A. Pople, J. Chem. Phys. 109 (1998) 7764 (b) L.A. Curtiss, K. Raghavachari, P.C. Redfern, V. Rassolov and J.A. Pople, J. Chem. Phys. 110 (1999) 4703.
47. P.M. Mayer, C.J. Parkinson, D.M. Smith and L. Radom, J. Chem. Phys., 108 (1998) 604.
48. For leading references see: (a) H. Friedrichs, G.A.McGibbon and H. Schwarz, Int. J. Mass Spectrom. Ion Processes, 1524 (1996) 217 (b) F. Turecek and C.J. Cramer, J. Am. Chem.Soc., 117 (1995) 12243 (c) S. Hammerum, Int. J. Mass Spectrom. Ion Processes 165/166 (1997) 63. (d) P.E. Andersen and S. Hammerum, Eur. Mass Spectrom. 1 (1995) 499. (d) W. Bertrand and G. Bouchoux, Rapid Comm. Mass. Spectrom. 12 (1998) 1697 (e) M. George, C.A. Kingsmill, D. Suh, J.K. Terlouw and J.L. Holmes, J. Am. Chem. Soc, 116 (1994) 7807.
49. (a) P.M. Mayer, M.N. Glukhovstev, J.W. Gauld and L.Radom, J. Am. Chem. Soc, 119 (1997) 12889 (b) B.J. Smith and L. Radom, Chem. Phys, Lett., 231 (1994) 345 (c) B.J. Smith and L. Radom, J. Am. Chem. Soc, 113 (1993) 4885.
50. (a) J.W. Gauld, M.N. Glukhovtsev and L. Radom, Chem. Phys. Lett., 262 (1996) 187 (b) J.W. Gauld and L. Radom, Chem. Phys. Lett., 275 (1997) 28 (c) N.L. Ma, B.J. smith, J.A. Pople and L.Radom, J. am. Chem. Soc., 113 (1991) 7903 (d) M.L. McKee and L. Radom, Org. Mass Spectrom., 28 (1993) 1238
51. (a) A.J. Chalk and L. Radom, J. Am. Chem. Soc., 121 (1999) 1574 (b) A.J. Chalk and L. Radom, J. Am. Chem. Soc., 119 (1997) 7573 (c) J.W. Gauld and L. Radom, J. Am. Chem. Soc., 119 (1997) 9831.
52. M.A. Trikoupis, P.C. Burgers and J.K. Terlouw, J. Am. Chem. Soc. 120 (1997) 12131.
53. T. Fridgen and J. Parnis, Int. J. Mass Spectrom. Ion Processes, in press.
54. (a) A.Nicolaides, A. Rauk, M.N. Glukhovstev and L. Radom, J. Phys. Chem. 100 (1996) 17460. (b) J.W. Ochterski, G.A. Petersson, and K.B. Wiberg, J. Am. Chem. Soc. 1995, 117, 11299. (c) K. Raghavachari, B.B. Stefanov, and L.A. Curtiss, J. Chem. Phys. 1997, 106, 6764. (e) Nicolaides, A. Radom, L. Mol. Phys. 1996, 88, 759. (f) L.A. Curtiss, K. Raghavachari, P.C. Redfern and B.B. Stefanov, J. Chem. Phys. 1998, 108, 692. (g) K. Raghavachari, B.B. Stefanov and L.A. Curtiss, Mol. Phys. 1997, 91, 555. (h) P.M. Mayer, M.N. Glukhovstev, J.W. Gauld and L. Radom, J. Am. Chem. Soc. 1997, 119, 12889. (i) K.B. Wiberg and J.W. Ochterski, J. Comp. Chem. 1997, 18, 108.
55. D. K. Malick, G.A. Petersson and J.A. Montgomery, Jr., J. Chem. Phys., 108 (1998) 5704.

CHAPTER 2

THE DISSOCIATION OF LOW ENERGY 1,2-PROPANEDIOL IONS : AN INTRIGUING MECHANISM REVISITED[1]

Abstract

The fascinating unimolecular chemistry of ionized 1,2-propanediol, $CH_3C(H)OHCH_2OH^{+\bullet}$, **1**, has been re-examined using computational chemistry (*ab initio* MO and density functional theories) in conjunction with modern tandem mass spectrometric and ^{13}C labelling experiments. The calculations allow a considerable simplification of a previously proposed complex mechanism (Org. Mass Spectrom. 23 (1988) 355). Again, the central intermediates are proposed to be stable hydrogen bridged ion-dipole complexes, but our present calculations indicate that the key transformation now is the rearrangement $CH_3C(H)OH^{+}\bullet\bullet\bullet O(H)\text{-}CH_2^{\bullet} \rightarrow CH_3C(H)OH^{+}\bullet\bullet\bullet{}^{\bullet}OCH_3$, which can best be viewed as the cation-catalyzed 1,2-hydrogen shift $^{\bullet}CH_2OH \rightarrow CH_3O^{\bullet}$, a rearrangement which does not occur so easily in the unassisted system. Another important process is the **electron** transfer $CH_3C(H)=O\bullet\bullet\bullet CH_3OH^{+\bullet} \rightarrow O=CH(CH_3)\ {}^{+\bullet}\bullet\bullet O(H)CH_3$ which allows **proton** transfer to generate $CH_3OH_2^{+} + CH_3C=O^{\bullet}$. Other dissociation processes (loss of $CH_3^{\bullet}$, H_2O, $H_2O + CH_3^{\bullet}$, $H_2O + CH_4$) are interpreted in terms of Bohme's "methyl cation shuttle" (J. Am. Chem. Soc.,118 (1996) 4500) taking place in ion-dipole complexes. The most stable intermediate is the hydrogen bridged ion-dipole complex $CH_2=CHOH^{+\bullet}\bullet\bullet\bullet O(H)CH_3$, which is the reacting configuration for loss of methanol.

Introduction

Ten years ago, in an important review, Professor Lifshitz wrote : " From the theoretical point of view, *ab initio* calculations have demonstrated predictive capabilities for ion structure determinations ..." [1]. As an example, and we quote further from the review : "The discovery of the methyleneoxonium radical cation, $[CH_2OH_2]^{+\bullet}$, was a

[1] This chapter has already appeared in print under the same title: P.C. Burgers, L.M. Fell, A. Milliet, M. Rempp, P.J.A. Ruttink and J.K. Terlouw, *Int. J. Mass Spectrom. Ion Processes*, **167/168** (1997) 291-308.

triumph of theory". Indeed, not only have such calculations uncovered surprisingly stable structures, for example distonic ions [2], but they have also led to a deeper understanding of the processes that lead to, what fifty years ago was referred to as "fragments that one would not expect in mass spectra" [3], i.e. rearrangement peaks. Especially long-lived ions (those that dissociate during flight through the mass spectrometer) show a pronounced tendency to transform prior to dissociation as reflected by their metastable ion (MI) mass spectra which can be very different from the normal EI mass spectra. Often, but not always, organic radical cations seem to undergo rearrangement reactions so as to produce the most economical set of products and the literature abounds with references dealing with rearrangement processes [4].

In the context of ionic rearrangements, ion-neutral complexes are often being proposed to account for otherwise unintelligible rearrangements [5]. This followed an earlier cunning suggestion by Rylander and Meyerson [6], forty years ago, that such complexes can rationalize puzzling "scrambling" reactions observed for ^{13}C labelled α,α-dimethylbenzylium ions. Increasingly, hydrogen-bridged O•H•O bonded ions, are being proposed as stable intermediates to rationalize otherwise problematic dissociations of oxygen containing cations [4,7]. This followed our earlier suggestion [8] that hydrogen-bridged cations might well be stable species, and this has been amply confirmed by *ab initio* calculations. For example, for ionized 1,2-ethanediol's fragmentation to $HC{=}O^{\bullet}$ + $CH_3OH_2^{+}$, the key intermediate was found to be the hydrogen bridged species $CH_2{=}O{\bullet\bullet\bullet}H^{+}{\bullet\bullet\bullet}O(H)CH_2^{\bullet}$ (**c**), which was observed, from *ab initio* calculations to lie 16 kcal/mol below the dissociation energy to $HC{=}O^{\bullet}$ + $CH_3OH_2^{+}$ [9].

More recently, C•H•O bonded ions have been invoked to rationalize some unexpected observations [10]. Although such species are not as stable as their O•H•O bonded counterparts, calculations indicate that they can be easily formed from O•H•O bonded ions by a dipole-catalyzed proton shift [9,10e], a process which is identical to Bohme's concept of "proton-transfer catalysis" [11]. (Our proposals [9] followed an earlier result [12] from *ab initio* calculations, that the barrier for the isomerization $H\text{-}C\text{-}OH^{+\bullet} \rightarrow H_2C{=}O^{+\bullet}$

is substantially lowered by the addition of CO via the catalytic conversion H-C-OH$^{+\bullet}$•••CO → H-C=O•••H^{+}-CO → O=C(H)-H$^{+\bullet}$•••CO).

A case in point is ionized 1,2-ethanediol for which *ab initio* calculations, see Scheme 1 (upper part), indicate the following pathway for loss of HC=O$^{\bullet}$.

Scheme 1

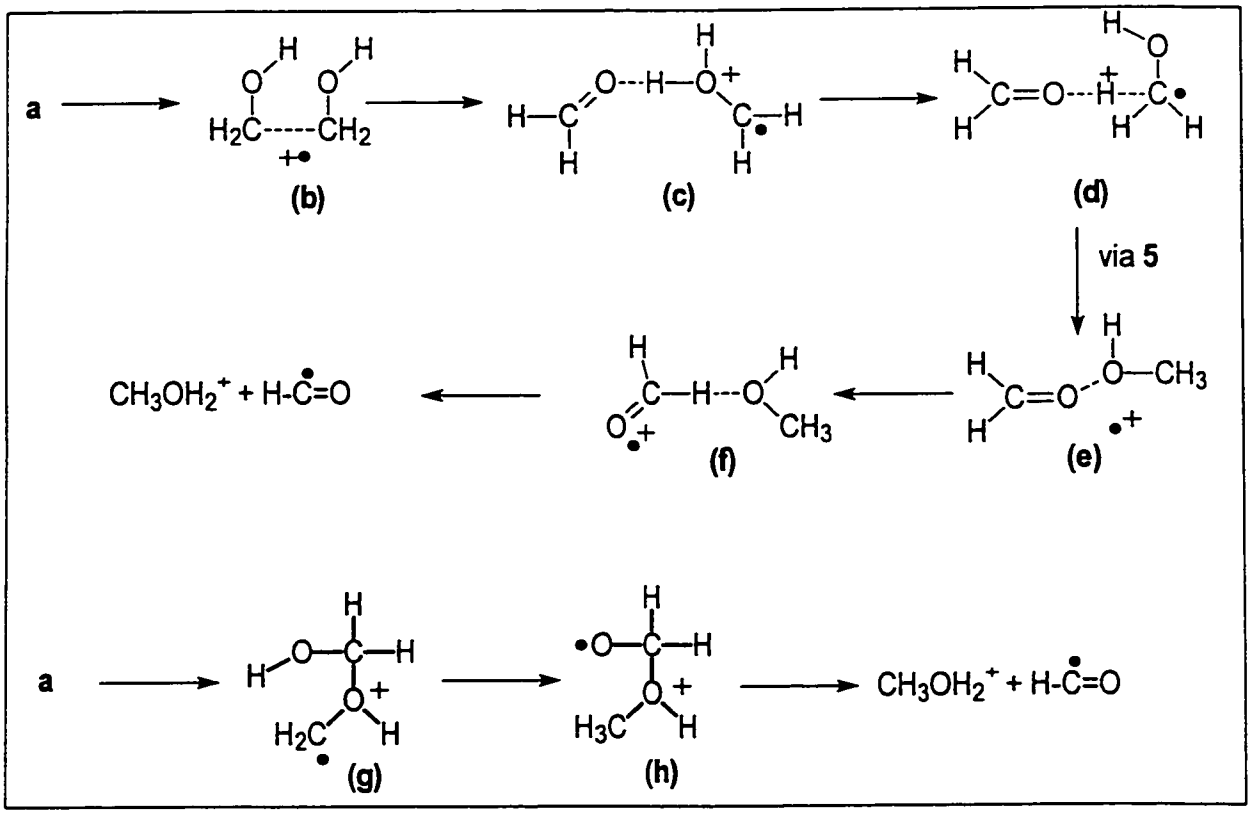

Ions **a** formed by vertical ionization spontaneously collapse to **b** which is a species containing a strong (26 kcal/mol) one-electron bond, i.e. it is **not** an ion-dipole complex. Upon further elongation of the C-C bond in **b**, proton donation leads to the hydrogen-bridged species **c**. This species undergoes a 1,2-hydrogen shift $CH_2OH_2^{+\bullet} \rightarrow CH_3OH^{+\bullet}$ catalyzed by formaldehyde [9] ("proton transfer catalysis" [11]) to produce the transient **d**. This species then rearranges to the ion-dipole complex **e**, a charge transfer complex, where the charge can be on the formaldehyde or the methanol unit. When the charge is on formaldehyde, this moiety can rotate along the dipole vector of methanol and can then

donate a second proton to form **f**. Thus the double hydrogen transfer is best viewed as two **proton** transfers and since they originate from the same moiety, a charge transfer complex, **e**, is implicated. Crucial in this mechanism are the proton transfer catalysis (**c** → **d**) and the charge transfer (**e**) for the following reason. The key intermediate **c** is best viewed as a hydrogen bridged ion-dipole complex of $CH_2OH_2^{\bullet+}$ and CH_2=O; it had been proposed previously [8c] that **c** could undergo a 1,5-hydrogen shift to directly produce the products $HC{=}O^{\bullet}$ + $CH_3OH_2^{\bullet}$. The reason [9] that this reaction does not occur is that in order to correctly orient one of the formaldehyde hydrogens in **c** for transport to $CH_2OH_2^{\bullet+}$, the formaldehyde unit must rotate within the electrostatic field of $CH_2OH_2^{\bullet+}$; this leads to ion-dipole repulsion and consequently to dissociation, rather than to hydrogen transfer.

Hence we proposed the circuitous, but more economical route **c**→**d**→ **e**→**f**. In a recent experimental study [13] it was observed that the isomerization $CH_3OH^{\bullet+}$ → $CH_2OH_2^{\bullet+}$, which does not occur unassisted, can be catalyzed by the addition of water ; this constitutes a prime example of "proton-transport catalysis" and it has recently been confirmed by *ab initio* calculations [14]. These results lend great support for our earlier key mechanistic proposal referred to above, i.e. catalysis of the transformation $CH_2OH_2^{\bullet+}$ → $CH_3OH^{\bullet+}$ by formaldehyde in ionized 1,2-ethanediol.

Audier et al. [15] have provided an alternative mechanism for the $HC{=}O^{\bullet}$ loss from **a** which, too, is in agreement with all observables. They propose that the reaction does not proceed via ion-dipole complexes but rather via distonic ions, i.e. via **a** → **g**, as depicted in the bottom part of Scheme 1. This mechanism involves the 1,4-hydrogen **atom** shift **g** → **h**. However, high level *ab initio* calculations [16] show that this transformation has a surprisingly high barrier which lies 26 kcal/mol above the Appearance Energy (AE) and is thus not feasible (i.e. in the above and other [10c,d,e] cases, separate transfer of a proton and an electron in ion-dipole complexes is more economical than prompt transfer of a hydrogen **atom** in distonic ions).

Before the above concepts of dipole-catalyzed proton shift [7] or "proton-transfer catalysis" [11] and charge transfer were known to operate, we attempted, almost ten years ago [17], to rationalize the complex dissociation behaviour of 1,2-ethanediol's next higher homologue, 1,2-propanediol, **1**, in terms of hydrogen bridged radical cations.

Whereas **a** shows only one dissociation, namely loss of $HC{=}O^{\bullet}$, **1** undergoes no less than six fragmentations, among which is the formation of $CH_3C{=}O^{\bullet} + CH_3OH_2^{\bullet}$, the equivalent of 1,2-ethanediol's dissociation. Apparently the additional methyl group opens up five other fragmentation routes.

By combining results from a variety of mass spectrometric techniques (Metastable Ion (MI), Collision Induced Dissociation (CID), Collision Induced Dissociative Ionization(CIDI), Neutralization-Reionization Mass Spectrometry (NRMS) and Appearance Energy (AE) measurements) as well as isotopic labelling, a unified mechanism was proposed [17] in which the key intermediates were hydrogen bridged radical cations. This mechanism will be reviewed below. At that time we made some reasonable assumptions : for example we discarded the possibility of 1,2-hydrogen shifts because such shifts usually have very large barriers [18], and so we proposed more circuitous routes via 1,4-, 1,5- and 1,6-hydrogen shifts. We were then forced to include an "all-or-nothing" isotope effect to account for the many labelling results. It recently occurred to us that a dipole-catalyzed proton shift (proton-transport catalysis [11]) in the proposed hydrogen bridged cations (as in **c** → **d**) would considerably simplify our proposed mechanism in that it would not only allow a 1,2-hydrogen shift, but at the same time it would dispense with the need of an "all-or-nothing" isotope effect. According to the *ab initio* calculations we present here this is indeed the case.

Results and Discussion

First, we will review the salient experimental results [1] for ionized 1,2-propanediol. The electron impact EI mass spectrum of **1** is dominated by m/z 45, CH_3CHOH^{+}, a simple bond breaking reaction. By contrast, the MI spectrum (Fig. 2-1a) contains six intense signals, m/z 33, 42, 43, 44, 58 and 61 but **no** m/z 45. The product ion structures of the metastable processes and the product ion enthalpies are given in Table 2-1.

Figure 2-1. MI spectra of : (a) $CH_3C(H)OHCH_2OH^{\bullet+}$; (b) $CH_3C(H)ODCH_2OD^{\bullet+}$ and (c) $CH_3C(H)OH^{13}CH_2OH^{\bullet+}$.

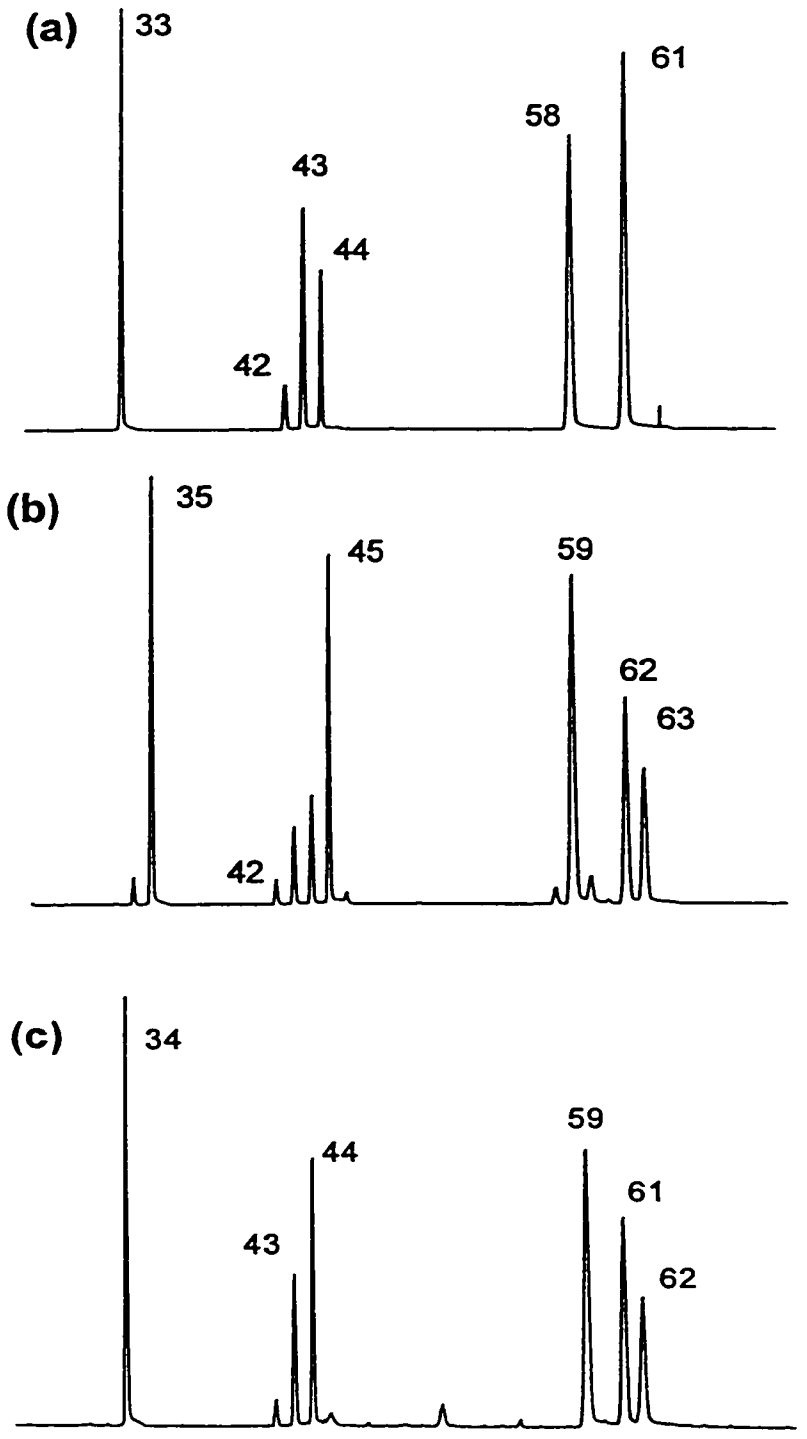

Table 2-1. Product ion structures and enthalpies (kcal/mol) for the dissociations of low energy 1,2-propanediol ions.

Reaction products		m/z	MI ? [a]	$\sum H_f$ [b]	$\sum H_f$ [c]
$CH_3OH_2^+$	+ $CH_3C{=}O^{\bullet}$	33	yes	131.5 [d]	132
$CH_3OH_2^+$	+ $CH_2{=}C(H)O^{\bullet}$	33	no	136	132
$CH_2{=}C{=}O^{+\bullet}$ + H_2O	+ CH_4	42	yes	133	-----
$CH_3{-}C{=}O^+$ + $CH_3^{\bullet}$	+ H_2O	43	yes	133	132
$CH_2{=}C(H)OH^{+\bullet}$	+ CH_3OH	44	yes	133, 135 [e]	133
$CH_3{-}C(H)OH^+$	+ $CH_2OH^{\bullet}$	45	no	135.5 [f]	
$CH_2{=}C(OH)CH_3^{+\bullet}$	+ H_2O	58	no	100	131
$CH_3C(=O)CH_3^{+\bullet}$	+ H_2O	58	yes	114	131
$CH_3C(=O)OH_2^+$	+ $CH_3^{\bullet}$	61	yes	117	133

[a] "Yes" signifies that the reaction is observed in the Metastable Ion (MI) spectrum; [b] Unless otherwise stated, calculated from ref. 19; [c] Calculated from AE measurements in ref.17, values ± 2 kcal/mol ; [d] Using $\Delta H_f\, CH_3C{=}O^{\bullet}$ = - 4.5 kcal/mol , see ref. 20 c ; [e] Using $\Delta H_f\, CH_2{=}C(H)OH^{\bullet +}$ = 183 kcal/mol as recommended in ref. 20 a,b ; [f] Using $\Delta H_f\, CH_2OH^{\bullet}$ = -3.6 kcal/mol as recommended in ref. 20d.

These reactions, except for the exothermic formation of m/z 58 and m/z 61, take place at threshold as evidenced by AE data and the very small kinetic energy releases, 0.5 - 9 meV [17]. Surprisingly, the direct bond cleavage reaction to CH_3CHOH^+ + $^{\bullet}CH_2OH$ is **not** observed, although its calculated energy requirement (135.5 kcal/mol) is very close to that for the other processes, see Table 2-1. The identity of the product ions, except that for m/z 58, was determined by CID mass spectrometry. The identity of the $C_2H_3O^{\bullet}$ neutral was determined by CIDI spectroscopy : $CH_3C{=}O^{\bullet}$ and not $CH_2{=}C(H)O^{\bullet}$ and this finding is in agreement with the data in Table 2-1.

The mechanism proposed previously [17] is presented in Scheme 2.

Scheme 2

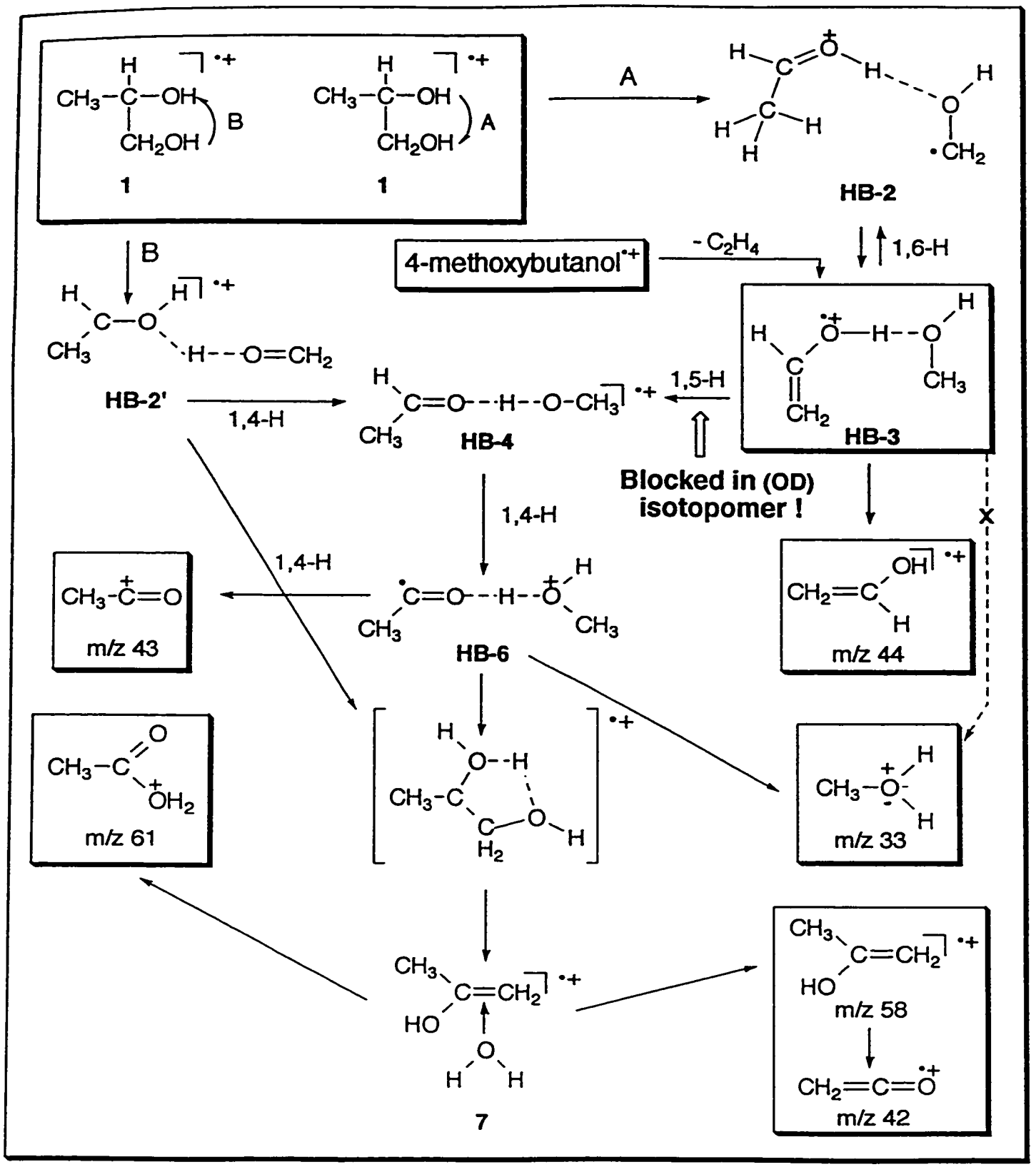
1
1
A
B
HB-2
4-methoxybutanol•+
- C2H4
1,6-H
HB-2'
1,4-H
HB-4
1,5-H
HB-3
Blocked in (OD) isotopomer !
1,4-H
1,4-H
m/z 43
HB-6
m/z 44
m/z 61
m/z 33
7
m/z 58
m/z 42

Starting with path [A], hydrogen bridge formation of the 2-hydroxyl hydrogen atom leads to **HB-2**. This ion can undergo a reversible 1,6-H shift **HB-2→HB-3**, and this explains the observed scrambling of the methyl and methylene hydrogen atoms [17]. **HB-3** is the most stable species encountered on the potential energy surface, see below ; it can be generated independently by loss of C_2H_4 from ionized 4-methoxybutanol and shows the same dissociation characteristics as **1** [17]. **HB-3** can dissociate to m/z 44 (but **not** to m/z 33, because the neutral generated is not CH_2=C(H)O$^{\bullet}$), or it can undergo a 1,5-H shift to generate **HB-4**, which then rearranges further by a 1,4-H shift to **HB-6**. This ion can then dissociate to m/z 33 and m/z 43. A further 1,4-H shift in **HB-6** would produce the transient depicted in Scheme 2 which was thought to collapse to the ion-dipole complex **7**, the precursor for m/z 58, 42 and 61.

This sequence of events could explain all of the experimental results, including all labelling results except for one : pathway [A] predicts that the **1**-$(OD)_2$ labelled ions should form m/z 34, CH_3OHD^+, but the MI spectrum, see Fig. 2-1b, shows that only m/z 35 is formed. Moreover, structure analysis of the metastably generated daughter ions showed these ions to be CH_2DOHD^+. Hence, we proposed that in ion **1**, the hydrogen atom of the 1-hydroxyl group , too, can form the hydrogen bridge to generate **HB-2'** (pathway [B]), which then can form **HB-4** via a 1,4-H shift ; this leads to CH_2DOHD^+ , as observed. However, since m/z 34 is not formed, **HB-3→HB-4** cannot occur in the $(OD)_2$ labelled ion and so we proposed that this hydrogen shift becomes blocked by an "all-or-nothing" isotope effect. Thus we were left in the unusual, but not impossible situation that a 1,5-H shift (**HB-3→HB-4**) becomes blocked by isotopic substitution but that the 1,4-H shift (**HB-2'→HB-4**) remains open. Also inevitable at that time was the conclusion, again from an analysis of labelling data, that the 1,5-H shift **HB-2'→HB-6** does not occur, not even in unlabelled ions, while the 1,4-H shift **HB-2'→HB-4** occurs easily. However, it can be seen from Scheme 2 that if we allow the transition **HB-2→HB-4** (formally a 1,2-H shift) all the peculiarities discussed above disappear, i.e. we can dispense entirely with path [B] and the "all-or-nothing" isotope effect.

In this paper we show that **HB-2** may undergo an acetaldehyde catalyzed proton shift to generate **HB-4** and that this hydrogen shift can occur at the thermochemical threshold.

This transformation, together with a charge transfer process, satisfactorily explains all experimental results.

A new mechanistic proposal : formation of $CH_3C{=}O^{\bullet} + CH_3OH_2^+$

Scheme 3 presents our new mechanistic proposal for the formation of $CH_3C{=}O^{\bullet}$ + $CH_3OH_2^+$, using the concepts of dipole-catalyzed proton shift cum charge (electron) transfer [9]. For discussion purposes, the mechanism is given for the $(OD)_2$ labelled compound and should be compared with the MI spectrum of $CH_3C(H)ODCH_2OD^{\bullet+}$ shown in Figure 2-1b. Also shown is the mechanism for the formation of ionized vinylalcohol, which remains unchanged, see also Scheme 2. This mechanistic proposal is substantiated by our *ab initio* calculations which are discussed below.

Scheme 3

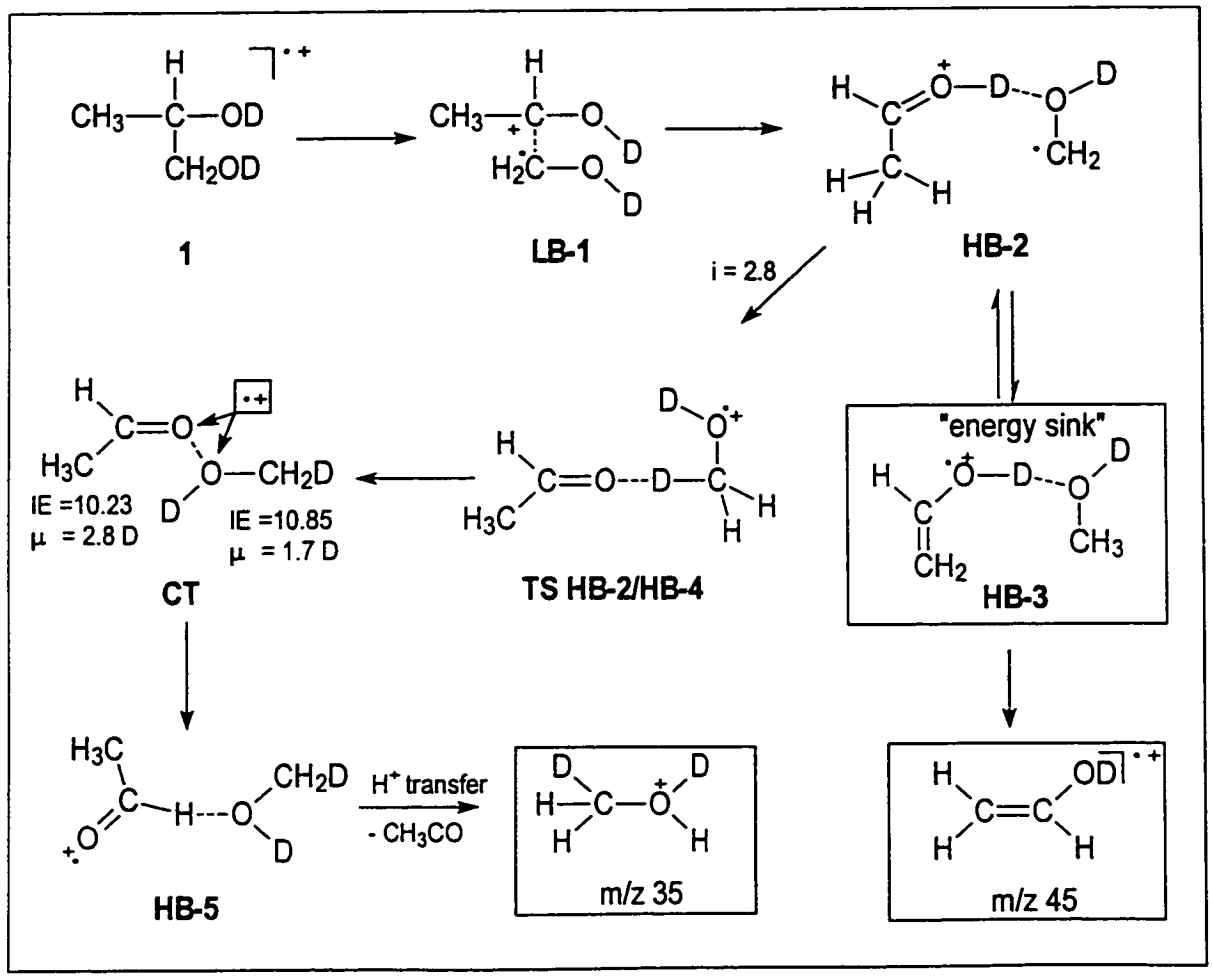

Analogous to 1,2-ethanediol, it is proposed that upon vertical ionization **1** collapses to the one-electron long bonded species **LB-1** which subsequently forms **HB-2** by hydrogen bonding. Since the proton affinity (PA) of $CH_3C(H)=O$ is larger than that of $^{\bullet}CH_2OH$, (by 21.5 kcal/mol [19]), the proton will be closer to $CH_3C(H)=O$; this is confirmed by our calculations, see below. As in 1,2-ethanediol, the $CH_3CHOH^{\bullet}$ group then moves to the carbon atom of the $^{\bullet}CH_2OH$ unit after which proton transfer takes place to generate the transient species represented by **TS HB-2→HB-4**. Since (and in contrast to 1,2-ethanediol) the proton in **HB-2** is closer to acetaldehyde, this transformation is not a "proton transfer catalysis" in the strict sense of the meaning, but rather a proton shuttle [11] . In **TS HB-2→HB-4** the charge is on the methanol part and so this moiety can rotate along the acetaldehyde dipole vector to produce the charge transfer complex **CT**. According to our calculations, see below, in **CT** the acetaldehyde and methanol unit are oriented towards each other in such a way that electron transfer is possible via interaction of the oxygen lone pairs. After charge transfer from the methanol part to the acetaldehyde unit, the now charged acetaldehyde moiety can rotate along the methanol dipole vector to produce **HB-5**. A proton transfer then leads to **HB-6**, see Scheme 5, from which dissociation into $CH_3C=O^{\bullet} + CH_3OH_2^{+}$ may occur. The purpose of electron transfer therefore is twofold : (i) it allows rotation of the acetaldehyde moiety along the methanol dipole vector so that the carbonyl hydrogen is correctly oriented for transfer and (ii) this transfer is then a proton rather than a hydrogen atom shift.

According to our calculations, see below, the transformation depicted in Scheme 3 can take place at the thermochemical threshold. We can therefore dispense with path [B] in Scheme 2 and the "all-or-nothing" isotope effect putatively associated with **HB-3→ HB-4**.

The NR mass spectrum of **1** is given in Fig. 2-2a. This spectrum appears to be dominated by CIDI peaks resulting from the (dissociative) reionization of neutrals generated by collision induced dissociation of **1** by the neutralization gas, compare Fig. 2-2b which shows the CIDI spectrum of the neutrals generated by CID of **1** using He. Thus the peaks at m/z 12-15, m/z 28-32 and m/z 41-43 in Fig. 2-2a are the result of (dissociative) reionization of neutral CH_3OH and $CH_3C=O^{\bullet}$. The peak at m/z 44 in Fig. 2-2a

is a genuine NR peak and its structure could be established (by a CID experiment in the 3ffr, result not shown) as ionized vinyl alcohol, not acetaldhyde. Similarly, the CID mass spectrum of ionized **1** [17] is dominated by m/z 44 and the structure of these ions, too, was shown (by a CID experiment in the 3ffr) to be ionized vinyl alcohol .

These experimental observations leave little doubt that the majority of the non dissociating ions derived from **1** (and also from 4-methoxybutanol, see Scheme 2, which yields closely similar NR and CID spectra [17]) are long-lived vinyl alcohol$^{\bullet+}$/CH_3OH complexes such as **HB-3**.

Such species are expected to dissociate upon neutralization and this may well be the reason that the NR spectrum (Fig. 2-2a) contains no survivor signal at m/z 76. Analogous to the computationally studied vinylalcohol$^{\bullet+}$/ water system [8d], the very stable hydrogen bridged species **HB-3** may be expected to interconvert with several other isomers, including the distonic ion $^{\bullet}CH_2$-C(H)(OH)-$^{+}$O(H)CH_3, **D-3**, and the ion-dipole complex $CH_3(H)O\cdots CH_2$=C(H)OH$^{\bullet+}$, **ID-3**, at energies considerably below the dissociation threshold CH_2=CHOH$^{\bullet+}$ + CH_3OH. Thus, the experiments testify that ions **1** can easily rearrange to the vinyl alcohol$^{\bullet+}$/CH_3OH system at energies below the threshold for the six dissociation reactions observed in the MI spectrum but the detailed pathway(s) for this transition remains to be established.

Figure 2-2. (a) Neutralization-Reionization (NR) spectrum and (b) Collision-Induced Dissociative Ionization (CIDI) spectrum of ionized 1,2-propanediol.

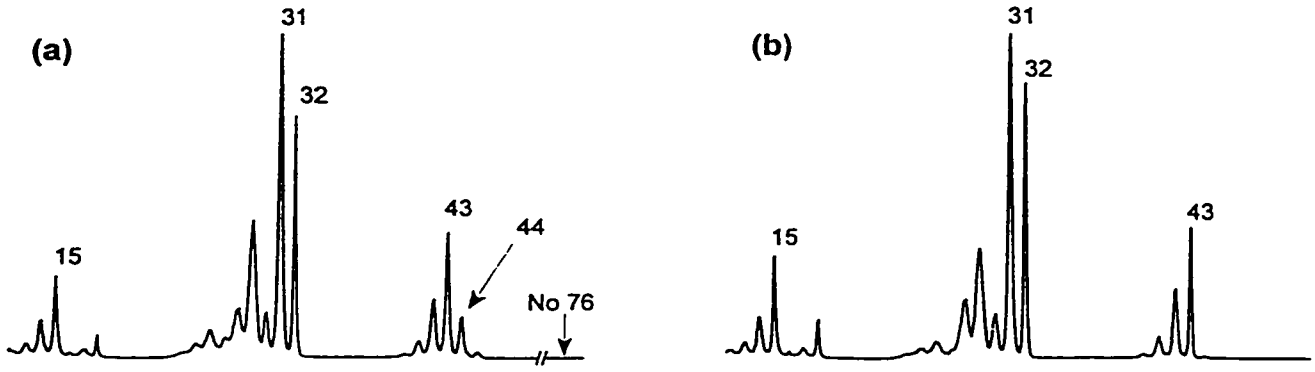

Theoretical calculations for proton (HB-2 → HB-4) and charge transfer (CT)

For ionized 1,2-ethanediol the crucial steps in its decay were the dipole-catalyzed proton transfer cum charge transfer processes and so for ions **1** our computational efforts were first focussed on these processes.

First, the transition state **HB-2→HB-4** and the charge transfer complex were located at the RHF/DZP level of theory using the UK GAMESS series of programs [21a] as described in ref. 9 for the ethylene glycol system. Next, electronic correlation effects were introduced by performing single + double excitation CI (MRSDCI) calculations, including the Pople size-consistency correction method [22]. The results will be presented in more detail elsewhere [16], but the essence is that both **TS HB-2→HB-4** and **CT** (whose geometry is shown in Figure 2-3) lie very close to the anchor point (-1.7 kcal/mol for **CT**), the dissociation limit $CH_3OH_2^+ + CH_3C{=}O^\bullet$, as required by experiment.

The above SDCI method proved to be too time consuming to more fully examine the PES for a system of this size. We therefore changed to the recently developed density functional/Hartree-Fock hybrid approach, Becke3LYP/6-31G* [23], available in the GAUSSIAN series of programs [21b]. This more economical procedure was recently successfully used in a related study of hydrogen bridged radical cations [24]. Satisfactory results were obtained for the various local minima on the PES (see Figure 2-3 and Table 2-2) but we were unable to locate the desired **TS HB-2 → HB-4** with this method. Therefore we resorted to additional UHF and RHF *ab initio* calculations available in the GAUSSIAN series of programs, using the D95** (Dunning and Hay double zeta plus polarization functions, equivalent to the DZP basis set used in ref. 9) basis set [25]. The UHF approach proved unsuccessful in locating **TS HB-2 → HB-4** : the charge in the initial geometries appeared to localize on the component of lowest IE, i.e. the $CH_3C(H){=}O$ moiety and that structure connects **HB-4** with **CT**.

RHF calculations on the other hand were successful : the optimized geometry for **TS HB-2 → HB-4** is shown in Figure 2-3 and its relative energy - obtained from single point QCISD(T)/6-31G** calculations including the usual zero point vibrational energy corrections, see Table 2-3 - lies 6.6 kcal/mol below the dissociation limit $CH_2{=}CHOH^{+\bullet} + CH_3OH$, or ~ 5 kcal/mol below that for $CH_3OH_2^+ + CH_3C{=}O^\bullet$, in satisfactory agreement with

both the above CI(MRSDCI) calculations and the energy constraints imposed by the experiments. We also note that for **HB-2** the relative energies from the single point QCISD(T)/6-31G** calculations in Table 2-2 (Becke3LYP/6-31G*) and Table 2-3 are closely similar.

The energy diagram derived from Tables 2-2 and 2-3, and from the MRSDCI calculation on **CT** is presented in Figure 2-4 and this Figure we believe represents a realistic dissociation pathway for metastable ions **1**.

As with 1,2-ethanediol, ions **1** formed by vertical ionization of 1,2-propanediol collapse to the long bonded species **LB-1** which have a C-C bond length of 1.964 Å. What is the fate of such a long-bonded species ? In the case of 1,2-ethanediol [9], the C--C bond strength of the long-bonded species, (**b**) in Scheme 1, is c. 26 kcal/mol, which is similar to the bond strength in $H_2^{\bullet+}$, i.e. it is similar to a one electron bond where the charge and the radical are both located in this bond. In 1,2-ethanediol further lengthening of the C--C bond raises the energy until at a distance of 2.633 Å a TS is reached which lies c. 10 kcal/mol above the long-bonded species (**b**) and which connects (**b**) with the hydrogen bridged ion $CH_2{=}O{\bullet\bullet\bullet}H\text{-}O(H)CH_2^{\bullet+}$ (structure (**c**) in Scheme 1). This transition takes place c. 16 kcal/mol below the energy for the separted products $CH_2OH^+ + CH_2OH^{\bullet}$.

In the case of 1,2-propanediol the C~C bond strength is somewhat lower, 18 kcal/mol, which may reflect the stabilizing influence of the electron donating methyl substituent in the $CH_3C(H)OH^+$ product ion. As a result, see Figure 2-4, the calculated (from thermochemical data, see Table 1) energy level of the (non observed!) dissociation products $CH_3C(H)OH^+ + CH_2OH^{\bullet}$ resulting from further elongation of the long bond in **LB-1** and also **HB-2**, coincides with that for the formation of the six observed metastable dissociations including the formation of $CH_3OH_2^+ + CH_3C{=}O^{\bullet}$. Thus, (i) the isomerization of **LB-1** into **HB-2** should be feasible since there is no reason that its transition state would lie above the completely separated products $CH_3C(H)OH^+ + CH_2OH^{\bullet}$ and (ii) unlike the ethylene glycol case, this TS may be as high as 18 kcal/mol. A definitive energy value for this TS is not yet available but, in agreement with the above expectations, we have found a TS **LB-1** → **HB-2** at the RHF/D95** level of theory with a structure akin

to that found in ethylene glycol [9] and which lies c. 5 kcal/mol below the dissociation limit.

Table 2-2. Electronic energies (hartree), ZPVE (kcal/mol), and relative energies (kcal/mol) of selected 1,2-propanediol$^{\bullet+}$ isomers, using B3LYP/6-31G* optimized geometries [a].

Species	ZPVE	UB3LYP/6-31G*	QCISD(T)/6-31G**	E_{rel} B3LYP	E_{rel} QCI
LB-1	70.4	-269.23542	-268.52435	-21.0	-18.1
HB-2	67.2	-269.23126	-268.52693	-21.6	-22.9
HB-3	68.0	-269.25042	-268.54358	-32.8	-32.5
HB-4	66.5	-269.23148	-268.51821	-22.4	-18.1
HB-6	68.2	-269.24075	-268.53697	-26.5	-28.2
ID-2	68.1	-269.21928	-268.50790	-13.1	-10.1
ID-3	69.9	-269.23209	-268.51972	-19.3	-15.6
D-3	69.9	-269.23209	-268.51973	-19.3	-15.6
D-1	69.5	-269.22026	-268.51088	-12.3	-10.5
CH_2=$CHOH^{\bullet+}$ + CH_3OH	67.8	-269.19786	-268.49144	**0.0**	**0.0**
$CH_3CO^{\bullet}$ + $CH_3OH_2^+$	67.6	-269.19558	-268.49474	1.3	- 2.2

[a] Optimized geometries for the species not given in Figure 2-3 will be discussed in Ref.16 and are available upon request from the authors.

Figure 2-3. Optimized geometries of selected ionized 1,2-propanediol isomers from UB3LYP/6-31G* (for LB-1, HB-2, HB-3 and HB-4) and RHF/D95** (for TS HB-2→HB-4, HB-5 and CT) calculations.

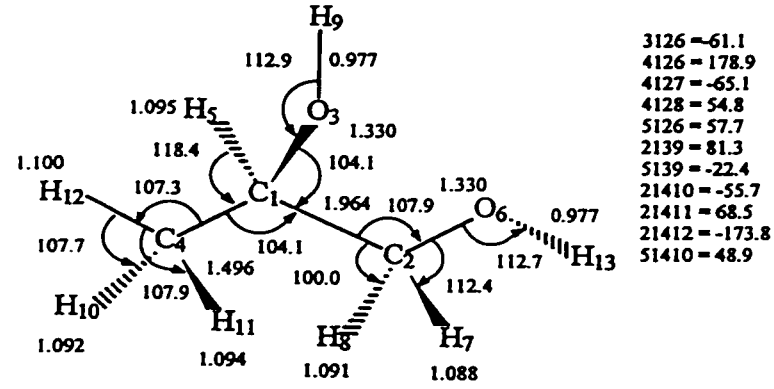

3126 = -61.1
4126 = 178.9
4127 = -65.1
4128 = 54.8
5126 = 57.7
2139 = 81.3
5139 = -22.4
21410 = -55.7
21411 = 68.5
21412 = -173.8
51410 = 48.9

LB-1

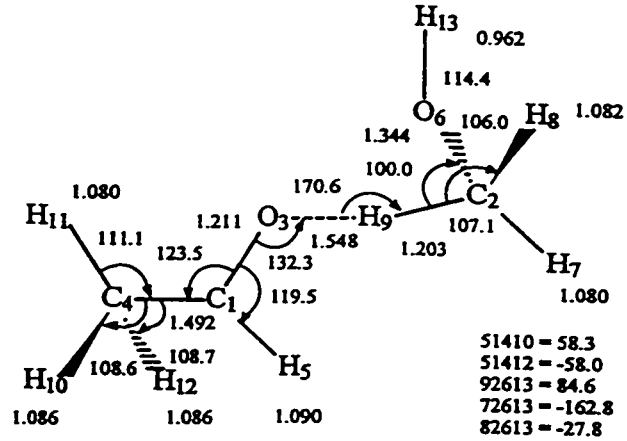

51410 = 58.3
51412 = -58.0
92613 = 84.6
72613 = -162.8
82613 = -27.8

TS HB-2 → HB-4

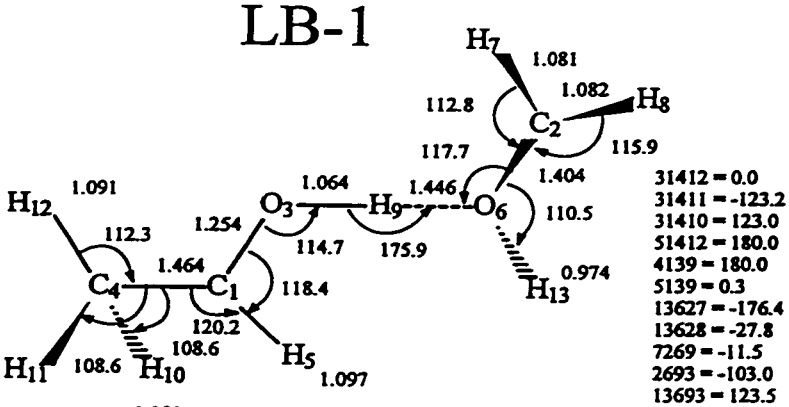

31412 = 0.0
31411 = -123.2
31410 = 123.0
51412 = 180.0
4139 = 180.0
5139 = 0.3
13627 = -176.4
13628 = -27.8
7269 = -11.5
2693 = -103.0
13693 = 123.5

HB-2

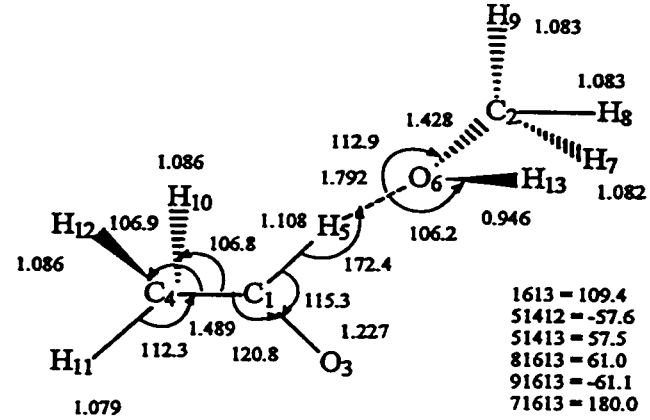

1613 = 109.4
51412 = -57.6
51413 = 57.5
81613 = 61.0
91613 = -61.1
71613 = 180.0

HB-5

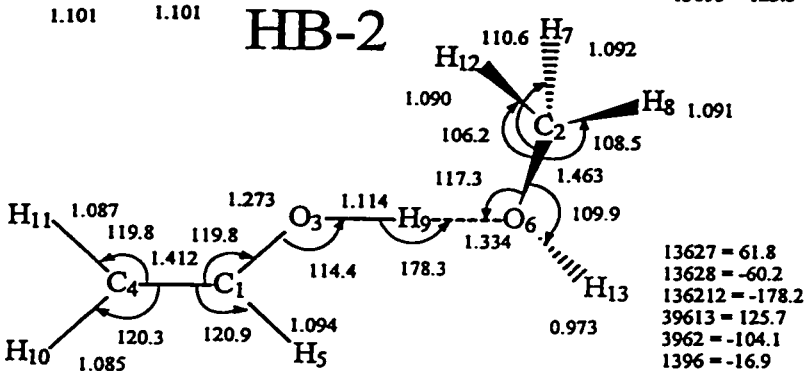

13627 = 61.8
13628 = -60.2
136212 = -178.2
39613 = 125.7
3962 = -104.1
1396 = -16.9

HB-3

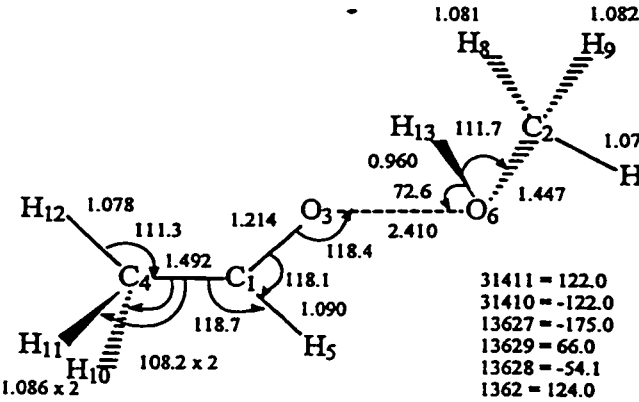

31411 = 122.0
31410 = -122.0
13627 = -175.0
13629 = 66.0
13628 = -54.1
1362 = 124.0
13631 = -127.2
12413 = 0.0
4136 = -179.5
3145 = 180.0
628 = 107.0
629 = 108.4
627 = 106.3
2631 = 124.0

CT

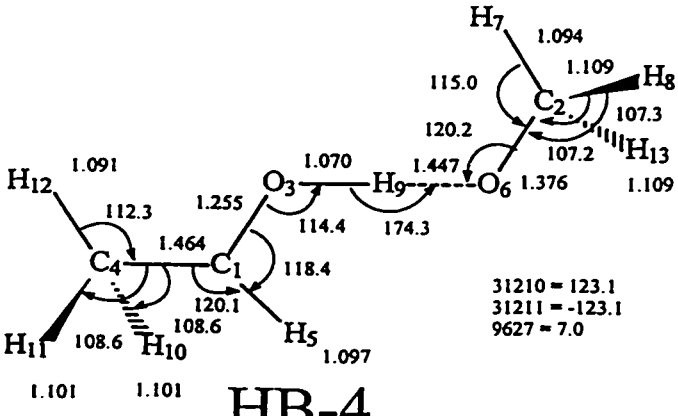

31210 = 123.1
31211 = -123.1
9627 = 7.0

HB-4

Figure 2-4. Energy diagram for the rearrangement and dissociation reactions of low energy 1,2-propanediol ions based upon experiment and theory as presented in Tables 2-1, 2-2 and 2-3.

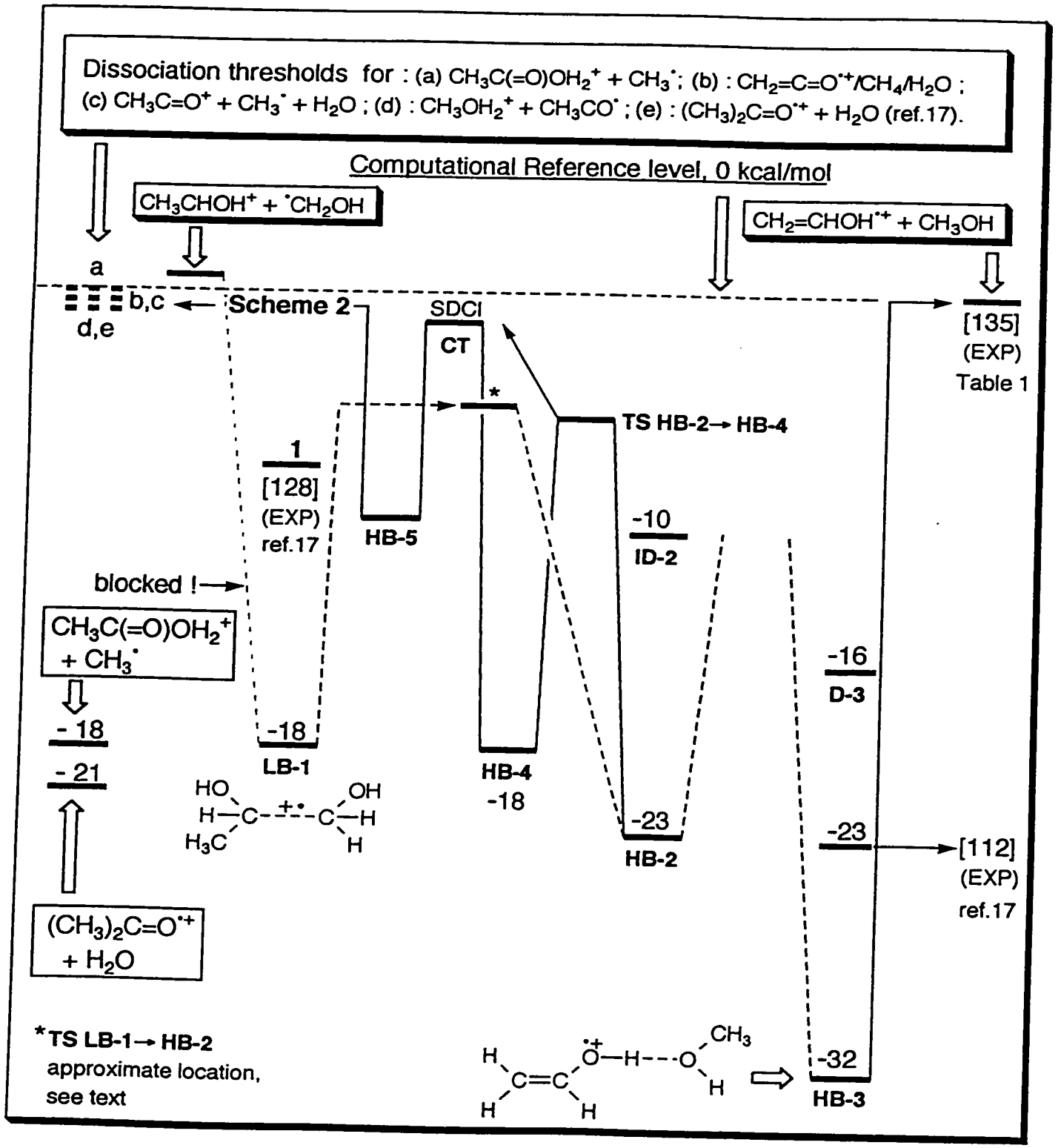

Table 2-3. Electronic energies (hartree), ZPVE (kcal/mol, scaled by 0.9), and relative energies (kcal/mol) of selected 1,2-propanediol$^{\bullet+}$ isomers, using RHF/D95** optimized geometries [a].

Species	ZPVE	RHF/D95**	QCISD(T)/6-31G**	E_{rel} RHF	E_{rel} QCI
LB-1	67.7	-267.72913	-268.52138	- 3.3	-17.9
HB-2	65.2	-267.74829	-268.52414	-17.9	-22.2
HB-4	65.6	-267.74889	-268.51509	-18.0	-16.0
HB-5	65.0	-267.72807	-268.50553	- 5.4	-10.7
TS HB-2 → HB-4	62.2	-267.68949	-268.49458	16.0	- 6.6
CH_2=$CHOH^{\bullet+}$ + CH_3OH	65.4	-267.72007	-268.48912	**0.0**	**0.0**

[a] Optimized geometries for the species not given in Figure 2-3 will be discussed in Ref.16 and are available upon request from the authors.

Once **HB-2**, a hydrogen bridged ion-dipole complex of $CH_3C(H)OH^{\bullet}$ and $^{\bullet}CH_2OH$, has been generated, it may shuttle the bridging proton to the methylene carbon, **TS HB-2→HB-4** . In actuality, see Figure 2-3, this TS connects the ions $CH_3C(H)$-$OH^{\bullet}$•••$O(H)CH_2^{\bullet}$ and $CH_3C(H)$-$OH^{\bullet}$•••$OCH_3^{\bullet}$. This transformation can be viewed as the charge-catalyzed 1,2-hydrogen shift $CH_2OH^{\bullet}$ → $CH_3O^{\bullet}$, the very transformation we had ruled out earlier [17] on the sound argument , at that time, that the unassisted 1,2-H shift $CH_2OH^{\bullet}$ → $CH_3O^{\bullet}$ would be far too energy demanding. Next, the charged methanol moiety rotates around the acetaldehyde molecule until a configuration is reached (**CT**) where the oxygen lone pairs are oriented towards each other so that electron transfer is possible. Now, the neutral methanol can migrate within the electrostatic field of the acetaldehyde radical cation, such that proton transfer is now possible to yield the key species **HB-5** as depicted in Scheme 3.

Alternatively, **HB-2** may isomerize into the very stable vinylalcohol$^{\bullet+}$/methanol complex **HB-3**, via a 1,6-H shift, as indicated in Schemes 2 and 3. We have not yet examined the energy barrier for this interconversion because (i) it is not directly relevant to the new mechanistic proposal presented in this study and (ii) whereas (see previous section) the experiments leave little doubt that a facile (inter)conversion of **1** into the

vinylalcohol$^{+\bullet}$/CH_3OH system takes place, several other pathways are conceivable. An attractive alternative, which will be explored in a separate computational study, would involve breaking of the hydrogen bridge in **HB-2** and **HB-3** followed by reorientation into their stable ion-dipole equivalents **ID-2** and **ID-3.** This could then lead to the alternative route **LB-1** → **HB-2** (Scheme 3) → **ID-2** → **ID-3** (Scheme 4) → **HB-3**.

Theoretical calculations for an alternative pathway to $CH_3C{=}O^{\bullet} + CH_3OH_2^+$

In Scheme 4 is given an alternative pathway for formation of $CH_3C{=}O^{\bullet} + CH_3OH_2^{+}$, based on the mechanism proposed by Audier et al. [15] for the dissociation of $CH_3OCH_2CH_2OH$. This mechanism involves the putative (nota bene, see below) distonic ions **ID-2** and **D-1**. This proposal, too, explains all labelling results including the key observation that 1-$(OD)_2$ specifically forms CH_2DOHD^+. According to this Scheme, ion 1 rearranges to the distonic ion **ID-2** which then undergoes a 1,4-H shift to form another distonic ion, **D-1**, which then can form **HB-5**, the reacting configuration for formation of $CH_3C{=}O^{\bullet} + CH_3OH_2^{+\bullet}$. If this system behaves like ionized 1,2-ethanediol [16] then the highest barrier will be associated with **ID-2→D-1** and so we focussed on this transition. Details will be presented elsewhere [16] and only the salient features are presented here.

As initial guesses of the structures of **ID-2** and **D-1** we took the distonic ones as depicted in Scheme 4. For **ID-2**, optimization at the Becke3LYP/ 6-31G*, UHF/6-31G* and UHF/D95** levels of theory yielded a long C-O linkage (2.4 Å), i.e. ion-dipole complexes $CH_3C(H)OH^{+}\bullet\bullet\bullet O(H)CH_2^{\bullet}$, whereas **D-1** remained distonic. Perhaps not too surprising, considering the very different structures of **ID-2** and **D-1**, we could not locate a transition state connecting the ions at these levels of theory. **ID-2** remained distonic (short bonded) in a UHF/D95V (i.e. basis set without polarization functions [25]) geometry optimization and at this level of theory a transition state for the 1,4-H shift could be located. However, its relative energy is very high : 25.5 kcal/mol above $CH_2{=}CHOH^{+\bullet}$ + CH_3OH in QCISD(T)/6-31G**//UHF/D95V calculations.

Scheme 3

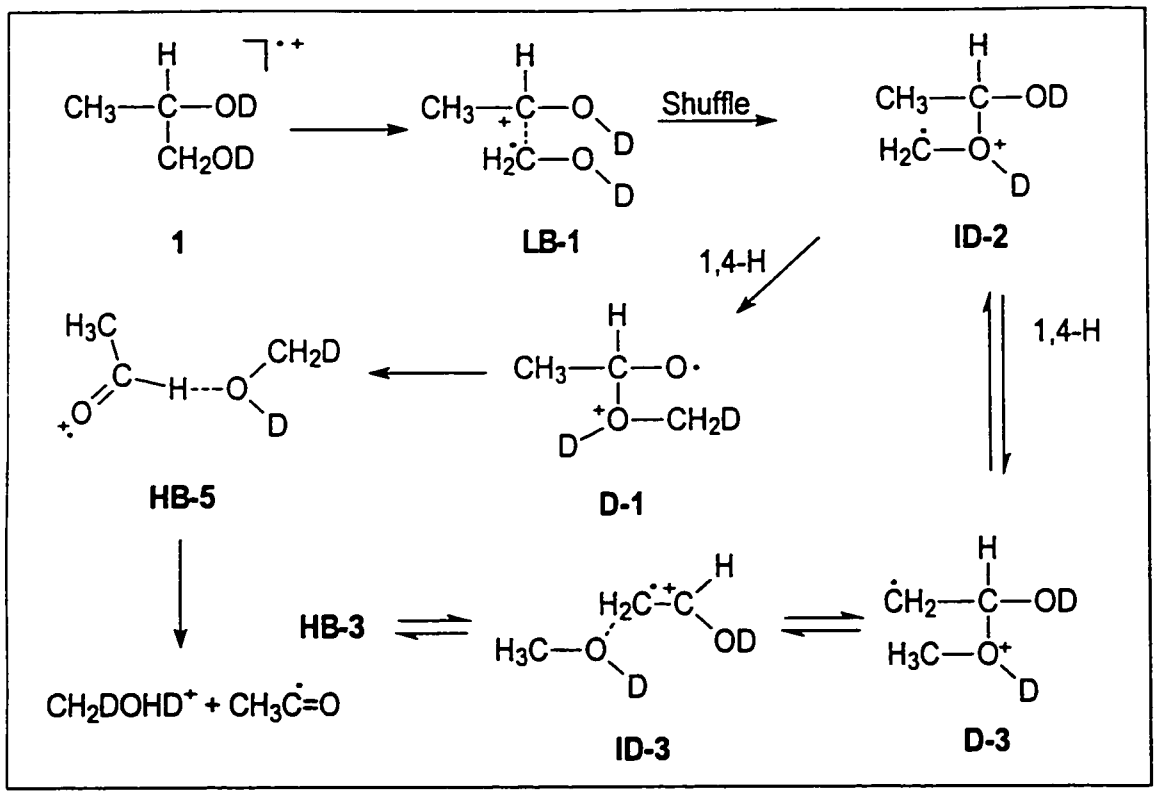

Thus it seems very unlikely that the dissociation of 1 proceeds via the mechanism depicted in Scheme 4, which parallels observations made from theory for ionized 1,2-ethanediol [16].

Formation of m/z 58, $CH_3C(=O)CH_3^{\bullet+}$ and m/z 61, $CH_3C(=O)OH_2^+$.

In our earlier work we could not decide from CID experiments whether metastable ions form keto or enol acetone ions, but we thought we had identified the ion by the following argument. The immediate precursor for m/z 58 was proposed to be an ion-dipole complex of either ionized acetone/H_2O or the ionized enol of acetone/H_2O. We also proposed that loss of $CH_3^{\bullet}$ occurred wholly from this ion-dipole complex. Now, we had observed that the complex $^{13}CH_2{=}C(OH)CH_3^{\bullet+}/H_2O$ or $^{13}CH_3C(=O)CH_3^{\bullet+}/H_2O$ formed from labelled 4-methoxy -butanol-O$^{13}CH_3$, see Scheme 2, lost $^{13}CH_3^{\bullet}$ and $^{12}CH_3^{\bullet}$ in a ratio of c. 3 : 2, whereas equal losses are expected for an acetone$^{\bullet+}/H_2O$ complex. Now, solitary ionized $^{13}CH_2{=}C(OH)CH_3^{\bullet+}$ shows nonstatistical behaviour in that prior to loss of methyl it

rearranges via a rate-determining 1,3-H shift to acetone which is so highly excited that it preferentially loses the newly formed methyl group [26] ; the ratio of $^{13}CH_3^{\bullet}$ and $^{12}CH_3^{\bullet}$ loss, 1.3, observed for $^{13}CH_2$=C(OH)$CH_3^{\bullet+}$ is close to that observed for 4-methoxybutanol-$^{13}OCH_3$, i.e. for the complex $^{13}CH_2$=C(OH)$CH_3^{\bullet+}$/H_2O, see Scheme 2, and so we inferred that loss of water leads to the enol of acetone and not to acetone itself.

We have now observed that the m/z 58 daughter ions formed from metastable ions 1 (and the $C_3H_6O_2$ ions derived from 4-methoxybutanol) spontaneously fragment further and the MI spectrum of the metastably generated m/z 58 ions (MI/MI) is shown in Figure 2-5a. The spectrum is dominated by a narrow peak at m/z 42, corresponding to the loss of CH_4, with a small peak at m/z 43. Now, metastable ionized acetone preferentially loses CH_4 [27], the loss of $CH_3^{\bullet}$ being slightly higher in energy (0.9 kcal/mol) [28]. By contrast, the enol ion preferentially loses $CH_3^{\bullet}$; these results show that the product ions formed from 1 are ionized acetone.

According to the data in Table 2-1, these acetone ions can dissociate further, but only just, by loss of CH_4 and $CH_3^{\bullet}$ and so the metastable acetone ions, generated from the metastable molecular ions are very "cold". This explains why these metastable acetone ions generated from 1 preferentially lose CH_4. The MI spectrum of the m/z 59 ions generated from metastable 1-$(OD)_2$ (Figure 2-5b), too, leaves no doubt that ionized acetone and not its enol is generated.

We tentatively rationalize the formation of $CH_3C(=O)CH_3^{\bullet+}$ and $CH_3C(=O)OH_2^{+}$ in terms of Bohme's concept of "methyl-cation shuttle" [29], closely related to proton-transfer catalysis, see Scheme 5.

Scheme 5

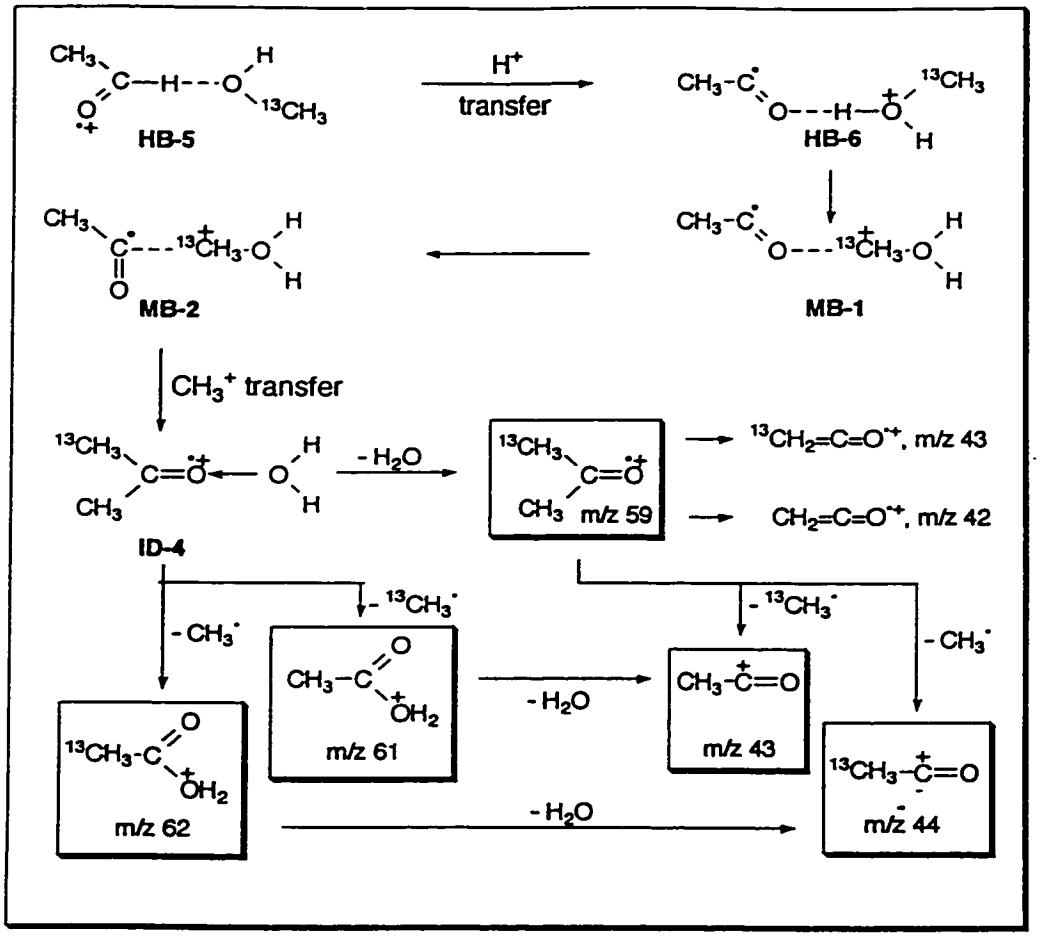

Figure 2-5. MI spectra (third field free region) of metastable ions generated in the second field free region : (a) m/z 58 from $CH_3C(H)OHCH_2OH^{\bullet+}$ and (b) m/z 59 from $CH_3C(H)ODCH_2OD^{\bullet+}$.

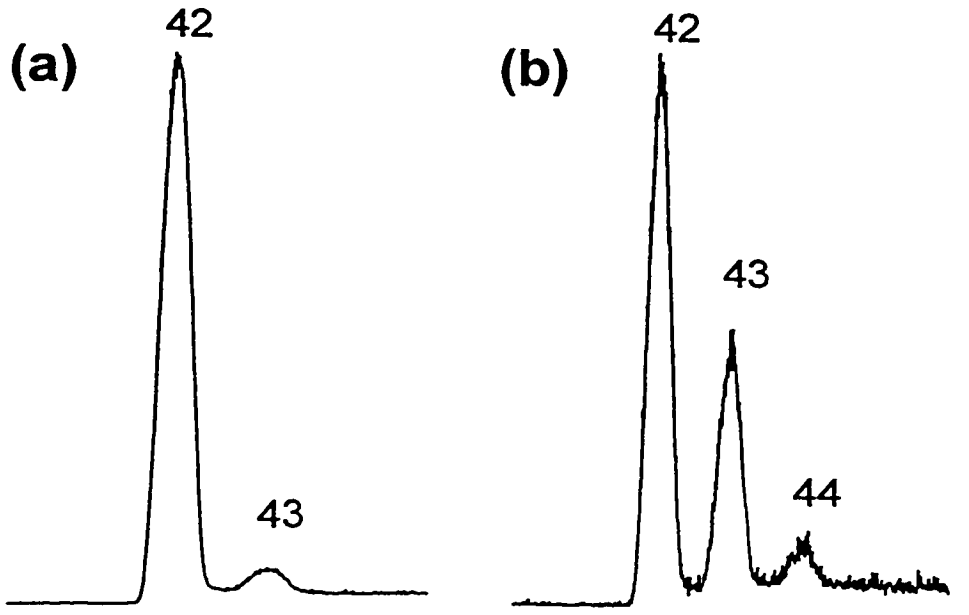

Since $CH_3OH_2^+$ ions are formed at threshold [17], the proton transfer **HB-5→HB-6** (→ $CH_3OH_2^+ + CH_3C{=}O^+$) is not exothermic. This means that **HB-6** may live sufficiently long to undergo other transformations. The $CH_3OH_2^+$ moiety may undergo rotation along the acetyl dipole vector to produce **MB-1**. Next, the $CH_3OH_2^+$ group moves to the carbon atom of the $CH_3C{=}O^+$ unit (**MB-2**) after which methyl transfer takes place to generate the $CH_3C(=O)CH_3^{+\bullet}/H_2O$ ion-dipole complex (**ID-4**) which then dissociates to ionized acetone. The rearrangement **MB-1→ID-4** can formally be viewed as a "methyl-cation shuttle" [29].

It is in principle possible for the methyl cation in **MB-1** to migrate to the oxygen atom of $CH_3C{=}O^+$ instead of to the carbon atom to produce the complex $CH_3\text{-}C\text{-}OCH_3^{+\bullet}/H_2O$ which would dissociate to the ionized carbene $CH_3\text{-}C\text{-}OCH_3^{+\bullet}$; since ionized carbenes have similar heats of formation as their keto counterparts [30], formation of $CH_3\text{-}C\text{-}OCH_3^{+\bullet}$ is energetically possible. Indeed, $CH_3\text{-}C\text{-}OCH_3^{+\bullet}$ has been generated and identified as a stable species [31]. However, the MI and CID mass spectra of the metastably generated m/z 58 ions showed they were ionized acetone with no ionized carbene present. Hence the methyl cation in **MB-1** moves to carbon (→ **MB-2**), not to oxygen. A similar observation was made for ionized acetol [10e], where the proton in the intermediate $CH_2O\text{-}H^+\bullet\bullet\bullet O{=}^\bullet C\text{-}CH_3$, too, moves to the acetyl carbon and not to oxygen.

Ion **ID-4** may also serve as the precursor for $CH_3C(=O)OH_2^+$, m/z 61 by losing $CH_3^\bullet$ (a QCISD(T)/6-31G**//B3LYP/6-31G* calculation shows that this protonated acetic acid isomer is in fact an ion-dipole complex with a stabilization energy of 16 kcal/mol relative to $CH_3C{=}O^+ + H_2O$, leading to ΔH_f $CH_3C(=O)OH_2^+$ = 82 kcal/mol , see Table 2-1 and Figure 2-4). The MI spectrum of $HOCH(CH_3)\text{-}^{13}CH_2OH$ is shown in Fig. 2-1c. Following Scheme 3, this labelled precursor should produce **HB-5** with the ^{13}C at the methanol carbon.

According to Scheme 5, this species in turn should form m/z 61 and 62 in a ratio 1 : 1. However, it can be seen from Fig. 2-1c that there is a clear preference for the loss of $^{13}CH_3^\bullet$ and this nicely parallels observations made for the $(OD)_2$ labelled compound which, see Fig. 2-1b, preferentially loses $CH_2D^\bullet$ over $CH_3^\bullet$. We interpret the above preferences in terms of a reaction similar to the methyl cation shuttle, to wit a water cation shuttle in **HB-6**, see Scheme 6.

Scheme 6

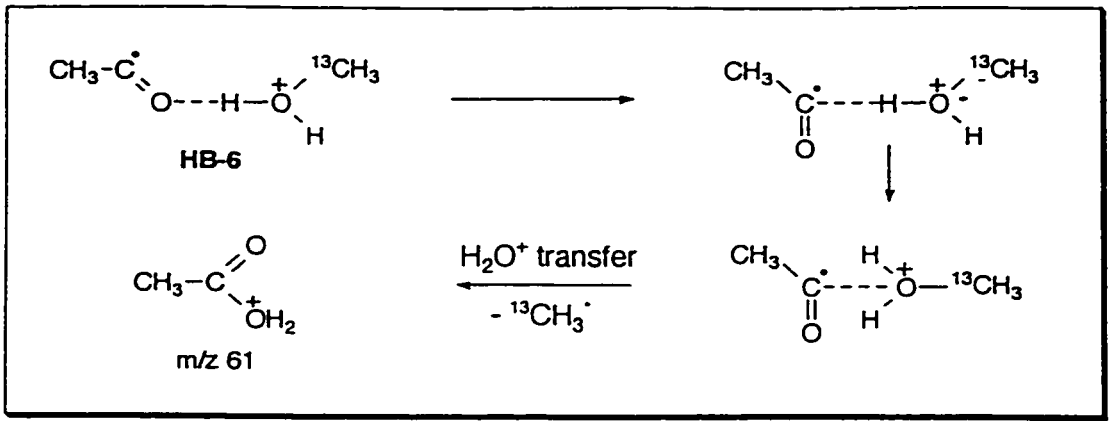

This mechanism, in combination with the equal methyl losses from **ID-4** in Scheme 5 would explain the preferred loss of $^{13}CH_3^{\bullet}$ and $CH_2D^{\bullet}$. It can be calculated from Figures 2-1a and 2-1b that for the $(OD)_2$ labelled compound an isotope effect of magnitude 2.8 operates for all dissociations, except that leading to ionized vinyl alcohol [17]. It is now easy to see where this isotope effect operates, namely for the acetaldehyde catalyzed proton shift **HB-2→HB-4**, see Scheme 3. An isotope effect of similar magnitude (3.0) was observed for the formaldehyde catalyzed proton shift in ionized 1,2-ethanediol [9]. For $HOCD(CH_3)CH_2OH$ we had observed an isotope effect of 1.7 for all fragmentations except for that leading to vinyl alcohol [17]. This effect was associated with the 1,4-H shift **HB-4→HB-6** in Scheme 2. We now attribute this effect to the proton transfer in **HB-5** (see Scheme 3) ; isotope effects of similar magnitude ($\sim \sqrt{2}$) have been observed for a variety of deuteron versus proton transfers [32].

Consecutive processes leading to m/z 43, $CH_3C{=}O^+$

The formation of the acetylium ion involves the consecutive losses of $CH_3^{\bullet}$ and H_2O, see Table 2-1, but in which order ? Acetylium may be formed from m/z 58, ionized acetone, by loss of $CH_3^{\bullet}$ or it may be formed by loss of H_2O from m/z 61, $CH_3C(=O)OH_2^+$, see Scheme 5. The answer is provided by an analysis of the MI spectrum of $HOCH(CH_3)$-$^{13}CH_2OH$, see Fig. 2-1c. From the intensities of m/z 43 and m/z 44 in Figures 2-1a and 2-1c it can immediately be seen that m/z 43 in Fig. 2-1a has been split in m/z 43, $^{12}CH_3C{=}O^+$, and m/z 44, $^{13}CH_3C{=}O^+$. After correction from the contributions of $^{13}CH_2{=}C{=}O^{+\bullet}$

to m/z 43 and from CH_2=C(H)OH$^{\bullet+}$ to m/z 44 the ratio $^{12}CH_3C{=}O^+/^{13}CH_3C{=}O^+$ = 0.82. If acetylium were to arise solely from m/z 59, $^{13}CH_3C(=O)CH_3^{\bullet+}$, the ratio would be 1.00, whereas if the acetylium ions arise only from m/z 61 and m/z 62 a ratio of 0.63 would ensue, i.e. the intensity ratio of m/z 61/ m/z 62 in Fig. 2-1c.

The observed ratio is intermediate and this indicates that half of m/z 43 in the unlabelled spectrum arises by loss of CH_3· from ionized acetone and the other half by loss of H_2O from m/z 61. Not in disagreement with this finding is the observation that the MI spectrum (not shown) of the metastably generated m/z 61 ions contains an intense signal at m/z 43. However, we had already observed that the MI spectrum of the metastably generated acetone ions (Fig. 2-5a) is dominated by m/z 42, whereas m/z 43 is very weak, in sharp contrast to the MI spectrum (Fig. 2-1a) of the molecular ions, where m/z 43 is much more intense than m/z 42. Now it is known, see above, that m/z 43 from ionized acetone rapidly increases with internal energy and so the above result is entirely compatible with the respective time-frames and thus rate constants of fragmentation : for the normal MI mass spectrum the intermediate acetone ions must fragment in the same field free region , whereas for the MI/MI spectrum the intermediate acetone ions are selectively transmitted to the 3rd ffr and are then allowed to fragment, i.e. these acetone ions fragment with a lower rate constant.

Using the above knowledge, namely that m/z 43 is formed from m/z 58 and m/z 61 in a ratio of 1 : 1, and by incorporating the isotope effects for the reactions **HB-2→HB-4** (k_h/k_d = 2.8) and for **HB-5→HB-6** (k_h/k_d = 1.7), we can now calculate the expected intensities for the peaks in the MI spectrum of the labelled ions **1**-$(OD)_2$ using the data from Fig. 2-1a of the unlabelled ions and compare them with the observed intensities in Fig. 2-1b. The results are given in Table 2-4. Agreement is very good for all peaks, except for m/z 43 which in reality seems to be suppressed by a factor of 2. In their infrared multiphoton study of acetone, Osterheld and Brauman [28] conclude that for low energy acetone ions, a large secondary isotope effect is associated with the loss of methyl. For the intermediate $CH_3C(=O)CH_2D^{\bullet+}$, m/z 59, formed from **1**-$(OD)_2$ this means that the loss of CH_2D· may be entirely suppressed in favour of loss of CH_3·. If this is the case and knowing that m/z 43 in the unlabelled material arises from intermediate m/z 58 and

m/z 61 ions in a ratio of 1 : 1, we can recalculate the m/z 43 (and m/z 44) intensity in the MI spectrum, see third entry in Table 4. The agreement now is excellent. Similar observations were made for the 1-(OH)(OD) labelled compound, where the deuterium can be on either oxygen, leading to a mixture of isotopomeric ions.

Table 2-4. Observed and calculated MI mass spectra [a] for the 1,2-propanediol isotopomer $CH_3C(H)ODCH_2OD$.

m/z	35	42	43	44	45	59	62	63
Calc. [b]	110	6	**41**	31	100	90	66	39
Obs.	120	6	**20**	30	100	90	60	35
Calc. [c]	110	6	**17**	32	100	90	66	39

[a] Relative to m/z 45 (CH_2=C(H)OD$^{\bullet+}$) = 100 for which no isotope effect operates; [b] Assuming no secondary isotope effect for the formation of m/z 43 from m/z 59, see text ; [c] Assuming a large secondary isotope effect for the formation of m/z 43 from m/z 59, see text.

There remains one question : why is m/z 45 absent in the MI spectrum ? According to the data in Table 2-1 this fragmentation should be competitive with the observed dissociations. According to Longevialle [33] and Ahmed et al. [34] once a bond is cleaved to generate an ion-dipole complex, recombination of the partners is prevented by a severe entropy barrier and is therefore exceptional. Longevialle [33] has presented evidence that competition between reactions in an ion-dipole complex can be governed by "reorientation" critical energies, rather than decomposition critical energies. Thus as soon as reorientation has occurred, fragmentation to separate partners is highly unlikely.

In summary the complex gas-phase chemistry of ionized 1,2-propanediol can be understood in terms of proton and electron transfers taking place in intermediate ion-dipole complexes, together with "classical" primary and secondary isotope effects.

Experimental

The experiments were performed with the McMaster University VG Analytical (Manchester, UK) ZAB-R instrument of BE_1E_2 geometry (B, magnet; E, electric sector) [35] using an accelerating voltage of 10 keV. Metastable ion (MI) mass spectra were recorded in the second field-free region (2ffr) ; Collision-induced dissociation (CID) mass spectra were recorded in the 2 and 3ffr using oxygen as collision gas (transmittance T = 70%). The CID mass spectra of the 2ffr metastable peaks were obtained in the 3ffr using O_2 as the collision gas. Neutralization-reionization (NR) [36] spectra were recorded in the 2ffr using N,N-dimethylaniline as reducing agent and oxygen gas for reionization. The CIDI spectrum shown in Figure 2b was obtained in the 2ffr by using He for CID of the ions in the second gas cell whereas oxygen was used for collisional ionization of the neutrals produced. In this experiment the He pressure used was such that the He CID spectrum became closely similar to N,N-dimethylaniline CID spectrum, both in terms of the intensity distribution of the fragment ions as well as the total ion current. All spectra were recorded using a small PC-based data system developed by Mommers Technologies Inc. (Ottawa).

All compounds were of research grade (Aldrich) and used without further purification. The D labelled isotopomers of 1,2-propanediol were obtained as described in ref. 17a. The $CH_3CH(OH)^{13}CH_2OH$ isotopomer was prepared by reduction of 1-^{13}C pyruvic acid (99 % isotopically pure, Eurisotop, France) using $AlLiH_4$ in diethyl ether.

References

1. C. Lifshitz, Int. Rev. Phys. Chem, 6 (1987) 35.
2. B.F. Yates, W.F. Bouma and L. Radom, Tetrahedron, 22 (1986) 6225.
3. (a) A.J. Langer, J. Phys. Colloid Chem., 54 (1950) 618. (b) S. Meyerson, Anal. Chem., 66 (1994) 960A.
4. (a) P.C. Burgers and J.K. Terlouw, in M.E. Rose (Ed.) Specialist Periodical Reports : Mass Spectrometry, The Royal Society of Chemistry, London, 1989, Vol. 10, Chapter 2. (b) J.S. Splitter in J.S. Splitter and F. Turecek (Ed.) Applications of Mass Spectrometry to Organic Stereochemistry, VCH, Weinheim, 1994, Chapter 3.
5. (a) D.J. McAdoo and T.H. Morton, Acc. Chem. Res., 26 (1993) 295. (b) P. Longevialle, Mass Spectrom. Rev., 11 (1992) 157. (c) R.D. Bowen, Acc. Chem. Res., 24 (1991) 364. (d) S. Hammerum in K.R. Jennings (Ed.) Fundamentals of Gas Phase Ion Chemistry, pp. 379-390. (e) D.J. McAdoo , Mass Spec. Rev., 7 (1988) 363. (f) T.H. Morton, Tetrahedron, 38 (1982) 3195. (g) R.D. Bowen, Org. Mass Spectrom., 28 (1993) 1577.
6. P. Rylander and S. Meyerson, J. Am. Chem. Soc., 78 (1956) 5799.

7. For selected reviews see : (a) N. Heinrich and H. Schwarz, in J.P. Maier (Ed.) Ion and Cluster Ion Spectroscopy and Structure, Elsevier, Amsterdam, 1989 , p. 329. (b) L. Radom, Org. Mass Spectrom. 26 (1991) 359. (c) E. Uggerud, Mass Spectrom. Rev. 11 (1992) 389. (d) T.H. Morton, Org. Mass Spectrom. 27 (1992) 353.
8. J.K. Terlouw, W. Heerma, P.C. Burgers and J.L. Holmes, Can. J. Chem., 62 (1984) 289. (b) R. Postma, P.J.A. Ruttink, F.B. van Duijneveldt, J.K. Terlouw and J.L. Holmes, Can. J. Chem., 63 (1985) 798 . (c) P.C. Burgers, J.L. Holmes, C.E.C.A. Hop, J. Am. Chem. Soc., 109 (1987) 7315. (d) R. Postma, S.P. an Helden, J.H. van Lenthe, P.J.A. Ruttink, J.K. Terlouw and J.L. Holmes, Org. Mass Spectrom., 23 (1988)503.
9. P.J.A. Ruttink and P.C.Burgers, Org. Mass Spectrom., 28 (1993) 1087.
10. (a) M. George, C.A. Kingsmill, D. Suh, J.K. Terlouw and J.L. Holmes, J. Am. Chem. Soc. 116 (1994)7807. (b) A. Pakarinen, K. M Stirk, P. Vainiotalo, T.A. Pakkanen and H.I. Kenttämaa, J. Am. Chem. Soc. 115 (1993) 12431. (c) D. Suh, C.A. Kingsmill, P.J.A. Ruttink, P.C. Burgers and J.K. Terlouw, Int. J.Mass Spectrom. Ion Processes, 146/147 (1995) 305. (d) D. Suh, P.C. Burgers and J.K. Terlouw, Int. J. Mass Spectrom. Ion Processes, 144 (1995) L1. (e) P.J.A. Ruttink, P.C. Burgers and J.K. Terlouw, Can. J. Chem., 74 (1996) 1078. (f) H. Friedrichs, G.A.McGibbon and H. Schwarz, Int. J. Mass Spectrom. Ion Processes, 1524 (1996) 217.
11. D.K. Bohme, Int. J. Mass Spectrom. Ion Processes, 115 (1992) 95.
12. P.J.A. Ruttink, in R. Naaman and Z. Vager (Ed.) The Structure of Small Radicals and Ions, Plenum Press, New York, 1989, p. 243.
13. (a) P. Mourges, H.-E. Audier, D. Leblanc and S. Hammerum, Org. Mass Spectrom., 28 (1993) 1098. (b) H.-E. Audier, D. Leblanc, P. Mourgues, T.B. McMahon and S. Hammerum, J. Chem. Soc. Chem. Commun. (1994) 2329.
14. J.W. Gauld, H.-E. Audier, J. Fossey and L. Radom, J. Am. Chem. Soc., 118 (1996) 6299.
15. H.-E. Audier, A. Milliet, D. Leblanc and T.H. Morton, J. Am. Chem. Soc., 114 (1992) 2027.
16. P.J.A. Ruttink, P.C. Burgers, L. M. Fell and J.K. Terlouw, see Chapter 2.
17. (a) B.L.M. van Baar, P.C. Burgers, J.L. Holmes and J.K. Terlouw, Org. Mass Spectrom., 23 (1988) 355. (b) J.K. Terlouw, in R. Naaman and Z. Vager (Ed.) The Structure of Small Radicals and Ions, Plenum Press, New York, 1989, p. 269.
18. See for example : W.J. Bouma, R.H. Nobes and L. Radom, J. Am. Chem. Soc., 104 (1982) 2929.
19. S. Lias, J.E. Bartmess, J.F. Liebman, J.L. Holmes, R.D. Levin and W.G. Mallard. J. Phys. Chem. Ref. Data, 17 (1988) Supplement 1.
20. (a) F. Turecek and C.J. Cramer, J. Am. Chem. Soc., 117 (1995) 12243. (b) G. Bouchoux, C. Alcaraz,
O. Dutuit and M.T. Nguyen, Int. J. Mass Spectrom. Ion Processes, 137 (1994) 93. (c) D. Griller, J.M. Kanabus-Kaminska and A. Maccoll, J. Mol. Structure (THEOCHEM), 163 (1988) 125. (d) C.W. Bauschlicher and H. Partridge, J. Phys. Chem., 98 (1994) 1826.
21. (a) M.F. Guest, J. Kendrick. GAMESS Users Manual, SERC Daresbury Laboratory, CCP/86/1, 1986 ; M. Dupuis, D. Spangler and J. Wendolowski. NRCC Software Catalog, Vol. 1, Program No. QG01 (GAMESS), 1980 ; M.F. Guest, R.J. Harrison, J.H. van Lenthe and L.C.H. van Corler, Theor. Chim. Acta ,71 (1987) 117. (b) Gaussian 94, Revision B.3, M. J. Frisch, G.W. Trucks, H.B. Schlegel, P.M.W. Gill, B.G. Johnson, M.A. Robb, J.R. Cheeseman, T.A. Keith, G.A. Peterson, J.A. Montgomery, K. Raghavachari, M.A. Al-Laham, V.G. Zakrevski, J.V. Ortiz, J.B. Foresman, C.Y. Peng, P.Y. Ayala, W. Chen, M.W. Wong, J.L. Andres, E.S. Replogle, R. Gomperts, R.L. Martin, D.J. Fox, J.S. Binkley, D.J. de Frees, J. Baker, J.P. Stewart, M. Head-Gordon, C. Gonzales and J.A. Pople, Gaussian Inc., Pittsburgh PA, 1995.
22. (a) V.R. Saunders and J.H. van Lenthe, Mol. Phys., 48 (1983) 923. (b) J.A. Pople, R. Seeger and R. Krishnan, Int. J. Quantum Chem., 11 (1977) 149.
23. (a) A.D. Becke, J. Chem. Phys., 98 (1993) 5648. (b) C. Lee, W. Yang and R.G. Parr, Phys. Rev. B, 37 (1988) 785. (c) B. Meihlich, A. Savin, H. Stoll and H. Preuss, Chem. Phys. Lett., 157 (1989) 200.
24. J. Hrusak, G.A. McGibbon, H. Schwarz and J.K. Terlouw, Int. J. Mass Spectrom. Ion Processes, 160 (1997) 117.
25. T.H. Dunning Jr and P.J. Hay, in H.F. Schaeffer III (Ed.) Modern Theoretical Chemistry, Vol.3, Methods of Electronic Structure Theory, Plenum Press, New York, 1977, pp.1-28.

26. (a) F.W. McLafferty, D.J. McAdoo, J.S. Smith and R. Kornfield, J. Am. Chem. Soc., 93 (1971) 3720. (b) R.C. Heyer and M.E. Russell, Org. Mass Spectrom., 16 (1981) 236. (c) G. Depke, C. Lifshitz, H. Schwarz and E. Tzidony, Angew. Chem. Int. Ed. Engl., 20 (1981) 792. (d) C. Lifshitz and E. Tzidony, Int. J. Mass Spectrom. Ion Phys., 39 (1981) 181. (e) C. Lifshitz, Int. J. Mass Spectrom. Ion Phys., 43 (1982) 179. (f) T.H. Osterheld and J.I. Brauman, J. Am. Chem. Soc., 115 (1993) 10311.
27. N. Heinrich, F. Louage, C. Lifshitz and H. Schwarz, J. Am. Chem. Soc., 110 (1988) 8183.
28. T.H. Osterheld and J.I. Brauman, J. Am. Chem. Soc., 114 (1992) 7158.
29. V. Baranov, S. Petrie and D.K. Bohme, J. Am. Chem. Soc., 118 (1996) 4500.
30. See for example : W.J. Bouma, P.C. Burgers, J.L. Holmes and L. Radom, J. Am. Chem. Soc., 108 (1986) 1767.
31. T. Wong, M. Sc. Thesis, McMaster University, 1992.
32. (a) E.L. Chronister and T.H. Morton, J. Am. Chem. Soc., 112 (1990) 133. (b) D. Harnish and J.L. Holmes, J. Am. Chem. Soc., 113 (1991) 9729. (c) D. Suh, J.T. Francis, J.K. Terlouw, P.C. Burgers and R.D. Bowen, Eur. Mass Spectrom., 1 (1995) 545.
33. (a) P. Longevialle, Rapid Commun. Mass Spectrom., 9 (1995) 1189. (b) P. Longevialle and O. Lefèvre, Rapid Commun. Mass Spectrom., 10 (1996) 621.
34. M.S. Achmed, C.S. Giam and D.J. McAdoo, Int. J. Mass Spectrom. Ion Processes, 130 (1994) 1.
35. H.F. van Garderen, P.J.A. Ruttink, P.C. Burgers, G.A. McGibbon and J.K. Terlouw, Int. J. Mass Spectrom. Ion Processes, 121 (1992) 159.
36. For a recent review see : N. Goldberg and H. Schwarz, Acc. Chem. Res., 27 (1994) 34.

CHAPTER 3

THE DISSOCIATION OF IONIZED 1,2-ETHANEDIOL AND 1,2-PROPANEDIOL: PROTON TRANSPORT CATALYSIS WITH ELECTRON TRANSFER[1]

Abstract

Ab initio Molecular Orbital (MO) calculations support the proposal that the key processes in the rearrangement of $HOCH_2CH_2OH^{\bullet+}$ and $HOCH_2CH(CH_3)OH^{\bullet+}$ (ionized 1,2-ethanediol and 1,2-propanediol) are sequential transfers of a *proton* and an *electron* taking place from one partner to the other in ion-dipole complexes, rather than prompt hydrogen *atom* shifts taking place in distonic ions. Although the proposed distonic ions in the alternative mechanism (*J. Am. Chem. Soc.* **1992**, *114*, 2027) are thermodynamically remarkably stable species, a surprisingly large barrier exists for their interconversion by way of a 1,4-H *atom* shift. This large barrier results from significant distortion, from planarity, of the transition state. The rearrangement process of ionized 1,2-ethanediol and 1,2-propanediol can therefore best be described in terms of intramolecular catalysis (proton transport catalysis, *Int. J. Mass Spectrom. Ion Processes*, **1992**, *115*, 95) in combination with an electron transfer taking place in intermediate ion-dipole complexes.

[1] This chapter has already appeared in print under the same title: P.J.A Ruttink, P.C. Burgers, L.M. Fell and J.K. Terlouw, *J. Phys. Chem. A*, **102** (1998) 2976-2980.

Introduction

The unimolecular chemistry of low energy 1,2-ethanediol radical cations, **1**, is very interesting for a number of reasons [1]. It is one of those cases where the time-honoured technique of isotopic labelling led to completely unexpected results. The radical cation $HOCH_2CH_2OH^{\bullet+}$, **1**, is but one of many that dissociate via a so-called double hydrogen transfer (DHT) and for **1** this reaction produces $CH_3OH_2^+$, m/z 33, + $HCO^{\bullet}$ [1]. Over the past decade no less than four mechanisms have been proposed for this reaction. Ten years ago, we proposed [2] that the reaction proceeded via a 1,5-hydrogen shift (**4**→**7**) in the hydrogen bridged intermediate **4** :

1 → CH_2=O•••H^+•••O(H)-$CH_2^{\bullet}$, **4** → $HC^{\bullet}$=O•••H^+•••O(H)-CH_3, **7** → $CH_3OH_2^+$ + $HCO^{\bullet}$

This followed an earlier elegant proposal by Morton [3] that hydrogen bonding in the neutral may persist upon ionization and that such bonding may account for otherwise problematic reactions. Indeed *ab initio* calculations indicated that species **4** and **7** enjoy considerable stabilization and that they therefore are attractive intermediates [2]. However, at that time the transition state **4**→**7** and its energy could not be evaluated due to computational limitations. A concurrent study by Radom et al. [4] led to an alternative mechanistic proposal i.e. a 1,2-H shift in the distonic isomer [5] (**2**) : **1** → $^{\bullet}OCH_2CH_2OH_2^+$, **2** → $CH_3OH_2^+$ + $HCO^{\bullet}$. The surprisingly stable ion **2** was calculated to be generated upon ionization of 1,2-ethanediol by a barrier-free 1,4-H shift.

These mechanistic proposals both prescribe that the **1**-$(OD)_2$ labelled ion undergoes a specific loss of $HCO^{\bullet}$ to yield the protonated methanol isotopomer $CH_3OD_2^+$ at m/z 35. The specific formation of m/z 35 had been observed in the initial study [2] but later MS/MS experiments [6,7] revealed that the m/z 35 ions had the connectivity CH_2DOHD^+ rather than $CH_3OD_2^+$ and this proved the above proposals to be incorrect. From the *ab initio* calculations, [2] it followed that **4** can best be viewed as a hydrogen bridged ion-dipole complex of the methyleneoxonium ion and neutral formaldehyde, CH_2=O•••H-O^+(H)$CH_2^{\bullet}$, i.e. with the bridging hydrogen closer to the moiety of higher proton affinity. This would imply that the transition state **4**→**7** may lie prohibitively high, because in order to transport one of the formaldehyde H atoms in **4** to the methylene radical site of $CH_2OH_2^{\bullet+}$, the formaldehyde molecule would have to rotate to such a

degree that the resulting ion-dipole repulsion would lead to separation of the partners, rather than to hydrogen transport. Nevertheless we felt that, because of their considerable stability, [2] hydrogen bridged intermediates would still be viable mediators. Indeed, using *ab initio* calculations we were able to trace a circuitous but energetically attractive route for hydrogen transfer [1] which satisfies the labelling results, see Scheme 1 and Figure 3-1 :

Figure 3-1: Theoretical results for the relative energies of isomers and transition states encountered in the dissociation of 1,2-ethandiol radical cations according to Schemes 1 and 2.

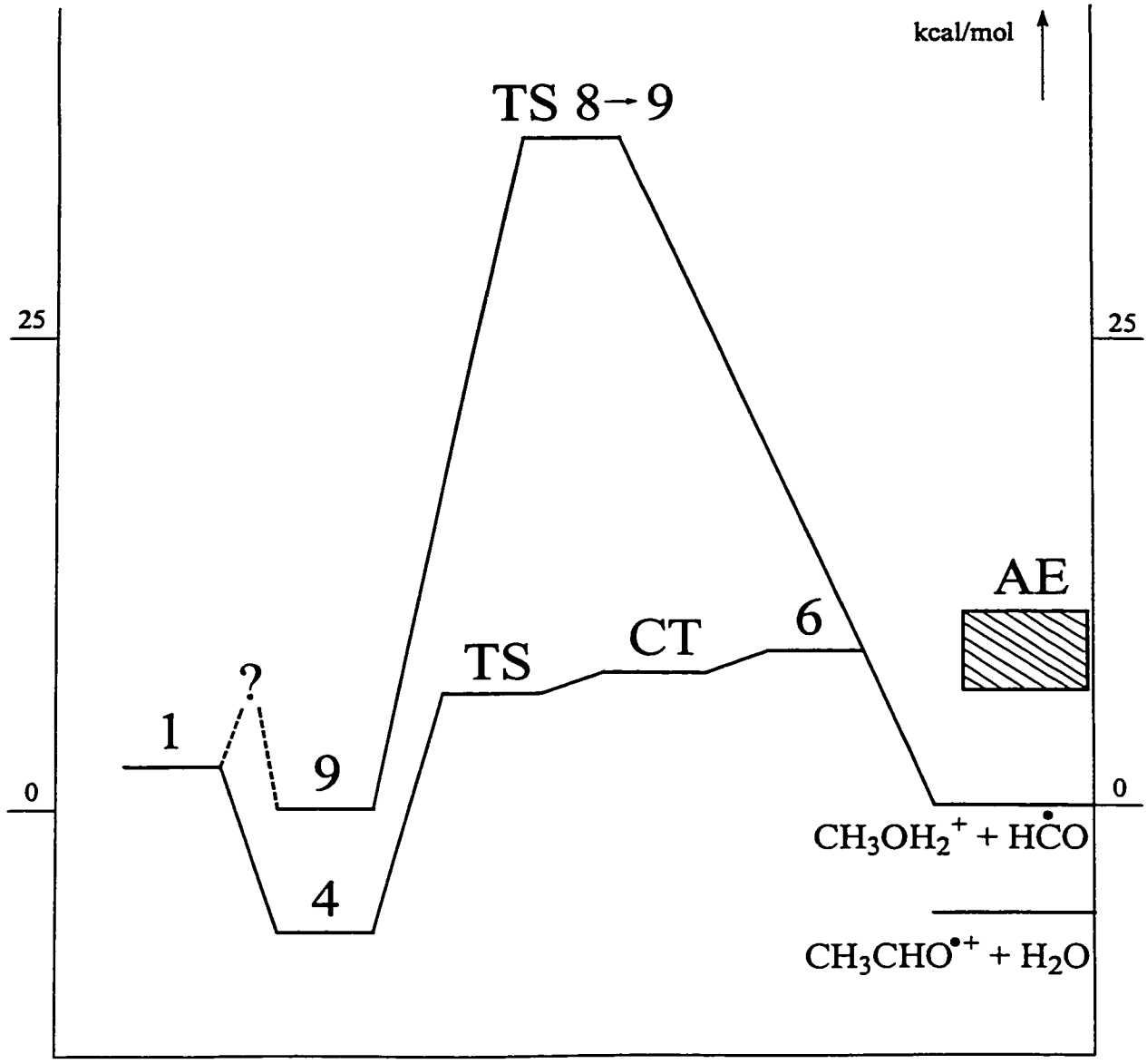

Scheme 1

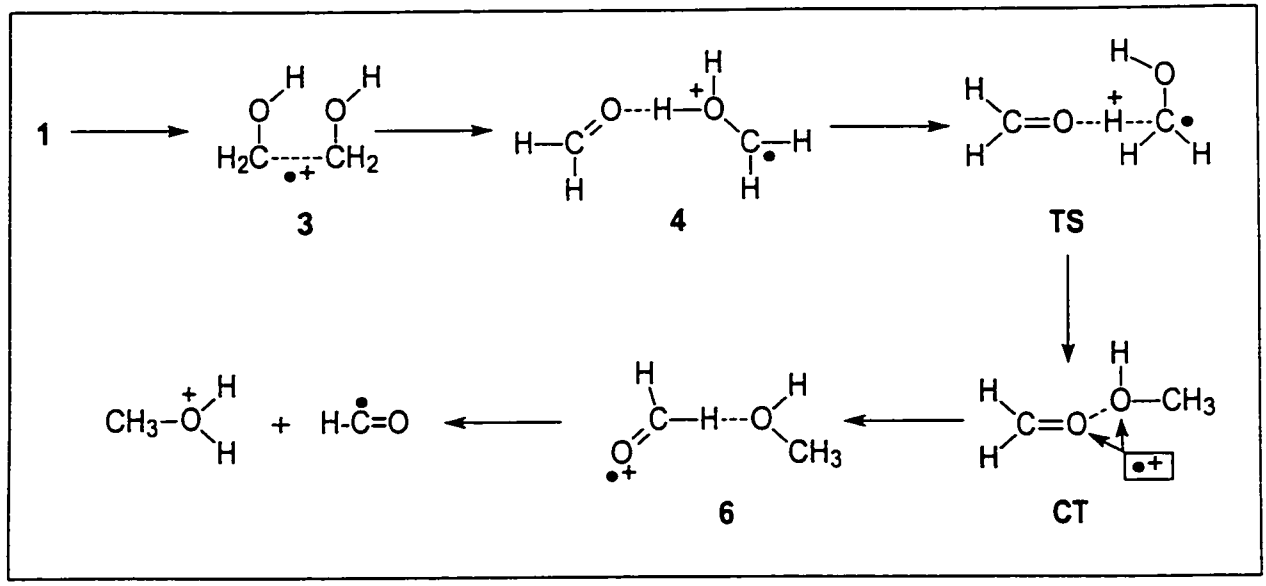

First, upon ionization of ethanediol, the resulting radical cation collapses to a species, **3**, containing a long (~ 2 Å), one electron C–C bond. Further elongation of this bond leads to the H-bridged radical cation **4**. In representing ion **4** as $CH_2{=}O{\bullet\bullet\bullet}M^{\bullet+}$, the key questions is: how can we achieve hydrogen transfer to produce $HCO^{\bullet}$ + MH^{+}? As stated above, rotation of the formaldehyde unit within the electrostatic field of $M^{\bullet+}$ would lead to ion-dipole repulsion ($O{=}CH_2{\bullet\bullet\bullet}M^{\bullet+}$) and so hydrogen transfer is not possible via this route. However, in an ion-dipole complex of the type $CH_2{=}O^{\bullet+}{\bullet\bullet\bullet}M$, where the formaldehyde moiety is now charged, the $CH_2{=}O^{\bullet+}$ unit can more or less freely rotate without too much loss of ion-dipole stabilization ; this would produce $O{=}CH_2^{\bullet+}{\bullet\bullet\bullet}M$ (ion **6** in Scheme 1) which could then undergo **proton** transfer to produce $HCO^{\bullet}$ + MH^{+}. Hence hydrogen (proton) transfer in $CH_2{=}O^{\bullet+}{\bullet\bullet\bullet}M$ is possible only if the charge is first transferred to $CH_2{=}O$, but this is not possible for ion **4**, because neutral CH_2OH_2, if it exists, is a very high energy species. We therefore proposed, and this was substantiated by *ab initio* calculations, that the $CH_2OH_2^{\bullet+}$ ions first rearrange to $CH_3OH^{\bullet+}$, by a formaldehyde catalyzed 1,2–proton shift (**4** → **TS**). This process is an example of Böhme's concept of "proton transport catalysis"[8,9]. It has recently been shown, [10] from chemical ionization experiments, that the reverse isomerization $CH_3OH^{\bullet+}$ → $CH_2OH_2^{\bullet+}$, which does

not occur unassisted, is greatly accelerated by the addition of water; this has also been established by *ab initio* calculations [11]. The result of this "proton-transport catalysis" for ion **4** is that an ion-dipole complex is produced for which both partners (CH_2=O and CH_3OH) represent stable neutral and ionic structures and so now charge transfer (**CT**) is possible via orbital interaction [1]. Once the formaldehyde moiety becomes charged, it can rotate such that one of its hydrogen atoms becomes correctly oriented for transfer (**6**) and this transfer then is a **proton** transfer. With regard to the transformation **4** → **TS** it is of interest to note that the proton affinity (PA) of CH_2=O (PA = 168 kcal/mol) lies between that of $CH_2OH^{\bullet}$ at oxygen (to produce $CH_2OH_2^{\bullet+}$), PA = 160 kcal/mol, and that of $CH_2OH^{\bullet}$ at carbon (to produce $CH_3OH^{\bullet+}$), PA = 170 kcal/mol [9] and so the proton transport catalysis **4** → **TS** is energetically possible as substantiated by our *ab initio* calculations.

Shortly before these results were reported, Audier et al. [7] reported a detailed study of the unimolecular chemistry of the methyl ether of **1**, $CH_3OCH_2CH_2OH$ which also dissociates via DHT to produce $CH_3O(H)CH_3^+$ + $HCO^{\bullet}$. Based on labelling results and observations from ion-molecule reactions they proposed a mechanism involving distonic ions and suggested that **1** would dissociate similarly, see Scheme 2:

Scheme 2

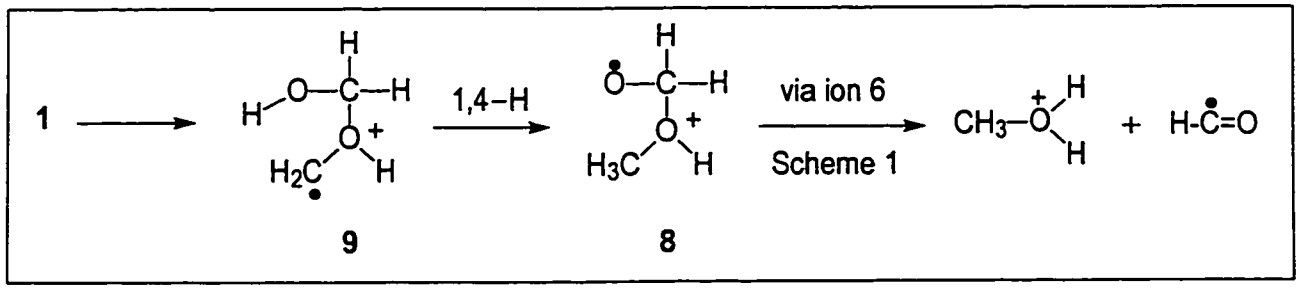

but no theoretical calculations were available for this process. Ion **9** could be formed from **3** via a shuffle of the two CH_2OH subunits. Both mechanisms, i.e. dissociation via either ion-dipole complexes (Scheme 1) or distonic ions (Scheme 2) are experimentally indistinguishable ; for example they both correctly predict the labelling results, see above. Note that we had already calculated [1] that if ions **8** can be formed from **1**, they could lose $HCO^{\bullet}$ via a low lying isomerization to **6**. The question is therefore: can ions **8** be

formed from **9** via a 1,4-hydrogen shift according to Scheme 2 at or below the experimentally determined Appearance Energy (AE)?

The next higher homologue of **1**, ionized 1,2-propanediol, $HOCH_2CH(CH_3)OH^{\bullet+}$ **1p**, also dissociates by DHT, yielding $CH_3OH_2^+ + CH_3CO^{\bullet}$ [12]. This process appears to be remarkably similar to that for **1**; for example, the isotopomer $CH_3CH(OD)CH_2OD^{\bullet+}$ specifically forms CH_2DOHD^+ to the exclusion of $CH_3OD_2^+$ [12]. Again, two mechanisms, one involving ion-dipole complexes (Proposal A), the other distonic ions (Proposal B) and which are very similar to those proposed for 1,2-ethanediol, may account for all observations, see Scheme 3. Again, the question is : which mechanism can occur at or below the AE ? To decide between the two mechanistic proposals for **1** and **1p**, we have performed *ab initio* MO calculations on the most relevant parts of the respective potential energy surfaces.

Scheme 3

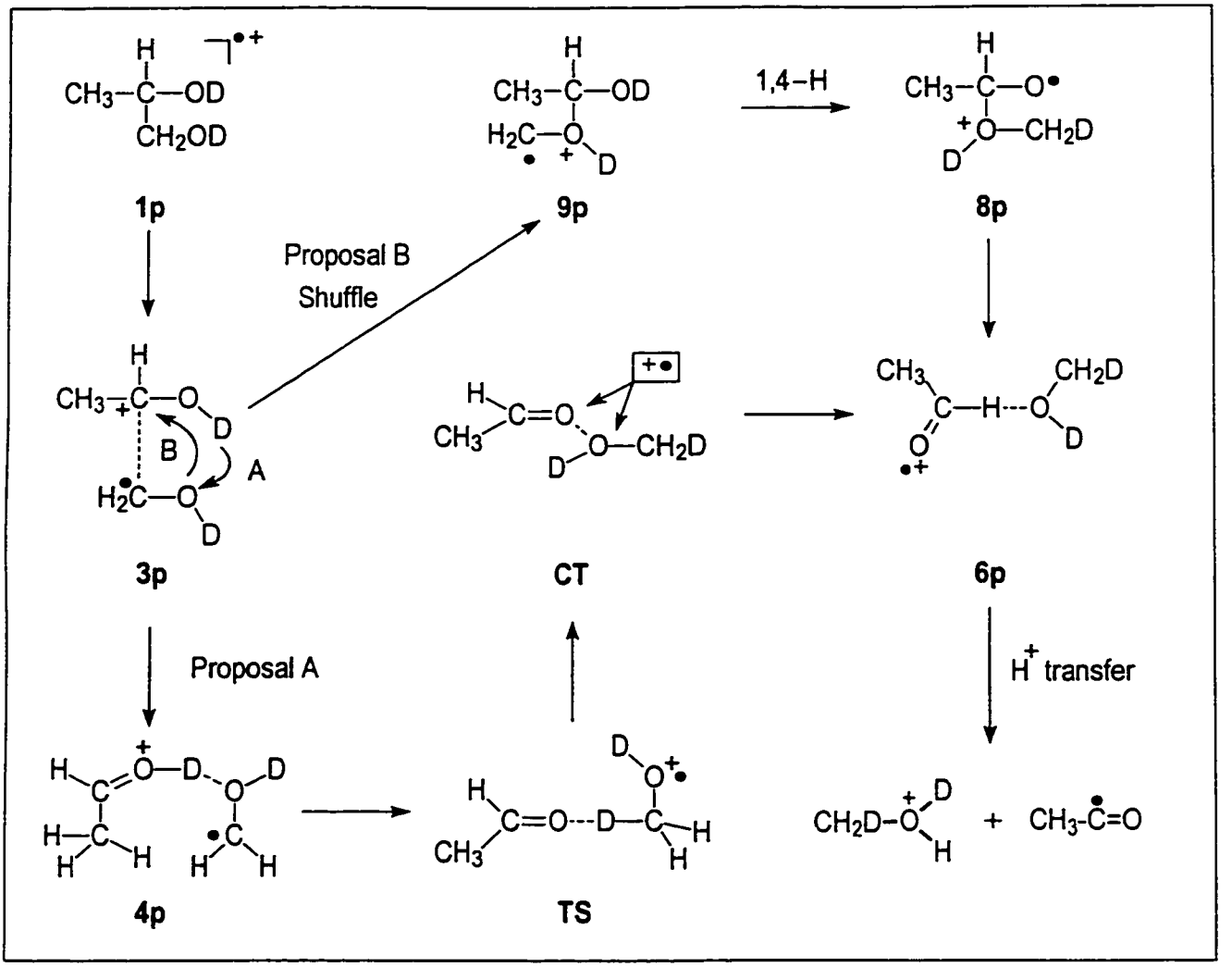

Results and Discussion

1,2-ethanediol

Building upon the results described in Ref. 1 and using the same computational procedures, we have located, at the RHF/DZP level of theory, the minima for the distonic structures **8** and **9** as well as the transition state (saddle point with one imaginary frequency) connecting these ions. Electron correlation effects were then introduced by performing single + double excitation CI (SDCI) calculations including the Pople size correction method [13a]. All minima and saddle points were checked for the correct number of imaginary frequencies and transition states were checked for connections to

appropriate minima. Note further that CT does not correspond to a minimum but to a Minimum Energy Crossing Point (see reference 1 for details). The results are given in Figure 3-1 and in Table 3-1, which include the highest barriers associated with the ion-dipole mechanism, **CT** and **6** in Scheme 1 [1]. All energies are relative to the products, which are set to zero. We find that the barrier for the 1,4-H shift **9** → **8** is surprisingly large and more importantly, that it lies 26 kcal/mol above the measured AE, see Figure 3-1. As stated, ions **8**, should they be formed, can isomerize to **6** at the AE after which dissociation to $CH_3OH_2^+$ + $HCO^•$ would take effect [1]. For ions **8**, **9** and **TS 8→9** we have also performed MO calculations at the QCISD/6-31G**//MP2(FC)/6-31G** level of theory [13], see Table 3-1, which gives results almost identical to our SDCI calculations. From the results presented in Table 3-1 and Figure 3-1 we conclude that the 1,4-hydrogen shift **9** → **8** does not occur for the low energy (metastable) ions and also that the dissociation of ionized 1,2-ethanediol may proceed via Scheme 1, i.e. via proton and electron transfers in ion-dipole complexes.

Table 3-1. Electronic energies of ionized 1,2-ethanediol (hartree), ZPVE (kcal/mol) and relative energies (E_{rel}, kcal/mol) of isomers and transition states for this system.

Structure	RHF/DZP	ZPVE[a]	SDCI/Pople	E_{rel}[b]	E_{rel}[c]
1	-228.66284	50.9	-229.31174	1.9	
4	-228.67266	47.8	-229.32113	-6.9	
TS	-228.62324	45.2	-229.29584	6.2	≤ 9 ± 2
CT	-228.65290	48.0	-229.29994	6.4	≤ 9 ± 2
6	-228.65027	47.8	-229.29873	7.2	≤ 9 ± 2
9	-228.66620	50.7	-229.31485	-0.2 [-1.8][d]	
8	-228.67560	51.4	-229.31653	-0.5 [-1.9][d]	
TS 8 → 9	-228.57775	48.3	-229.25428	35.4 [34.7][d]	≤ 9 ± 2
$HCO^•$ + $CH_3OH_2^+$	-228.65174	47.3	-229.30887	0	

[a] RHF/DZP scaled by 0.9 ; for the geometries of the ions (except for **TS 8→9**) see Ref. 1. [b] Energies including ZPVE. [c] Experimental Appearance Energy, Ref. 1. [d] QCISD/6-31G**//MP2(FC)/6-31G** result, see text.

The barrier for the conversion **8** → **9** is 36 kcal/mol relative to **8**, much larger than that associated with a 1,4-H shift in other oxygen containing cations ; for example the 1,4-H shift in ionized methyl acetate, $CH_3C(=O)OCH_3^{\bullet+}$ → $CH_3C(OH)OCH_2^{\bullet+}$ requires only 12 kcal/mol [14]. A possible explanation for the increased barrier height in the present system comes from an analysis of the computational results in Table 3-2 on 1,4-H shifts in the ionic and neutral systems shown in Scheme 4 (Case B, $X=OH^+$ represents ions **8** and **9** for ionized 1,2-ethanediol).

Scheme 4

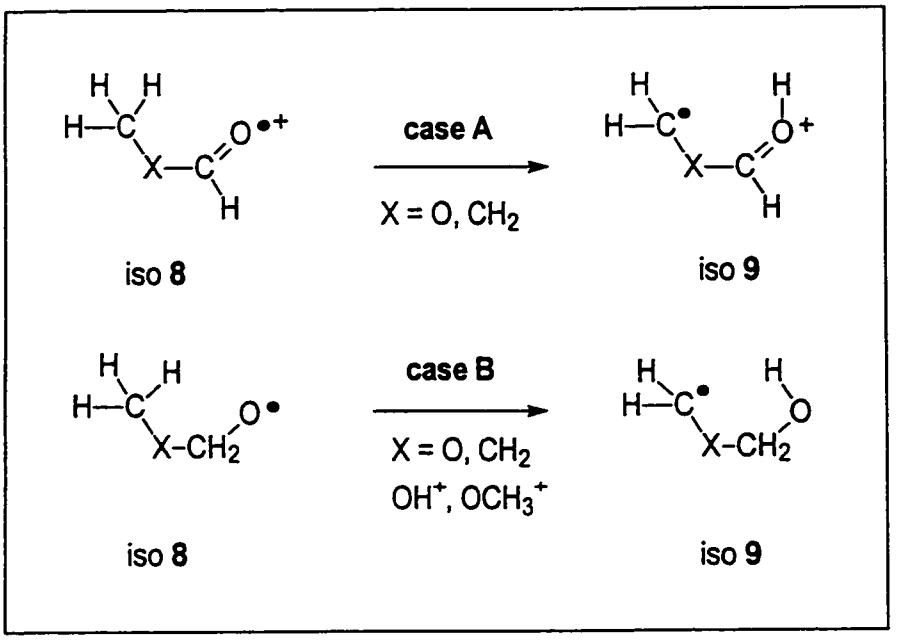

Table 3-2. Relative energies (kcal/mol) for molecules or ions analogous to the ionized 1,2-ethanediol isomers **8** and **9** and their 1,4-H shift transition states. The orientation of the singly occupied orbital in iso **8** and iso **9** is indicated as σ or π (see text for details). The non-planarity of the structures is indicated via the dihedral angle CXCO (between parenthesis after **TS** and after iso **9**).

	X	iso 8	TS	iso 9
Case A	O	0 (σ) 14 (π)[a]	14 (0°)	-12 (σ)
	CH_2	0 (σ) 54 (π)	15 (0°)	-4 (σ)
Case B	O	0 (π)	27 (30°)	-4 (78°)
	CH_2	0 (π)	26 (31°)	1 (180°)
	OH^+	0 (π) 21 (σ)	35 (29°)	-1 (50°)
	OCH_3^+	0 (π)	31 (28°)	-2 (163°)

[a] π-ionization of the ether oxygen is favoured over the carbonyl oxygen

In Table 3-2 the orientation of the singly occupied orbital, which in all cases is almost completely localized on an O atom, is indicated by σ or π. This is possible, even if the structure has no overall symmetry. Here σ indicates that the open shell orbital lies in the XCO plane, whereas π indicates an orbital perpendicular to this plane. The (non)planarity of the skeleton is measured by the dihedral angle CXCO.

The main feature of these results is that the stabilities of the two ionization states (σ or π) apparently reverse when we go from case A to case B. This may be an important factor in determining the magnitude of the activation energy for the H shift. In case A, the σ-symmetry corresponds to the ground state, the transition state for the 1,4-H shift is planar and the barrier is relatively low. However, in case B the π state is more stable than the σ state. This is a property of the radical O atom in both the neutral molecules and the cations. The 1,4-H shift is thus more difficult for case B since here the molecule or ion has to be distorted before the shift can take place. This is further illustrated in Figure 3-2 which shows the transition state structures for the 1,4-H shift in $CH_3OC(H)=O^{\bullet+}$ → $^{\bullet}CH_2OC^+(H)OH$ (case A, X = O) and that for $CH_3O^+(H)CH_2O^{\bullet}$ → $^{\bullet}CH_2O^+(H)CH_2OH$ (case B,

X = OH^+, TS **8→9** in Fig. 3-1). It is seen that for case A, the dihedral angle is zero, while for case B, the ion is significantly distorted from planarity.

Figure 3-2. [A] Transition state for the 1,4-hydrogen shift in methyl formate : $CH_3OC(H)=O^{\bullet+}$ → $^{\bullet}CH_2OC^+HOH$. [B] Transition state for the 1,4-hydrogen shift : $CH_3O^+(H)CH_2O^{\bullet}$ → $^{\bullet}CH_2O^+(H)CH_2OH$.

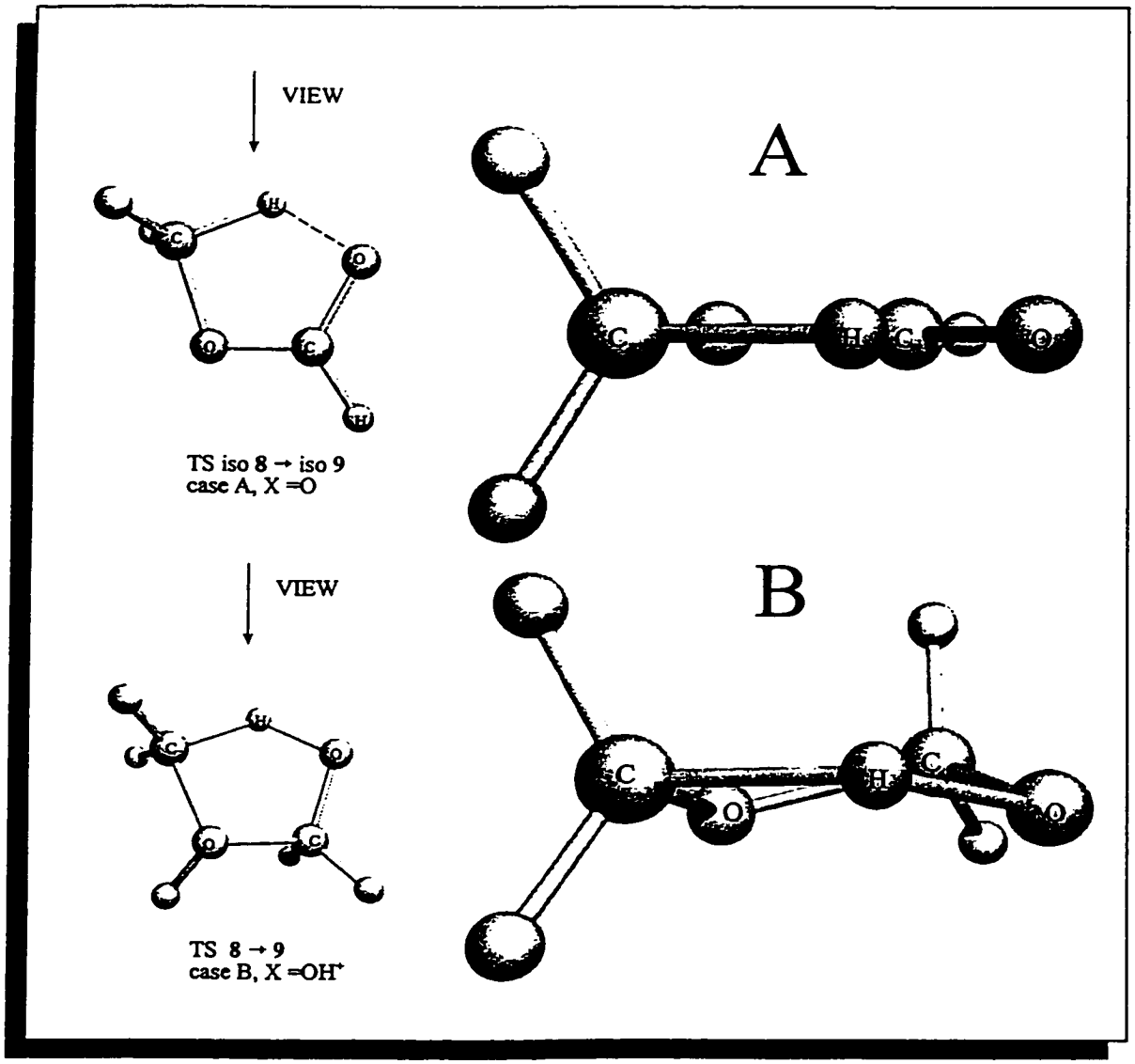

1,2-propanediol.

The sequence depicted in Scheme 3 (Proposal A) has been the subject of a recent experimental and computational study [15] and a brief discussion will suffice. Unlike 1,2-ethanediol, the reactions for 1,2-propanediol all take place below or at the dissociation limit [12], that is to say all species involved must have energies at or below that for $CH_3OH_2^+ + CH_3CO^\bullet = 0$. First, the charge transfer complex (**CT**) was located and its energy was calculated by the procedure described in Reference 1. It was found that its energy lies just below (-1.7 kcal/mol) the above anchor point and so charge transfer is energetically possible. For economical reasons, see Ref. 15, other relevant parts of the surface were calculated from UB3LYP/6-31G* optimized geometries followed by single point QCISD(T)/6-31G** calculations including the usual zero point vibrational energy corrections; the obtained energies are given below in parentheses. The calculated energy diagram is given in Figure 3-3. As with 1,2-ethanediol, ions **1p**, formed by vertical ionization of 1,2-propanediol collapse to the long bonded species **3p** (-15.9 kcal/mol) which has a C-C bond length of 1.964 Å, see Scheme 3. The species can undergo reorientation to form the hydrogen bridged species **4p** (-20.7 kcal/mol). Because the proton affinity of acetaldehyde is greater than that of $CH_2OH^\bullet$, while that of formaldehyde is smaller than that of $CH_2OH^\bullet$, the proton will now be closer to acetaldehyde, compare **4p** (Scheme 3) and **4** (Scheme 1). Ions **4p** may then shuttle [8] the bridging proton to the methylene carbon, **TS** (-4.4 kcal/mol, RHF/D95** optimized geometry, see Ref. 15). Next, the charged methanol rotates around the acetaldehyde molecule until a configuration is reached (**CT**) where the oxygen lone pairs are oriented towards each other so that charge transfer is possible. Now, the neutral methanol in turn can migrate within the electrostatic field of the charged acetaldehyde such that proton transfer is possible to generate **6p** (-8.5 kcal/mol, RHF/D95** optimized geometry, see Ref. 15) which then dissociates. Note that all these transformations take place below the dissociation limit and so the ion-dipole mechanism is energetically possible.

Figure 3-3. Theoretical results for the relative energies of isomers and transition states encountered in the dissociation of 1,2-propanediol radical cations according to Scheme 3.

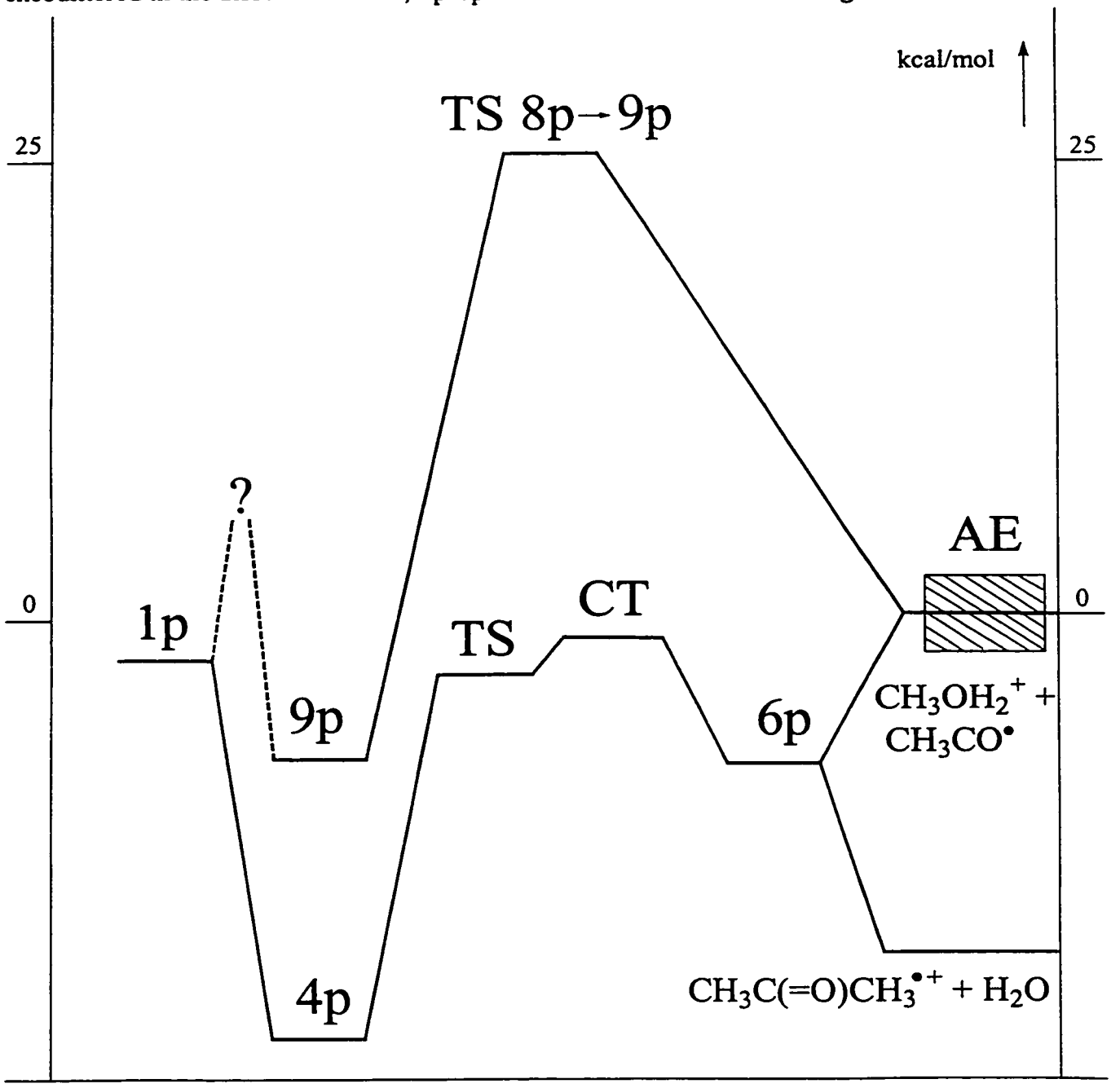

With respect to the distonic ion mechanism, the barrier for the transformation **9p** → **8p** was determined by a QCISD(T)/6-31G** calculation as 25.5 kcal/mol above the dissociation threshold ($CH_3OH_2^+$ + $CH_3CO^•$). Thus this transformation takes place far above the dissociation limit and so the distonic ion mechanism can be ruled out for the low energy ions.

Summarizing, the above computational results show that the rearrangement processes observed in the radical cations of 1,2-ethanediol and 1,2-propanediol can best be understood in terms of proton and electron transfers taking place in ion-dipole complexes rather than hydrogen atom shifts in distonic ions. Thus the sequential transfer of a proton and an electron in ion-dipole complexes appears much more "economical" than a prompt hydrogen atom shift in a distonic ion.

Why only one fragmentation for ionized 1,2-ethanediol?

Our computational results allow a comparison of the dissociation behaviour of ionized 1,2-ethanediol and 1,2-propanediol, compare Figures 3-1 and 3-3. As was stated above, formation of $CH_3OH_2^+$ + $HCO^\bullet$ are the sole dissociation products for ionized 1,2-ethanediol. By contrast 1,2-propanediol undergoes, in addition to loss of $CH_3CO^\bullet$, five other dissociations [12,15]. Apparently the additional methyl substituent makes available dissociation routes and products which are not possible for ionized 1,2-ethanediol.[15] However, there is one abundant dissociation observed for ionized 1,2-propanediol, namely the loss of H_2O, which, too, should occur easily for ionized 1,2-ethanediol, but which is nevertheless not observed. For **1p** the reactions proposed to occur from **6p** via a proton shift followed by a "methyl cation shuttle" [16] to produce ionized acetone [15] are (R = CH_3) :

1p → $O{=}C(R){-}H^{\bullet+}\bullet\bullet\bullet H{-}O(H)CH_3$ **6p** → $R{-}C^\bullet{=}O\bullet\bullet\bullet H{-}O(H)CH_3^+$ **11p** → $R{-}C^\bullet{=}O\bullet\bullet\bullet CH_3^+{-}OH_2$

12p → $R{-}C^\bullet(=O)\bullet\bullet\bullet CH_3^+{-}OH_2$ **13p** → $R{-}C^\bullet(=O){-}CH_3^+\bullet\bullet\bullet OH_2$ **14p** → $R{-}C(=O){-}CH_3^{\bullet+}$ + H_2O

Rotation of the charged $CH_3OH_2^+$ group in **11p** leads to the methyl cation bridged species **12p** after which the methyl cation shuttles to the carbon atom of $R{-}C^\bullet{=}O$ followed by dissociation of the intermediate ion-dipole complex **14p**. As can be seen from Fig. 3-3, for ionized 1,2-propanediol these products lie below the anchor point $CH_3OH_2^+$ + $CH_3CO^\bullet$, but the same is true for ionized 1,2-ethanediol, see Fig. 3-1, yet loss of water is not observed. Our *ab initio* calculations provide an explanation for this puzzling result. According to our results ions **6p** lie below the anchor point, see Fig. 3-3, that is to say, proton transfer is endothermic. Hence the resulting ions **11p** live sufficiently long to undergo other transformations such as a "methyl cation shuttle". By contrast ions **6** lie

above the anchor point, see Fig. 3-1, and so proton transfer now is exothermic and fast; therefore ions **11**, $H\text{-}C^{\bullet}{=}O\bullet\bullet\bullet H\text{-}O(H)\text{-}CH_3^+$, have a fleeting existence only and cannot undergo other transformations. A confirmation of these findings is provided by an assessment of the Stabilization Energies (SE) of ions **6** and **6p**. Using for $\Sigma\Delta H_f$ [$CH_3OH_2^+$ + $HCO^{\bullet}$] = 144 kcal/mol [17], we calculate, using the results of Table 3-1, for ions **6**, ΔH_f = 152 kcal/mol. Using ΔH_f [$CH_2O^{\bullet+}$] = 225 kcal/mol [17] and ΔH_f [$CH_3OH^{\bullet+}$] = -48 kcal/mol [17], we obtain a SE(**6**) of 25 kcal/mol. A similar procedure for ions **6p** (using ΔH_f [$CH_3OH_2^+$ + $CH_3CO^{\bullet}$] = 132 kcal/mol [17] and ΔH_f [$CH_3CHO^{\bullet+}$] = 196 kcal/mol [17]) yields SE(**6p**) = 26 kcal/mol. Not only are these SE's entirely reasonable in magnitude, they are also equal. The reason that many of the intermediates and transition states for ionized 1,2-propanediol lie below the anchor point is that these ionic intermediates are stabilized by the additional methyl group, but the product ion $CH_3OH_2^+$ obviously is not.

References

1. Burgers, P.C.; Ruttink, P.J.A.R. *Org. Mass Spectrom.* **1993**, *28*, 1087.
2. Burgers, P.C.; Holmes, J.L.; Hop, E.C.A.;Postma, R.; Ruttink, P.J.A.R.; Terlouw, J.K. *J. Am. Chem. Soc.* **1987**, *109*, 7315.
3. Morton, T.H. *Tetrahedron* **1982**, *38*, 3195 ; see also Morton, T.H. *Org. Mass Spectrom.* **1992**, *27*, 353 and Biermann, H.W.; Morton, T.H. *J. Am. Chem. Soc.* **1983**, *105*, 5025.
4. Yates, B.F.; Bouma, W.J.; MacLeod, J.K.; Radom, L. *J. Chem. Soc., Chem. Commun.* **1987**, *207*.
5. Yates, B.F.; Bouma, W.J.; Radom, L. *J. Am. Chem. Soc.* **1984**, *106*, 5805.
6. Cao, J.R.; George, M.; Holmes, J.L.; Sirois, M.; Terlouw, J.K.; Burgers, P.C. *J. Am. Chem. Soc.* **1992**, *114*, 2017.
7. Audier, H. E.; Millet, A.; Leblanc, D.; Morton, T.H. *J. Am. Chem. Soc.* **1992**, *114*, 2020.
8. Bohme, D.K. *Int. J. Mass Spectrom. Ion Processes* **1992**, *115*, 95.
9. For recent reviews and leading references see:
   (a) Radom, L.; Gauld, J.W. *J. Am. Chem. Soc.* **1997**, *119*, 9831.
   (b) Chalk, A.J.; Radom, L. *J. Am. Chem. Soc.* **1997**, *119*, 7573.
10. (a) Mourges, P.; Audier, H.E.; Leblanc, D.; Hammerum, S. *Org. Mass Spectrom.* **1993**, *28*, 1098.
    (b) Audier, H.E.; Leblanc, D.; Mourges, P.; McMahon, T.B.; Hammerum, S. *J. Chem. Soc. Chem. Commun.* **1994**, 2329
11. Gauld, J.W.; Audier, H.E.; Fossey, J.; Radom, L. *J. Am. Chem. Soc.* **1996**, *118*, 6299.
12. Van Baar, B.L.M.; Burgers, P.C.; Holmes, J.L.; Terlouw, J.K. *Org. Mass Spectrom.* 1988, 23, 355.
13. (a) Pople J.A.; Seeger R.; Krishnan R., *Int. J. Quantum Chem.* **1977**, *11*, 149; Saunders V.R.; van Lenthe J.H., *Mol. Phys.* **1983**, *48*, 923. (b) Foresman, J.B.; Frisch, A. *Exploring Chemistry with Electronic Structure Methods*, Gaussian Inc: Pittsburgh, 1996.
14. Heinrich, N.; Schmidt, J.; Schwarz, H.; Apeloig, Y. *J. Am. Chem. Soc.* **1987**, *109*, 1317.
15. Burgers, P.C.; Fell, L.M.; Milliet, A.; Rempp, M.; Ruttink, P.J.A.R.; Terlouw, J.K. *Int. J. Mass 16. Spectrom. Ion Processes*, **1997**, *166/167*, 291.
16. Baranov, V.; Petrie, S.; Bohme, D. *J. Am. Chem. Soc.* **1996**, *118*, 4500.
17. Lias, S.; Bartmess, J.E.; Liebmann, J.F.; Holmes, J.L.; Levin, R.D.; Mallard,W.G. *J. Phys. Chem. Ref. Data*, **1988**, *17*, Supplement 1.

CHAPTER 4

THE INTRIGUING BEHAVIOUR OF (IONIZED) OXALACETIC ACID INVESTIGATED BY TANDEM MASS SPECTROMETRY[1]

Abstract

Tandem mass spectrometry based experiments on commercial oxalacetic acid (OAA) samples confirm the indirect evidence from the elegant study of Flint et al. (J. Org. Chem., 57 (1992) 7270) that solid OAA exists solely in the (Z)-enol form of HOOCC(H)=C(OH)COOH. It is further shown that : (i) the samples contain a minor impurity in the low % range, assigned as a dehydration product of 4-hydroxy-4-methyl-2-ketoglutaric acid ; (ii) careful evaporation of solid OAA samples yields mass spectra representative of the (Z)-enol form. The (E)-enol is not present in the solid, nor is its ion generated in the gas phase via isomerization of the ionized (Z)-enol form. However, even under gentle sample introduction conditions, a partial ketonization of the neutral (Z)-enol takes place. The resulting keto OAA molecules are either ionized intact or decarboxylate to yield a mixture of α-hydroxyacrylic acid, CH_2=C(OH)COOH, and its keto isomer pyruvic acid, CH_3C(=O)COOH. From computational quantum chemistry (CBS-4) and experimental data, ionic enthalpies of formation of 95 and 109 kcal/mol were derived for CH_2=C(OH)COOH$^{\bullet+}$ and CH_3C(=O)COOH$^{\bullet+}$ respectively ; (iii) under less controlled sample introduction conditions, thermal dehydration may take place to yield $C_4H_2O_4$ molecules whose mass spectral characteristics are indistinguishable from those of ionized hydroxymaleic anhydride.

Introduction

Oxalacetic acid (OAA) is an important primary metabolite and can in principle have three isomers : the keto isomer, **1a**, and the two enolic forms hydroxyfumaric acid, **1b**, (trans- or (Z)-enol) and hydroxymaleic acid, **1c**, (cis- or (E)-enol) :

---

[1] This chapter has already appeared in print under the same title: L.M. Fell, J.T. Francis, J.L. Holmes and J.K. Terlouw, *Int. J. Mass Spectrom. Ion Processes*, **165/166** (1997) 179-194.

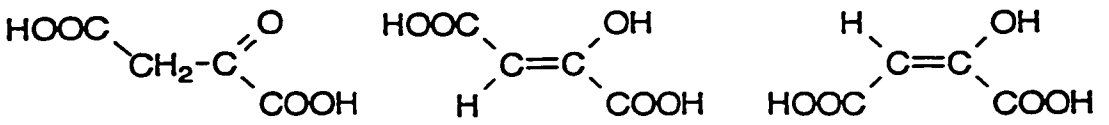

1a **1b** **1c**

The unambiguous identification of which of these structures OAA assumes in the solid state has been a longstanding problem which dates back nearly one hundred years. Wohl and coworkers [1] reported in one of the earliest studies that OAA exists as the enol in the solid state. Moreover, these authors proposed that they obtained crystalline enol isomers **1b** (m.p. 182 °C) or **1c** (m.p. 152 °C), depending upon the sulfuric acid concentration in the mother liquor. Since that time, others have claimed to have synthesized both **1b** and **1c** with melting points very similar to Wohl's samples, and further, that **1b** could be converted to **1c** via dissolution in water followed by immediate recrystallization [2]. Indeed, as Flint et al. [3] have pointed out, the monograph "oxalacetic acid" in the Centennial Edition of the *Merck Index* [4a] reflects this proposed scenario and the 1990 Sigma Catalogue listed the hydroxymaleic acid form of OAA, **1c**, for sale. In the same vein, Beyer-Walter's 1988 textbook of Organic Chemistry [4b] states that free OAA is not known in the solid state but that it can be isolated as either hydroxyfumaric acid **1b** or hydroxymaleic acid **1c**.

In spite of the above, the work of Gruber and co-workers in 1956 [5] had already cast serious doubt concerning the existence of the cis isomer **1c** in the solid state. It was discovered that solid samples with respective melting points of 152 °C and 182 °C had identical infrared spectra, leading to the proposal that there was really only one structure present and that impurities gave rise to the melting point depression. A few years later, Banks [6] reported a similar observation in a study, which further concluded that the lone structure was the (Z)-isomer, based upon the absence of an enolic OH stretching frequency in the IR spectrum. The argument was that the (Z)-isomer could form a six membered, intramolecularly H-bonded structure involving the enolic H and the carbonyl group cis to it across the double bond thus altering the OH stretching frequency.

In the most comprehensive study to date, Flint and co-workers in 1992 tried to determine the crystal structure of OAA directly via X-ray crystallography [3]. Due to poor quality crystals this direct approach remained inconclusive. The authors did,

however, *infer* indirectly that OAA has the (Z)-enol form **1b** in the solid state (and that the enol form in solution is also **1b**). This was based upon X-ray crystallographic data for crystalline di-*tert*- butyl OAA, ^{1}H and ^{13}C NMR data for di-*tert*- butyl OAA in solution and low temperature ^{1}H NMR and ^{13}C data for OAA in solution. Flint and co-workers concluded that the so-called hydroxymaleic acid **1c** solid state products reported in the literature were actually hydroxyfumaric acid **1b** with varying levels of impurities which lower the melting point from 182 °C. Despite the strong arguments which indicate that OAA exists solely as isomer **1b** in the solid state [3,5,6], there is still no definitive evidence from direct experiments on crystalline OAA.

To the best of our knowledge, the only mass spectral information on OAA reported to date is that by Wiley [7] who found its 70 eV EI mass spectrum to be of little diagnostic value stating : "The spectrum of OAA showed a prominent peak at 113 amu for the molecular ion less 19 amu but no peak for the molecular ion itself, which is presumably lost in the source heater ". This observation is at odds with our recent work on the related compound dihydroxyfumaric acid [8] which - albeit only under carefully controlled conditions - yields clearly structure diagnostic mass spectra with an intense molecular ion (~ 60 % of base peak). Further, the work of Chen and Holmes [10] shows that the (Z)- and (E)-isomers of ethenedicarboxylic acid can easily be distinguished by mass spectrometric methods and many more examples of the use of this technique to differentiate between geometrical isomers have been reported [11].

The above observations prompted us to investigate a number of commercial OAA samples using modern tandem mass spectrometric techniques including Collision-Induced Dissociation (CID) - the technique so fruitfully pioneered by K.R. Jennings [9a] and F.W. McLafferty [9b] - and Neutralization-Reionization mass spectrometry (NRMS) [9c]. The samples, obtained from Aldrich and Fluka and sold under the generic name oxalacetic acid, had melting points in the 157-162 °C range, i.e. close to that of the putative (E)-enol isomer **1c**. Samples with a m.p. of 182 °C, assigned to the pure (Z)-enol isomer, are not commercially available.

In view of the labile nature of OAA - numerous sources report decomposition at the melting point and a facile decarboxylation in aqueous solutions [12] - special care was taken to introduce the solid sample under the gentlest conditions feasible.

It will be shown that careful mass spectrometric experiments can both confirm and significantly enlarge our knowledge of this unusual molecule.

Results and Discussion

(i) Conventional EI mass spectra

The rather striking differences between the mass spectra displayed in Figures 4-1a and b, illustrate how strongly the EI mass spectrum of solid OAA (M = 132) depends upon the method of sample introduction.

Fig. 4-1a is representative of a typical spectrum obtained from a "bulk" sample : a probe tube (glass, 15 mm, ϕ = 1 mm) filled with tightly packed sample (~ 15 mg) was introduced via the direct solids insertion probe into the ion chamber such that the tip of the capillary just protruded into the source, which was kept at 120 °C. The bottom part of the sample tube was kept at 50 °C using the probe heater. Radiative heat transfer from the ion chamber to the sample tube caused the sample to slowly evaporate into the source yielding a stable ion current over long periods of time (h). The overall appearance of the spectrum obtained under these conditions remained fairly constant : compare Fig. 4-1a with its inset, which shows the high mass region of the spectrum recorded when the sample had been in the instrument for about an hour. The spectra displayed a molecular ion at m/z 132 and, in the absence of further information, all of the other ions could be rationalized as fragment ions generated therefrom.

Fig. 4-1b shows a typical EI spectrum of the **same** sample introduced in a different way. Now only a fraction of a mg of the finely powdered sample was put in the bottom of a 15 mm quartz probe tube in which a 17 mm gold wire was inserted to promote a better heat transfer to the sample. The sample tube was again inserted into the ion source with the direct solids insertion probe but now such that the tip of the gold wire just protruded into the source, which was again kept at 120 °C. Evaporation of the sample was realized by slowly increasing the sample probe heater, up to 80 °C, until a stable ion current of magnitude comparable to that in the previous experiment was observed. The overall appearance of the spectrum obtained under these conditions, see Fig. 4-1b, remained constant *with the exception of a peak at m/z 113 which was present in the*

initial spectra but disappeared over time. Similar results were obtained with much smaller quantities of sample (in the mg range) which permitted us to monitor the spectra under conditions where the entire sample was consumed (no visible residue was left in the sample tube). These samples were introduced as a thin film on the inside surface of the quartz tube by evaporating the solvent from a freshly prepared concentrated solution of OAA in dry acetone. Increasing the source temperature (up to 150 °C) in these experiments had a negligible effect on the spectra.

Figure 4-1. Typical 70 eV EI mass spectra of commercial oxalacetic acid samples. See text for details.

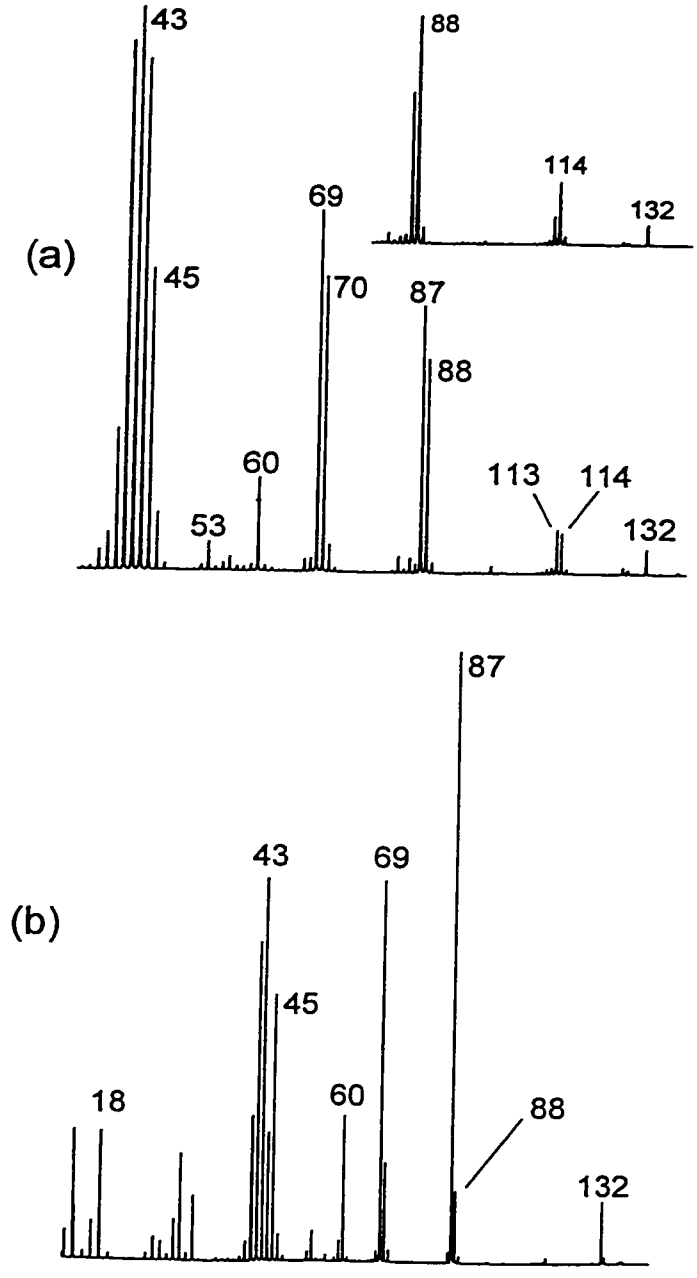

In the above experiments the Aldrich and Fluka samples behaved in the same way.

Comparison of the two sets of mass spectra of OAA leads to the following (tentative) conclusions :

(i) in contrast to the statement by Wiley et al. (see above), OAA yields an EI mass spectrum which features a reasonably intense molecular ion and major fragment ions which can readily be accomodated by its keto/enol structure, *viz.* m/z 87 (loss of $COOH^{\bullet}$), m/z 69 (loss of $COOH^{\bullet} + H_2O$), m/z 45 ($COOH^{+}$) and m/z 43 ($C_2H_3O^{+}$) ;

(ii) the method of sample introduction is of critical importance and the procedure used to obtain spectrum Fig. 4-1a leads to chemical transformations in the probe tube, viz. decarboxylation and dehydration, which give rise to the ions at m/z 114 ($[M - H_2O]^{+\bullet}$), 88 ($[M - CO_2]^{+\bullet}$), 70 and 44 ($CO_2^{+\bullet}$); (iii) the peak at m/z 113 arises from an impurity in the sample.

Before describing the various tandem mass spectrometry based experiments to probe the structure of OAA and the chemical transformations it may undergo prior to ionization, we will first briefly address the origin of the m/z 113 peak. The elemental composition of this ion, $C_5H_5O_3^{+}$, is incompatible with its formation from ionized OAA ($C_4H_4O_5^{+\bullet}$) and thus this even electron ion must arise from an impurity in the sample. Its CID mass spectrum features prominent peaks at m/z 85, 69, 67 and 43 and would be compatible with a structure such as $CH_3C(COOH)=C(H)C=O^{+}$. CID experiments show that the very weak m/z 158 ion in the normal mass spectrum may serve as its precursor. Assuming that the loss of 45 Daltons corresponds with $COOH^{\bullet}$, the impurity could be the keto dicarboxylic acid $CH_3C(COOH)=C(H)C(=O)COOH$, a logical dehydration product of $CH_3C(COOH)(OH)CH_2C(=O)COOH$, 4-hydroxy-4-methyl-2-ketoglutaric acid. The ketoglutaric acid has been reported to be formed [7b] (via an aldol type condensation) in aqueous OAA solutions along with $HOOCC(=O)CH_2C(COOH)(OH)CH_2COOH$, citroylformic acid. The latter species is formed by bimolecular decarboxylative self-condensation of OAA [7] and it is reported [7a] to have prominent peaks at m/z 112, 139 and 184 in its mass spectrum. Peaks at these m/z values were either absent in our spectra or, when present, of negligible intensity (< 0.05 % of base peak).

Thus, whereas the identity and origin of the m/z 158 and 113 ions remains somewhat speculative, it is clear that the commercially obtained samples contain an

impurity, which we estimate to be in the low % range. Since in general, melting points are depressed by the presence of impurities, our observations support the conclusion of Flint et al. that : "all previously reported samples of enol OAA with melting points lower than 182 °C were not (E)-enol OAA, **1c**, but were in fact samples of crystalline (Z)-enol OAA, whose melting points had been lowered by impurities", provided that it can be shown that the mass spectrum shown in Fig. 4-1b is that of the (Z)-enol OAA, **1b**.

Evidence that this is indeed the case will be presented in the next sections. It will be argued, see Scheme 1 which summarizes our findings, that the sample consists of the (Z)-enol isomer which, to some extent, ketonizes during evaporation.

Under the conditions of Fig. 4-1a, a large fraction of these keto molecules, **1a**, decarboxylates to produce **2a**, α-hydroxyacrylic acid, which partially further ketonizes to pyruvic acid, **2b**, prior to ionization. Some dehydration also takes place to generate hydroxymaleic anhydride molecules, which accounts for the telltale peaks at m/z 114 and m/z 70.

Scheme 1

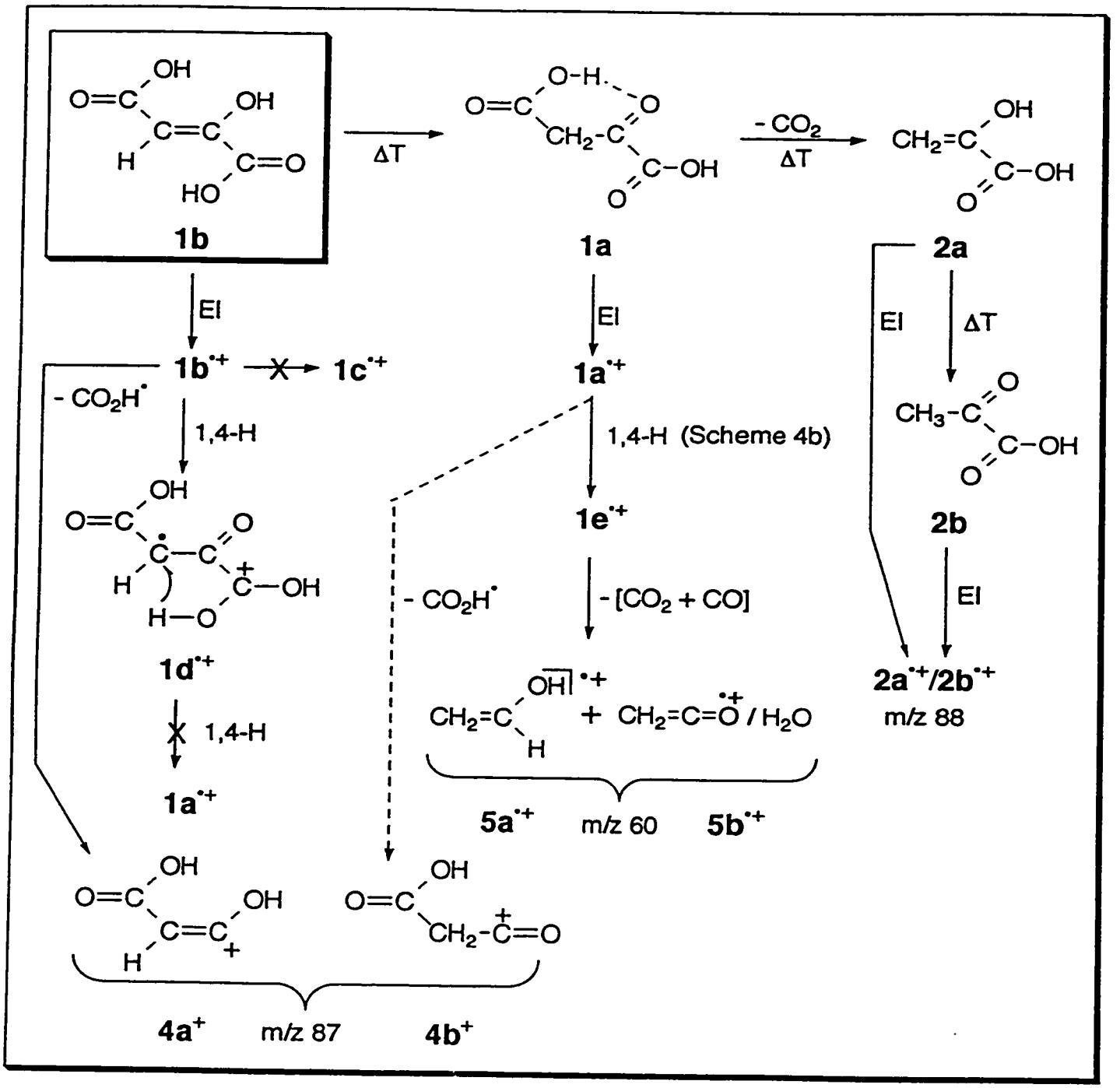
1b
ΔT
1a
- CO2
ΔT
2a
EI
1b•+
1c•+
- CO2H•
1,4-H
1d•+
1,4-H
1a•+
EI
1a•+
1,4-H (Scheme 4b)
1e•+
- CO2H•
- [CO2 + CO]
5a•+
m/z 60
5b•+
+ CH2=C=O•+ / H2O
EI
ΔT
2b
EI
2a•+/2b•+
m/z 88
4a+
m/z 87
4b+

(ii) MS/MS experiments on the molecular ion : evidence for the presence of the (Z)-enol isomer $1c^{\bullet+}$

We begin our analysis by noting that Holmes et al. [10] have convincingly showed that the metastable ionized (Z)- and (E)- isomers of ethenedicarboxylic acid do not readily interconvert and that the ionized (E) isomer, maleic acid, shows a geometry-specific dissociation, viz. loss of CO_2 , see Scheme 2 (X=H). By analogy, it is reasonable to expect ionized hydroxymaleic acid, **1c**, to undergo a similar carboxyl-carboxyl interaction and subsequent elimination of CO_2 within the metastable time frame, see Scheme 2, X = OH.

Scheme 2

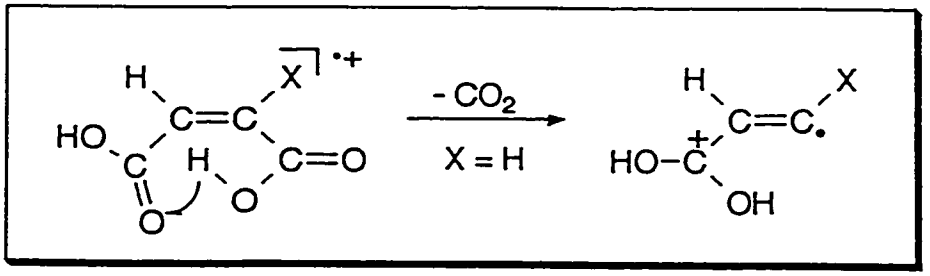

However, the OAA molecular ion does not behave in this manner : the MI mass spectrum contains only one peak, m/z 87, which corresponds to the loss of $COOH^{\bullet}$. Loss of CO_2 is also entirely absent in the CID mass spectrum which, in addition to m/z 87 (base peak), contains one more prominent ion, m/z 69 (~15 %). Because the energy requirement for CO_2 loss is considerably lower than that for the loss of $COOH^{\bullet}$, the possibility that the m/z 132 ions in Fig. 4-1 are the enol isomer **1c** can be essentially ruled out.

These experimental observations also support the proposal that the m/z 88 peaks observed in Fig. 4-1 result from thermal decarboxylation of the sample prior to ionization, which will be discussed in detail below.

That the molecular ions do not have the structure of the keto ion, $\mathbf{1a}^{\bullet+}$, follows from the following observations. If the OAA molecular ions had the keto structure, then loss of $COOH^{\bullet}$ therefrom would yield a m/z 87 product ion of structure $\mathbf{4b}^{+}$, see Scheme 1. The CID mass spectrum of $\mathbf{4b}^{+}$ was obtained from a collision experiment on the prominent

m/z 87 ion in the mass spectrum of malonic acid, $HOOCCH_2COOH$, and is shown as item (a) in Figure 4-2. The spectrum is dominated by structure characteristic fragment ions at m/z 42 ($CH_2=C=O^{+\bullet}$), 45 ($HO-C=O^{+}$) and the rearrangement ion at m/z 43 which also dominates the MI spectrum : $CH_3C=O^{+}$ (structure verified by a double collision experiment).

On the other hand, the m/z 87 ions generated from OAA yield a distinctly different CID mass spectrum, item (b) in Fig. 4-2, which is dominated by m/z 69 (loss of H_2O) and which further features an intense doubly charged ion. The CID mass spectrum of these m/z 69 ions (MS/MS experiment) appeared to be closely similar to that of the source generated m/z 69 ions and comparison with literature spectra [13] leaves little doubt that these ions are $[O=C=CH-C=O]^{+}$, carbon-protonated carbon suboxide. This result is entirely compatible with the proposal that the OAA ions have the enol structure $\mathbf{1b}^{\bullet+}$, which by loss of $COOH^{\bullet}$ produce the m/z 87 product ion $\mathbf{4a}^{+}$ from which a facile loss of H_2O (via a 1,5-H shift) can easily be envisaged. In agreement with this proposal the corresponding m/z 89 ion generated from the ^{18}O labelled OAA isotopomer $HOOCC(^{18}OH)=CHCOOH$ (see next section for further details) shows a specific loss of $H_2{}^{16}O$.

Figure 4-2. Collision-induced dissociation (CID) mass spectra of source generated m/z 87 ions from ionized malonic acid (a) and ionized oxalacetic acid (b) ; item (c) represents the CID mass spectrum of m/z 87 ions generated from metastable oxalacetic acid molecular ions.

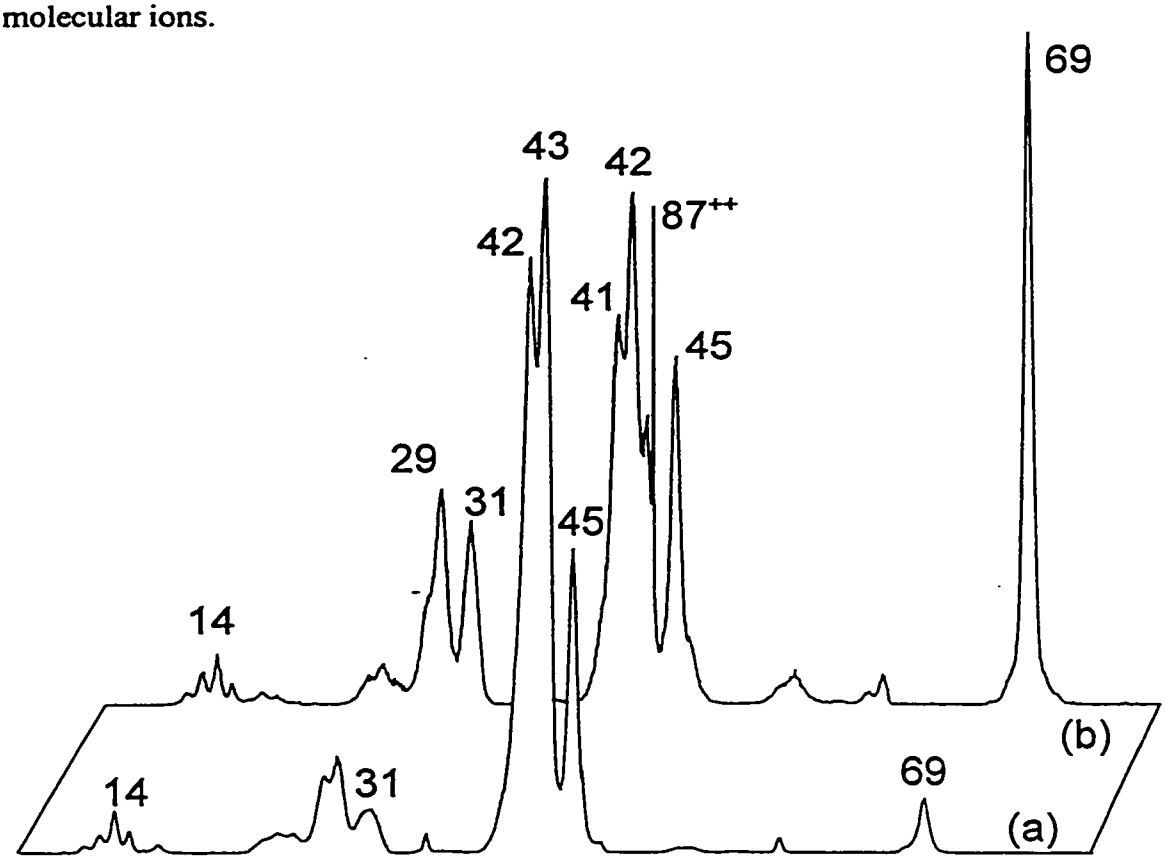

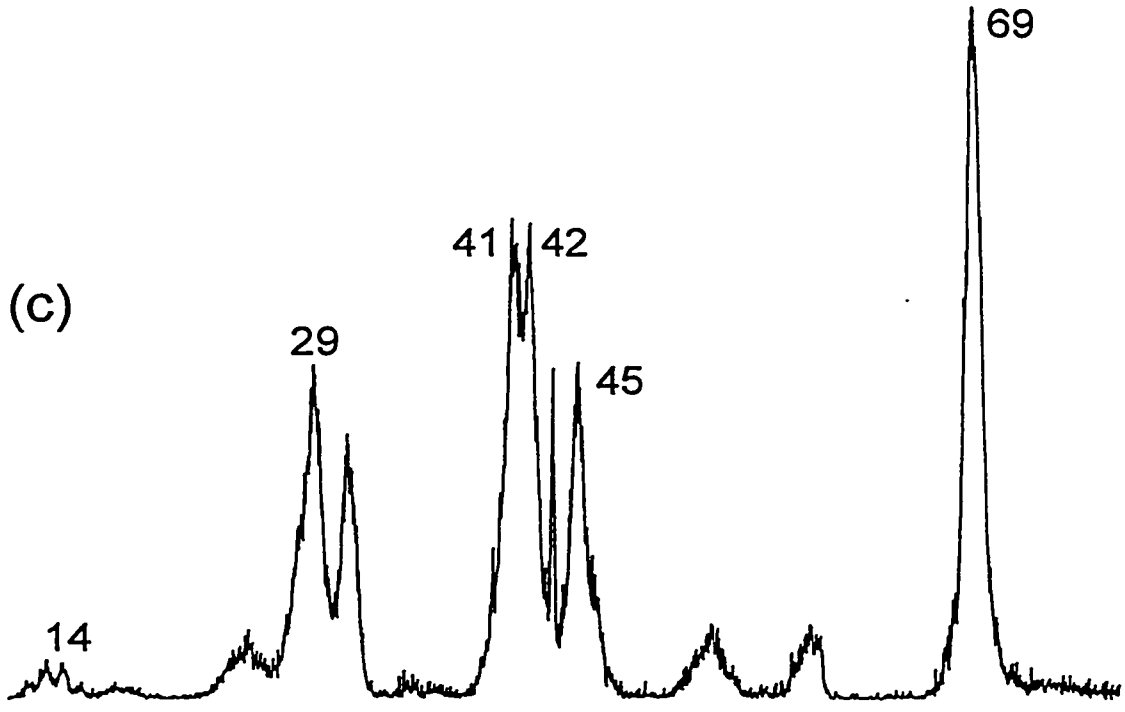

The isomeric m/z 87 ions **4a**$^+$ and **4b**$^+$ can be considered as carboxyl substituted analogues of the isomeric pair of $C_2H_3O^+$ ions CH_2=C-OH^+ and $CH_3C{=}O^+$. Of these, the acetyl cation is much more stable, by ~36 kcal/mol [14a]. Carboxyl substitution is not expected to greatly affect this difference and, in agreement with this, an AM1 calculation [15] predicted **4a**$^+$ to be 33 kcal/mol higher in energy than **4b**$^+$. This finding not only reinforces our proposal that we are dealing with ions **1b**$^{\bullet+}$ but it also stipulates that these ions cannot easily convert into the keto form, e.g. via the two consecutive 1,4-H shifts depicted in Scheme 1, because such a conversion would readily produce the m/z 87 ion of lower energy, *viz.* **4b**$^+$. That these ions are also not generated from *metastable* OAA ions was verified by examining the (third field free region) CID mass spectrum of m/z 87 ions metastably generated in the second field free region, see item (c) in Fig. 4-2.

Nevertheless, the above experimental observations do not exclude the possibility that a small fraction of the source generated m/z 87 ions from OAA have the **4b**$^+$ structure.

(iii) The m/z 88 ions : a mixture of ionized α-hydroxyacrylic and pyruvic acid generated by ionization of decarboxylation products from OAA.

As argued in the previous section, the m/z 88 ion is not a fragment generated from the OAA molecular ion. Indeed, when the energy of the ionizing electrons was lowered to c. 10 eV, the resulting mass spectrum displayed only five peaks of which m/z 88 had now become the most prominent : m/z 132 (7 %), m/z 88 (100 %), m/z 87 (6 %), m/z 60 (7 %) and m/z 43 (12 %). We have already noted that the method of sample introduction has a pronounced effect upon the m/z 88 ion intensity, compare Fig. 4-1a and b, and this strongly suggests that it originates from a chemical transformation (decarboxylation) during the evaporation process. Kokesh et al. [12] have shown that aqueous solutions of OAA are prone to decarboxylate into pyruvic acid, via the keto-acid anion.

Fig. 4-3a-c show the CID mass spectra of (i) the m/z 88 ion in the EI spectrum of OAA (conditions Fig. 1a), (ii) the m/z 88 ion in the low eV spectrum of OAA and (iii)

the molecular ion of an authentic sample of pyruvic acid ($CH_3C(=O)COOH$). From a comparison of these spectra we conclude that the m/z 88 ions from OAA consist of pyruvic acid in admixture with a second isomer having a lower ionization energy.

The most logical explanation is that this second isomer is α-hydroxyacrylic acid, the enol of pyruvic acid, structure **2a** in Scheme 1. It is likely the primary decarboxylation product of OAA is generated from the keto form **1a** by incipient proton transfer to the C=O through hydrogen bonding [16]. Neutral enol molecules are easily converted into their more stable keto counterparts via **inter**molecular isomerization and we propose that this occurs to some extent during the evaporation of the OAA sample, forming pyruvic acid, **2b**.

Figure 4-3. Collision-induced dissociation (CID) mass spectra of source generated m/z 88 ions generated from oxalacetic acid (a) and pyruvic acid acid (c) ; item (b) represents the CID mass spectrum of the m/z 88 ions from oxalacetic acid obtained at low ionizing electron energies.

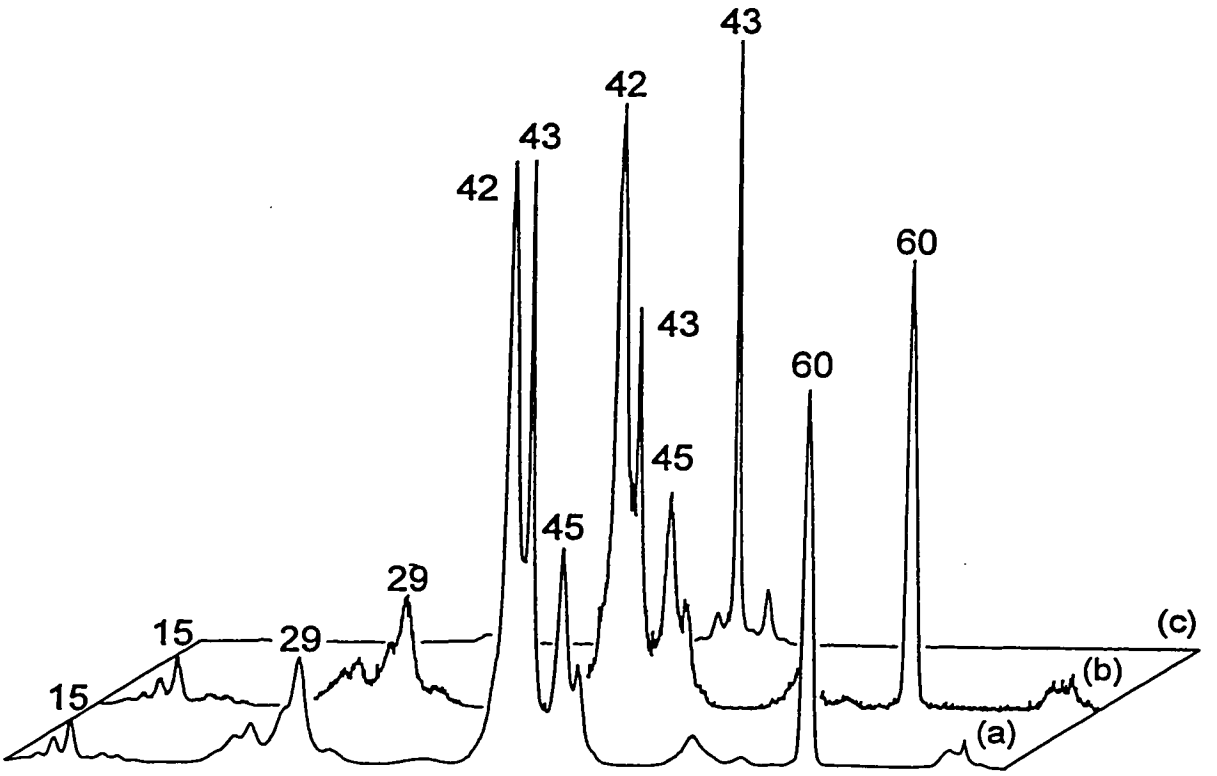

Fig. 4-4 compares the NR mass spectra of pyruvic acid (item (b)) with that of the m/z 88 ions derived from OAA. It is seen that **2b** generates no NR survivor signal, which is not surprising because the molecular ion in the normal mass spectrum of **2b** is very weak, ~ 5 % of m/z 43, base peak. (The dominant m/z 45 ($HO\text{-}C{=}O^+$) peak in the NR mass spectrum is largely due to collision induced dissociative ionization (CIDI) [9c] rather than neutralization.

In contrast, Fig. 4-4a shows, apart from the m/z 45 pyruvic acid signal, a clear survivor signal at m/z 88 which must be representative of the second component in the mixture and which has a stable neutral counterpart. The survivor ions were selectively transmitted to the third field free region of the instrument where they were subjected to collision induced dissociation. The resulting CID mass spectrum, see Fig. 4-4b, is that of this "purified" second component in the mixture. Its major fragment ions are at m/z 42 ($CH_2{=}C{=}O^{\bullet+}$), 45 ($HO\text{-}C{=}O^+$) and 60 ($C_2H_4O_2^{\bullet+}$, loss of CO), entirely compatible with the proposed enol structure $\mathbf{2a}^{\bullet+}$.

The rearrangement leading to the m/z 60 ion is the only process observed in the MI mass spectrum of the survivor ion and to probe its structure and mechanism of formation a sample of OAA was exchanged with $H_2{}^{18}O$. In aqueous solutions OAA largely exists in the keto form and a facile carbonyl exchange may therefore be expected to occur [17]. Indeed, the EI mass spectrum of the exchanged sample, see Fig. 4-5a (spectrum obtained under the conditions of Fig. 4-1b), shows that only one ^{18}O atom is incorporated to yield the isotopomer $HOOCC(^{18}OH){=}CHCOOH$. Following our proposal, the m/z 90 ions in this spectrum should be a mixture of $CH_3C(={}^{18}O)COOH$ and $CH_2{=}C(^{18}OH)COOH$ and the CID mass spectrum of these ions shown in Fig. 4-5b confirms this : the m/z 43 ion characteristic of **2b** has shifted to m/z 45 ($CH_3C{=}{}^{18}O^+$) , whereas the m/z 42 ($CH_2{=}C{=}O^{\bullet+}$) and m/z 60 ions characteristic of **2a** have shifted to m/z 44 ($CH_2{=}C{=}{}^{18}O^{\bullet+}$) and m/z 62 respectively.

Figure 4-4. Neutralization-reionization (NR) mass spectra of source generated m/z 88 ions generated from oxalacetic acid (a) and pyruvic acid acid (b) ; item (c) represents the CID mass spectrum of the m/z 88 survivor ions shown in item (a).

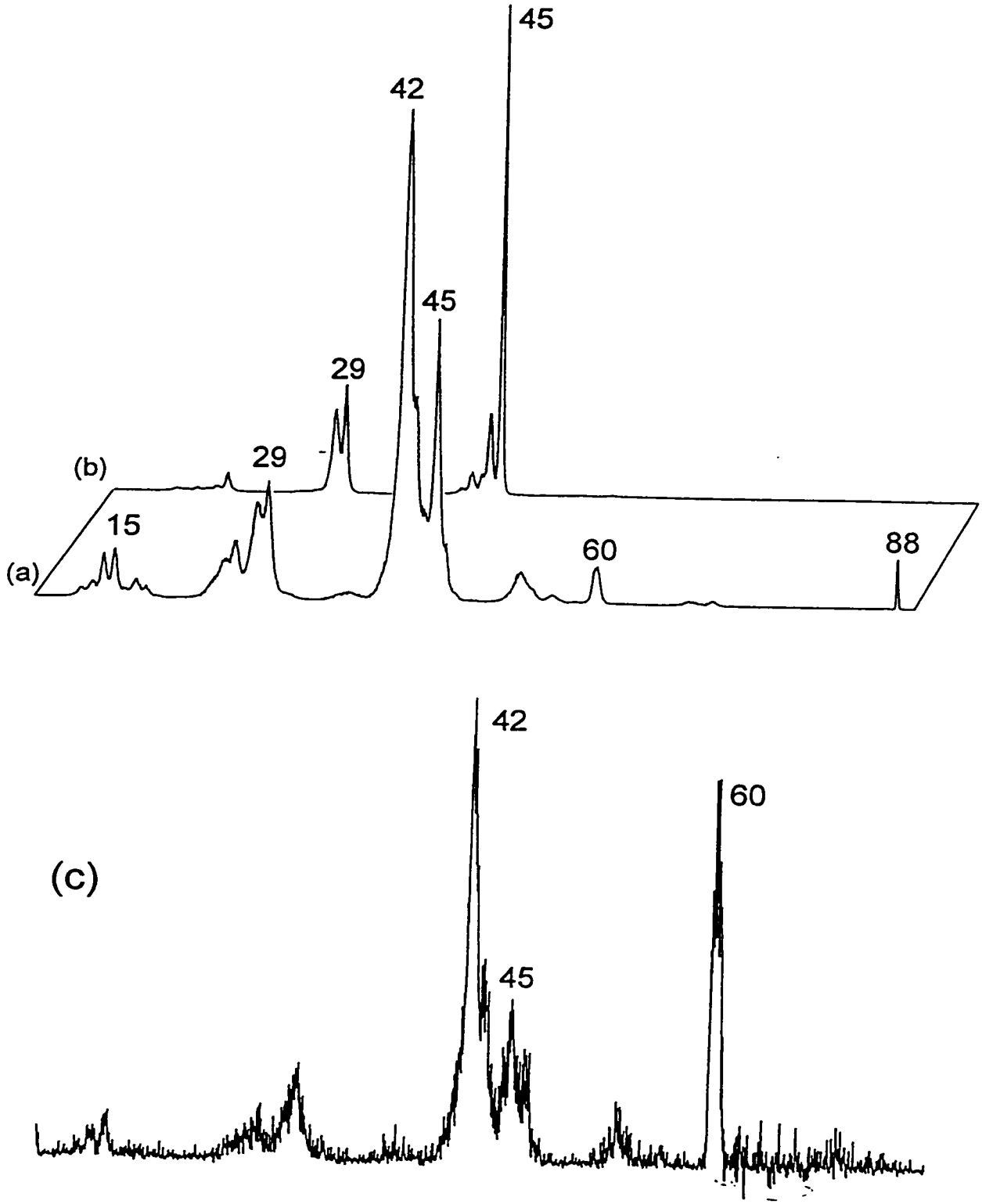

Figure 4-5. (a) partial 70 eV EI mass spectrum of the ^{18}O-carbonyl labelled oxalacetic acid isotopomer; (b) the CID mass spectrum of the source generated m/z 90 ions generated from this isotopomer.

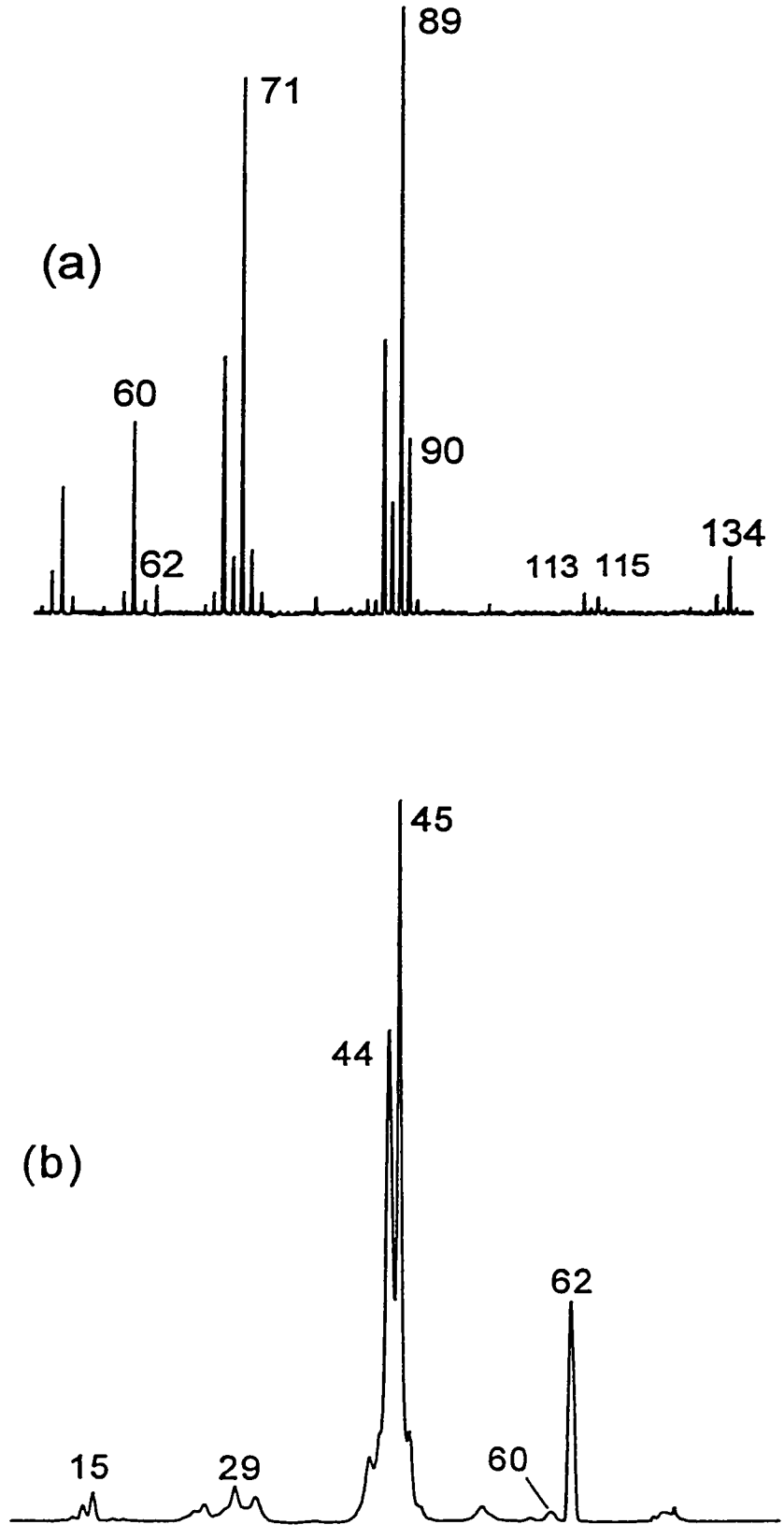

However, these ^{18}O labelling experiments also show that the majority of the m/z 60 ions in the EI mass spectrum of the unlabelled compound are **not** generated from the enol ion. Fig. 4-5b clearly shows that the enol shows an almost specific loss of $C^{16}O$ yielding the much weaker m/z 62 ion in the EI mass spectrum, see Fig. 4-5a. CID mass spectra were obtained of both the source generated m/z 62 ions, item (a) in Fig. 4-6 and the m/z 62 ions in the CID mass spectrum of Fig. 4-5b (MS/MS experiment, result not shown) : the two closely similar spectra are dominated by an intense very narrow peak at m/z 44, $CH_2{=}C{=}{}^{18}O^{\bullet+}$ generated by a specific loss of H_2O. Comparison with reference spectra of $C_2H_4O_2^{\bullet+}$ isomers [18] leaves little doubt that it is the well characterized [19] ketene/water ion-dipole complex, whose generation from the enol ion $\mathbf{2a}^{\bullet+}$ may occur as follows (Scheme 3) :

Scheme 3

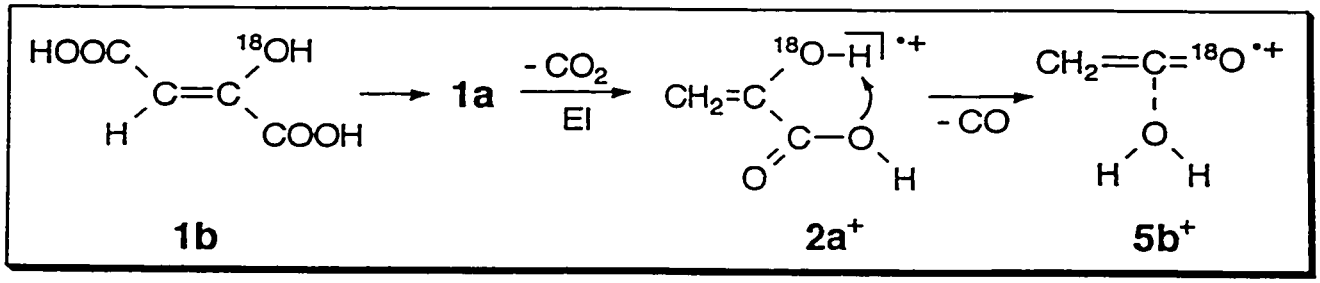

Figure 4-6. Collision-induced dissociation (CID) mass spectra of the source generated m/z 62 and m/z 60 ions derived from the the ^{18}O-carbonyl labelled oxalacetic acid isotopomer, items (a) and (b) respectively ; item (c) represents the CID mass spectrum of the source generated m/z 60 ions generated from ionized butyric acid.

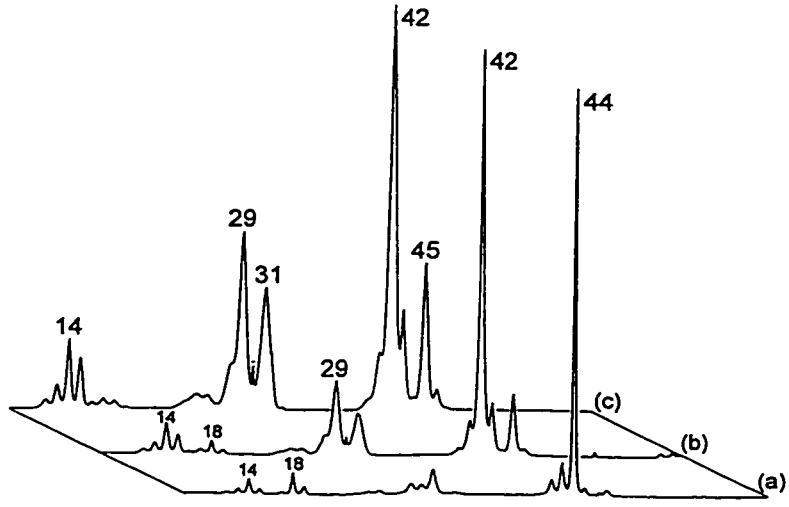

The same product ion, **5b**$^+$, is generated from ionized β-hydroxyacrylic acid, HOC(H)=C(H)COOH$^{\bullet+}$, an isomer of **2a**, but which displays characteristically different CID and MI mass spectra, dominated by loss of H_2O [10b].

Thus, there is solid evidence that the m/z 88 ions in the normal mass spectra consist of a keto/enol mixture of **2a**$^{\bullet+}$ and **2b**$^{\bullet+}$ which originates from ionization of the decarboxylation products of OAA as indicated in Scheme 1.

The Ionization Energy of the m/z 88 ion was measured by a comparative method [14b] and was found to be 9.50 ± 0.1 eV , significantly below that reported for pyruvic acid (9.9 eV [14a]) and that recently obtained by ourselves, 10.4 ± 0.1 eV.

The heat of formation of pyruvic acid's enol, **2a**, can be estimated from the effect of carboxyl substitution in olefinic molecules, giving ΔH_f [**2a**] = - 120 ± 1 kcal/mol and a value of - 124 kcal/mol from the computational quantum chemistry approach described in the Experimental. The same level of theory gave - 131 kcal/mol for ΔH_f [pyruvic acid] , in excellent agreement with an earlier estimate [14a]. The energy difference between the neutral tautomers, 10 kcal/mol, is reasonable (compare acetone and its enol, ref. 14a) and the ionic heats of formation, 95 kcal/mol for the enol and 109 kcal/mol for the keto acid are comparable with those of ionized acetone and its enol [14a].

As stated above, the enol ions do **not** serve as the precursor for the majority of the m/z 60 ions which comprise a peak of significant intensity in the normal mass spectrum. Its origin and structure will be discussed in the next section.

(iv) The m/z 60 ions : a mixture of CH_2=C(OH)$_2^{\bullet+}$ and CH_2=C=O$^{\bullet+}$/H_2O ions generated from the ionized keto form of OAA.

Acetic acid has been reported as a minor impurity in OAA samples [12] and this might serve as an explanation for the presence of the m/z 60 peak in the EI spectra. However, this is definitely not the case : Fig. 4-6b shows the CID mass spectrum of the source generated m/z 60 ions of the ^{18}O isotopomer HOOCC(^{18}OH)=CHCOOH and this spectrum effectively rules out ionized acetic acid, whose CID mass spectrum [18] is dominated by peaks at m/z 43 and 45. The spectrum bears some resemblance to that of the CH_2=C=O$^{\bullet+}$/H_2O ion, **5b**$^{\bullet+}$, but it is much closer to that of the 1,1-dihydroxy-ethene isomer, **5a**$^{\bullet+}$, whose CID mass spectrum is given in Fig. 4-6c. The CID mass spectra of

other common $C_2H_4O_2^{\cdot+}$ isomers have different characteristic peaks [18] but the spectrum of Fig. 4-6b can be reproduced from a 13 : 1 mixture of **5a**$^{\cdot+}$ and **5b**$^{\cdot+}$ respectively (see Experimental).

Further evidence for a mixture of these $C_2H_4O_2^{\cdot+}$ isomers comes from the NR experiments shown in Fig. 4-7. Unlike **5a**$^{\cdot+}$, whose neutral counterpart is a stable molecule, the ionized ketene/water isomer **5b**$^{\cdot+}$ is expected to completely dissociate into CH_2=C=O and H_2O upon neutralization to yield m/z 42 and m/z 18 ions in the collisional ionization step. Thus, the increased m/z 42 and m/z 18 intensities in the NR spectrum of the OAA m/z 60 ions, Fig. 4-7b, relative to that in the spectrum of the pure ions **5a**$^{\cdot+}$, Fig. 4-7a, is due to the contribution from **5b**$^{\cdot+}$, whereas the m/z 60 survivor ion should be representative of **5a**$^{\cdot+}$. The survivor ions were selectively transmitted to the third field free region where their CID mass spectrum was obtained. This spectrum, Fig. 4-7c, is indeed that of pure ions **5a**$^{\cdot+}$.

Figure 4-7. Neutralization-reionization (NR) mass spectra of source generated m/z 60 ions generated from butyric acid (a) and oxalacetic acid ; item (c) represents the CID mass spectrum of the m/z 60 survivor ions shown in item (b).

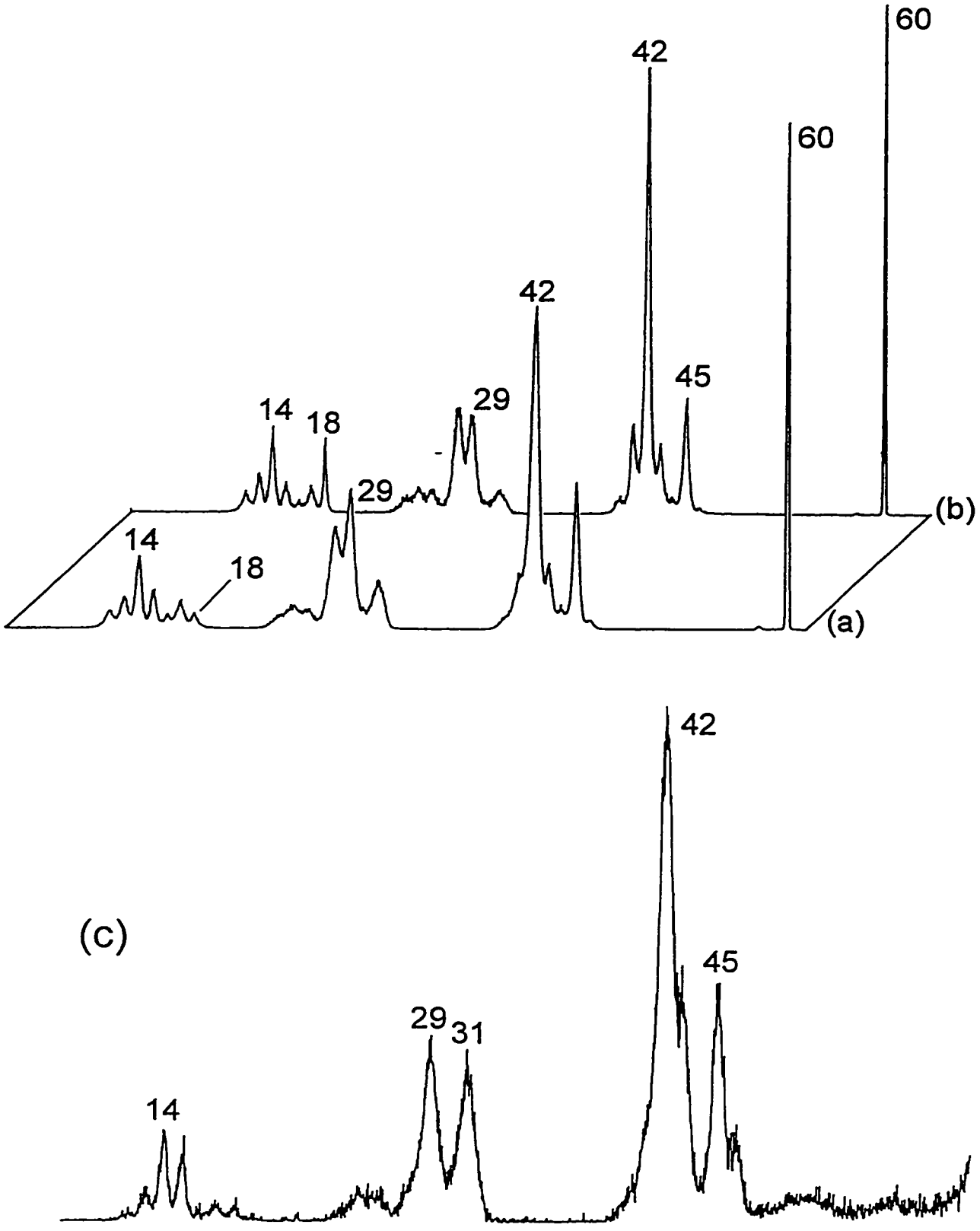

Considering the reactivity and stability of the neutral counterparts of these ions, they must originate from a dissociative ionic rearrangement rather than direct ionization. This raises the intriguing question of the identity of their precursor.

Neither the MI nor the CID mass spectrum of the OAA molecular ion, see section (ii), shows a detectable signal at m/z 60 and thus we conclude that the m/z 60 rearrangement ions are not generated from the (Z)-enol OAA molecular ions $\mathbf{1b}^{\bullet+}$ which comprise the m/z 132 peak.

On the other hand, we do have indirect evidence that the keto form is generated during the evaporation of the sample as it is the most probable precursor of the m/z 88 ions examined in the previous section. Could the m/z 60 ions then originate from a fraction of **keto** OAA molecules which do not undergo decarboxylation but rather evaporate intact into the source to become ionized ? This may well be the case, but **only** if the ionized keto OAA molecules would completely dissociate in the ion source. This seems quite reasonable considering that ionized keto acids have a very weak or no molecular ion (cf. the NR spectrum of pyruvic acid, Fig. 4-4b).

A further clue to our m/z 60 problem comes from the behaviour of $HOOCCH(OH)CH_2COOH$, malic acid, a compound akin to OAA, but which does not suffer from any thermal decomposition during evaporation. Malic acid's EI mass spectrum displays no detectable molecular ion at m/z 134 but it does show a prominent m/z 60 peak (~20 % of base peak, m/z 89), whose CID mass spectrum appears to be closely similar to that presented in Fig. 4-6a ! (compatible with a 10 : 1 mixture of $\mathbf{5a}^{\bullet+}$ and $\mathbf{5b}^{\bullet+}$).

Formation of its m/z 60 ions can be envisaged to occur as proposed in Scheme 4a.

Scheme 4a

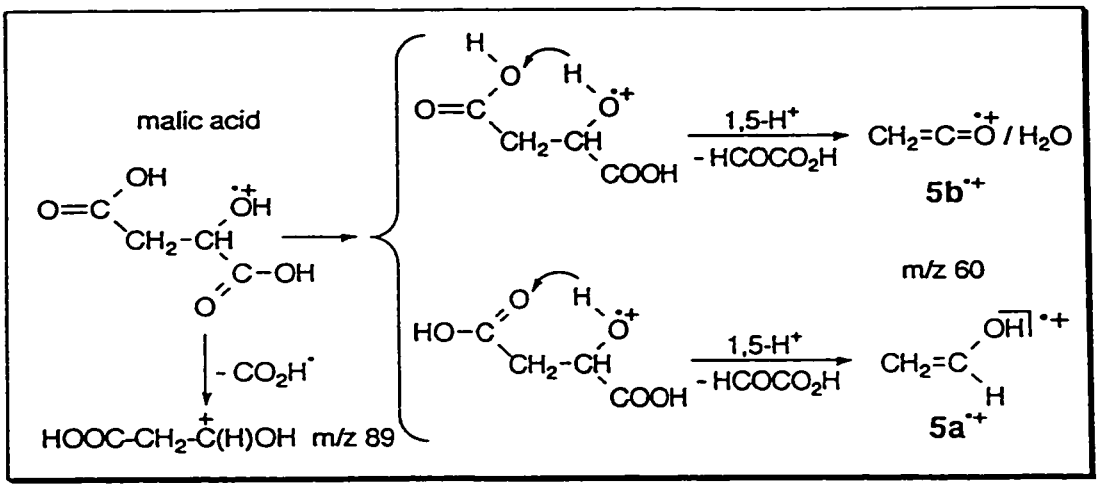

At first sight it may seem surprising that the rearrangement yields two product ions which differ considerably in stability - ion $\mathbf{5b}^{\bullet+}$ is 18 kcal/mol higher in energy than $\mathbf{5a}^{\bullet+}$ [14,19] - but it should be noted that the dissociation is undoubtedly exothermic and is best formulated as a proton rather than a hydrogen radical transfer.

By analogy, we propose that the m/z 60 ions in the spectrum of OAA are generated as depicted in Scheme 4b.

Scheme 4b

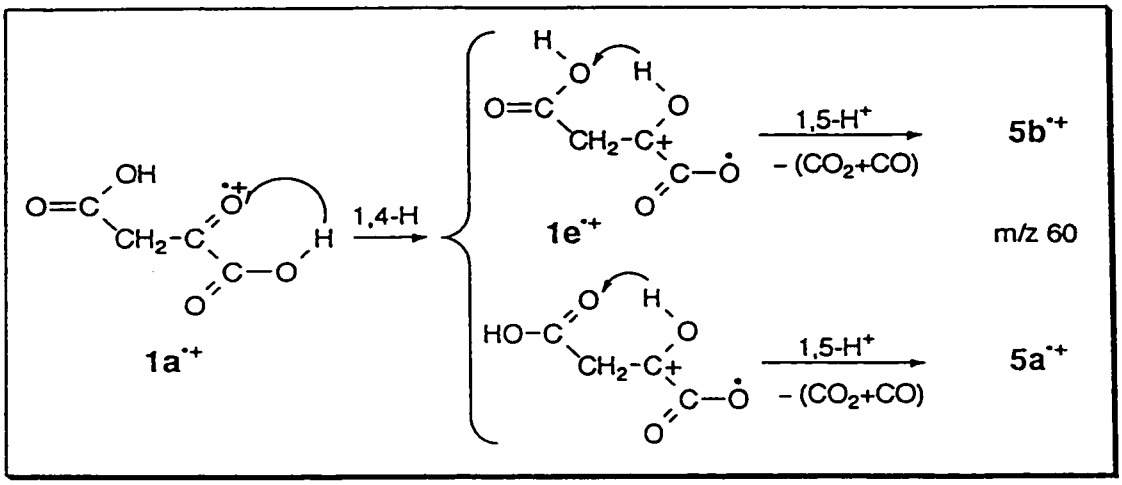

In the above scenario for the formation of the m/z 88 and m/z 60 ions we have tacitly assumed that the keto form is generated during the evaporation of the sample and thus is absent in the original sample. This point will be addressed in the last section (**vi**) but first we will consider the structure and origin of the m/z 114 ions present in the mass spectra of "bulk" samples, see Fig. 4-1a.

(v) The m/z 114 ions : ionized hydroxymaleic anhydride resulting from a slow thermal dehydration.

As discussed in section (i), the m/z 114 ion is **not** present in OAA mass spectra obtained from submilligram samples and so it is not a truly representative fragment ion of OAA.

We propose that the m/z 114 ions have the structure of ionized hydroxymaleic anhydride, ion $\mathbf{3a}^{\bullet+}$ in Scheme 5a below, and that it is a thermal dehydration product of the acid. Evidence for this structure assignment comes from the following :

1. The mass spectrum of an authentic sample of the (pyridine salt of) the anhydride [2c] was obtained, which shows principal ions at m/z 114 [$M^{\bullet+}$,17 %], 70 [loss of CO_2, 75 %], 69 [loss of $CO_2H^{\bullet}$, 95 %] and m/z 42 [$C_2H_2O^{\bullet+}$, 100 %]. Next, CID mass spectra of these ions were obtained and these were indistinguishable from those obtained from the corresponding ions derived from OAA. The CID mass spectrum of the m/z 69 ions (not shown) was easily identified as that of $[O{=}C{=}CH{-}C{=}O]^{+}$ [13], that of the other ions is presented as items (a) to (c) in Fig. 4-8. The spectrum of the m/z 42 ions, item (c) in Fig. 4-8, clearly is that of the high energy ketene isomer $H{-}C'C{-}OH^{\bullet+}$ [20]. *This removes any doubt that the enolic anhydride converts into its keto form prior to ionization.*
2. The m/z 42 ions in the m/z 70 CID mass spectra were subjected to a collision experiment and the resulting spectrum (not shown) was very close to that presented in Fig. 4-8(c), thus showing that the ketene isomer hydroxyacetylene is the product ion generated.

Figure 4-8. Collision-induced dissociation (CID) mass spectra of source generated ions from ionized hydroxymaleic anhydride : (a) m/z 114, (b) m/z 70 and (c) m/z 42.

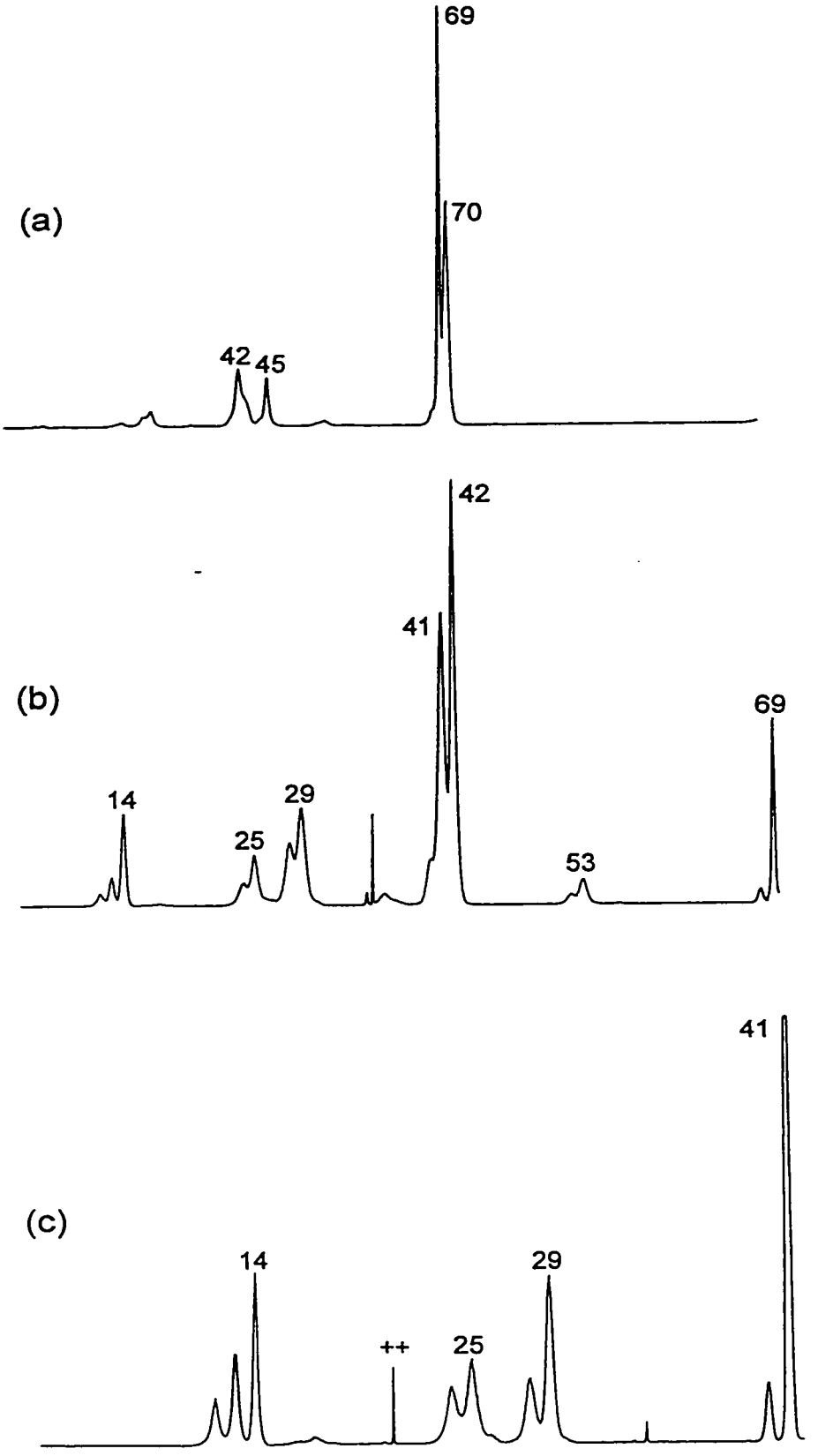

These observations leave little doubt that the m/z 114 ions in the OAA mass spectrum Fig. 4-1a have the structure of ionized hydroxymaleic anhydride whose major dissociations are rationalized in the following Scheme :

Scheme 5a

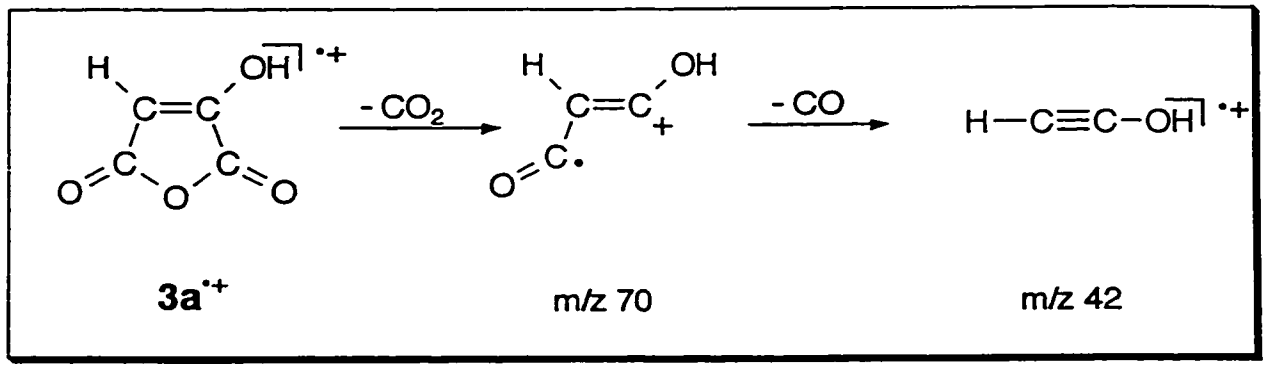

In agreement with this proposal is the observation that the ^{18}O label is retained in the dehydration of the ^{18}O isotopomer HOOCC(^{18}OH)=CHCOOH and that the ionized dehydration product shows atom specific losses of $C^{16}O_2$ and $C^{16}O_2H^{\bullet}$ in its CID mass spectrum.

What is the origin of these hydroxymaleic anhydride ions? It seems obvious that they originate from direct ionization of the neutral anhydride generated by thermal dehydration of OAA. However, it is less clear which of the three OAA isomers serves as the immediate precursor for the dehydration (and also why this process only occurs during the evaporation of the "bulk" sample). Scheme 4-5b presents two reasonable possibilities : (i) the (Z)-enol, **1b**, undergoes the thermal dehydration via a mechanism analogous to the (facile and reversible) hydration of acylketenes [21], i.e. water loss occurs via a 6-membered transition state to yield the ketene **3b** which readily undergoes cyclization and concomitant intermolecular proton transfer to yield the anhydride **3a**; (ii) the keto form of the acid partially enolizes to **1c**, which has a geometry favouring a facile loss of water to directly generate **3a**. Note, however, that the second possibility can only be entertained if dehydration of the incipient (E)-enol,**1c**, in the solid is much faster than its evaporation : the experiments described in section (ii) clearly show that the ionized (E)-enol is not present in the gas phase.

Scheme 5b

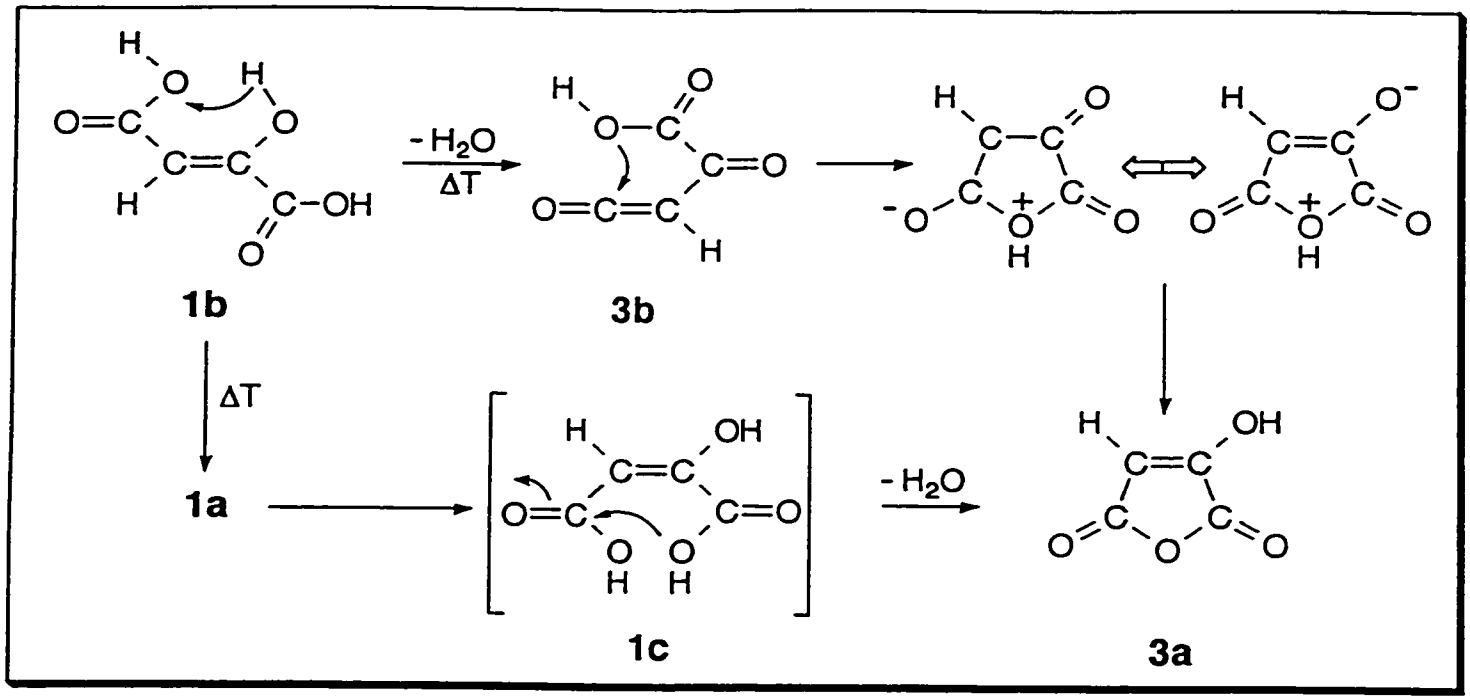

Comparison of the mass spectra (a) and (b) in Fig. 4-1 and the associated sample introduction procedures, shows that the "bulk" sample procedure not only leads to dehydration but also to a considerably higher degree of decarboxylation, as witnessed by the enhanced intensities of m/z 88 and 44 ($CO_2^{\bullet+}$). Since the ion chamber temperature does not greatly affect the spectra obtained from submilligram samples, it seems likely that the dehydration and decarboxylkation reactions occur in the solid, i.e. prior to evaporation. Now, when the probe tubes with the samples are heated (by the combined effect of radiative heat transfer from the chamber and the sample heater of the probe) poor heat dissipation may cause higher local temperatures in the "bulk" samples than in thin films, thus promoting decomposition. Another contributing factor could be the presence of traces of water in the samples. In the evaporation of thin film samples any moisture present in the sample is quickly pumped off. In contrast, the moisture present in a "bulk" sample has to diffuse through a thick layer of sample and so may long remain trapped in the sample, as witnessed by a persistent intense m/z 18 peak in the mass spectra, and where it could promote the ketonization of OAA.

(vi) Summary and conclusions

The mass spectrometry based experiments on commercial OAA samples described above lead to the following conclusions :

(i) the samples contain a minor impurity in the low % range, tentatively assigned as a dehydration product of 4-hydroxy-4-methyl-2-ketoglutaric acid.

(ii) careful evaporation of the solid OAA samples yields mass spectra representative of the (Z)-enol form **1b**. The (E)-enol is not present in the solid, nor is it generated in the gas phase via isomerization of the ionized (Z)-enol form. However, even under gentle sample introduction conditions, a partial ketonization of the neutral (Z)-enol takes place. The resulting keto OAA molecules are either ionized as intact molecules or decarboxylate to yield a mixture of α-hydroxyacrylic acid and its keto isomer pyruvic acid.

(iii) under less controlled sample introduction conditions, thermal dehydration may also take place to yield M=114 molecules whose mass spectral characteristics are indistinguishable from that of ionized hydroxymaleic anhydride.

To verify our conclusion that the partial ketonization of the OAA (Z)-enol takes place during the evaporation of the sample, i.e. that the keto form is **not** present in the original sample, we have obtained a solid state ^{13}C NMR spectrum. Flint et al. [3] have reported ^{13}C NMR spectra of OAA dissolved in acetone and concluded from their thorough analysis of the data that at room temperature both the keto and the (Z)-enol form are present, with chemical shifts characteristic of the keto form, $HOOC^1C^2(=O)C^3(H_2)C^4OOH$, at δ = 161.60 ($C^1$), 189.22 ($C^2$), 45.12 ($C^3$), 168.36 ($C^4$) , and for the (Z)-enol form, $HOOC^1C^2(OH)C^3(H)C^4OOH$, at δ = 162.85 ($C^1$), 161.81 ($C^2$), 96.51 ($C^3$), 174.18 ($C^4$). Our solid state spectrum showed only four signals, at 167.95, 159.33, 98.69 and 177.46, which is entirely compatible with solid OAA samples of a > 95 % purity having the structure of the (Z)-enol.

Experimental

The OAA samples used in this study were obtained from Aldrich (two different batches, m.p. 162 °C) and Fluka (m.p. 157 °C). The ^{18}O OAA isotopomer was prepared on a mg scale by equilibration of the acid with $H_2{}^{18}O$ (90 % ^{18}O, 3.7 % ^{17}O) (Ventron GMBH,

Karlsruhe) at room temperature for c. 30 min. The pyruvic acid sample came from Eastman and was used without further purification. The pyridine salt of hydroxymaleic anhydride was synthesized from diacetyltartaric anhydride (Aldrich) using the procedure described in ref. 2c.

The mass spectrometric experiments were performed with the McMaster University VG Analytical (Manchester, UK) ZAB-R instrument of BE_1E_2 geometry (B, magnet; E, electric sector) [22] using an accelerating voltage of 8 or 10 keV. Metastable ion (MI) mass spectra were recorded in the second field-free region (2ffr) ; Collision-induced dissociation (CID) mass spectra were recorded in the 2 and 3ffr using oxygen as collision gas (transmittance T = 70%). Neutralization-reionization (NR) spectra were recorded in the 2ffr using N,N-dimethyl-aniline as reducing agent and oxygen gas for reionization. All spectra were recorded using a small PC-based data system developed by Mommers Technologies Inc. (Ottawa). The CID mass spectra in Fig. 4-3 and Fig. 4-4c have been corrected for MI contributions to the m/z 60 signal. The relative proportion of the two isomeric m/z 60 ions represented by Fig. 4-6b was evaluated on the basis of the collision efficiencies of the pure reference ions and corrected for the contribution of unlabelled material. Ionization energy measurements were performed on an AEI MS 902 mass spectrometer, using the IE of benzene as the electron energy calibrant.

The computational quantum chemistry procedure used to obtain ΔH_f values for α-hydroxyacrylic acid, **2a**, and pyruvic acid, **2b**, involved the following : for the enol the neutral conformers were investigated by the B3LYP/ 6-31G* hybrid density functional method [23] in the Gaussian 94 package of programs [24]. The most stable conformer was found to be planar, with both hydroxylic hydrogens oriented towards the carbonyl of the carboxylic acid group. This conformer was then used in a CBS-4 [25] (Complete Basis Set) type calculation which yielded ΔH_f^{298} = - 124.1 kcal/mol for the most stable conformer of **2a** (- 119.2 kcal/mol @ 0 K). For pyruvic acid CBS-4 calculations were performed on two of its conformers, both having (except for two of the methylic hydrogens) almost planar geometries with the carbonyl groups in the *trans* position. The conformer of lowest energy had the hydroxylic H bridging with the keto-carbonyl in a geometry closely similar to that derived from microwave experiments [26]. Its derived

ΔH_f^{298} value was -130.9 kcal/mol (-126.0 kcal/mol @ 0 K) whereas the non H-bridged conformer yielded -128.5 kcal/mol (-123.7 kcal/mol @ 0 K).

The high-powered proton-decoupled solid state ^{13}C NMR spectrum of OAA was run at 25.18 MHz at a magnetic field strength of 2.35 T on a Bruker MSL 100 spectrometer with cross polarization and magic angle spinning (CP-MAS). The sample was contained in a 7 mm (OD) alumina oxide rotator and spun at a rate of 4 kHz.

References

1. (a) A. Wohl and C. Oesterlin, Chem. Ber., 34 (1901) 1139. (b) A. Wohl , Chem. Ber., 40 (1907) 2282. (c) A. Wohl and P. Claussner, Chem. Ber., 40 (1907) 2308.
2. (a) C. Heidelberger and R.B. Hurlburt, J. Am. Chem. Soc., 72 (1950) 4704. (b) C. Heidelberger, Biochem. Prepn., 3 (1953) 59. (c) J.C. Roberts, J. Chem. Soc., (1952) 3315.
3. D.H. Flint, A. Nudelman, J.C. Calabrese and H.E. Gottlieb, J. Org. Chem., 57 (1992) 7270.
4. (a) The Merck Index , S. Budavari (Ed.), Merck & Co., Inc., Rahway, N.J.,1989, entry 6863 ; the same information is presented under entry 7041 in the latest (1996) edition. (b) H. Beyer and W. Walter, Lehrbuch der Organischen Chemie, S. Hirzel Verlag,Stuttgart, 1988, Chapter 2, p. 351.
5. W. Gruber, G. Pfleiderer and T. Wieland, Biochem. Z., 328 (1956) 245.
6. B.E.C. Banks, J. Chem. Soc., (1961) 5043.
7. (a) R.H. Wiley and K-S Kim, J. Org. Chem., 38 (1973) 3582. (b) G. Buldain, C. de los Santos and B. Frydman, Magn. Reson. Chem., 23 (1985) 478.
8. J. Hrusak, G.A. McGibbon, H. Schwarz and J.K. Terlouw, Int. J. Mass Spectrom. Ion Processes, 1997, in press.
9. (a) K.R. Jennings, Int. J. Mass Spectrom. Ion Phys. 1 (1968) 227 . (b) W.F. Haddon and F.W. McLafferty, J. Am. Chem. Soc., 90 (1968) 4745. (c) For a recent review see : N. Goldberg and H. Schwarz, Acc. Chem. Res., 27 (1994) 34.
10. (a) F. Benoit, J.L. Holmes and N.S. Isaacs, Org. Mass Spectrom., 2 (1969) 591. (b) C.H. Chen and J.L. Holmes, J. Mass Spectrom., 30 (1995) 1083.
11. J.S. Splitter and F. Tureçek (Ed.) Applications of Mass Spectrometry to Organic Stereochemistry, VCH, Weinheim, 1994.
12. (a) F.C. Kokesh, J. Org. Chem., 41 (1976) 3593. (b) M. Cocivera, F.C. Kokesh, V. Malatesta and
J.J. Zinck, J. Org. Chem., 42 (1977) 4076.
13. J. Tortajada, G. Provot, J.-P. Morizur, J.-F. Gal, P.-C. Maria, R. Flammang and Y. Govaert, Int. J. Mass Spectrom. Ion Proc., 141 (1995) 241.
14. (a) S. Lias, J.E. Bartmess, J.F. Liebman, J.L. Holmes, R.D. Levin and W.G. Mallard. J. Phys. Chem. Ref. Data, 17 (1988) Supplement 1. (b) P.C. Burgers and J.L. Holmes, Org. Mass Spectrom., 17 (1982) 123.
15. M.J.S. Dewar and C.H. Reynolds, J. Comp. Chem., 2 (1986) 140 and references cited therein.
16. P. Sykes, A guidebook to mechanism in organic chemistry, Longman Scientific & Technical, Harlow, England, 1986, p. 286.
17. G.W.A. Milne, Mass Spectrometry : Techniques and Applications, Wiley-Interscience, London, 1971, p. 279.
18. J.K. Terlouw, C.G. de Koster, W. Heerma, J.L. Holmes and P.C. Burgers, Org. Mass Spectrom., 18 (1983) 222.
19. R. Postma, P.J.A. Ruttink, J.K. Terlouw and J.L. Holmes, J. Chem. Soc., Chem. Commun., 683 (1986).
20. B.L.M. van Baar, T. Weiske, J.K. Terlouw and H. Schwarz, Angew. Chem. Int. Ed. Engl., 25 (1986) 282.
21. A.D. Allen, M.A. McAllister and T.T. Tidwell, Tetrahedron Letters, 34 (1993) 1095.
22. H.F. van Garderen, P.J.A. Ruttink, P.C. Burgers, G.A. McGibbon and J.K. Terlouw, Int. J. Mass Spectrom. Ion Processes, 121 (1992) 159.

23. (a) A.B. Becke, J. Chem. Phys., 98 (1993) 5648. (b) C. Lee, W. Yang and R.G. Parr, Phys. Rev. B, 37 (1988) 785. (c) B. Meihlich, A. Savin, H. Stoll and H. Preuss, Chem. Phys. Lett., 157 (1989) 200.
24. Gaussian 94, Revision B.3, M. J. Frisch, G.W. Trucks, H.B. Schlegel, P.M.W. Gill, B.G. Johnson, M.A. Robb, J.R. Cheeseman, T.A. Keith, G.A. Peterson, J.A. Montgomery, K. Raghavachari, M.A. Al-Laham, V.G. Zakrevski, J.V. Ortiz, J.B. Foresman, C.Y. Peng, P.Y. Ayala, W. Chen, M.W. Wong, J.L. Andres, E.S. Replogle, R. Gomperts, R.L. Martin, D.J. Fox, J.S. Binkley, D.J. de Frees, J. Baker, J.P. Stewart, M. Head-Gordon, C. Gonzales and J.A. Pople, Gaussian Inc., Pittsburgh PA, 1995.
25. J.W. Ochterski, G.A. Petersson and J.A. Montgomery Jr., J. Chem. Phys., 104 (1996) 2598 and references cited therein.
26. (a) C.E. Kaluza, A. Bauder and Hs. H. Günthard, Chem. Phys. Lett., 22 (1973) 454. (b) K.-M. Marstokk and H. Møllendal, J. Mol. Struc., 20 (1974) 257.

CHAPTER 5

THE DECARBONYLATION OF IONIZED β-HYDROXYPYRUVIC ACID : THE HYDROGEN-BRIDGED RADICAL CATION $[CH_2{=}O{\bullet\bullet\bullet}H{\bullet\bullet\bullet}O{=}C\text{-}OH]^{\bullet+}$ STUDIED BY EXPERIMENT AND THEORY[1]

Abstract

The intriguing gas-phase ion chemistry of β-hydroxypyruvic acid (HPA), $HOCH_2C(=O)COOH$, has been investigated using tandem mass spectrometry - Metastable Ion (MI) and (multiple) Collision Induced Dissociation (CID) experiments, Neutralization- Reionization Mass Spectrometry (NRMS), ^{18}O and D isotopic labelling on both the acid and its methyl ester - in conjunction with computational chemistry (*ab initio* MO and density functional theories).

HPA does not enolize upon evaporation but it retains its keto structure. When ionized, decarbonylation occurs and depending on the internal energy content, this dissociation reaction proceeds via two distinct routes.

The source generated, high energy ions lose the keto C=O, not *via* a least-motion extrusion into ionized glycolic acid, $HOCH_2COOH^{\bullet+}$, but *via* a rearrangement that yields the title H-bridged radical cation $CH_2{=}O{\bullet\bullet\bullet}H{\bullet\bullet\bullet}O{=}C\text{-}OH^{\bullet+}$ for which $\Delta H_f^o = 99 \pm 3$ kcal/mol.

The long-lived low energy ions enolize prior to decarbonylation and lose the carboxyl C=O. Again, this is not a least-motion extrusion (which would produce the most stable isomer, $HOC(H){=}C(OH)_2^{\bullet+}$, $\Delta H_f^o = 73$ kcal/mol) but a rearrangement yielding the ion-dipole complex $HOC(H)C{=}C{=}O^{\bullet+}/H_2O$. The methyl ester of HPA behaves analogously, yielding $CH_2{=}O{\bullet\bullet\bullet}H{\bullet\bullet\bullet}O{=}C\text{-}OCH_3^{\bullet+}$ and $HOC(H)C{=}C{=}O^{\bullet+}/CH_3OH$ upon decarbonylation of the high and low energy ions, respectively.

Decarboxylation into the ylidion $CH_2OH_2^{\bullet+}$ characterizes the dissociation chemistry of both the title H-bridged ion and its glycolic acid isomer $HOCH_2COOH^{\bullet+}$. A computational analysis of this reaction (which satisfies the experimental observations) leads to the proposal that the decarboxylation of the acid occurs via $CH_2\text{-}O(H){\bullet\bullet\bullet}H{\bullet\bullet\bullet}O{=}C{=}O^{\bullet+}$ as the key intermediate, whereas the title H-bridged ion follows a

[1] This chapter has already appeared in print under the same title: L.M. Fell, P.C. Burgers, P.J.A. Ruttink and J.K. Terlouw, *Can. J. Chem.*, **76** (1998) 335-349.

higher energy route that involves ion-dipole rotations leading to the ionized carbene $HO(H_2)CO\text{-}C\text{-}OH^{\bullet+}$ and the distonic ion $H_2O\text{-}C(H_2)\text{-}O\text{-}C{=}O^{\bullet+}$ as key intermediates.

Introduction

In the context of ionic rearrangements, hydrogen-bridged radical cations [1], particularly O•••H•••O and N•••H•••O bonded ions are being proposed with increasing frequency as intermediates to rationalize the dissociation behaviour of low energy radical cations. This growing realization [2] follows findings from both theory and experiment that such hydrogen-bridged species can be thermodynamically more stable than the non - rearranged reactant, which makes them energetically attractive intermediates. *Ab initio* calculations on such species do not only attest to their stability, they also confirm the intuitive expectation that the bridging H in these complexes is more closely connected to the moiety of higher proton affinity (PA). In fact, such (necessarily asymmetric) O•••H•••O bridged radical cations can best be described as H-bridged ion-dipole complexes of the type $[M•••H\text{-}R]^{\bullet+}$ or $[M\text{-}H•••R]^{\bullet+}$ (M = molecule, R = radical), where most of the stabilization energy is provided by ion-dipole interactions. As shown in recent studies on ionized ethylene glycol, $HOCH_2CH_2OH^{\bullet+}$ [3], acetol, $CH_3C(=O)CH_2OH^{\bullet+}$ [4] and several related molecules [5], the O•••H•••O intermediates undergo a facile isomerization leading to C-H•••O bridged ions and these are the key intermediates in the low energy dissociation reactions of the molecular ions. Such C-H•••O species are not as stable as their O•••H•••O bonded counterparts, but calculations indicate that they can be easily formed from O•••H•••O bonded ions by a dipole-catalyzed proton shift [3,4], a process which is identical to Bohme's concept of "proton-transfer catalysis" [6]. In a recent experimental study [7] it was observed that the isomerization $CH_3OH^{\bullet+} \rightarrow CH_2OH_2^{\bullet+}$, which does not occur unassisted, can be catalyzed by the addition of water ; this constitutes a prime example of "proton-transport catalysis" which has recently been confirmed and elegantly rationalized by the *ab initio* computational studies of Radom and coworkers [7c-e].

Despite their role as key intermediates in dissociation reactions, only relatively few H-bridged radical cations have been characterized as stable product ions, in part because of the experimental difficulties to differentiate such ions from their distonic counterparts

[1c]. The well characterized species include the vinylalcohol/water and methanol ions CH_2=C(H)O•••H•••$OH_2^{+\bullet}$ and CH_2=C(H)O•••H•••$HOCH_3^{+\bullet}$ [2], the carbonic acid isomer HO•••H•••O=C=$O^{+\bullet}$ [8], CH_3(H)O•••H•••O=C-$H^{+\bullet}$ [9], which is also a key intermediate in the dissociation chemistry of ionized ethylene glycol [3] and most recently H_2O•••H•••O=C-$OH^{+\bullet}$. The latter ion was shown in a combined experimental and theoretical study to be the stable product ion formed by the consecutive loss of three CO molecules from HOOC(OH)=C(OH)$COOH^{+\bullet}$, ionized dihydroxyfumaric acid (ΔH_f) [10].

In the present study we report on the identification of a related H-bridged radical cation, *viz.* CH_2=O•••H•••O=C-$OH^{+\bullet}$, which forms part of the $C_2H_4O_3^{+\bullet}$ (m/z 76) system of ions and which *inter alia* comprises ionized glycolic acid, $HOCH_2COOH^{+\bullet}$, and its enol $HOC(H)=C(OH)_2^{+\bullet}$ [11] as members whose neutral counterpart are molecules of conventional structure. A combination of tandem mass spectrometric techniques (Metastable Ion (MI), Collision Induced Dissociation (CID), Neutralization-Reionization Mass Spectrometry (NRMS) and MS/MS/MS experiments) and computational chemistry (using *ab initio* MO and density functional theories) is used to show that the decarbonylation of ionized β-hydroxypyruvic acid (HPA), $\mathbf{1}^{+\bullet}$, does **not** lead, via a least-motion extrusion, to ionized glycolic acid, $\mathbf{2}^{+\bullet}$, nor to its enol, $\mathbf{1}^{+\bullet}$, but rather to the H-bridged radical cation $\mathbf{3a}^{+\bullet}$:

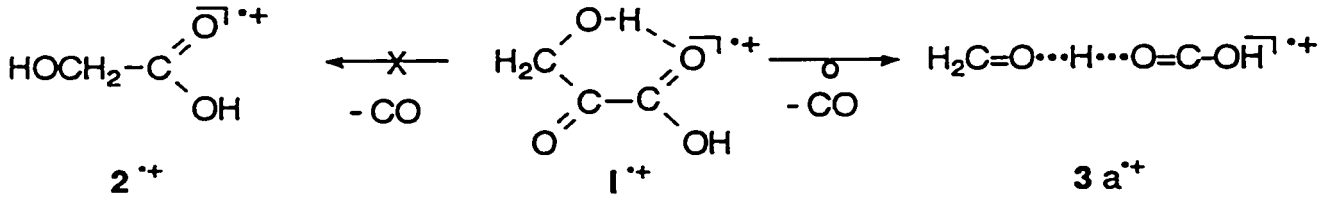

This H-bridged ion has two closely related isomers, *viz.* CH_2=O•••H•••O(H)-C=$O^{+\bullet}$, $\mathbf{3b}^{+\bullet}$ and $CH_2O(H)$•••H•••O=C=$O^{+\bullet}$, $\mathbf{3c}^{+\bullet}$ of which the latter, as shown in the theoretical section below, is by far the most stable. Since formation of $CH_2OH_2^{+\bullet}$ and CO_2 represents the dissociation reaction of lowest energy requirement in $\mathbf{3a}^{+\bullet}$ and also in $\mathbf{2}^{+\bullet}$, the participation of $\mathbf{3c}^{+\bullet}$ in their isomerization *cum* dissociation reactions will be considered using results of *ab initio* MO theoretical calculations.

The above scenario refers to the decarbonylation reaction in the ion source, i.e. the loss of CO from high energy HPA ions. Low energy (metastable) HPA ions also lose CO

but , it will be shown, from molecular ions that have isomerized into their enol counterpart, *viz.* ionized 1,2-dihydroxyacrylic acid, $\mathbf{II}^{\bullet+}$:

$$\underset{\mathbf{I}^{\bullet+}}{HOCH_2\text{-}C(=O)\text{-}COOH^{\bullet+}} \xrightarrow{-O} \underset{\mathbf{II}^{\bullet+}}{HOC(H)=C(OH)\text{-}COOH^{\bullet+}} \xrightarrow[-CO]{-O} \underset{\mathbf{4}^{\bullet+}}{HO(H)C=C=O^{\bullet+}} / H_2O$$

The resulting product ion is not the H-bridged species $\mathbf{3a}^{\bullet+}$ but the more stable ion-dipole complex $\mathbf{4}^{\bullet+}$ whose dissociation chemistry is related to that of the enol ion $HOC(H)=C(OH)_2^{\bullet+}$, $\mathbf{1}^{\bullet+}$, [11].

The principal precursor molecule used in this study, β-hydroxypyruvic acid, has been the subject of numerous biochemical studies [12,13] but unlike pyruvic acid itself, HPA is a thermally labile compound that decomposes vigorously at its melting point, 82 °C [13a].

This facile decomposition of the pure solid at elevated temperatures is a decarboxylation that also occurs in aqueous solutions of varying acidity at room temperature where it has been proposed [13c,d] to yield glycol aldehyde, $HOCH_2CHO$, as the final reaction product. HPA's reaction in the solid melt may well occur analogously to that established for the decarboxylation of oxalacetic acid [14] i.e. as shown in Scheme 1 :

Scheme 1

$$\underset{\mathbf{I}}{HOCH_2\text{-}C(=O)\text{-}COOH} \rightleftharpoons \underset{\mathbf{II}}{HOC(H)=C(OH)\text{-}COOH} \rightleftharpoons \underset{\mathbf{III}}{H\text{-}C(=O)\text{-}C(H)OH\text{-}COOH}$$

$$HOCH_2\text{-}C(=O)H \;\text{<}\!\text{- - -}\; HOC(H)=C(H)OH \xleftarrow[\Delta T]{-CO_2} \mathbf{III}$$

In this context we note that the statement in entry H-0-03641 of the latest edition of the Dictionary of Organic Compounds [15] that HPA would consist of an equilibrium mixture of **I** with its enol 1,2-dihydroxyacrylic acid, **II**, is clearly incorrect. The IR spectroscopic findings of Bellamy and Williams [13b], the polarographic and UV results of Fleury et al. [13e] and also the results of our own deuterium incorporation experiments described in the Experimental section, leave little doubt that at room temperature solid β-hydroxypyruvic acid and aqueous solutions thereof consist of the keto structure **I.**

Results and Discussion

(i) Conventional EI mass spectra of β-hydroxypyruvic acid : thermal decarboxylation vs electron impact induced decarbonylation.

The rather striking differences between the mass spectra displayed in Figures 5-1a and b, illustrate how strongly the EI mass spectrum of HPA (M = 104) depends upon the method of sample introduction. Fig. 5-1a is representative of a typical spectrum obtained from a "bulk" sample introduced at the lowest possible temperature (see Experimental for further details). The overall appearance of the spectrum obtained under these conditions remained fairly constant. The spectrum displays a molecular ion at m/z 104 and, in the absence of further information, most of the other peaks including the base peak at m/z 31, CH_2OH^+, can readily be assigned as fragment ions generated from $\mathbf{I}^{\bullet+}$.

Fig. 5-1b shows the spectrum obtained from the same sample but now using a much higher source temperature, 170 °C. Comparison with Fig. 5-1a shows that the relative intensity of the signals at m/z 60 and m/z 44 has greatly increased. CID spectra of these ions were obtained (spectra not shown) and comparison with reference spectra [16a] shows that the m/z 60 ions are a mixture of $HOCH{=}C(H)OH^{\bullet+}$ and $HOCH_2CHO^{\bullet+}$, whereas the m/z 44 ions are $CO_2^{\bullet+}$.

Thus at elevated temperatures **I** is prone to decarboxylate and the structure of the reaction products supports the mechanism presented in Scheme 1 of the Introduction.

On the other hand, the decarbonylation responsible for the m/z 76 ions appears to be a genuine electron impact induced process. This reaction is even more prominent in the EI spectrum of the methyl ester of **I** [17] which does not suffer from thermal decarboxylation and which is sufficiently volatile to be introduced into the ion source as

vapour at room temperature. As will be shown in detail elsewhere [17], the molecular ions of the methyl ester decarbonylate via two distinct mechanisms yielding product ions of a different structure, see Scheme 2 : at high internal energies (source generated ions) the product ion is the H-bridged radical cation CH_2=O•••H•••O=C-$OCH_3^{\bullet+}$ [5a] whereas the low energy molecular ions (metastable ions) also produce this ion, but as further discussed in section (v), these ions are produced in admixture with the more stable isomer $HO(H)C=C=O^{\bullet+}/CH_3OH$ [9]. The latter ion's generation involves a slow isomerization of the keto molecular ion into its enolic counterpart which then loses CO via a mechanism analogous to that for the decarbonylation of ionized CH_2=C(OH)$COOH^{\bullet+}$ which was recently shown [14] to specifically yield $CH_2=C=O^{\bullet+}/H_2O$ and not the more stable isomer $CH_2=C(OH)_2^{\bullet+}$.

A similar situation obtains, we propose, for the parent acid **I** : Fig. 5-1c shows the CID mass spectrum of $\mathbf{I}^{\bullet+}$ and even a cursory inspection indicates that the (majority of the) HPA molecular ions must have lost their parent keto structure as witnessed by the greatly reduced intensity of the m/z 31 CH_2OH^+ ion and the appearance of the prominent peak at m/z 58, $HO(H)C=C=O^{\bullet+}$ (structure identified from a MS/MS experiment and comparison with reference spectra [9], result not shown). It will be shown in section (v) that most of these long lived ions have rearranged to the enol $HOC(H)=C(OH)COOH^{\bullet+}$, $\mathbf{II}^{\bullet+}$.

Fig. 5-2 shows the CID mass spectra of the source generated m/z 76 M-CO ions (item a) along with that of the m/z 76 ions found in the MI spectrum of the molecular ions (item b) . Also given are the CID mass spectra of the isomeric ions $HOC(H)=C(OH)_2^{\bullet+}$, $\mathbf{1}^{\bullet+}$ and $HOCH_2COOH^{\bullet+}$, $\mathbf{2}^{\bullet+}$, whose ion chemistry has been discussed in considerable detail in a previous study [11]. Comparison of the four spectra shows (i) that the source generated m/z 76 ions from HPA are neither $\mathbf{2}^{\bullet+}$ nor its enol nor a mixture thereof and (ii) that the structure of the low energy m/z 76 ions from $\mathbf{I}^{\bullet+}$ must be different from that of the source generated ions and that it is akin to that of the ionized enol $\mathbf{1}^{\bullet+}$. Thus the source generated ions and the metastably generated ions (high and low energy ions) appear to have different structures (and also different precursor structures) and we will therefore deal with these in different sections.

Figure 5-1. EI mass spectrum of β-hydroxypyruvic acid (**I**) : item a : obtained from a "bulk" sample at an ion source temperature of 110 °C, see text, item b : ibid., using an ion source temperature of 170 °C ; item c : CID mass spectrum [2ffr,O_2] of $\mathbf{I}^{\bullet+}$; item d : Neutralization -Reionization (NR) mass spectrum of $\mathbf{I}^{\bullet+}$ (S denotes the Survivor ion).

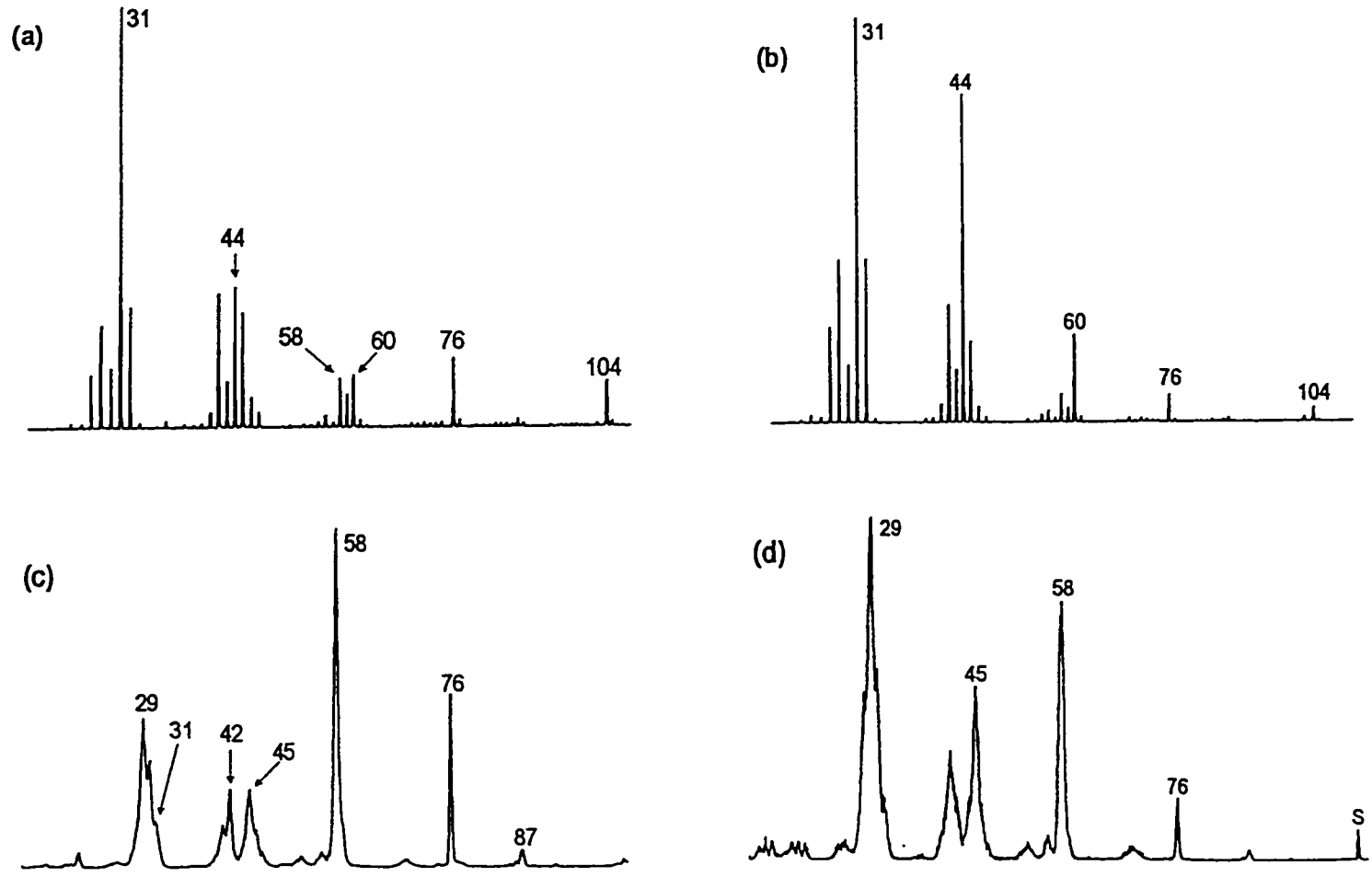

Scheme 2

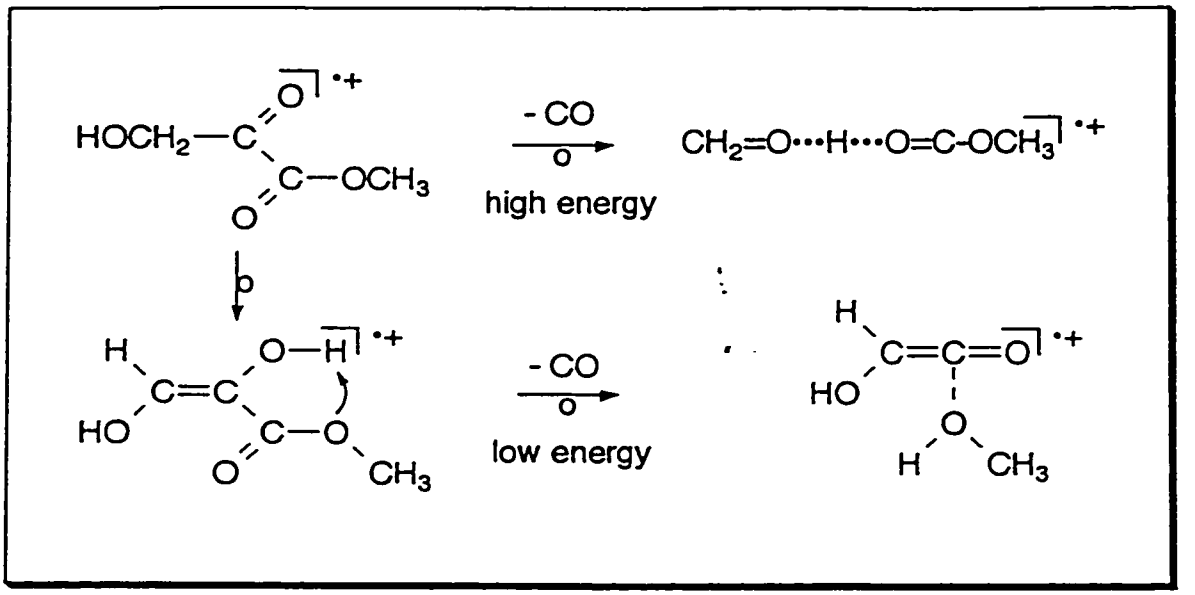

(ii) The decarbonylation of high energy HPA ions : generation of the H-bridged radical cation CH_2=O•••H•••O=C-OH$^{\bullet+}$, 3a$^{\bullet+}$.

The CID mass spectrum of the m/z 76 $C_2H_4O_3^{\bullet+}$ ions generated from HPA, **I**$^{\bullet+}$, shows a tell-tale peak at m/z 46, $C(OH)_2^{\bullet+}$, which differentiates this spectrum from that of the two isomers of conventional structure, *viz.* ionized glycolic acid, **2**$^{\bullet+}$, and its more stable enol **1**$^{\bullet+}$. The MI spectrum of the m/z 76 ions is dominated by a signal at m/z 32, $CH_2OH_2^{\bullet+}$, (ion structure established by a MS/MS experiment, result not shown) and m/z 46 is completely absent. Further, the threshold energy for the most prominent dissociation taking place upon collisional activation, 76$^{\bullet+}$ → CH_2OH^+ (m/z 31) + HOCO$^{\bullet}$, 122 kcal/mol [18], is considerably lower than that for the formation of m/z 46, i.e. 149 kcal/mol [18a] for 76$^{\bullet+}$ → $C(OH)_2^{\bullet+}$ + CH_2=O. That the m/z 46 ions are ionized dihydroxycarbene ions and not the isomeric ionized formic acid, H-C(=O)OH$^{\bullet+}$, follows from a MS/MS experiment, see Fig. 5-3a , and comparison with reference spectra of the two isomeric ions [19].

Figure 5-2. CID mass spectra of the $[M\text{-}CO]^{\bullet+}$ ions (m/z 76) from ionized β-hydroxypyruvic acid, $\mathbf{I}^{\bullet+}$: item a : **source** generated ions , item b : **metastably** generated ions. Items (c) and (d) represent reference spectra of ionized trihydroxyethylene, $\mathbf{1}^{\bullet+}$, and ionized glycolic acid, $\mathbf{2}^{\bullet+}$, respectively [9].

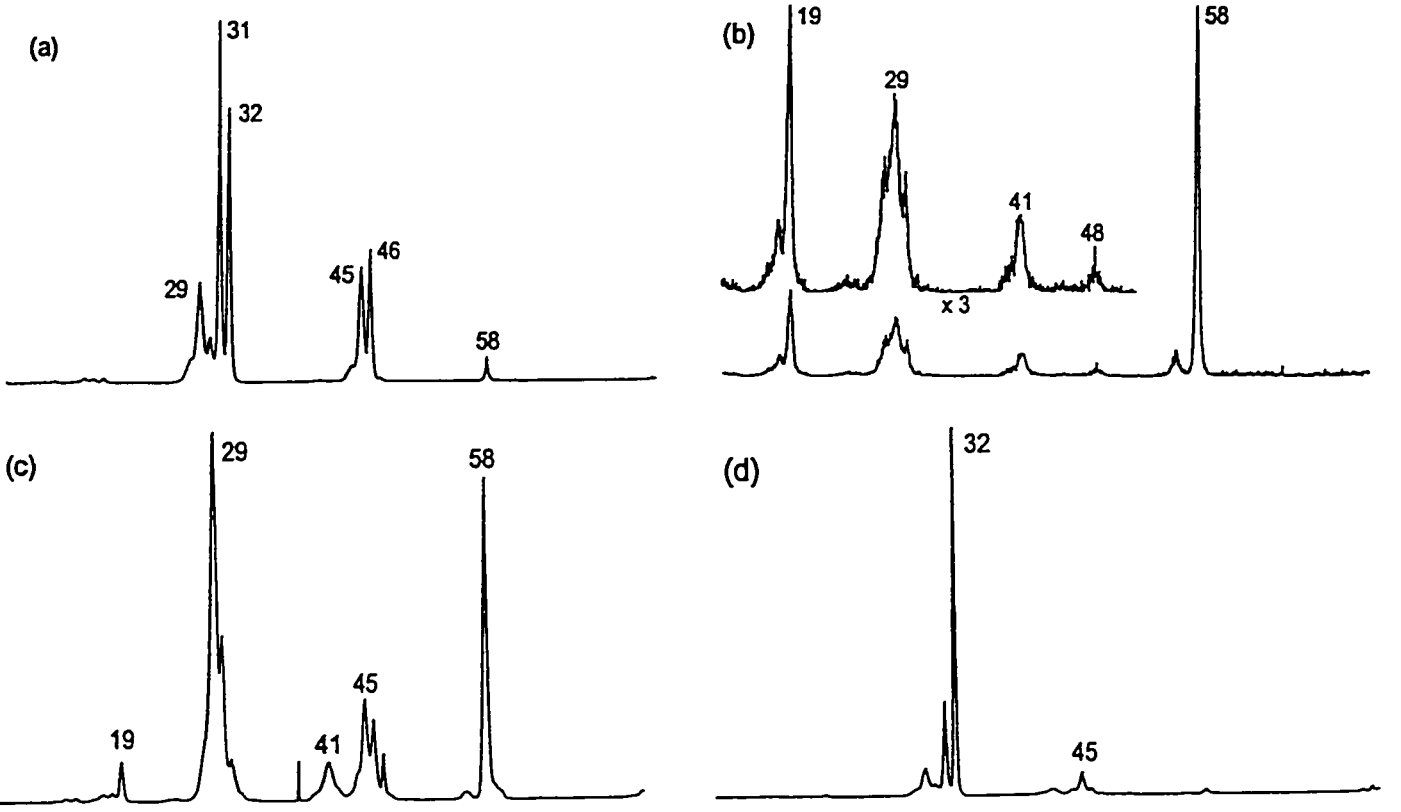

Figure 5-3. Item a : partial CID mass spectrum [3ffr/O_2] of the m/z 46 ion in the CID mass spectrum of Figure 5-2a ; item b : NR mass spectrum of the source generated m/z 76 ions from β-hydroxypyruvic acid.

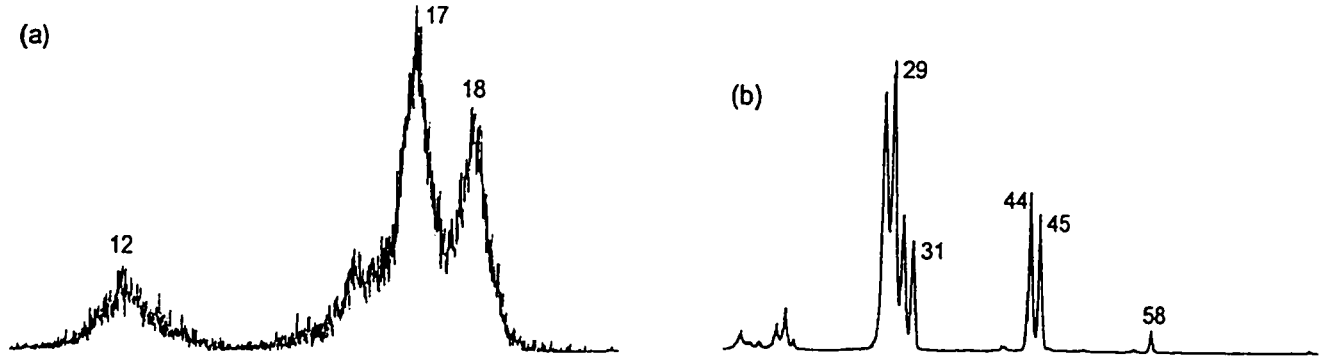

Thus it is reasonable to assume that the formation of m/z 46, $C(OH)_2^{\bullet+}$, and $CH_2{=}O$ involves a high energy direct bond cleavage reaction and this narrows down possible structures for the m/z 76 ions to either the H-bridged ion $CH_2{=}O{\bullet\bullet\bullet}H{\bullet\bullet\bullet}O{=}C{-}OH^{\bullet+}$, $\mathbf{3a}^{\bullet+}$ or its distonic isomer $CH_2OC(OH)_2^{\bullet+}$, $\mathbf{5}^{\bullet+}$. Plausible mechanisms for the generation of either ion involve a common 1,5-H transfer and the loss of the carbonyl CO group, as depicted in the following (Scheme 3) :

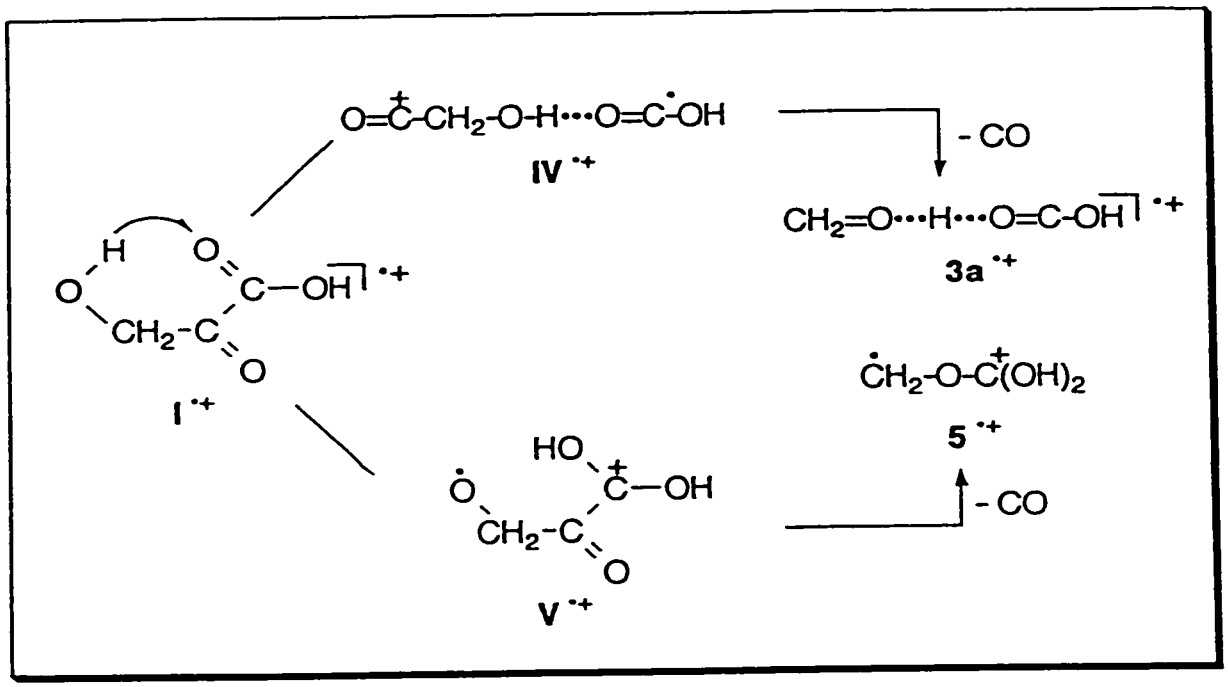

That the ion generated is not the distonic ion $\mathbf{5}^{\bullet+}$ but rather the H-bridged ion $\mathbf{3a}^{\bullet+}$ is supported by the following arguments :

(a) The first step in the proposed mechanism for the formation of $\mathbf{5}^{\bullet+}$, an undoubtedly facile 1,5-H shift, leads to a stable intermediate, $\mathbf{V}^{\bullet+}$, see section (v), which may be expected to competitively dissociate into $(HO)_2C{=}C{=}O^{\bullet+}$ (m/z 74) + $CH_2{=}O$ by direct bond cleavage[2], either in the ion source or upon collisional activation of the long lived molecular ions. However, neither the EI spectrum of **I** nor the CID mass

[2] the threshold energy for this reaction is 88.6 kcal/mol, from $\Delta H_f^{298}(HO)_2C{=}C{=}O^{\bullet+}$ is 114.6 kcal/mol (neutral is - 76.4 kcal/mol, G2(MP2) [20a,b] values, this work) and ΔH_f^{298} $CH_2{=}O$ is - 26.0 kcal/mol [18a]. Note also that $(HO)_2C{=}C{=}O^{\bullet+}$ is a prominent fragment ion in the 70 eV EI mass spectrum of meso-oxalic acid, HOOCC(=O)COOH.

spectrum of $\mathbf{I}^{\bullet+}$ shows a signal at m/z 74 indicative of this reaction. This also excludes formation of $\mathbf{3a}^{\bullet+}$ via the H-bridged intermediate $CH_2{=}O{\bullet\bullet\bullet}H\text{-}O\text{-}C(OH){=}C{=}O^{\bullet}$.

(b) The ionized methyl ester of $\mathbf{I}^{\bullet+}$, see above, also shows a prominent decarbonylation and here the corresponding product ions would be either $CH_2{=}O{\bullet\bullet\bullet}H{\bullet\bullet\bullet}O{=}C\text{-}OCH_3^{\bullet+}$ or $CH_2OC(OH)(OCH_3)^{\bullet+}$. The latter ion was independently generated and examined in previous study [5a] and from a comparison of the exchange behaviour of multiple (^{13}C and D) labelled isotopomers, it follows that the methyl ester ion does not generate $CH_2OC(OH)(OCH_3)^{\bullet+}$ but rather $CH_2{=}O{\bullet\bullet\bullet}H{\bullet\bullet\bullet}O{=}C\text{-}OCH_3^{\bullet+}$, and also that the two isomers do not easily communicate [17].

(c) The $CH_2OC(OH)(OCH_3)^{\bullet+}$ ion undergoes a facile reversible isomerization, via a 1,4-H shift, into $CH_3OC(=O)(OCH_3)^{\bullet+}$ [5a] and by analogy ion $\mathbf{5}^{\bullet+}$, $CH_2OC(OH)_2^{\bullet+}$, may be expected to communicate with $CH_3OC(=O)(OH)^{\bullet+}$. However, this process leads to loss of positional identity of the C and O bonded H atoms and this is not what is observed. Comparison of the CID mass spectrum of the source generated m/z 78 $[M\text{-}CO]^{\bullet+}$ ions from the D labelled HPA isotopomer $DOCH_2C(=O)COOD^{\bullet+}$ with that of the unlabelled m/z 76 ion shown in Fig. 5-2a, showed that the m/z 31, 32, 45 and 46 ions are cleanly shifted to m/z 32, 34, 46 and 48 respectively, in agreement with the proposed H-bridged structure $CH_2{=}O{\bullet\bullet\bullet}D{\bullet\bullet\bullet}O{=}C\text{-}OD^{\bullet+}$, not $CH_2OC(OD)_2^{\bullet+}$.

Thus we propose that the parent acid $\mathbf{I}^{\bullet+}$ also produces the H-bridged ion, $CH_2{=}O{\bullet\bullet\bullet}H{\bullet\bullet\bullet}O{=}C\text{-}OH^{\bullet+}$, $\mathbf{3a}^{\bullet+}$ and that it is generated by the mechanism depicted above.

Two peaks in the CID mass spectrum of $\mathbf{3a}^{\bullet+}$ deserve further comment : the signal at m/z 32, $CH_2OH_2^{\bullet+}$, which dominates the MI spectrum and the peak at m/z 58. The latter ion, $(HO)HC{=}C{=}O^{\bullet+}$ (structure established by a MS/MS experiment, result not shown) is the principal fragment ion in the CID spectrum of the low energy decarbonylation of $\mathbf{I}^{\bullet+}$, see Fig. 5-2b, and its presence in the spectrum of the source generated m/z 76 ions most likely reflects a small contribution of the low energy decarbonylation product ion $\mathbf{4}^{\bullet+}$ which will be further discussed in section (v). This may also explain the presence of the weak m/z 58 ion in the NR spectrum [21] of the $[\mathbf{I} - CO]^{\bullet+}$ source generated ions, see Fig. 5-3b. The other features of the NR spectrum are readily accommodated by the proposed $\mathbf{3a}^{\bullet+}$ structure and CIDI [21] contributions from its metastable dissociation (responsible for the larger part of the peak at m/z 44, $CO_2^{\bullet+}$). The neutral counterpart of the hydrogen

bridged ion is not expected to be stable and indeed the m/z 76 survivor signal is of negligible intensity. Neutralized $3a^{\bullet+}$ may (formally) dissociate by direct bond cleavage into $HOCO^{\bullet} + CH_2OH^{\bullet}$ and/or $:C(OH)_2 + CH_2{=}O$ and upon collisional ionization these neutrals would give rise to ions at m/z 45 and m/z 31 for the first process and m/z 46 and m/z 30 for the second, and lower mass fragment ions generated therefrom. The fact that m/z 46, $C(OH)_2^{\bullet+}$, ions are barely detectable in the NR spectrum is not due to the NR properties of $C(OH)_2^{\bullet+}$ [19] nor to the energetic demands of the $:C(OH)_2$ generation vis `a vis that of $HOCO^{\bullet}$, but rather to the charge distribution in $3a^{\bullet+}$, which, as discussed below, is best represented as a CH_2OH^+ **ion** interacting via an H-bridge with a $HOCO^{\bullet}$ dipole. The related H-bridged radical cation $H_2O{\bullet\bullet\bullet}H{\bullet\bullet\bullet}O{=}C\text{-}OH^{\bullet+}$ shows a similar NR behaviour [10].

The CO_2 loss, which dominates the MI but not the CID spectrum of the source generated $[\mathbf{I} - CO]^{\bullet+}$ ions, is obviously a rearrangement reaction since the threshold energy for the generation of $CH_2OH_2^{\bullet+} + CO_2$, 101 kcal/mol , is considerably lower than that associated with the base peak in the CID spectrum : CH_2OH^+ (m/z 31) + $HOCO^{\bullet}$ = 122 kcal/mol [18]. This observation further supports our proposal that the source generated $[\mathbf{I} - CO]^{\bullet+}$ ions have structure $3a^{\bullet+}$ and not that of the isomeric H-bridged radical cations $3b^{\bullet+}$ or $3c^{\bullet+}$, although the latter may be involved as a stable intermediate en route to the loss of CO_2 from $3a^{\bullet+}$. Loss of CO_2 also dominates the MI spectrum of the isomeric glycolic acid ion $2^{\bullet+}$ and two mechanisms involving a 1,4-H transfer can be envisaged, of which one involves the H-bridged ion $3c^{\bullet+}$, see Scheme 4 :

Scheme 4

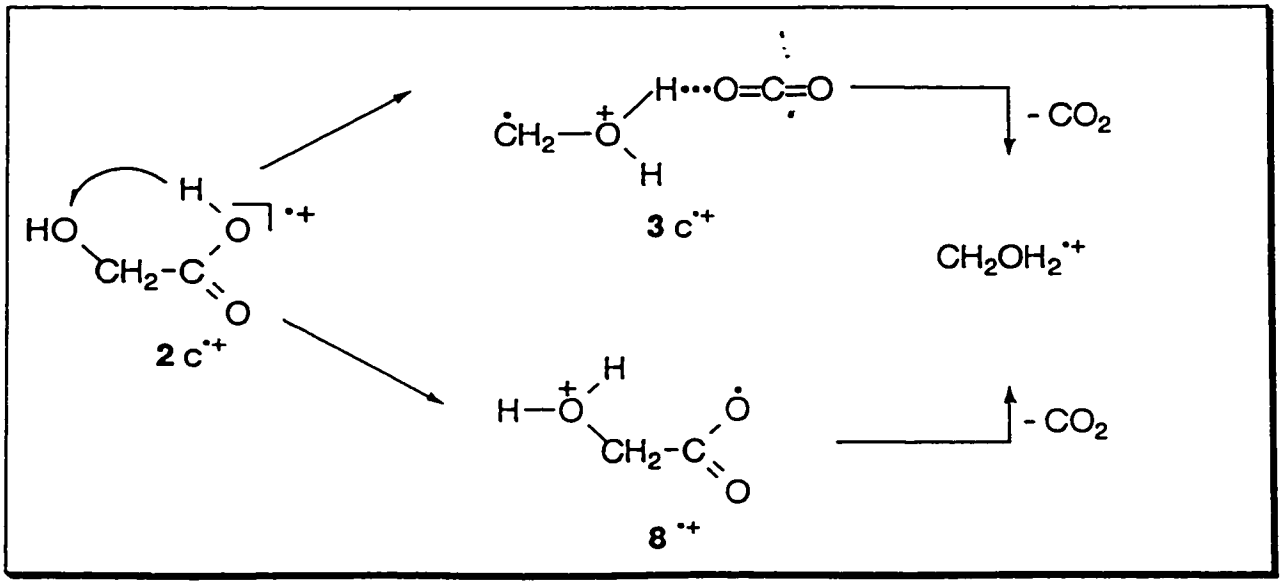

This raises the question : does the H-bridged ion $3a^{\bullet+}$ communicate with $2^{\bullet+}$ prior to the common CO_2 loss and if not, how then does $3a^{\bullet+}$ isomerize to lose CO_2? Analysis of the metastable peak shapes for the two reactions rules out a facile interconversion - albeit not a communication - between $3a^{\bullet+}$ and $2^{\bullet+}$: the two isomeric ions display Gaussian shaped metastable peaks [22] but that for loss of CO_2 from $3a^{\bullet+}$, $T_{0.5}$ = 43 meV, is significantly larger than that from $2^{\bullet+}$, whose $T_{0.5}$ value is only 21 meV (0.5 kcal/mol). Unfortunately, another valuable piece of experimental information i.e. an accurate appearance energy (AE) for the two CO_2 losses is not available : the involatility (glycolic acid) and additional thermal lability (HPA) of the acids precludes AE measurements with the currently accessible instrumentation. In this context we also note that an AE of the m/z 76 ions from $\mathbf{I}^{\bullet+}$ would not lead to an experimental heat of formation of the H-bridged ion $3a^{\bullet+}$ but rather to that of the low energy isomer $4^{\bullet+}$.

However, the intriguing mechanistic question regarding the loss of CO_2 from $3a^{\bullet+}$ and its relationship with $2^{\bullet+}$ can be addressed computationally. This is done in section (iv) but first we will discuss the computational results of the $[\mathbf{I}\text{-}CO]^{\bullet+}$ isomers.

(iii) The structure and stability of CH_2=O•••H•••O=C-OH$^{\bullet+}$ and its principal isomers : *ab initio* computational results and considerations.

The isomers examined are : ionized trihydroxyethylene, $\mathbf{1}^{\bullet+}$; ionized glycolic acid, $\mathbf{2}^{\bullet+}$; the H-bridged radical cations 3a-c$^{\bullet+}$; the hydroxyketene$^{\bullet+}$/water ion-dipole complex $\mathbf{4}^{\bullet+}$; the β-distonic ion $\mathbf{5}^{\bullet+}$ of Scheme 3 ; $HO(H_2)C\bullet\bullet\bullet O{=}C\text{-}OH^{\bullet+}$, $\mathbf{6a}^{\bullet+}$, an ion-dipole complex derived from $\mathbf{3a}^{\bullet+}$ and its carbenic conformer $HO(H_2)C\text{-}O\text{-}C\text{-}OH^{\bullet+}$, $\mathbf{6b}^{\bullet+}$; the distonic ions $H_2O\text{-}C(H_2)\text{-}O\text{-}C{=}O^{\bullet+}$,$\mathbf{7}^{\bullet+}$, and $H_2O\text{-}C(H_2)\text{-}C(=O)\text{-}O^{\bullet+}$, $\mathbf{8}^{\bullet+}$, precursor ions for the direct loss of CO_2 discussed in the next section. Their MP2(full) optimized geometries and CCSD(T) derived relative energies [20a] are presented in Figure 5-4 and Table 5-1 respectively, along with the transition states for loss of CO_2 discussed in the next section. Geometries were also optimized using the UHF and B3LYP methodology (using standard basis sets, see theoretical section for further details) and we will refer to those results that are relevant to the discussion.

The optimized geometry for $\mathbf{1}^{\bullet+}$ in Fig. 5-4 represents the lowest energy conformer of the ionized enol [11] which is the most stable of the isomers examined. Its G2(MP2) derived enthalpy of formation, ΔH_f^{298} = 71.6 kcal/mol [11], was chosen as the anchor point because accurate experimental data are not available for any of the isomeric ions. The energy differences between the anchor point and the experimental (thermochemical) values of the dissociation limits $CH_2OH_2^{\bullet+}$ + CO_2 and CH_2OH^+ + $HOCO^{\bullet}$ are 29 and 52 kcal/mol respectively, see last column of Table 5-1. These values are gratifyingly close to those derived from our CCSD(T) calculations, 29.8 and 53.4 kcal/mol (note that these refer to 0 K, whereas the estimated energies were evaluated at 298 K). The last column of Table 5-1 also lists values for those isomeric ions whose ionic enthalpy can be reliably estimated and here, too, comparison with the calculated energy differences is satisfactory. In particular, the calculated keto ion (**2c**)-enol ion (**1**) energy difference, 35.5 kcal/mole, is close to the estimate, 34 kcal/mol, and also compatible with ionic keto-enol energy differences established in related systems [26]. In view of these facts, we propose that ΔH_f for the key H-bridged ion $\mathbf{3a}^{\bullet+}$ = 99 kcal/mole with an estimated uncertainty of ± 3 kcal/mol.

For ionized glycolic acid, $\mathbf{2}^{\bullet+}$, various conformers were examined to determine the most stable conformer and to probe potential routes for the loss of CO_2. The MP2(full) calculations yielded seven stable species, represented by items **2a-e** in Figure 5-4. Two of these, $\mathbf{2d}^{\bullet+}$ and $\mathbf{2c'}^{\bullet+}$, have a greatly elongated C-C bond, whereas optimization starting from glycolic acid's most stable neutral conformer [27] led to a spontaneous rearrangement via a 1,4-H shift into the energetically favourable distonic ion $\mathbf{2e}^{\bullet+}$. No such rearrangement occurs without electron correlation : at the Hartree-Fock (UHF/6-31G*) level of theory, structure $\mathbf{2e}^{\bullet+}$ **[UHF]** (see Fig. 5-4) was obtained with a relative energy (37.5 kcal above ion $\mathbf{1}^{\bullet+}$) in reasonable agreement with the keto-enol differences mentioned above.

Table 5-1. UMP2(Full)/6-31G* and CCSD(T)/cc-pVDZ//UMP2(Full)/6-31G* energies, zero-point vibrational energies (ZPVEs) and relative energies, E [rel.], for ionized glycolic acid and its most important isomers.

Ions	UMP2(Full) /6-31G*	ZPVE[a]	CCSD(T) /cc-pVDZ	E [rel.] MP2	E [rel.] CCSD(T)	E [rel.] estimated
	Hartree, -303.	kcal/mol	Hartree, -303.	kcal/mol	kcal/mol	kcal/mol
[1]$^{\bullet+}$	-0.14285	41.2	-0.24898	0.0	0.0	0 [b]
[2a]$^{\bullet+}$	-0.05941	38.4	-0.15320	49.6	57.3	
[2b]$^{\bullet+}$	-0.06414	39.8	-0.17869	48.0	42.7	
[2c]$^{\bullet+}$	-0.07481	40.5	-0.19122	42.0	35.5	34 [c]
[2c']$^{\bullet+}$	-0.08404	41.0	-0.19094	36.7	36.2	
[2d]$^{\bullet+}$	-0.08871	41.2	-0.19387	34.0	34.6	
[2e]$^{\bullet+}$	-0.09437	40.6	-0.20459	29.8	27.3	
[3a]$^{\bullet+}$	-0.09607	38.2	-0.19848	26.4	28.7	
[3a']$^{\bullet+}$	-0.09484	38.7	-0.20239	27.7	26.8	27 [d]
[3b]$^{\bullet+}$	-0.08637	39.0	-0.19360	33.2	32.6	
[3c]$^{\bullet+}$	-0.12254	38.5	-0.22138	10.0	14.6	10 [d]
[4]$^{\bullet+}$	-0.10501	39.1	-0.21321	21.7	20.3	
[4']$^{\bullet+}$	-0.10692	38.5	-0.21464	19.8	18.8	
[4"]$^{\bullet+}$	-0.12187	38.3	-0.22888	10.2	9.7	
[5]$^{\bullet+}$	-0.11518	39.8	-0.21850	16.0	17.7	
[6a]$^{\bullet+}$	-0.08480	40.0	-0.19108	35.2	35.1	
[6b]$^{\bullet+}$	-0.07628	41.0	-0.17917	41.6	43.6	
[7]$^{\bullet+}$	-0.07451	41.2	-0.17439	42.9	46.8	
[8]$^{\bullet+}$	-0.06511	40.3	-0.17503	47.8	47.3	
TS [2c' → 3c] $^{\bullet+}$	-0.07718	38.6	-0.18148	38.6	39.8	
TS [2c → 8] $^{\bullet+}$	-0.06424	38.5	-0.17589	46.6	51.3	
TS [6b → 7] $^{\bullet+}$	-0.06605	39.0	-0.16979	46.0	49.7	
$CO_2 + CH_2OH_2^{\bullet+}$	-0.09992	36.9	-0.19468	26.2	29.8	29 [e]
$CH_2OH^+ + HOCO^{\bullet}$	-0.05112	37.8	-0.15845	54.2	53.4	52 [f]
H(HO)C=C=O $^{\bullet+}$ + H_2O	-0.07281	36.7	-0.18163	39.5	37.6	33 [g]

Legend to Table 5-1.

[a] Scaled by a factor of 0.9646, see reference [22].
[b] Using ΔH_f [**1**]$\bullet^+$ = 71.6 kcal/mol as the anchor point (G2(MP2) 298K value from [11]) ; ΔH_f[**1**] values (298K) from G2(MP2) and CBS-4 are -107.5 and -108.5 kcal/mol respectively.
[c] Using ΔH_f[**2**] = -139.5 kcal/mol [11] and IE [**2**] = 10.6 eV ; the CBS-4 value for the lowest energy conformer of **2** (the neutral counterpart of the UHF/6-31G* geometry **2e**$\bullet^+$ shown in Figure 5-2) is -137.6 kcal/mol at 298K (this work) ;
[d] Using ΔH_f[**3a**]$\bullet^+$ = 99 kcal/mol and ΔH_f[**3c**]$\bullet^+$ = 82 kcal/mol, estimates based on the empirical relationship for O•••H•••O proton bound dimers : SE (kcal/mol) = 30.4 - 0.30ΔPA [23] ; SE, stabilization energy relative to the dissociation products of lowest combined enthalpy, PA, proton affinity : PA[CH_2=O] = 170.4 kcal/mol [24a], PA[CO_2] = 129.4 kcal/mol [24b] ; PA[$\bullet CH_2OH \rightarrow CH_2OH_2\bullet^+$] = 166 kcal/mol ; PA[$\bullet COOH \rightarrow C(OH)_2\bullet^+$] = 145 kcal/mol, from ΔH_f[•COOH] = -46 kcal/mol [18b] and ΔH_f[$C(OH)_2\bullet^+$] = 175 kcal/mol, [18a].
[e] Using the following 298 K ΔH_f values : $CH_2OH_2\bullet^+$ = 195 kcal/mol and CO_2 = -94 kcal/mol [18a].
[f] Using the following 298 K ΔH_f values : CH_2OH^+ = 169.3 kcal/mol [24a] and •COOH = -46 kcal/mol [18b].
[g] Using ΔH_f^{298} (H_2O) = -58 kcal/mol and ΔH_f^{298} ($HO(H)C{=}C{=}O\bullet^+$) = 163 kcal/mol, final value obtained from the isodesmic reaction $HO(H)C{=}C{=}O\bullet^+ + CH_4 \rightarrow H_2C{=}C{=}O\bullet^+ + CH_3OH$ calculated using the G2 model chemistry and values from reference [18a]. Note ionized ketene value was obtained from the G2 value of neutral ketene and the ionization energy from reference [24d].

Figure 5-4. MP2(full)/6-31G* optimized geometries of various $C_2H_4O_3^{\bullet+}$ (m/z 76) isomers, values in parentheses refer to geometries optimized with B3LYP/6-31G*.

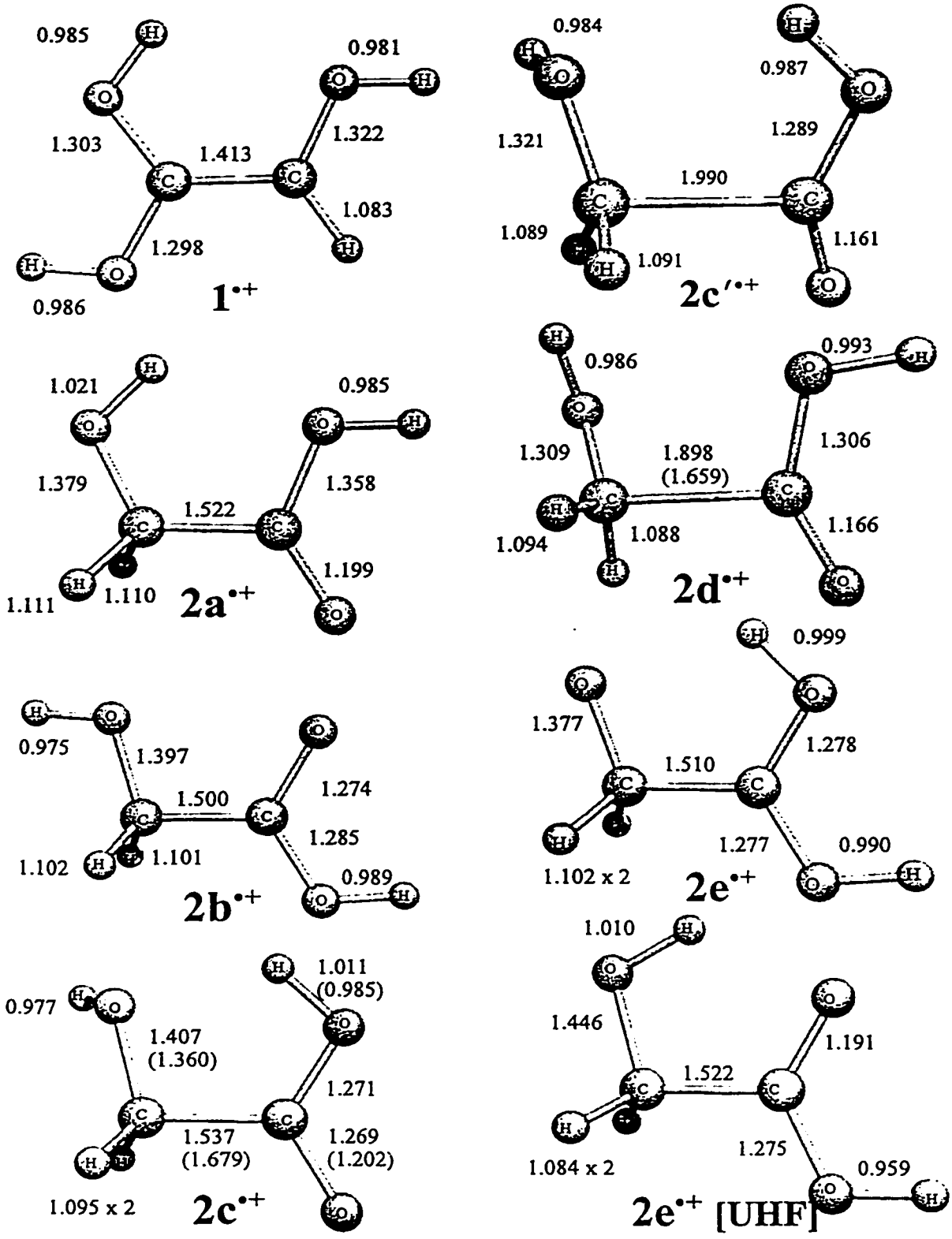

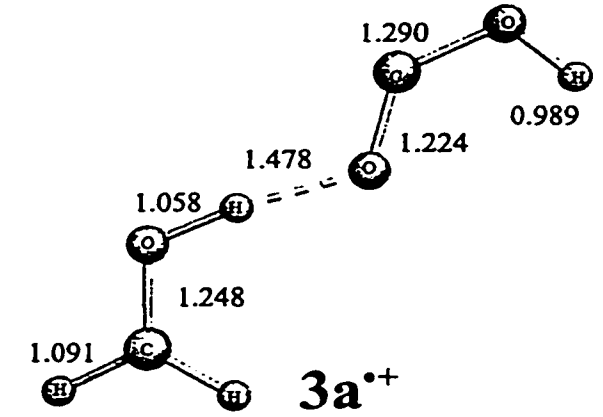

3a$^{\bullet+}$

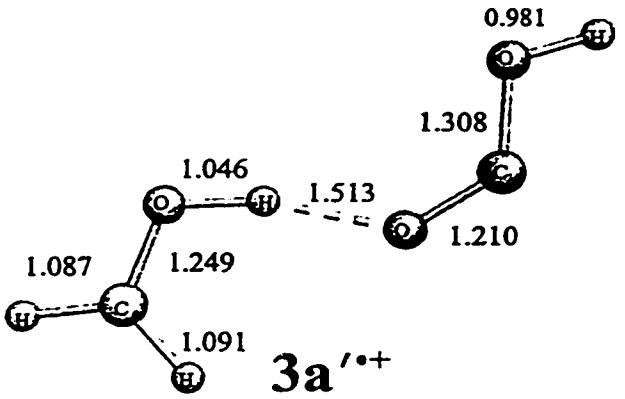

3a′$^{\bullet+}$

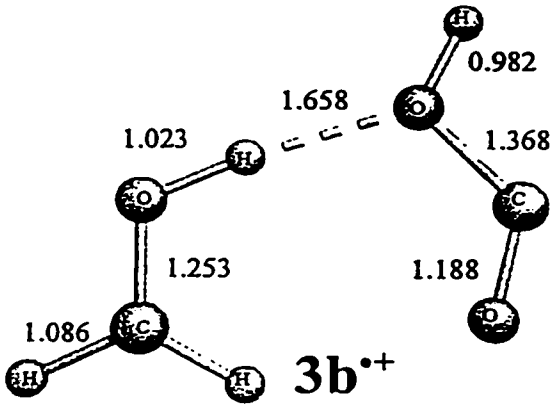

3b$^{\bullet+}$

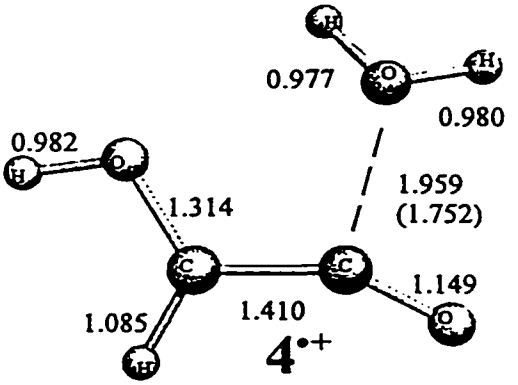

4$^{\bullet+}$

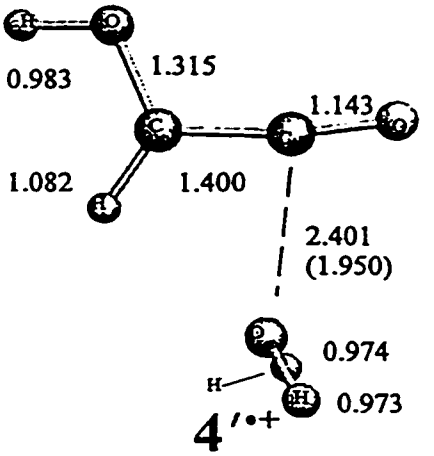

4′$^{\bullet+}$

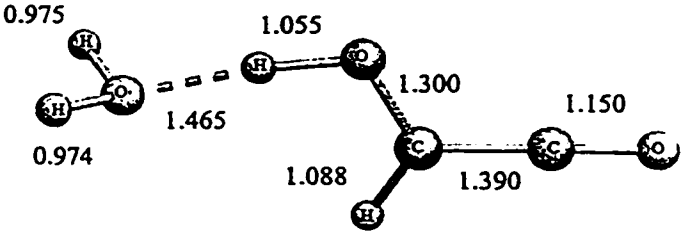

4′′$^{\bullet+}$

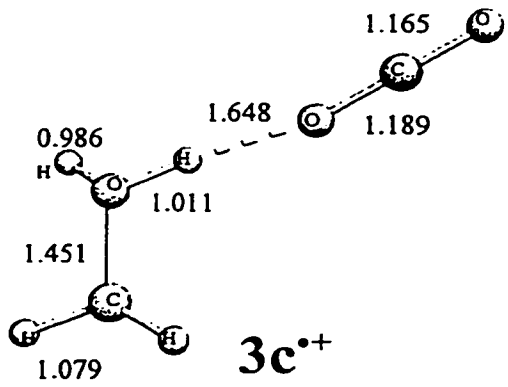

3c$^{\bullet+}$

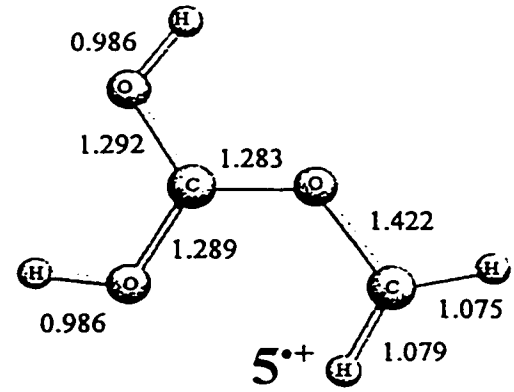

5$^{\bullet+}$

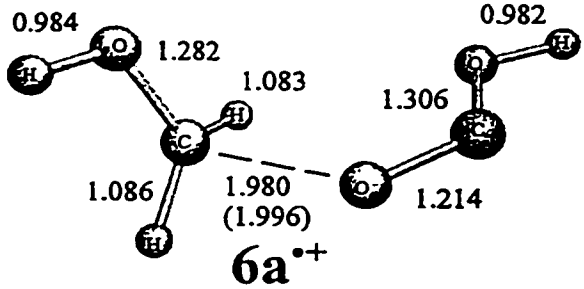

6a$^{\bullet+}$

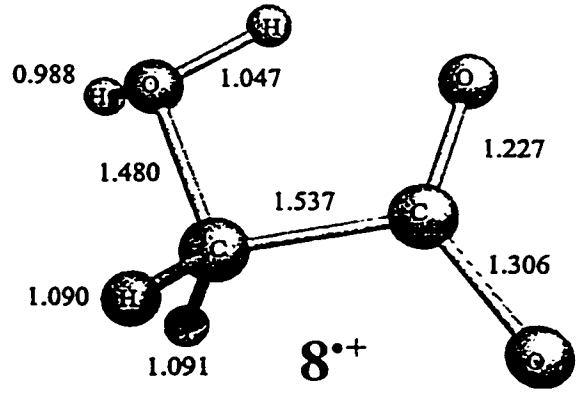

8$^{\bullet+}$

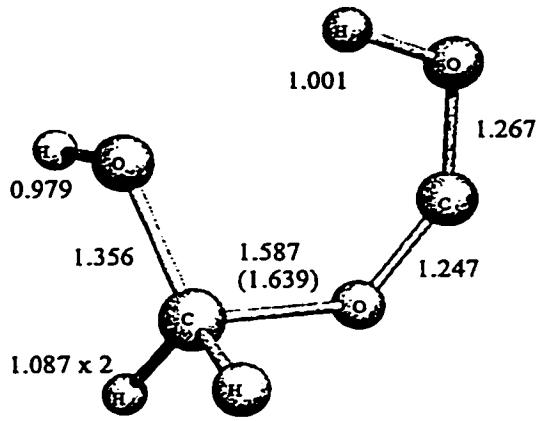

$6b^{\bullet+}$

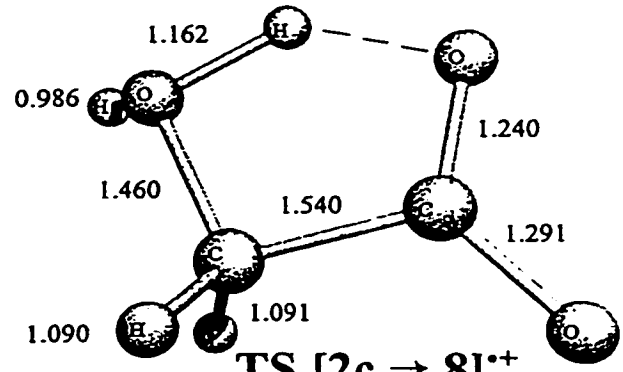

TS [2c → 8]$^{\bullet+}$

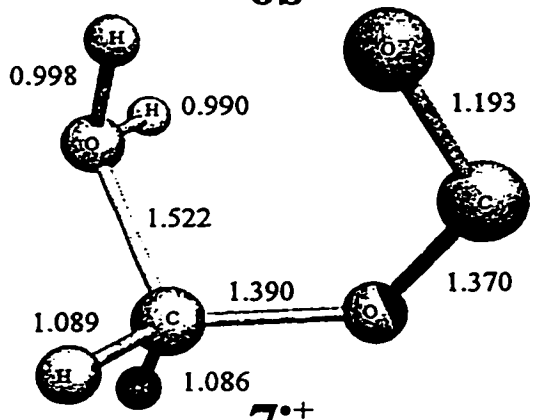

$7^{\bullet+}$

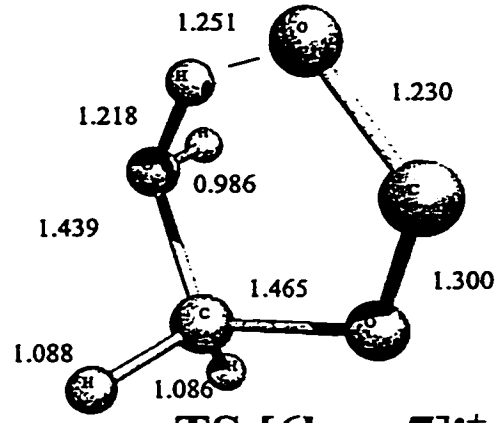

TS [6b → 7]$^{\bullet+}$

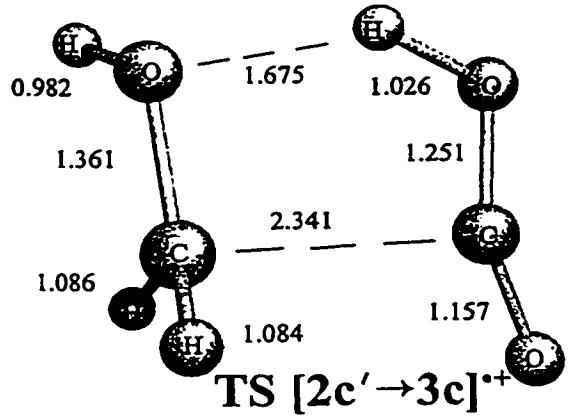

TS [2c′→3c]$^{\bullet+}$

Ion $\mathbf{2a}^{\bullet+}$ is considerably higher in energy (by ~ 15 kcal/mol) than $\mathbf{2b}^{\bullet+}$ and $\mathbf{2c}^{\bullet+}$, the other conformers of conventional C-C bond length. This is likely due to differing electronic structures which is reflected in the geometries shown in Figure 5-4. In ion $\mathbf{2a}^{\bullet+}$, the charge and the radical are largely located on the oxygen atom of the CH_2OH group since the O-H (1.021 Å) bond is slightly elongated and the C-O (1.379 Å) bond slightly shortened relative to the corresponding bond length in the neutral, 0.997 Å and 1.407 Å [27]. For $\mathbf{2b}^{\bullet+}$ and $\mathbf{2c}^{\bullet+}$, the values are much closer to neutral CH_2OH and moreover, their carbonyl C=O bond (1.274 Å and 1.269 Å) is much longer than that in $\mathbf{2a}^{\bullet+}$ (1.199 Å, the corresponding neutral value is 1.211 Å [27]) indicating that the charge and radical electron are now localized in the carbonyl moiety. These proposals are confirmed by population analysis of these species. Note further that the relative energy of $\mathbf{2a}^{\bullet+}$ is such that it lies above the direct bond cleavage dissociation into CH_2OH^+ (m/z 31) + $HOCO^{\bullet}$. Thus, $\mathbf{2a}^{\bullet+}$ may play a significant role in the high energy source reactions represented by the conventional 70 eV EI spectrum of **2** (where m/z 31 is the base peak) but not in the chemistry of the long-lived ions $\mathbf{2}^{\bullet+}$ sampled by MI and CID experiments.

Conformers $\mathbf{2d}^{\bullet+}$ and $\mathbf{2c'}^{\bullet+}$ are so-called long bonded species [3a] having C-C bond lengths of 1.898 Å and 1.990 Å respectively (on the DFT surface, values in parentheses in Fig. 5-4, the effect is less pronounced). Both are low energy species with geometrical parameters of the HOCO moiety that lie in between that of the HOCO ion and its neutral counterpart, indicating that the charge and the radical are localized in the long C-C bond. Note also that one of these conformers, $\mathbf{2c'}^{\bullet+}$, along with its short bonded counterpart, $\mathbf{2c}^{\bullet+}$, has the correct orientation for a 1,4-H transfer leading to the ultimate loss of CO_2 as depicted in Scheme 4.

The H-bridged radical cations $\mathbf{3a\text{-}c}^{\bullet+}$ are among the most stable isomers and their calculated relative energies agree well with the estimates. In all these H-bridged structures the moiety with the largest proton affinity (PA, see legend Table 5-1 for numerical values) covalently binds the bridging hydrogen. Thus, the best description of ions $\mathbf{3a}^{\bullet+}$ and $\mathbf{3b}^{\bullet+}$ is a CH_2OH^+ ion interacting with a $HOCO^{\bullet}$ dipole, that is $\mathbf{3a}^{\bullet+}$ and $\mathbf{3b}^{\bullet+}$ have different connectivities but the same distribution of charge and radical, as confirmed by standard population analysis. Similarly, ion $\mathbf{3c}^{\bullet+}$ represents the interaction of a CO_2 molecule with the ylid ion $CH_2OH_2^{\bullet+}$. This ion is the most stable of the H-bridged ions and

a prime candidate for the dissociation reaction of lowest energy requirement, *viz.* loss of CO_2 by separation of the two moieties.

For the ionized hydroxyketene$^{\bullet+}$/water complex, the conformers examined (**4**$^{\bullet+}$, **4'**$^{\bullet+}$ and **4''**$^{\bullet+}$) were the analogues of the lowest energy conformers in the ketene$^{\bullet+}$/water system [16]. Conformers **4**$^{\bullet+}$ and **4'**$^{\bullet+}$ represent "pure" ion-dipole complexes with computationally derived stabilization energies (SE) of 17.3 and 18.8 kcal/mol respectively. These SE values are in reasonable agreement with those calculated for **4**$^{\bullet+}$ and **4'**$^{\bullet+}$ from SE = 68.8 μ/r^2 kcal/mol, using μ [H_2O] = 1.85 D and r values of 2.7 Å and 2.4 Å derived from the optimized structures in Figure 5-4, : 17.5 and 22 kcal/mol. Not unexpectedly, conformer **4''**$^{\bullet+}$ is considerably lower in energy, by ~ 10 kcal/mol, because it benefits from the added stabilization of the hydrogen bridge.

The distonic ion **5**$^{\bullet+}$ is indeed quite a stable intermediate as it lies 18 kcal/mole above ion **1**$^{\bullet+}$, but as argued above, it is not generated from ionized HPA. Also presented in Table 5-1 and Figure 5-4 are ions **6**$^{\bullet+}$- **8**$^{\bullet+}$, key intermediates in the decarboxylation of **3a**$^{\bullet+}$ and **2**$^{\bullet+}$ which will be discussed in the next section along with three strategic transition states.

(iv) Mechanistic proposals for the loss of CO_2 from CH_2=O•••H•••O=C-OH$^{\bullet+}$, 3a$^{\bullet+}$, participation of the stable isomer $CH_2O(H)$•••H•••O=C=O$^{\bullet+}$, 3c$^{\bullet+}$?

First, we will consider how the low energy glycolic acid ions lose CO_2. Following Scheme 4, one pathway involves isomerization into **3c**$^{\bullet+}$, via a 1,4-H transfer and C-C bond cleavage, whereas the alternative route leads to the distonic ions **8**$^{\bullet+}$, via a 1,4-H transfer without C-C cleavage. As discussed in the previous section, the long and short bonded conformers **2c'**$^{\bullet+}$ and **2c**$^{\bullet+}$ may serve as the immediate precursors. Transition states could be located for both pathways : TS [**2c**→**8**]$^{\bullet+}$ and TS [**2c'**→**3c**]$^{\bullet+}$ in Figure 5-4. TS [**2c**→**8**]$^{\bullet+}$ lies very high in energy, c. 16 kcal/mol above **2c**$^{\bullet+}$ and only a few kcal/mol below the direct bond cleavage dissociation limit CH_2OH^+ + HOCO$^{\bullet}$, see Figure 5-5. If this were the principal route by which glycolic acid ions lose CO_2, one would predict the normal mass spectrum to have a sizable molecular ion and the CID spectrum to be dominated by m/z 31 CH_2OH^+ ions. This is clearly not the case : the normal mass spectrum displays a very weak molecular ion (< 1 % of base peak, m/z 31) while the CID

mass spectrum (Fig. 5-2d) is dominated by loss of CO_2, not HOCO$^{\bullet}$. Thus, there must be a pathway of much lower energy and indeed the alternative route $\mathbf{2c'^{\bullet+}} \rightarrow$ TS $[\mathbf{2c'} \rightarrow \mathbf{3c}]^{\bullet+} \rightarrow \mathbf{3c}^{\bullet+} \rightarrow CH_2OH_2^{\bullet+} + CO_2$ is calculated to have a critical energy of only a few kcal/mol, see Fig. 5-5.

Now that we have established that the majority of the low energy ions $\mathbf{2}^{\bullet+}$ lose CO_2 via the H-bridged ion $\mathbf{3c}^{\bullet+}$, the question arises whether the CO_2 loss from ions $\mathbf{3a}^{\bullet+}$ may follow the same route, via the isomerization $\mathbf{3a}^{\bullet+} \rightarrow \mathbf{2}^{\bullet+}$. The one way for this to occur is that the CH_2OH^+ and HOCO$^{\bullet}$ moieties in $\mathbf{3a}^{\bullet+}$ separate and recombine, carbon to carbon or ion center to radical center, to form glycolic acid ions $\mathbf{2}^{\bullet+}$.

Figure 5-5. Energy level diagram for the decarboxylation of ionized glycolic acid $\mathbf{2}^{\bullet+}$, versus that of the H-bridged radical cation $\mathbf{3a}^{\bullet+}$.

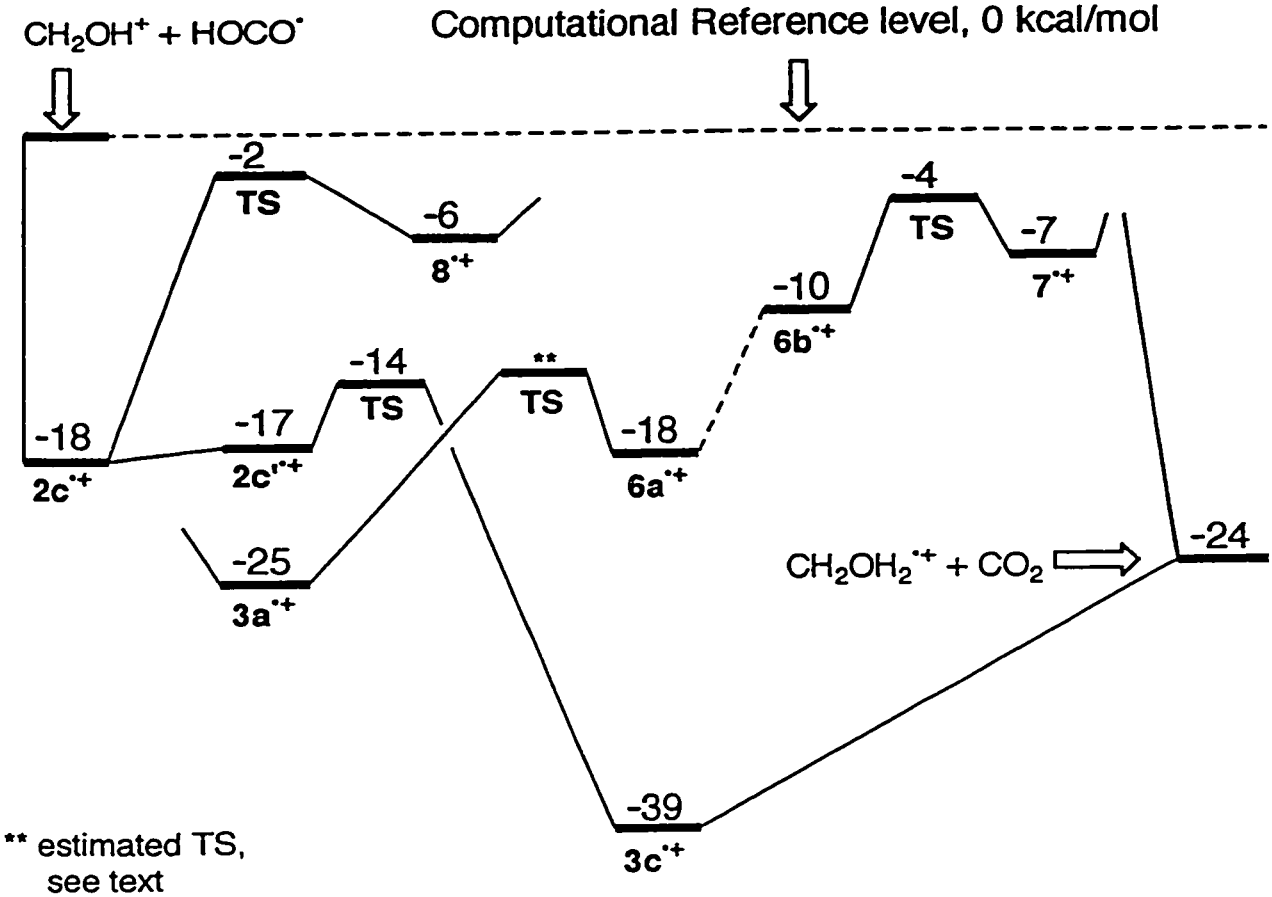

However, such a recombination reaction is highly unlikely since it requires rotation of the dipole of the HOCO$^{\bullet}$ moiety such that the ion-dipole stabilization is completely lost

and the moieties would fly apart, i.e. dissociation into CH_2OH^+ + HOCO$^\bullet$ would ensue. The same arguments apply to the isomerization **3a**$^{\bullet+}$ → **3c**$^{\bullet+}$. That the loss of CO_2 from **2**$^{\bullet+}$ and **3a**$^{\bullet+}$ would involve a common pathway is therefore unlikely, in agreement with the experimental observations (KER differences) discussed in section (ii).

How then does ion **3a**$^{\bullet+}$ lose CO_2 ? Recombination of the separated moieties of **3a**$^{\bullet+}$ such that the dipole vector remains pointed to the ionic center would allow the ion to isomerize and this forms the basis of our mechanistic proposal presented in Scheme 5. The CH_2OH^+ group in **3a**$^{\bullet+}$ can freely rotate in the dipole field of HOCO$^\bullet$. Such a motion sacrifices the stabilization energy (SE) of the H-bridge but it leaves the ion-dipole stabilization intact. The SE of the H-bridged ion **3a'**$^{\bullet+}$ is 24 kcal/mol (from data in Table 5-1) whereas all configurations resulting from the rotation of the CH_2OH^+ moiety about the charged carbon atom at the original ion-dipole distance (4.3 Å) retain a SE of ~13 kcal/mol, still well below the dissociation limit (denoted as ** in Figure 5-5). When the rotation is coupled with a shortening of the ion-dipole distance, the SE increases and this process may eventually lead to the formation of **6a**$^{\bullet+}$, whose stability is close to that of ionized glycolic acid (Table 5-1). Via not too energy demanding rotations, **6a**$^{\bullet+}$ may convert into its "conformer" **6b**$^{\bullet+}$ (an ionized carbene). A 1,5-H^+ transfer in this ion would yield the distonic ion **7**$^{\bullet+}$ which by direct bond cleavage exothermically decarboxylates, see Scheme 5 and Fig. 5-5. We have located (Fig. 5-4 and Table 5-1) the key transition state **6b**$^{\bullet+}$ → **7**$^{\bullet+}$ in this proposal and, as shown in Fig. 5-5, it indeed lies below the dissociation limit CH_2OH^+ + HOCO$^\bullet$. Note that our calculations predict that ions **3a**$^{\bullet+}$ should dissociate with a significantly larger KER than ions **2c**$^{\bullet+}$.

Scheme 5

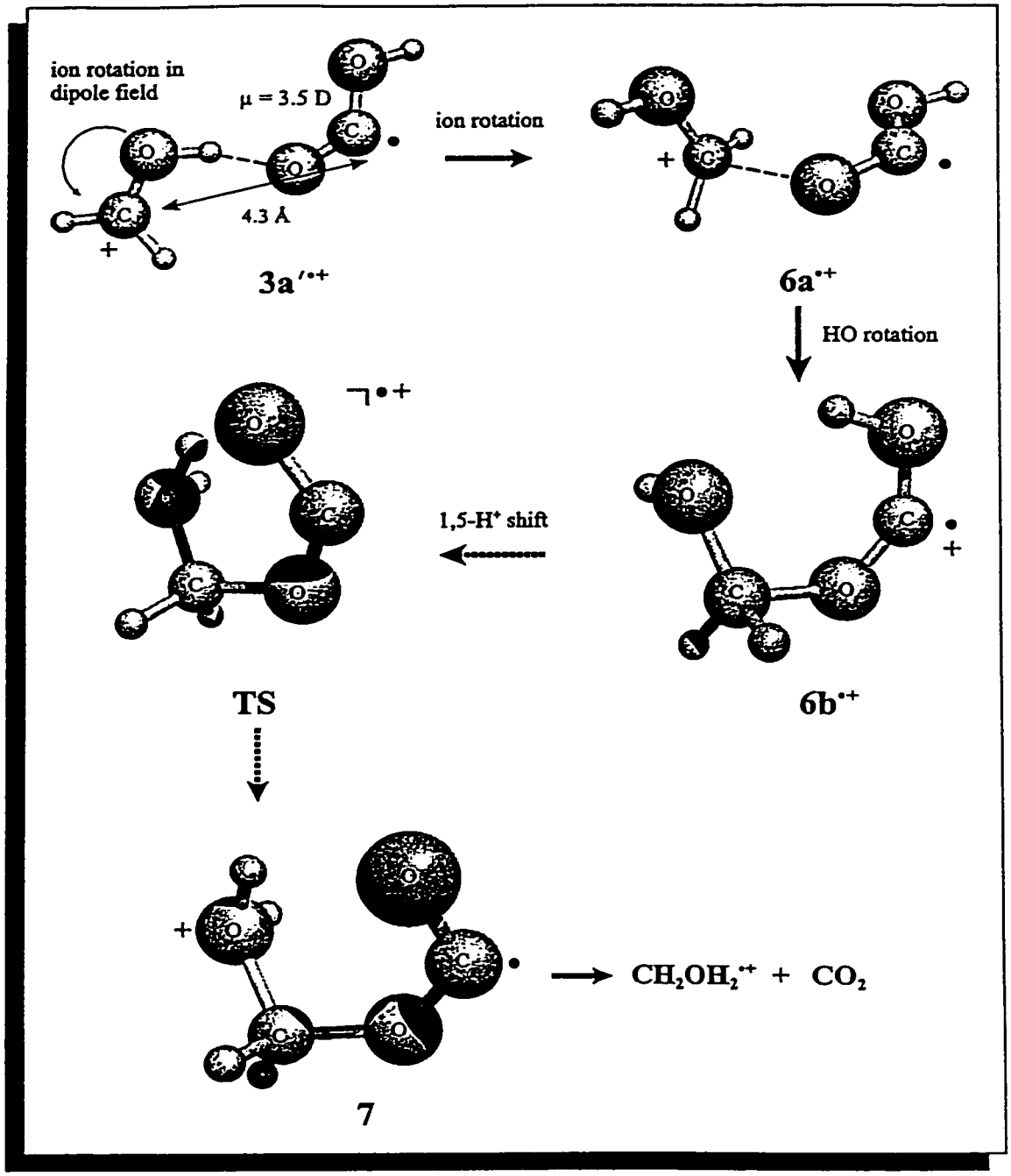
ion rotation in dipole field
μ = 3.5 D
4.3 Å
ion rotation
3a'•+
6a•+
HO rotation
1,5-H+ shift
TS
6b•+
7
CH2OH2•+ + CO2

(v) The decarbonylation of low energy HPA ions $I^{\bullet+}$: isomerization into the enol $II^{\bullet+}$ and generation of the ion-dipole complex $HO(H)C=C=O^{\bullet+}/H_2O$, $4^{\bullet+}$ therefrom. Comparison with the behaviour of the ionized methyl ester.

We will begin our discussion of the decarbonylation of the metastable HPA ions with a brief analysis of the behaviour of its methyl ester. As was mentioned in section (i) the decarbonylation of the **metastable** molecular ions of the methyl ester occurs via two distinct mechanisms yielding two different product ions i.e. the methyl(ated) analogue of the H-bridged ion $\mathbf{3a}^{\bullet+}$, $CH_2=O\bullet\bullet\bullet H\bullet\bullet\bullet O=C-OCH_3^{\bullet+}$ (which is the sole product ion generated in the source [17]) in admixture with the more stable isomer $HO(H)C=C=O^{\bullet+}/CH_3OH$ [9], see Scheme 2. A first indication that we are dealing with two mechanisms comes from the observation that the metastable peak for the decarbonylation is a Gaussian shaped composite [22] whose $T_{0.5}$ value is 60 meV. Next a sample of the specifically labelled ^{18}O isotopomer $HOCH_2C(=O^{18})COOCH_3$ was prepared and the MI spectrum of its molecular ion was examined : it displayed two non composite Gaussian shaped peaks, at m/z 92 (loss of CO^{16}) and m/z 90 (loss of CO^{18}) with an intensity ratio of 3 : 2 and $T_{0.5}$ values of 43 and 96 meV respectively. Following the proposal in Scheme 2, it is expected that the source generated ions exclusively lose CO^{18} and this is substantiated by the EI mass spectrum (not shown) where I [m/z 92] is < 5% of I [m/z 90]. The CID mass spectra of the metastably generated m/z 92 and m/z 90 ions are presented in Figure 5-6 : it is seen that these spectra are entirely different. Loss of CO^{18} yields a spectrum dominated by peaks at m/z 60 ($CH_3O\text{-}C\text{-}OH^{\bullet+}$), 45 ($HO\text{-}C=O^{+}$) and 31 ($CH_2OH^{+}$) which is closely similar to that of the source generated ions and which is entirely compatible with the formation of the H-bridged ion $CH_2=O\bullet\bullet\bullet H\bullet\bullet\bullet O=C-OCH_3^{\bullet+}$ [5a, 17]. Loss of CO^{16} yields a spectrum dominated by ions at m/z 62, 60 and 33 which we assign to the ion-dipole complex $HO(H)C=C=^{18}O^{\bullet+}/CH_3OH$ whose principal disociation routes are rationalized in the following Scheme (Scheme 6) :

Scheme 6

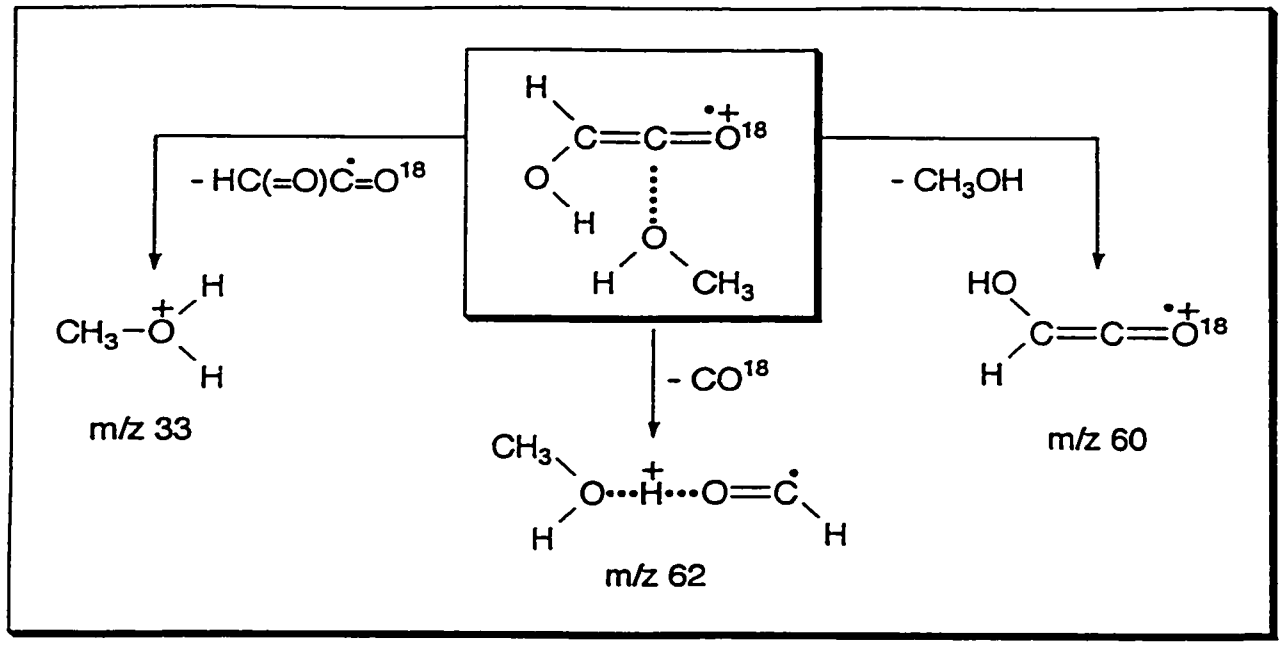

Figure 5-6. CID mass spectra of the **metastably** generated decarbonylation products from ionized O^{18} labelled methyl β-hydroxypyruvate, $HOCH_2C(=O^{18})COOCH_3$; item a : the spectrum of the $[M\text{-}CO^{16}]^{\bullet+}$ (m/z 92) ions, item b : the spectrum of the $[M\text{-}CO^{18}]^{\bullet+}$ (m/z 90) ions.

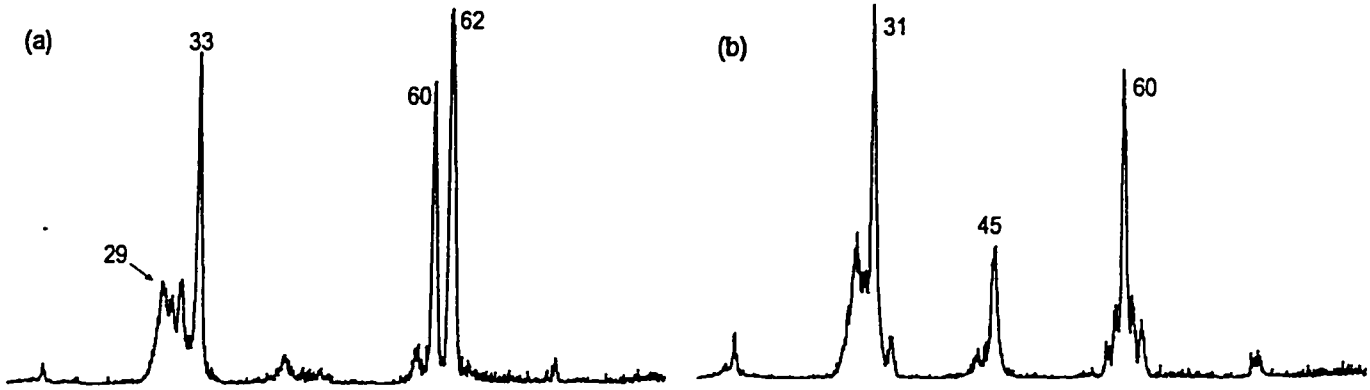

The proposal in Scheme 6 finds strong support from a previous study [9] on the enol of methyl glycolate ion, $HOC(H)=C(OH)OCH_3^{\bullet+}$, and several D and ^{18}O labelled isotopomers, where it was concluded that part of the low energy enol ions slowly isomerize into the ion-dipole complex $HO(H)C=C=O^{\bullet+}/CH_3OH$ prior to dissociation (see Scheme 1 in ref. 9). In this study it was also established, from an MS/MS/MS/MS experiment, that the m/z 62 ion is the H-bridged radical cation $CH_3O(H)\bullet\bullet\bullet H\bullet\bullet\bullet O=C\text{-}H^{\bullet+}$.

Unlike the methyl ester, the metastable peak for the decarbonylation of the low energy ions of the parent acid, $\mathbf{I}^{\bullet+}$, is a simple Gaussian ($T_{0.5}$ = 23 meV) and this suggests that we are dealing with a single mechanism. We have already noted, see section (i) and Fig. 5-2, that the product ions generated are not $\mathbf{3a}^{\bullet+}$ but rather $HO(H)C=C=O^{\bullet+}/H_2O$, $\mathbf{4}^{\bullet+}$, a species akin to the enol ion $HOC(H)=C(OH)_2^{\bullet+}$, $\mathbf{1}^{\bullet+}$, but nevertheless characteristically different. The spectrum of the enol ion features a unique m/z 46 ion ($HOCOH^{\bullet+}$ [3a]) whereas m/z 48 is absent and the intensity of m/z 19 (H_3O^+) is greatly reduced. We also note that the dissociation reactions that characterize $HO(H)C=C=O^{\bullet+}/CH_3OH$, see Scheme 6 and Fig. 5-6a are also found in the spectrum (Fig. 5-2b) of the putative ion $HO(H)C=C=O^{\bullet+}/H_2O$, $\mathbf{4}^{\bullet+}$, *viz.* loss of H_2O yielding $HO(H)C=C=O^{\bullet+}$ (m/z 58), loss of CO yielding $H_2O(H)\bullet\bullet\bullet H\bullet\bullet\bullet O=C\text{-}H^{\bullet+}$ [28] (m/z 48) and loss of $HC(=O)C=O^{\bullet}$ yielding H_3O^+ (m/z 19), albeit that their relative abundances are greatly different.[3]

Analysis of a small sample of $HOCH_2C(=O^{18})COOH$, prepared under carefully controlled conditions (see Experimental) shows that the **source** generated ions exclusively lose CO^{18} (providing further support for the high energy decarbonylation mechanism in Scheme 3) whereas both the MI and the CID spectrum, see Fig. 5-7, of its molecular ion show a specific loss of CO^{16}. This supports our proposal that the **metastable** ions decarbonylate via a mechanism analogous to that depicted in Scheme 2 for the low energy methyl ester ions, yielding $HOC(H)=C=O^{\bullet+}/H_2O$, $\mathbf{4}^{\bullet+}$, as the product ion (Scheme 7)
:

[3] The combined product enthalpies for the direct bond cleavage loss of H_2O from $HO(H)C=C=O^{\bullet+}/H_2O$ and CH_3OH from $HO(H)C=C=O^{\bullet+}/CH_3OH$ are 105 and 115 kcal/mol respectively [18a, Legend Table 1, item g]. For the rearrangement leading to loss of CO, the corresponding numbers are 111 [28] and 102 [11] kcal/mol. These differences in energy requirement may explain why the loss of CO from $\mathbf{4}^{\bullet+}$ is only a minor reaction, whereas it is prominent in the spectrum of $HO(H)C=C=O^{\bullet+}/CH_3OH$

Scheme 7

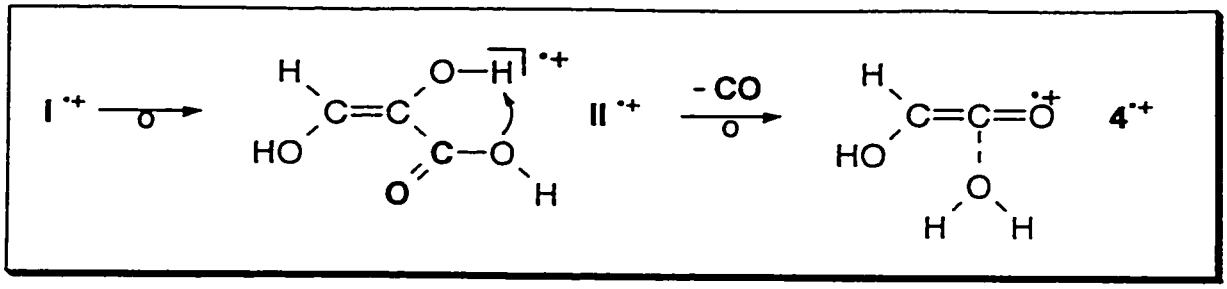

Figure 5-7. CID mass spectrum of the molecular ion of the ^{18}O labelled β-hydroxypyruvic acid isotopomer $HOCH_2C(=O^{18})COOH$.

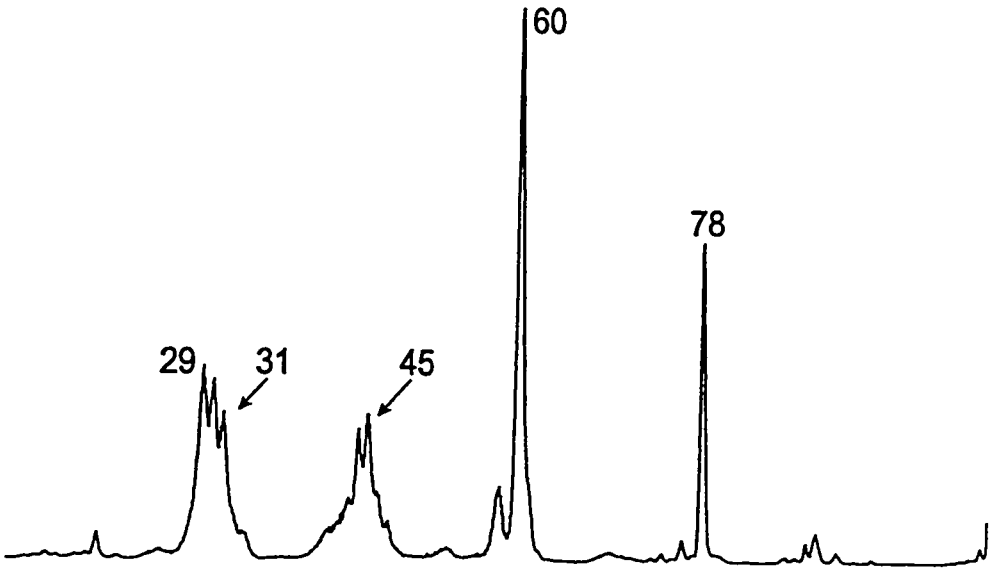

That the majority of the long lived non dissociating HPA ions have isomerized followed already from a comparison of the CID mass spectrum of $\mathbf{I}^{\bullet+}$ with the EI mass spectrum of the acid, see section (i) and Figure 5-1, and also from the observation that the low energy isomer ($\mathbf{4}^{\bullet+}$ vis `a vis $\mathbf{3a}^{\bullet+}$) is not formed at high internal energies.

That it is the enol ion 1,2-dihydroxyacrylic acid, $\mathbf{II}^{\bullet+}$, which is predominantly generated comes from a comparison of the MI, CID and NR spectra of the independently generated enol : when solid samples of dihydroxyfumaric acid (ΔH_f) are evaporated into

the ion source at elevated probe temperatures some thermal decarboxylation takes place which, analogous to the mechanism for the loss of CO_2 from oxalacetic acid (OAA) [14], may reasonably be expected to yield the gaseous enol **II** :

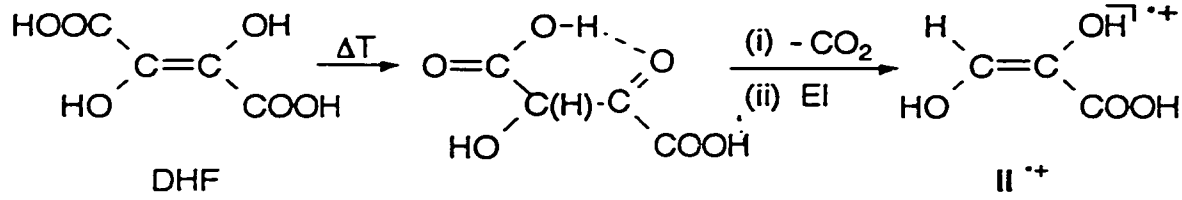

DHF

II $^{\bullet+}$

The NR mass spectrum of the m/z 104 ion generated from DHF appeared to be indistinguishable from that of HPA shown in Fig. 5-1d, whereas its CID mass spectrum was closely similar to that presented in Fig. 5-1c : the only notable difference was the reduced abundance of the m/z 42 (CH_2=C=O$^{\bullet+}$) ion. The latter ion is also present in the MI spectrum of the HPA derived ions (10 % of base peak at m/z 76) but not in that of the DHF derived ion, which exclusively decarbonylates yielding m/z 76 ions whose CID mass spectrum is indistinguishable from that presented in Fig. 5-2b for HPA. Thus, we conclude that the long-lived HPA ions have largely isomerized into their enol counterpart which may decarbonylate as shown in Scheme 7, i.e. analogous to the decarbonylation of its lower homologue ionized α-hydroxyacrylic acid, CH_2=C(OH)COOH$^{\bullet+}$ [14].

A plausible mechanism for the keto-enol tautomerization of the HPA ions involves two consecutive 1,4-H shifts with the distonic ion **VI**$^{\bullet+}$ as the key intermediate, see Scheme 8 :

Scheme 8

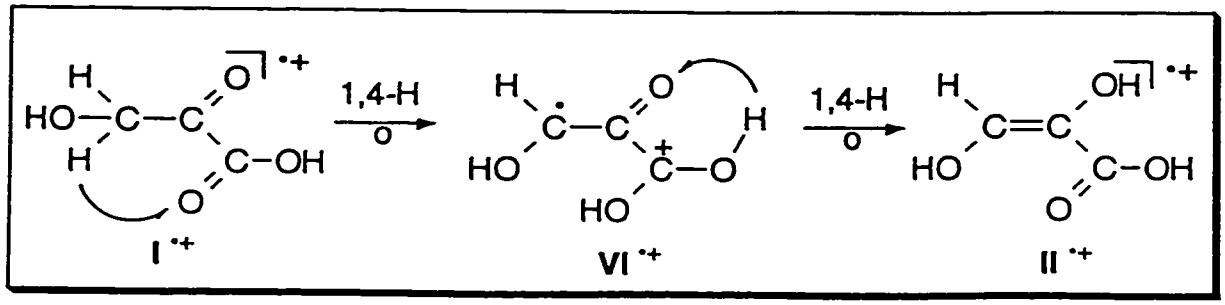

I $^{\bullet+}$ VI $^{\bullet+}$ II $^{\bullet+}$

Considering the size and complexity of the system, a detailed computational treatment of the mechanisms for the high and low energy decarbonylation reactions of HPA ions presented in Schemes 3, 7 and 8 would be a formidable task. We have therefore confined ourselves to exploratory calculations at the B3LYP/6-311+G(3df,3pd)//B3LYP/6-31G(d,p) level of theory [20a] on the HPA isomers $\mathbf{I}^{\bullet+}$- $\mathbf{VI}^{\bullet+}$ that are proposed in the Schemes. Fig. 5-8 shows their optimized geometries, all of which represent stable minima on the $C_3H_4O_4^{\bullet+}$ PES. The enol ion $\mathbf{II}^{\bullet+}$ and the distonic ion $\mathbf{VI}^{\bullet+}$ are found to be considerably more stable than the keto ion $\mathbf{I}^{\bullet+}$, which is in agreement with expectation [26]. More importantly, all of the proposed intermediate species are calculated to lie below the dissociation limit for the direct bond cleavage reaction of lowest energy requirement, $\mathbf{I}^{\bullet+} \rightarrow HOCH_2C{=}O^{+} + {}^{\bullet}COOH$, calculated to lie 22 kcal/mol above $\mathbf{I}^{\bullet+}$.

Figure 5-8. B3LYP/6-31G(d,p) optimized geometries for ionized β-hydroxypyruvic acid, $I^{\bullet+}$ and selected stable isomers thereof. Values in parentheses refer to relative energies (kcal/mol) calculated at the B3LYP/6-311+G(3df,3pd) + ZPVE level of theory.

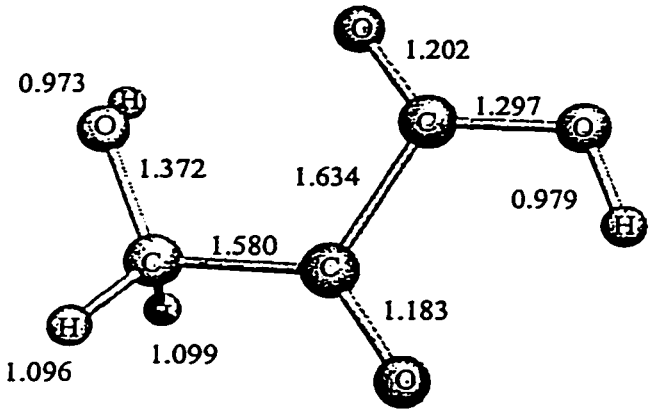

$I^{\bullet+}$ [0.0]

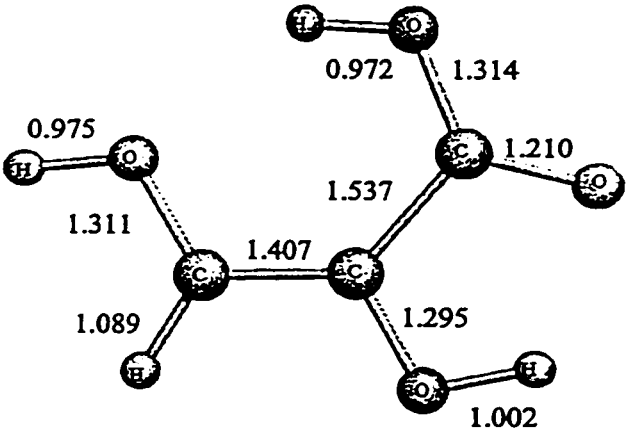

$II^{\bullet+}$ [-21.6]

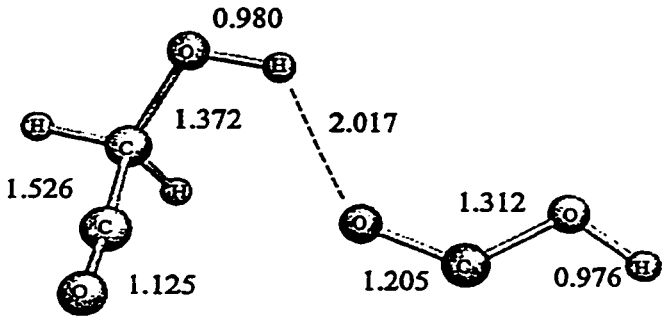

$IV^{\bullet+}$ [6.1]

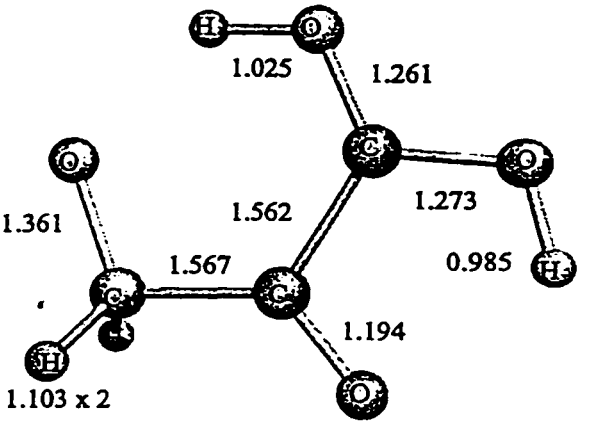

$V^{\bullet+}$ [18.3]

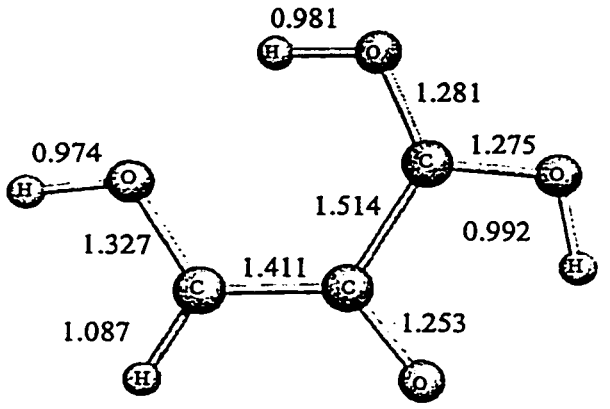

$VI^{\bullet+}$ [-22.9]

Conclusion

Ionized β-hydroxypyruvic acid (as well as its methyl ester) undergoes decarbonylation and depending on the internal energy content, fragmentation occurs via two distinct mechanisms, leading to two distinct product structures, see Scheme 9.

Scheme 9

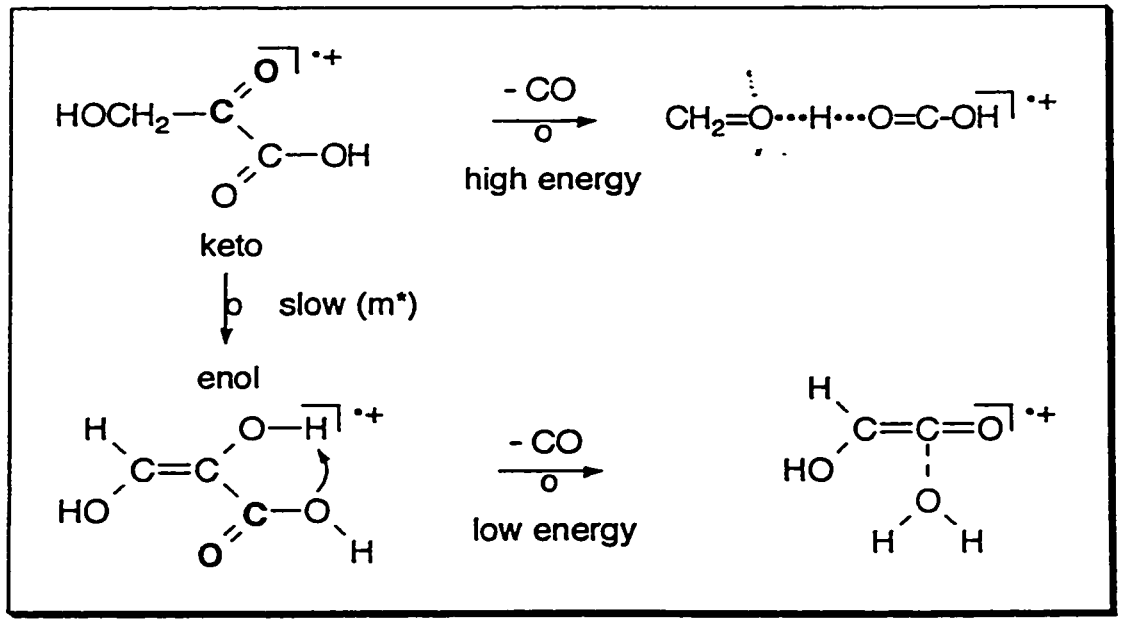

(i) At high internal energies, specific elimination of the keto C=O is observed ; this reaction is not a least-motion extrusion into ionized glycolic acid, $HOCH_2COOH^{\bullet+}$, but a rearrangement which produces the title H-bridged radical cation $CH_2{=}O{\bullet\bullet\bullet}H{\bullet\bullet\bullet}O{=}C\text{-}OH^{\bullet+}$.

(ii) By contrast, at low internal energies, it is the carboxyl C=O which is specifically lost. Comparative collision induced dissociation experiments show that the long lived, non-decomposing molecular ions have irreversibly rearranged to the more stable enol structure, $HOCH{=}C(OH)COOH^{\bullet+}$ which serves as precursor for CO loss and which contains only one C=O functionality. Again, decarbonylation is not a least-motion extrusion but a rearrangement yielding the ion-dipole complex $HOC(H){=}C{=}O^{\bullet+}/H_2O$ which is more stable than the above radical cation.

Hence, the more stable product ions are generated only at low internal energies i.e. from molecular ions that dissociate slowly, whereas the lesser stable product ions are formed only at elevated energies, i.e. from molecular ions that dissociate rapidly. This is

precisely what is expected as the more stable product ion can only be formed after slow isomerization of the molecular ions into the enol structure.

(iii) The H-bridged ion and its conventional isomer glycolic acid, $HOCH_2COOH^{+\bullet}$ both undergo decarboxylation into the ylidion $CH_2OH_2^{+\bullet}$. *Ab initio* calculations indicate that for the acid, stretching of the C-C bond leads eventually to proton transfer to generate the stable H-bridged radical cation CH_2-O(H)•••H•••O=C=O$^{+\bullet}$ which then sheds CO_2. The titled H-bridged ions dissociate via a higher energy route which involves the ionized carbene $HO(H_2)CO$-C-$OH^{+\bullet}$.

Experimental and theoretical

The β-hydroxypyruvic acid (HPA) samples used in this study were obtained from Sigma and used without further purification. The EI mass spectrum of HPA shown in Fig. 5-1a was obtained as follows : a probe tube (glass, 15 mm, d = 1 mm) filled with tightly packed sample (~ 15 mg) was introduced via the direct solids insertion probe into the ion chamber such that the tip of the capillary just protruded into the source, which was kept at 110 °C. The bottom part of the sample tube was kept at ambient temperature and radiative heat transfer from the ion chamber to the sample tube caused the sample to slowly evaporate into the source yielding a stable ion current for c. 1h. The spectrum shown in Fig. 5-1b was obtained by increasing the source temperature to 170 °C. All other experiments on HPA and the samples described below were performed at a source temperature of 110 °C.

Samples of the methyl ester of HPA were prepared on a mg scale by dissolving c. 30 mg of the acid in 150 mL of dry methanol and leaving the clear solution at room temperature. A ^{13}C NMR control experiment showed that the esterification of this rather strong acid is essentially complete in 30 min.

Next, the alcohol and the water were quickly removed from the reaction mixture using a rotary pump and the residual viscous liquid was then introduced into the ion chamber of the mass spectrometer using the all quartz direct liquids insertion probe.The sample reservoir of this probe was kept at ambient temperature and under these conditions the parent acid does not noticably evaporate. The ^{18}O labelled isotopomer

$HOCH_2C(=O^{18})COOCH_3$ was obtained by first preparing the methyl ester as described above and then adding 20 mL of $H_2{}^{18}O$ (90 % ^{18}O, 3.7 % ^{17}O) (Ventron GMBH, Karlsruhe) to allow the carbonyl oxygen to exchange [29]. The mixture was left at room temperature for 10 minutes and was then worked up and introduced as described above. EI mass spectra of the molecular ion region showed that only one ^{18}O atom had been incorporated in the ca. 40 % enriched ester. The ^{18}O labelled isotopomer of the acid, $HOCH_2C(=O^{18})COOH$, M = 106, was prepared by dissolving ca. 30 mg of the acid in 200 mL of 3 : 1 mixture of CH_3OH and $H_2{}^{18}O$ and leaving the clear solution at room temperature for 10 min (at much longer reaction times and when using $H_2{}^{18}O$ only, a noticable exchange of the carboxyl group also takes place). The sample was then worked up and introduced as described above for the acid. EI mass spectra of the molecular ion region showed that only one ^{18}O atom had been incorporated (m/z 108 < 5 % of m/z 106) in the ca. 50 % enriched ester. The D labelled HPA isotopomer $DOCH_2C(=O)COOD$ was prepared by dissolving ca. 30 mg of the acid in 150 mL of CH_3OD followed by immediate work up as described above. EI mass spectra of the sample showed that not more than two D atoms had been incorporated, thus showing that the acid does not equilibrate with its enol form under these conditions (see Introduction). The dihydroxyfumaric acid (DHF) sample came from Aldrich and was used without further purification. The intensity of the m/z 104 ion resulting from EI ionization of its *in situ* generated thermal decarboxylation product $HO(H)C{=}C(OH)COOH$, **II**, was comparable to that of the DHF molecular ion (see experimental and Table 1 of ref. 10 for further details).

The mass spectrometric experiments were performed with the McMaster University VG Analytical (Manchester, UK) ZAB-R instrument of BE_1E_2 geometry (B, magnet; E, electric sector) [30] using an accelerating voltage of 8 or 10 keV. Metastable ion (MI) mass spectra were recorded in the second field-free region (2ffr) ; Collision-induced dissociation (CID) mass spectra were recorded in the 2 and 3ffr using oxygen as collision gas (transmittance T = 70%). The CID mass spectra of the 2ffr metastable or CID peaks (MS/MS experiments) were obtained in the 3ffr using O_2 as the collision gas. Neutralization-reionization (NR) spectra were recorded in the 2ffr using N,N-dimethyl-aniline as reducing agent and oxygen gas for reionization. All spectra were recorded using a small PC-based data system developed by Mommers Technologies Inc. (Ottawa).

Standard *ab initio* and density functional MO calculations were performed with the Gaussian 94 suite of programs [31]. Key results (transition states) were verified with the GAMESS [31] computational chemistry program using the RHF/DZP methodology (see reference [3] for details). For the $C_2H_4O_3^{\cdot+}$ isomers geometry optimizations and frequency calculations were performed at the UHF/6-31G*, UB3LYP/6-31G* [32] and UMP2(full) /6-31G* levels of theory. The coupled cluster approximation [33] utilizing singles, doubles and estimated triple excitations (CCSD(T)) was used to obtain our best relative energies on UMP2(full)/6-31G* optimized structures. The CCSD(T) calculations used the double zeta correlation consistent basis set of Dunning, cc-pVDZ [34]. Scaling factors for zero-point vibrational energies (ZPVE) were : HF = 0.9, B3LYP = unscaled and MP2(full) = 0.9646 [23]. All transition states had the correct number of negative eigenvalues of the corresponding Hessian matrix. The reaction pathways were verified with IRC calculations, at the same level of theory as the geometry optimizations. The HPA isomeric ions (Fig. 5-8) were optimized with the B3LYP/6-31G(d,p) method. The relative energies reported in Fig. 5-8 were generated using the same hybrid functional but with a much larger basis set, 6-311+G(3df,3pd) which reproduced typical keto(**I**)-enol(**II**) energy differences. The spin contamination of the UHF wavefunctions was acceptable for all species investigated, i.e. less than 10 % of 0.75. The ray-traced images of the optimized structures in Figure 5-4 and 5-8 were generated from their Gaussian output using a combination of PovChem [35] and POV-Ray [36]. Numerical values for the (dihedral) bond angles in the structures presented are available on request.

References

1. For selected reviews see : (a) T.H. Morton. Tetrahedron, **38**, 3195 (1982) ; (b) N. Heinrich and H. Schwarz. *In* Ion and cluster ion spectroscopy and structure. *Edited by* J.P. Maier. Elsevier, Amsterdam. 1989. p. 329 ; (c) P.C. Burgers and J.K. Terlouw. *In* Specialist Periodical Reports : Mass Spectrometry. *Edited by* M.E. Rose. The Royal Society of Chemistry, London. **10**, 35 (1989) ; (d) T.H. Morton. Org. Mass Spectrom. **27**, 353 (1992) ; (e) J.S. Splitter. *In* Applications of Mass Spectrometry to Organic Stereochemistry. *Edited by* J.S. Splitter and F. Turecek. VCH, Weinheim. 1994. Chapter 3.
2. (a) J.K. Terlouw, W. Heerma, P.C. Burgers and J.L. Holmes. Can. J. Chem. **62**, 289 (1984) ; (b) R. Postma, P.J.A. Ruttink, F.B. van Duijneveldt, J.K. Terlouw and J.L. Holmes. Can. J. Chem. **63**, 2798 (1985) ; (c) R. Postma, S.P. van Helden, J.H. van Lenthe, P.J.A. Ruttink, J.K. Terlouw and J.L. Holmes. Org. Mass Spectrom. **23**, 503 (1988) ; (d) P. George, J.P. Glusker and C.W. Bock. J. Am. Chem. Soc. **117**,10131 (1995) .
3. (a) P.J.A. Ruttink and P.C.Burgers. Org. Mass Spectrom. **28**, 1087 (1993) and references cited therein ; (b) P. C. Burgers , L. M. Fell , A. Milliet , M. Rempp , P.J.A. Ruttink and J. K. Terlouw. Int. J. Mass

Spectrom. Ion Processes, (1997) in press ; (c) P.J.A. Ruttink, P.C. Burgers, L. M. Fell and J.K. Terlouw. J. Phys. Chem. submitted for publication.
4. P.J.A. Ruttink, P.C. Burgers and J.K. Terlouw. Can. J. Chem. **74**, 1078 (1996) and references cited therein.
5. (a) D. Suh, C.A. Kingsmill, P.J.A. Ruttink, P.C. Burgers and J.K. Terlouw. Int. J.Mass Spectrom. Ion Processes, **146/147**, 305 (1995) ; (b) D. Suh, P.C. Burgers and J.K. Terlouw. Int. J. Mass Spectrom. Ion Processes, **144**, L1 (1995) ; (c) H. Friedrichs, G.A. McGibbon and H. Schwarz. Int. J. Mass Spectrom. Ion Processes, **152**, 217 (1996) .
6. D.K. Böhme. Int. J. Mass Spectrom. Ion Processes, **115**, 95 (1992) ; see also : P.J.A. Ruttink. *In* The Structure of Small Radicals and Ions. *Edited by* R. Naaman and Z. Vager. Plenum Press, New York. 1989, p. 243 ; for CH_3^+ shuttle see : V. Baranov, S. Petrie and D.K. Böhme. J. Am. Chem. Soc. **118**, 4500 (1996).
7. (a) P. Mourges, H.-E. Audier, D. Leblanc and S. Hammerum. Org. Mass Spectrom. **28**, 1098 (1993) ; (b) H.-E. Audier, D. Leblanc, P. Mourgues, T.B. McMahon and S. Hammerum. J. Chem. Soc. Chem. Commun. (1994) 2329 ; (c) J.W. Gauld, H.-E. Audier, J. Fossey and L. Radom. J. Am. Chem. Soc.**118** , 6299 (1996). (d) J.W. Gauld and L. Radom, J. Am. Chem. Soc. **119**, 9831 (1997) ; (e) A.J. Chalk and L. Radom, J. Am. Chem. Soc. (1997) in press. 8.D. Sülzle, J.K. Terlouw and H. Schwarz. Angew. Chem. Int. Ed. Engl. **29**, 404 (1990).
9. D. Suh, P.C. Burgers and J.K. Terlouw. Rapid Commun. Mass Spectrom. **9**, 862 (1995).
10. J. Hrusak, G.A. McGibbon, H. Schwarz and J.K. Terlouw. Int. J. Mass Spectrom. Ion Processes. **160**,117 (1997)
11. D. Suh, J.T. Francis, J.K. Terlouw, P.C. Burgers and R.D. Bowen. Eur. Mass Spectrom. **1**, 545 (1995).
12. J.L. Hedrick and H.J. Sallach. J. Biol. Chem. **236**, 1872 (1961).
13. (a) F. Dickens and D.H. Williamson. Biochem. J. **68**, 74 (1958) ; (b) L.J. Bellamy and R.L. Williams, ibid., **68**, 81 (1958) ; (c) F. Dickens and D.H. Williamson. ibid. **68**, 84 (1958) ; (d) C.T. Chow and B. Vennesland. J. Biol. Chem. **233**, 997 (1958) ; (e) M.B. Fleury and D. Fleury. Biological Aspects of Electrochemistry. Proc. 1st Int. Symp. Rome (Italy) 1971 Experientia Supplementum 18.
14. L.M. Fell, J.T. Francis, J.L. Holmes and J.K. Terlouw. Int. J. Mass Spectrom. Ion Processes, **165/166b,** 179 (1997) .
15. F. Mer, The Dictionary of Organic Compounds, 6th Edition, Vol. 4, Chapman & Hall, London, 1996, p. 3778.
16. (a) J.K. Terlouw, C.G. de Koster, W. Heerma, J.L. Holmes and P.C. Burgers. Org. Mass Spectrom. **18**, 222 (1983) ; (b) R. Postma, P.J.A. Ruttink, J.K. Terlouw and J.L. Holmes. J. Chem. Soc., Chem. Commun. 683 (1986).
17. P.C. Burgers, L. M. Fell, P.J.A. Ruttink and J.K. Terlouw, Chapter 6.
18. (a) S. Lias, J.E. Bartmess, J.F. Liebman, J.L. Holmes, R.D. Levin and W.G. Mallard. J. Phys. Chem. Ref. Data, **17** (1988) Supplement 1 ; (b) J.L. Holmes, F.P. Lossing and P.M. Mayer. J. Am. Chem. Soc. **113**, 9723 (1991).
19. P.C. Burgers, G.A. McGibbon and J.K. Terlouw. Chem. Phys. Lett. **224**, 539 (1994).
20. (a) For a concise description and evaluation of the various computational methods and strategies see : J.B. Foresman and A. Frisch, Exploring Chemistry with Electronic Structure Methods, Gaussian, Inc., Pittsburgh, PA, 1996, Ch. 7 ; (b) L.A. Curtiss, K. Raghavachari and J.A. Pople. J. Chem. Phys. **98** , 1293 (1993) ; (c) J.W. Ochterski, G.A. Petersson and J.A. Montgomery Jr., J. Chem. Phys. **104**, 2598 (1996) and references cited therein.
21. For a recent review see : N. Goldberg and H. Schwarz. Acc. Chem. Res. **27**, 34 (1994).
22. J.L. Holmes and J.K. Terlouw, Org. Mass Spectrom. **15**, 383 (1980).
23. J.A. Pople, A.P. Scott, M.W. Wong and L. Radom. Israel J. Chem. **33**, 345 (1993).
24. M. Meot-Ner (Mautner). J. Am. Chem. Soc. **106**, 1257 (1984).
25. (a) B.J. Smith and L. Radom. J. Phys. Chem. **99**, 6468 (1995) ; (b) J. E. Szulejko and T.B. McMahon, J. Am. Chem. Soc. **115**, 7839 (1993) ; (c) H.E. Audier, J. Fossey, P. Mourgues, D. Leblanc, S. Hammerum.Int. J. Mass Spectrom. Ion Processes, **157/158**, 275 (1996) ; (d) A.P. Scott and L. Radom. Int. J. Mass Spectrom. Ion Processes, **160**, 73 (1997).
26. F. Turecek. *In* The Chemistry of Enols. *Edited by* Z. Rappoport. John Wiley & Sons, Chichester. 1990. pp.95-146.

27. K. Iijima, M. Kato, B. Beagley. J. Mol. Struc. **295**, 289 (1993).
28. (a) E. Coitino, A. Lledos, R. Serra, J. Bertran and O.N. Ventura. J. Am. Chem. Soc. **115**, 9121 (1993) ; (b) E. Coitino, A. Pereira and O.N. Ventura. J. Chem. Phys. **102**, 2833 (1995).
29. G.W.A. Milne. *In* Mass Spectrometry : Techniques and Applications. Wiley-Interscience, London.1971. p. 279.
30. H.F. van Garderen, P.J.A. Ruttink, P.C. Burgers, G.A. McGibbon and J.K. Terlouw. Int. J. Mass Spectrom. Ion Processes, **121**, 159 (1992).
31. (a) Gaussian 94, Revision B.3, M. J. Frisch, G.W. Trucks, H.B. Schlegel, P.M.W. Gill, B.G. Johnson, M.A. Robb, J.R. Cheeseman, T.A. Keith, G.A. Peterson, J.A. Montgomery, K. Raghavachari, M.A. Al-Laham, V.G. Zakrevski, J.V. Ortiz, J.B. Foresman, C.Y. Peng, P.Y. Ayala, W. Chen, M.W. Wong, J.L. Andres, E.S. Replogle, R. Gomperts, R.L. Martin, D.J. Fox, J.S. Binkley, D.J. de Frees, J. Baker, J.P. Stewart, M. Head-Gordon, C. Gonzales and J.A. Pople, Gaussian Inc., Pittsburgh PA, 1995.
(b) M.F. Guest, J. Kendrick. GAMESS Users Manual, SERC Daresbury Laboratory, CCP/86/1, 1986 ; M. Dupuis, D. Spangler and J. Wendolowski. NRCC Software Catalog, Vol. 1, Program No. QG01 (GAMESS), 1980 ; M.F. Guest, R.J. Harrison, J.H. van Lenthe and L.C.H. van Corler, Theor. Chim. Acta ,71 (1987) 117.
32. (a) A.D. Becke. J. Chem. Phys. **98**, 5648 (1993) ; (b) C. Lee, W. Yang and R.G. Parr. Phys. Rev. B, **37**, 785 (1988) ; (c) B. Meihlich, A. Savin, H. Stoll and H. Preuss. Chem. Phys. Lett. **157**, 200 (1989).
33. (a) J. Cizek. Adv. Chem. Phys. **14**, 35 (1969) ; (b) J.A. Pople, R. Krishnan, H.B. Schlegel and J.S. Binkley. Int. J. Quant. Chem. **14**, 545 (1978) ; (c) R.J. Bartlett and G.D. Purvis. Int. J. Quant. Chem. **14**, 516 (1978).
34. (a) T.H. Dunning Jr., J. Chem. Phys. **90**, 1007 (1989) ; (b) R.A. Kendall,T.H. Dunning Jr and R.J. Harrison. J. Chem. Phys. **96**, 6796 (1992).
35. P. A. Thiessen, see http://ludwig.scs.uiuc.edu/~paul/PovChem.html
36. Rendered images were generated using the copyrighted freeware Persistance of Vision Ray Tracer, POV-Ray Version 3.01 available at http://www.povray.org.

ADDENDUM TO CHAPTER 5

A REVISED MECHANISTIC PROPOSAL FOR THE DECARBOXYLATION OF THE HYDROGEN-BRIDGED RADICAL CATION CH_2=O•••H•••O=C-OH$^{\bullet+}$

INTRODUCTION

In the preceding Chapter the fascinating gas-phase ion chemistry of β-hydroxypyruvic acid and its high energy decarbonylation product the hydrogen-bridged radical cation CH_2O•••H•••O=C-OH$^{\bullet+}$, was studied by theory and experiment. This Addendum complements the previous investigation where it concerns the proposed multistep decarboxylation mechanism of low energy ions **3a**$^{\bullet+}$ into $CH_2OH_2^{\bullet+}$. We have found that the last step in this mechanism (Figure 5 and Scheme 5 of Chapter 4), i.e. the decarboxylation of the energetically high lying distonic ion, **7**$^{\bullet+}$, H_2O^+-CH_2-O-C$^{\bullet}$=O, into $CH_2OH_2^{\bullet+}$ + CO_2 is not continuously endothermic but involves an appreciable reverse barrier. This barrier lies above the experimentally imposed energy limit, i.e. the energy required for the formation of $^+CH_2OH$ + O=C-OH$^{\bullet}$. Therefore, we have continued the computational investigation of this system to find a more plausible description of this decarboxylation mechanism. The $C_2H_4O_3^{\bullet+}$ system represents an intriguing and complex surface with many stationary points, which is still not fully explored with computational chemistry but we believe we have found a connection between glycolic acid ions and the isomeric hydrogen-bridged radical cation which satisfactorily describes the experimental observations on this decarboxylation process.

RESULTS AND DISCUSSION

PREAMBLE

Before discussing the energetics of the dissociation of two ions which can directly form the low energy decarboxylation product $CH_2OH_2^{\bullet+}$, we will first deal with higher level computations of the dissociation limits. This was done to verify the reliability of the heat of formation of our previous anchor point, ionized trihydroxyethylene, **1**$^{\bullet+}$. The value that we had used for ΔH_f^0(**1**$^{\bullet+}$) = 73.4 kcal/mol, was obtained from a G2MP2 calculation. Advancing the level of theory to G2 for this ionized species we find, via an atomization

reaction, 69.8 kcal/mol and using ΔH_T = -1.8 kcal/mol yields $\Delta H_f^{298}(\mathbf{1}^{\bullet+})$ = 68.0 kcal/mol. The same calculation on ion $\mathbf{3a'}^{\bullet+}$ renders, $\Delta H_f^0(\mathbf{3a'}^{\bullet+})$ = 101.2 kcal/mol or 100.4 kcal/mol at 298 K and this value is in excellent agreement with our previous empirical estimate of 99 kcal/mol (see chapter 4). G2 calculations were also performed on the dissociation levels [CO_2 + $CH_2OH_2^{\bullet+}$] and [$^+CH_2OH$ + $HOCO^\bullet$] and their energies are also presented in Table 1, along with our previous results obtained at the CCSD(T)/cc-pVDZ//MP2(Full)/6-31G* + ZPVE level of theory. The agreement between the G2 0K level and the CCSD(T) level is quite satisfactory. The difference in relative energy being close to the proposed accuracy, ± 3 kcal/mol, for this method (see Chapter 4). It should also be realized that G2 calculations are not yet feasible nor meaningful for an entire ionic PES.

Table 1. Comparison of G2 and CCSD(T) relative energies of two key ions and dissociation limits on the $C_2H_4O_3^{\bullet+}$ potential energy surface.

Species	G2(0K) -303. hartree	G2(298K) -303. hartree	E_{rel} (0K) kcal/mol	E_{rel} (298K) kcal/mol	E_{rel} CCSD(T) + ZPVE[a] kcal/mol
$\mathbf{1}^{\bullet+}$	0.55652	0.55119	**0.0**	0.0	**0.0**
$\mathbf{3a'}^{\bullet+}$	0.50641	0.49925	**31.4**	32.6	**26.8**
$CO_2 + CH_2OH_2^{\bullet+}$	0.50442	0.49780	**32.7**	33.5	**29.8**
$^+CH_2OH + HOCO^\bullet$	0.46818	0.46198	**55.4**	56.0	**53.4**

[a] Zero-point vibrational energy scaled by 0.9646 [1]

Next, we computationally identified the transition state for the loss of CO_2 from ion $\mathbf{7}^{\bullet+}$, **TS 1**, by the now verified CCSD(T)//MP2 method. Surprisingly, it lies significantly above the dissociation limit $^+CH_2OH$ + $HOCO^\bullet$ by some 16 kcal/mol (see Table 2). Since the experimental observations show that dissociation into $^+CH_2OH$ does not take place in the metastable time frame to any significant extent. We conclude that the decarboxylation of ions **3a** does not occur via **TS 1**, at least not form the low energy (metastable) ions. On the other hand, the decarboxylation of ion $\mathbf{3c}^{\bullet+}$ requires little or no activation energy. This was verified by scanning the potential energy surface by stepwise lengthening the distance between ionic and neutral moieties up to ~ 30 Å. These two

dissociations are depicted in the energy level diagram of Figure 1. Hence it became clear that our former mechanism for the dissociation of the hydrogen-bridged radical cation needs revision.

Figure 1. Computational energy level diagram for the formation of CO_2 + $CH_2OH_2^{\bullet+}$ from the distonic ion $7^{\bullet+}$ and the hydrogen-bridged radical cation $\mathbf{3c}^{\bullet+}$.

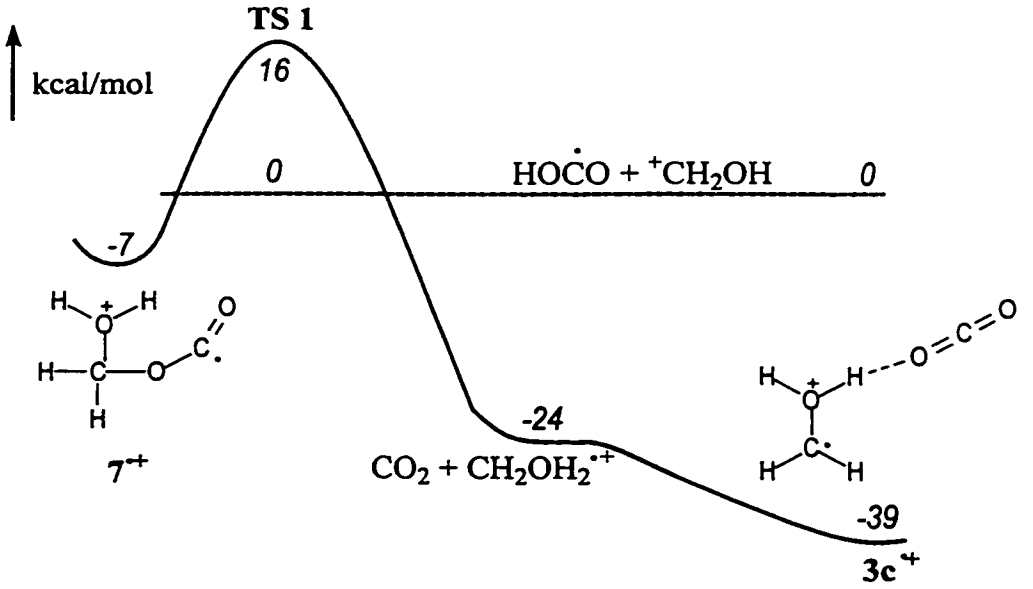

A New Proposal for the Decarboxylation of the Hydrogen-Bridged Radical Cation CH_2=O•••H•••O=C-OH$^{\bullet+}$

Further exploration of the MP2(Full)/6-31G* PES of glycolic acid$^{\bullet+}$ and its HBRC isomer, CH_2=O•••H•••O=C-OH$^{\bullet+}$, yielded two new key minima and two important transition states. A summary of the *ab initio* calculations on these new species and pertinent previous values is presented in Table 2. Note that the anchor point used for evaluation is now the dissociation limit [$^{+}CH_2OH$ + O=C-OH$^{\bullet}$]. The new structures and their key structural parameters are presented in Figure 2, which depicts our revised decarboxylation mechanism of CH_2=O•••H•••O=C-OH$^{\bullet+}$. The associated energy level diagram is presented in Figure 3.

Table 3 presents selected results from an Atoms in Molecules (AIM) analysis of this reaction pathway [2]. This theory defines the properties of atoms in molecules based

on an analysis of the charge density. It can also provide an elegant characterization of the structure and bonding in a molecule, it is this aspect of the theory which is presented in Table 3. This bonding analysis was performed on MP2(Full)/6-31G* [6d 10f] wave functions generated from the optimized geometries. All species obeyed the Poincare-Hopf relationship: n - b + r - c = 1, where n = number of nuclei, b = number of bond paths, r = number of rings and c = number of cages [2]. The results presented in Table 3 center on the value of the electronic charge density at a bond critical point, ρ_b, between two carbon atoms or between oxygen and hydrogen atoms. For both the C-C and O-H bonds, as these bonds are lengthened the charge density in the bond decreases as expected [2]. For comparison an AIM analysis was also performed on ion $\mathbf{2c}^{\bullet+}$, so that long C-C bonds can be compared to short ones.

The new structures are rotamers of previous structures, starting at the top of Figure 2 with the well characterized HBRC, $\mathbf{3a''}^{\bullet+}$, where in comparison with its rotamer $\mathbf{3a'}^{\bullet+}$, the $HOCO^{\bullet}$ moiety has rotated along its dipole axis. This new conformer is the most stable of the four hydrogen-bridged $\mathbf{3a}^{\bullet+}$ species studied thus far. The next new stable ion, labelled $\mathbf{2c''}^{\bullet+}$, is another "long-bonded" rotamer of glycolic acid. This turns out to be a crucial minimum, it is this structure which provides a connection to the HBRC $\mathbf{3a}^{\bullet+}$ surface by a transition state, $\mathbf{TS\ (3a''\rightarrow 2c'')}^{\bullet+}$, which lies well below the energy limit dictated by experiments whereas it also represents the highest point along the new pathway. The last new structure is a rotational transition state between two long bonded glycolic acid conformers, $\mathbf{TS\ (2c'\rightarrow 2c'')}^{\bullet+}$ involving a rotation of the $HOCO^{\bullet}$ moiety with respect to the $^{+}CH_2OH$ ion part.

It was argued in Chapter 4 that a rotation of the $HOCO^{\bullet}$ dipole away from the ionized moiety would result in a loss of ion-dipole stabilization and hence the moieties would fly apart. A cursory inspection of the results presented in Figure 2 seems to confirm this view since in the first transition state, $\mathbf{TS\ (3a''\rightarrow 2c'')}^{\bullet+}$, the dipole has clearly turned away from the ion. However, a closer look at the geometries presented in this Figure negates this arguement. The stabilization energy of ion $\mathbf{3a}^{\bullet+}$, ~ 13 kcal (see Chapter 4), is proportional to cos θ and thus as the dipole rotates away from the ion (θ = 0° → 60°) it decreases but at the same time a one-electron long bond is being formed, as indicated by the bond critical point between the carbon atoms (see Table 3), so

stabilization is being gained in this way. Hence the transformation **3a**$''^{\bullet+}$→**2c**$''^{\bullet+}$ is quite possible and indeed, as shown in Figure 3, it lies below the energy threshold representing an energy barrier of only 17 kcal/mol relative to ion **3a**$''^{\bullet+}$.

The final step in the rearrangement is a rotation of the $HOCO^{\bullet}$ moiety which orients the glycolic acid ions such that a hydrogen transfer can occur from the $HOCO^{\bullet}$ part to the $^{+}CH_2OH$ side. This yields, via a low barrier, ions **3c**$^{\bullet+}$ which undergo a facile decarboxylation as discussed in the previous section.

Table 2. The UMP2(Full) and CCSD(T) energies, zero-point vibrational energies (ZPVE) and relative energies (CCSD(T) + ZPVE kcal/mol) of the key ions and dissociation limits on the $C_2H_4O_3^{\bullet+}$ potential energy surface.

Species	UMP2(Full) /6-31G* Hartree, -303.	ZPVE kcal/mol	CCSD(T)/ cc-pVDZ Hartree, -303.	E_{rel} CCSD(T) + ZPVE kcal/mol
3a$''^{\bullet+}$	-0.09583	38.5	-0.203616	-27.65
TS [3a''→2c'']$^{\bullet+}$	-0.07065	39.4	-0.178242	-10.86
2c$''^{\bullet+}$	-0.07910	40.7	-0.184049	-13.16
TS [2c''→2c']$^{\bullet+}$	-0.07868	40.8	-0.184092	-13.09
2c$'^{\bullet+}$	-0.08404	41.0	-0.19094	-17.19
TS [2c'→3c]$^{\bullet+}$	-0.07718	38.6	-0.18148	-13.65
3c$^{\bullet+}$	-0.12254	38.5	-0.22138	-38.79
$CO_2 + CH_2OH_2^{\bullet+}$	-0.09992	36.9	-0.19468	-23.63
$^{+}CH_2OH + HOCO^{\bullet}$	-0.05112	37.8	-0.15845	0.00

Table 3. AIM analysis of the decarboxylation mechanism for CH_2=O•••H•••O=C-$OH^{\bullet+}$, the charge density at bond critical points (ρ_b).

Species	Bond Length C-C, Å	ρ_{C-C} x 10^{-2}, au	Bond Length O•••H, Å	$\rho_{O\cdots H}$ x 10^{-2}, au	Bond Length O-H, Å	ρ_{O-H} x 10^{-2}, au
3a$''^{\bullet+}$	-	-	1.484	7.2	1.054, 0.981	25.0, 31.9
TS [3a''→2c'']$^{\bullet+}$	2.548	2.4	-	-	0.991, 0.979	30.9, 32.2
2c$''^{\bullet+}$	1.982	8.3	-	-	0.986, 0.982	31.4, 31.6
TS [2c''→2c']$^{\bullet+}$	1.969	8.5	-	-	0.987, 0.981	31.4, 31.6
2c$'^{\bullet+}$	1.990	8.1	-	-	0.987, 0.984	31.8, 30.9
TS [2c'→3c]$^{\bullet+}$	2.341	4.0	1.675	4.9	1.026, 0.982	26.6, 32.0
3c$^{\bullet+}$	-	-	1.640	4.3	1.011, 0.986	28.1, 31.1
2c$^{\bullet+}$	1.536	24.2	1.824	3.8	1.011, 0.977	28.8, 32.4

Figure 2. The revised mechanism for the decarboxylation of the hydrogen-bridged radical cation $CH_2{=}O{\bullet\bullet\bullet}H{\bullet\bullet\bullet}O{=}C{-}OH^{\bullet+}$ (**3a**$^{\bullet+}$).

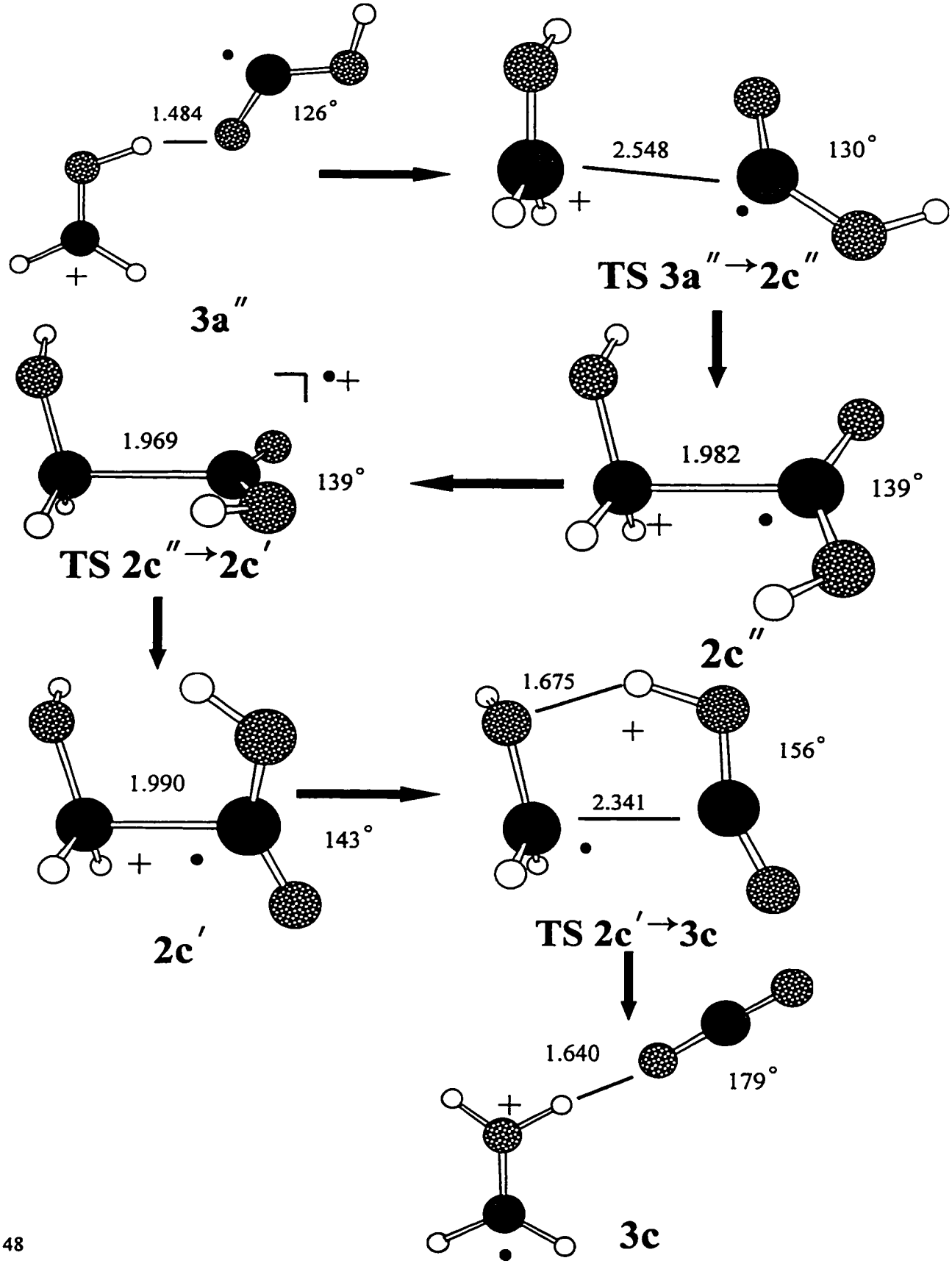

Figure 3. Calculated energy level diagram for the isomerization of ions **3a**$''^{\bullet+}$ into **3c**$^{\bullet+}$

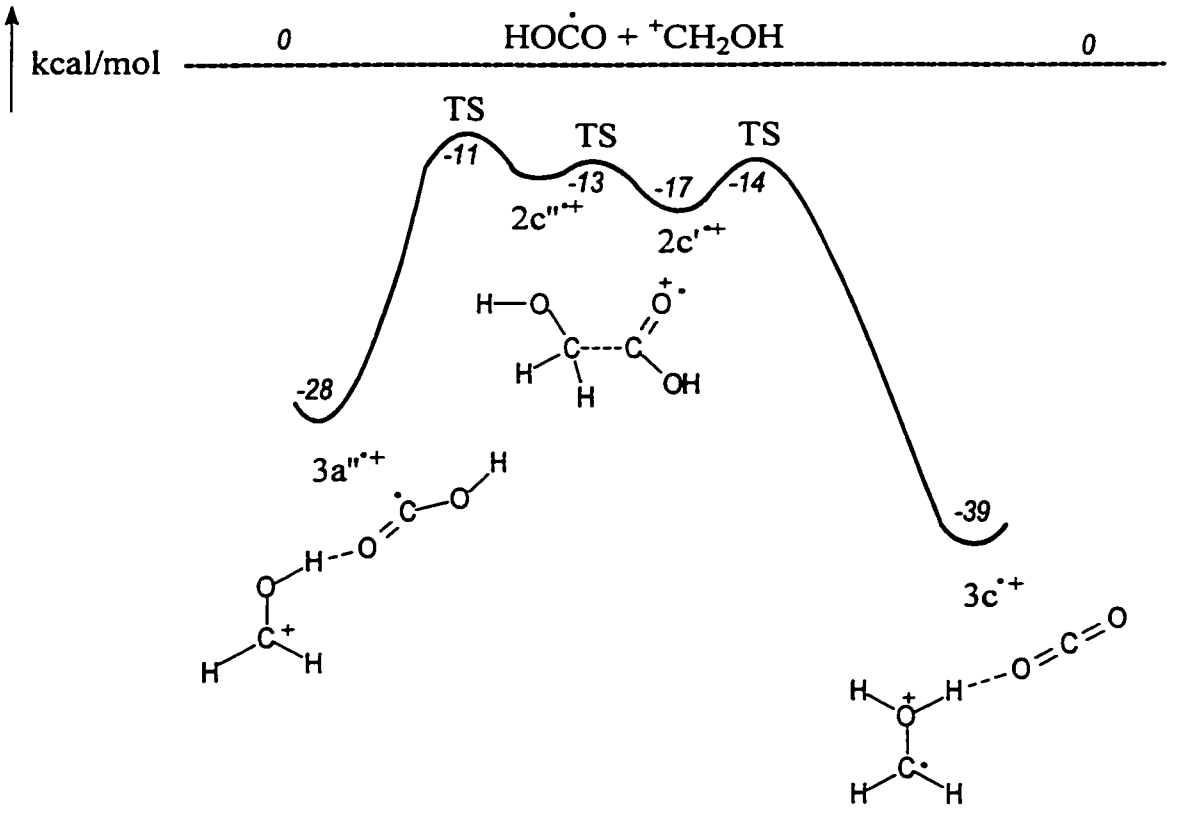

References:

1. Smith, B.J.; Radom, L. *J. Phys. Chem.* **1995**, *99*, 6468.
2. Bader, R.F.W. *Atoms in Molecules*, Pergamon Press : Toronto, 1996.

CHAPTER 6

THE DISSOCIATION CHEMISTRY OF THE HYDROGEN-BRIDGED RADICAL CATION $[CH_2{=}O{\bullet\bullet\bullet}H{\bullet\bullet\bullet}O{=}C{-}OCH_3]^{\bullet+}$: PROTON TRANSPORT CATALYSIS AND CHARGE TRANSFER[1]

Abstract

Tandem mass spectrometry based experiments on the decarbonylation products of ionized methyl-β-hydroxypyruvate and dimethyloxalate show that the hydrogen-bridged radical cation (HBRC) $CH_2{=}O{\bullet\bullet\bullet}H{\bullet\bullet\bullet}O{=}C{-}OCH_3^{\bullet+}$ is a stable species in the gas-phase. Its low energy dissociation products are protonated methylformate, $HOC(H)OCH_3^+$ and the formyl radical, $HC{=}O^\bullet$. The HBRC isomers $HOCH_2C(=O)OCH_3^{\bullet+}$ (ionized methylglycolate) and $(CH_3O)_2C{=}O^{\bullet+}$ (ionized dimethylcarbonate) show the same dissociation characteristics. Deuterium labelling experiments dictate that loss of $HC{=}O^\bullet$ from the title HBRC cannot be formulated as a simple H shift from the formaldehyde moiety to the C-atom of the $O{=}C^\bullet{-}OCH_3$ group. *Ab initio* molecular orbital (MO) calculations support the proposal that this dissociation proceeds via sequential transfers of a *proton*, *electron* and another *proton* within ion-dipole complexes. The first step in this rearrangement process is a 1,2-proton shift catalyzed by a formaldehyde dipole. This yields an ion/dipole complex, $CH_2{=}O{\bullet\bullet\bullet}H{-}C(=O)OCH_3^{\bullet+}$, which is in the correct configuration for electron transfer to occur at the energetic threshold dictated by experiment. The resulting intermediate triggers the transfer of yet another *proton* from the formaldehyde unit thereby generating another stable H-bridged radical cation *viz.* $HC{=}O{\bullet\bullet\bullet}H{\bullet\bullet\bullet}OC(H)OCH_3^{\bullet+}$. This final intermediate dissociates with little or no activation energy into $HOC(H)OCH_3^+$ and $HC{=}O^\bullet$. It is further predicted by the calculations that ionized methylglycolate isomerizes into the title hydrogen-bridged radical cation by a fairly high barrier which makes the communication between ionized

[1] This chapter has been submitted for publication under the same title: L.M. Fell, P.J.A. Ruttink, P.C. Burgers, M.A. Trikoupis and J.K. Terlouw, *Int. J. Mass Spectrom. Ion Processes*,

methylglycolate and dimethylcarbonate via the title ion quite unlikely ; instead an alternative route for this communication is proposed.

Introduction

In a previous study the decarbonylation of ionized β-hydroxypyruvic acid (HPA) was investigated and it was shown that the high energy molecular ions dissociate into the hydrogen-bridged radical cation (HBRC), CH_2=O•••H•••O=C-OH$^{\bullet+}$ [1]. It was further reported that the methyl ester of HPA, methyl-β-hydroxypyruvate, also readily decarbonylates upon ionization and it was tentatively proposed that the methyl substituted HBRC CH_2=O•••H•••O=C-$OCH_3^{\bullet+}$ was the product ion generated in the ion source. This interesting ion belongs to the m/z 90, $C_3H_6O_3^{\bullet+}$ family of ions which includes ionized methyl glycolate, $HOCH_2C(=O)OCH_3^{\bullet+}$, **1** and ionized dimethyl carbonate, $CH_3OC(=O)OCH_3^{\bullet+}$, **2**. The ion chemistry of **1** and **2** has been studied before and it was found that their low energy (metastable) ions predominantly lose a formyl radical, HC=O$^{\bullet}$, to yield $CH_3OC(H)OH^+$, protonated methylformate, as the product ion [2]. The kinetic energy releases (KER) as well as the dissociation levels for the two ions were found to be the same within experimental error and this was taken as evidence that **1** and **2** lose HC=O$^{\bullet}$ via the same mechanism. From extensive labeling experiments it was further concluded that **1** and **2** are separated by a sizable energy barrier and that **2** dissociates via **1** and not vice versa. Ab initio calculations were also performed, at the MP3/6-311G**/HF/6-31G** level of theory, and from experiment and theory a mechanism was derived which is presented in Scheme 1. In this mechanism the title HBRC CH_2=O•••H•••O=C-$OCH_3^{\bullet+}$, denoted as structure **7**, is proposed to be a key intermediate in the dissociation chemistry of low energy ions **1** and **2**.

We were curious then to see if **7** behaved analogously to ionized methylglycolate and indeed, in the metastable time frame it, too, readily loses HC=O$^{\bullet}$, with the same KER as **1** and **2**. Thus, the mechanism by which the HBRC loses HC=O$^{\bullet}$ may well be related to that of ions **1** and **2** and a detailed computational analysis of this mechanism forms the theme of this article.

Scheme 1

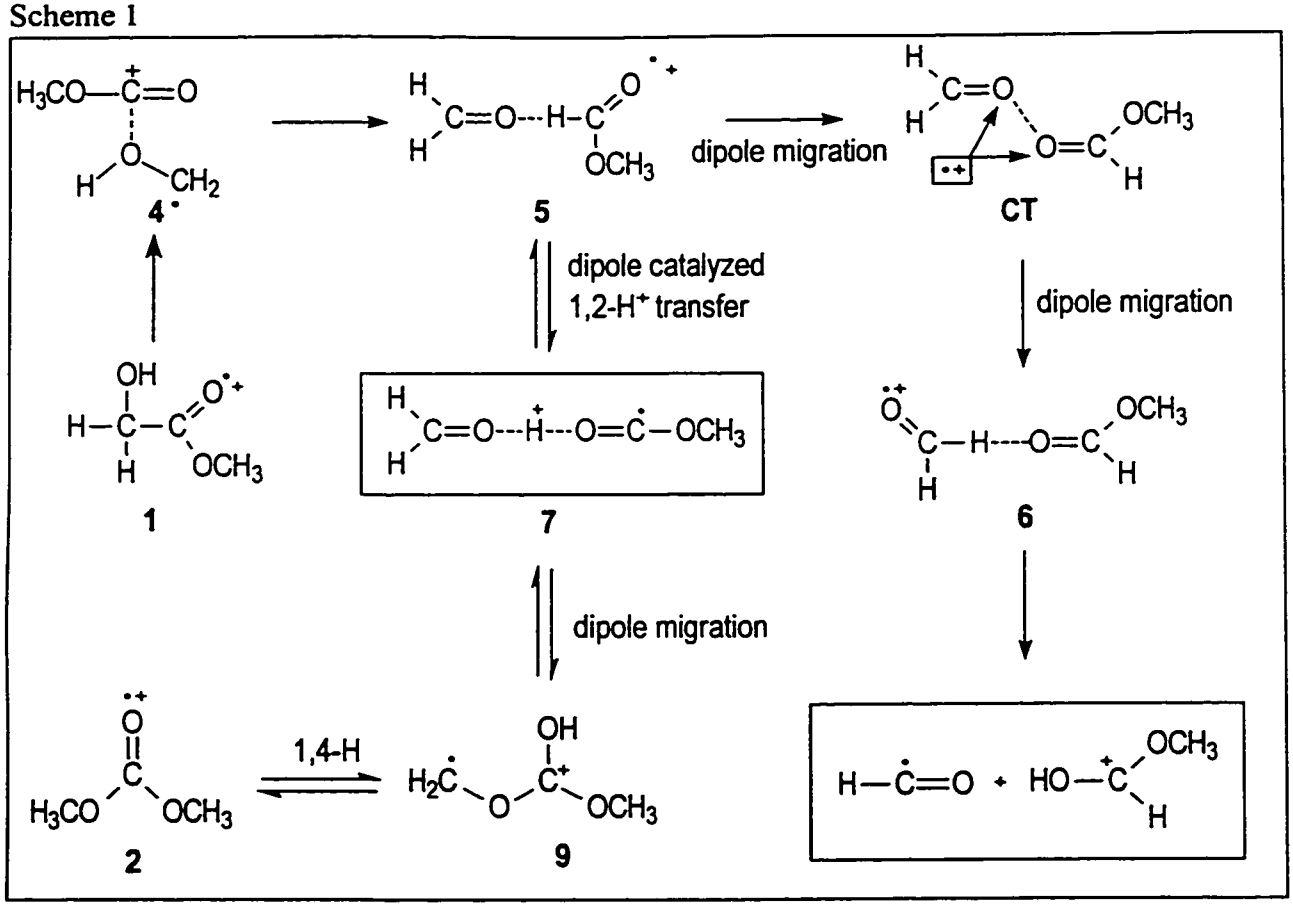

A key experimental result from the previous study of **1** and **2** was that OD labeled ions **1** lose HC=O$^{\bullet}$ to produce the following C-D labeled product ion [2]:

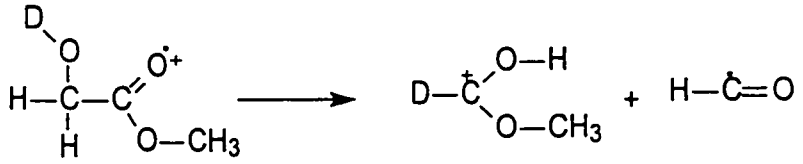

From extensive D, ^{13}C and ^{18}O labeling experiments, it was further concluded that this reaction is 75% atom specific for ions **1**. The D labeled isotopomer $CH_2{=}O{\bullet\bullet\bullet}D{\bullet\bullet\bullet}O{=}C{-}OCH_3^{\bullet+}$ of **7** produces the same C-D labeled protonated methylformate ion as shown above for 1-OD, but with an even higher atom specificity. This specific deuterium transfer eliminates many otherwise plausible mechanisms for the loss of HC=O$^{\bullet}$.

One mechanism that does satisfy the D labeling results in **1** involves conversion of the methylglycolate ion to its more stable enol counterpart, *viz*:

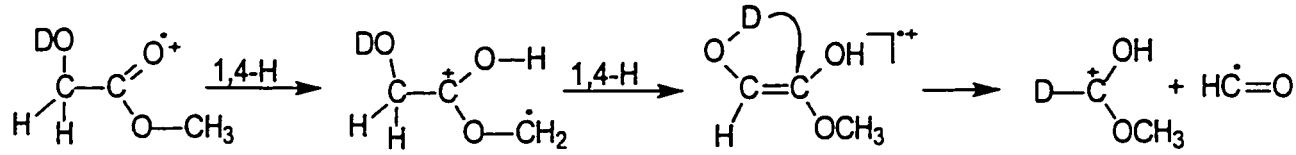

However, the dissociation chemistry of the enol ion appears to be quite different from that of the keto ion **1** [3], showing that enolization of **1** as proposed above does **not** occur.

A more plausible mechanistic proposal considered in ref. 1 involves a mechanism akin to that for the loss of $HC{=}O^{\bullet}$ from ionized acetol [4a], $CH_3C(=O)CH_2OH^{\bullet+}$, and ethanediol [4b], $HOCH_2CH_2OH^{\bullet+}$, which features the concept of proton transport catalysis with electron transfer [4c]. For ions **1** the first step in this mechanism involves a 1,4-H transfer of the hydroxylic hydrogen to the ester's carbonyl group with concomitant C-C cleavage to form the HBRC **7** :

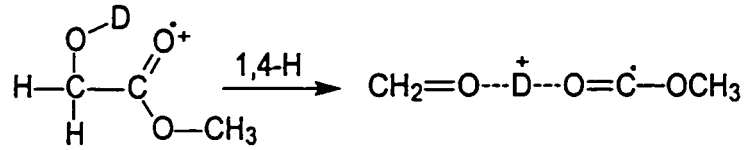

However, it was suggested in ref. 1 that ion **7** cannot be generated directly from **1** : the computations indicated that migration of the hydroxyl hydrogen to the keto oxygen is not accompanied by C-C cleavage but rather leads to the unreactive stable distonic ion **8**, via a low lying transition state :

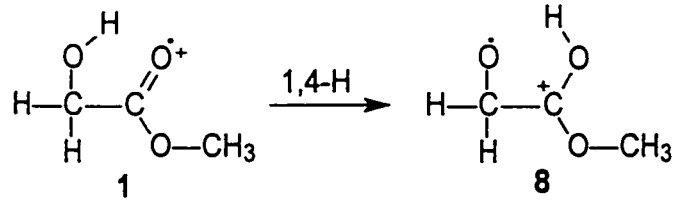

As an alternative, the mechanism of Scheme 1, which still features the concepts of dipole-catalyzed proton shift cum charge (electron) transfer, was proposed. Starting from methylglycolate ions, **1**, elongation of the C-C bond yields the ion-dipole complex, **4**. Once generated, the $^{\bullet}CH_2OH$ dipole rotates and donates the hydroxylic hydrogen to the methoxycarbonyl cation to generate the high energy C-H•••O bridged ion **5**. In this

methoxycarbonyl cation to generate the high energy C-H•••O bridged ion **5**. In this intermediate the formaldehyde dipole was proposed to move around the ionized methylformate and orient itself such that charge transfer occurs without affecting the total energy of the system [4b]. Because it is now charged, the CH_2=O moiety can rotate along the dipole vector of the O=C$^{\bullet}$-OCH_3 radical, to produce the C-H•••O bridged ion **6**. This final intermediate can smoothly donate a proton to the $CH_3OC(H)$=O part leading to the low energy product ion $CH_3OC(H)OH^+$. As already mentioned, our HBRC CH_2=O•••H•••O=C-$OCH_3^{\bullet+}$ also figures in this proposal (ion **7** in Scheme 1), not as an intermediate en route to the dissociation of **1** but rather as a link between ions **1** and **2**.

Although ion **4** could not be identified as a stable minimum in the calculations in ref. 1, it was argued that this ion-dipole complex would be sufficiently low in energy to be able to participate as a connecting intermediate in the generation of ion **5**. However, a recent re-evaluation of the combined heats of formation of the ion-dipole components of **4**, CH_3OC=O^+ and $^{\bullet}CH_2OH$, leads to a value for $\Sigma\Delta H_f$ [CH_3OC=O^+ + $^{\bullet}CH_2OH$] which is 11 kcal/mol higher than that used in ref. 1.[2] Hence the conversion of **1** into **4** is much more energy demanding than originally proposed and considering the low energy requirement for the HC=O$^{\bullet}$ loss, ca. 12 kcal/mol, the route **1**→**4**→**5** becomes unlikely. It is one of the goals of this paper to further investigate this part of the reaction mechanism and in particular to re-examine the feasibility of the isomerization **1**→**7** discussed above at a higher (correlated) level of theory.

The 25% non-atom specific loss of HC=O$^{\bullet}$ from **1** was proposed to originate from a partial interconversion with ions **2**, whose D-labeled isotopomers quickly lose their positional identity because of a facile interconversion with the very stable distonic ions **9** and **9′** via 1,4-H and 1,5-H shifts, *viz.*

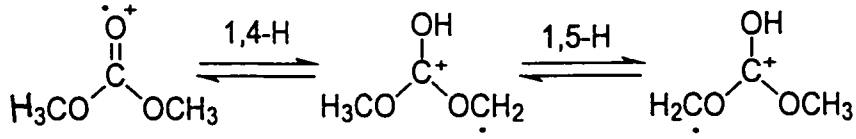

2 **9** **9'**

[2] ΔH_f^{total} changes from 114 to 125 kcal/mol, since ΔH_f (CH_2OH^+) = - 6 kcal/mol [5a] has been revised to - 4 kcal/mol [5b] and ΔH_f (CH_3OC=O^+) = 120 kcal/mol [5a] becomes 129 kcal/mol [5c].

However, both the loss of HC=O$^{\bullet}$ from **2** and the non-specific loss of HC=O$^{\bullet}$ from **1** were proposed to occur via the mechanism proposed for the specific loss of HC=O$^{\bullet}$ from **1**, as outlined in Scheme 1. Note that there is solid experimental evidence for the proposal that **1** and **2** lose HC=O$^{\bullet}$ via a single common dissociation route but the problematic part in Scheme 1 is that it is our HBRC **7** which is supposed to form the link in the communication between **1** and **2**. It was argued in ref. 1 that **7** could fulfill this role because the calculations had shown that the HBRC is best represented as CH_2=O•••H-O-C-$OCH_3^{\bullet+}$, that is a methoxy-hydroxycarbene ion interacting with the formaldehyde dipole, and in such a species one can indeed envisage a facile CH_2=O migration to generate ion **9**. However, this proposal implies that the HBRC exhibits a higher degree of non-specific D/H exchange than **1**. This is clearly not the case, see below, and thus ion **7** is **not** the connecting intermediate between **1** and **2** and there must be another route for the conversion **2**→**1**. We reiterate that a relatively high barrier must separate **1** (and **7**) from **2** to allow for the atom specific HC=O$^{\bullet}$ loss from **1**.

In summary, the experimental identification and characterization of the HBRC **7** questions some aspects of the mechanistic proposal presented in Scheme 1 and we have therefore investigated selected parts of this potential energy surface with calculations at a more advanced level of theory. In the first part of the Results and Discussion section, the experimental findings on the identification and the dissociation of the new HBRC **7** will be reviewed. In the second section the computational results on the process **7** → HC=O$^{\bullet}$ + $CH_3OC(H)OH^+$ are presented and it will be shown that they support the proposal that ions **7** dissociate via a catalyzed 1,2-H^+ shift, an electron transfer between moieties and a final spontaneous proton transfer. In the final section, it will be shown that **1** can isomerize into **7** prior to loss of HC=O$^{\bullet}$, via the sequence **1**→**7**→**5**→**CT**→**3/6**→products, and that this pathway is more likely than that proposed previously [2], i.e. **1**→**4**→**5**→**CT**→**6**→products, see Scheme 1. This section also deals with a tentative new proposal for the communication between **1** and **2** which accounts for the partial H/D exchange in D-labeled isotopomers of **1**.

Results and Discussion

1. Experimental observations on the HBRC $[CH_2{=}O{\bullet\bullet\bullet}H{\bullet\bullet\bullet}O{=}C\text{-}OCH_3]^{\bullet+}$

We will begin our discussion with the experimental identification of $CH_2{=}O{\bullet\bullet\bullet}H{\bullet\bullet\bullet}O{=}C\text{-}OCH_3^{\bullet+}$. The EI mass spectra of methyl-β-hydroxypyruvate, (MHP) $HOCH_2C(=O)COOCH_3$, and dimethyloxalate, (DMO) $CH_3OC(=O)C(=O)OCH_3$, (spectra not shown) both exhibit an interesting rearrangement product ion at m/z 90 corresponding to $C_3H_6O_3^{\bullet+}$ [1,6]. This m/z 90 ion results from a decarbonylation of the molecular ions : from MHP this likely occurs via formation of an intramolecular H bond and C-C cleavage followed by loss of the keto CO moiety [1] and from DMO via a 1,5-H shift and $CH_2{=}O$ migration [6], as depicted in Scheme 2.

Scheme 2

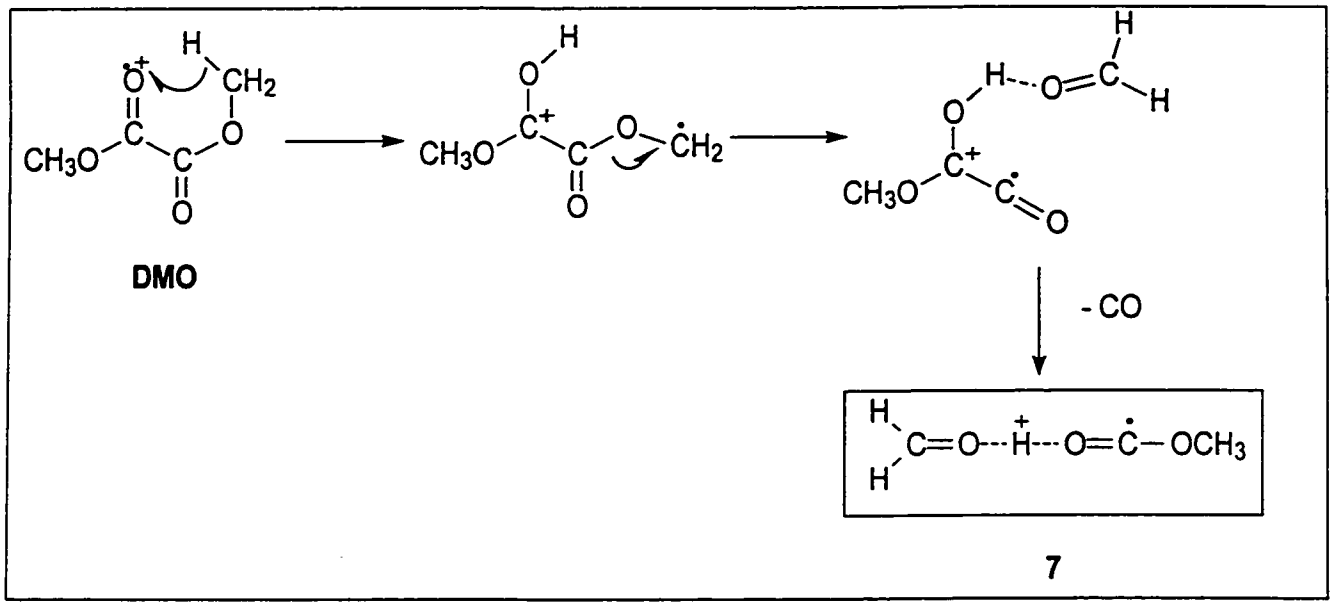

The CID mass spectra [10 keV ions, collision gas O_2] of the product ions from these two decarbonylation processes are identical and the spectrum obtained using DMO as the precursor molecule is presented in Figure 6-1a. It features intense signals at m/z 31, CH_2OH^+, and m/z 60, $CH_3OCOH^{\bullet+}$ (the carbene's structure was identified from a double collision experiment, result not shown) of almost equal intensity and considering the very similar proton affinities of $CH_3OC{=}O^{\bullet}$ and $CH_2{=}O$ (168 and 170 kcal/mol respectively[3]) this is precisely what is expected for the proposed HBRC :
$CH_2{=}O{\bullet\bullet\bullet}H{\bullet\bullet\bullet}O{=}C{-}OCH_3^{\bullet+}$.

[3] From $CH_3OC{=}O^{\bullet} + H^+ \rightarrow CH_3OCOH^{\bullet+} + PA$, using ΔH_f ($CH_3OC{=}O^{\bullet}$) = - 40 kcal/mol [7] and ΔH_f ($CH_3OCOH^{\bullet+}$) = 158 kcal/mol [5a] ; PA ($CH_2{=}O$) from ref 5d.

Figure 6-1. Collision-Induced Dissociation (CID) mass spectra of : (a) the (8 keV) source generated $[M\text{-}CO]^{\bullet+}$ ions $CH_2{=}O{\bullet\bullet\bullet}H{\bullet\bullet\bullet}O{=}C\text{-}OCH_3^{\bullet+}$ from dimethyloxalate ; (b) the $[M\text{-}CO]^{\bullet+}$ ions generated from metastable (10 keV) dimethyloxalate ions ; (c) source generated (8 keV) methylglycolate ions, $HOCH_2COOCH_3^{\bullet+}$, with the dominating metastable peak at m/z 61 removed, see text ; (d) source generated (8 keV) methylglycolate ions, uncorrected spectrum ; (e) the $CH_3OC(D)OH^+$ ions generated from metastable ions $CH_2{=}O{\bullet\bullet\bullet}D{\bullet\bullet\bullet}O{=}C\text{-}OCH_3^{\bullet+}$, formed by the decarbonylation of OD labelled methyl-β-hydroxypyruvate, $DOCH_2C(=O)COOCH_3^{\bullet+}$.

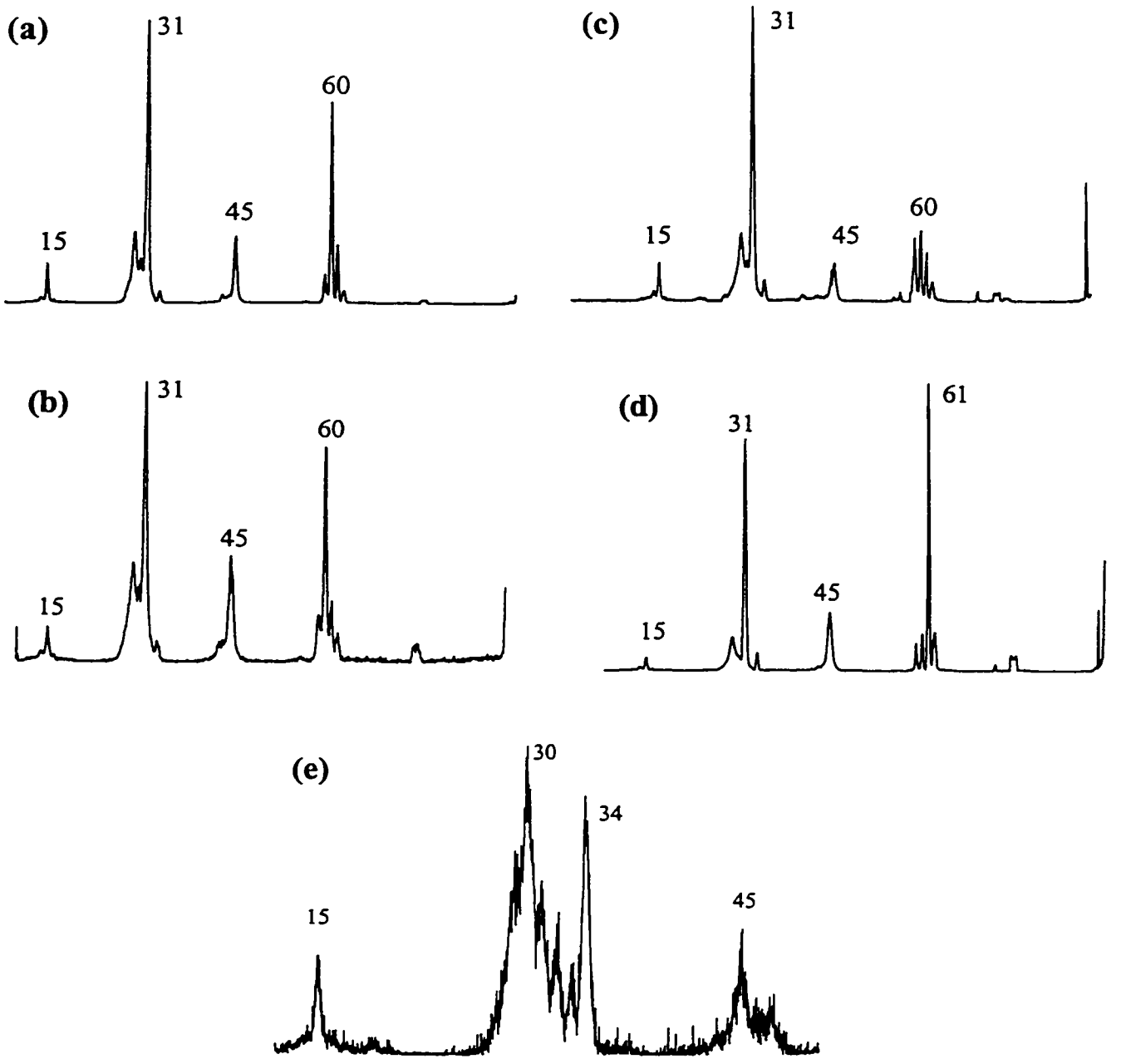

A closely similar CID mass spectrum, see Figure 6-1b, was obtained for the decarbonylation product of the *metastable* DMO ions (3ffr CID spectrum of 10 keV metastable precursor ions dissociating in the 2ffr of the instrument) and this strengthens our proposal that we are dealing with a single ion structure.

Figures 6-1c and 1d present the CID mass spectra of the isomeric methylglycolate ions, $HOCH_2C(=O)OCH_3^{\bullet+}$, **1**. Figure 6-1d represents the conventional CID spectrum. It is dominated by the m/z 61 peak but almost all of the $CH_3OC(H)OH^+$ ions represented by this signal originate from spontaneous (metastable) dissociations rather than collision induced processes. In fact, the fraction of the stable ions **1** that is metastable is remarkably high (c. 10%). We have therefore recorded a more representative CID spectrum of **1** which is presented in Fig. 6-1c (this spectrum was obtained by applying a voltage (+1000V) on the collision gas chamber to separate the metastable m/z 61 ions from the CID generated ions and by deleting the MI peak from the recorded spectrum). It is seen that the CID characteristics of **1** and **7** are similar but nonetheless distinctly different. Note in particular the decreased m/z 60 and the increased m/z 59 intensities in the spectrum of **1** which is in keeping with the differences in structure of the two ions.

In contrast, the MI spectra of ions **1** and **7** are virtually identical : both ions predominantly lose $HC=O^{\bullet}$ with the same kinetic energy release ($T_{0.5}$ = 23 meV) to yield the same product ion, $CH_3OC(H)OH^+$, whose structure was established from a double collision experiment. Moreover, the D labeled isotopomers $DOCH_2C(=O)OCH_3^{\bullet+}$ and $CH_2=O\bullet\bullet\bullet D\bullet\bullet\bullet O=C-OCH_3^{\bullet+}$ (generated from $DOCH_2C(=O)COOCH_3$) both yield the same D labeled product ion $CH_3OC(D)OH^+$ with a high degree of atom specificity. Figure 6-1e shows the CID spectrum of the metastably generated m/z 62 product ions generated by loss of $HC=O^{\bullet}$ from $CH_2=O\bullet\bullet\bullet D\bullet\bullet\bullet O=C-OCH_3^{\bullet+}$ and comparison with the reference spectrum (Figure 1b in ref. 1) leaves no doubt that the ions have the $CH_3OC(D)OH^+$ structure. Thus it is indeed likely that metastable ions **1** and **7** lose $HC=O^{\bullet}$ via the same mechanism and considering the arguments presented in the introduction the dissociation route **1**→**7**→**5**→**CT**→**6**→products is the most promising candidate for computational analysis. We further note that the reaction sequence **1**→**7**→products is more plausible than any route **7**→**1**→products and that there must be a sizable barrier for the isomerization **1**→**7**. This is because the degree of atom specificity in the loss of $HC=O^{\bullet}$ from isotopomers of **1** is fairly high but nevertheless lower than that

observed from isotopomers of **7** (cf. $DOCH_2C(=O)OCH_3^{\bullet+}$ and $CH_2=O\bullet\bullet\bullet D\bullet\bullet\bullet O=C-OCH_3^{\bullet+}$ for which the ratio of loss of $HC=O^{\bullet}$ versus $DC=O^{\bullet}$ are 97:3 and 98:2 respectively whereas $DOCH_2C(=O)OCD_3^{\bullet+}$ and $CH_2=O\bullet\bullet\bullet D\bullet\bullet\bullet O=C-OCD_3^{\bullet+}$ yield ratios of 83:17 and 88:12 respectively). One final experimental observation deserves to be mentioned : for the loss of $HC=O^{\bullet}$ from ions **1** and **2** it could be established (from appearance energy measurements, see ref. 2) that the highest transition state in any proposed mechanism should lie at ca 12 kcal/mol[4] above the dissociation products $CH_3OC(H)OH^+$ and $HC=O^{\bullet}$. For ions **7** no such experimental observations are available but, if it indeed is a key intermediate in the dissociation chemistry of **1** and **2**, this energetic constraint applies to its dissociation too.

2. Loss of $HC=O^{\bullet}$ from ion 7, $CH_2=O\bullet\bullet\bullet H\bullet\bullet\bullet O=C-OCH_3^{\bullet+}$: ***computational evidence for the double proton and single electron transfer mechanism.***

Our calculations confirm the proposal derived from the experiments that ion **7** is a stable species in the gas-phase. From a standard population analysis on its optimized structure presented in Fig. 6-2, it follows that the ion is best described as a CH_2OH^+ ion interacting via a H-bridge with the $CH_3OC=O^{\bullet}$ dipole. The bridging H atom is closer to the $CH_2=O$ moiety than the $CH_3OC=O^{\bullet}$ component and this is in line with the observation that the proton affinity (PA) of $CH_2=O$ is higher than that of $CH_3OC=O^{\bullet}$, albeit that the difference is only 2 kcal/mol. This may explain why ion **7**'s UHF optimized geometry [2] is found to have the bridging H attached to the methoxycarbonyl moiety, *viz.* $CH_2=O\bullet\bullet\bullet H-O-C^{\bullet+}-OCH_3$. It seems likely that little energy is required to shift the bridging H between the two moieties and that at the level where the HBRC undergoes isomerization, it can adopt either charge distribution. From the results in Table 6-1, it follows that the ion is stabilized by 33 kcal/mol relative to the dissociation products **C**, from which we derive ΔH_f (**7**) = 95 kcal/mol, in excellent agreement with an empirical estimate [10].

---

[4] From AE (m/z 61) [**1**] = 10.74 ± 0.05 eV and ΔH_f [**1**] = -133.1 kcal/mol [8a], AE (m/z 61) [**2**] = 10.94 ± 0.05 eV and ΔH_f [**2**] = -136.5 kcal/mol [8b] and using $\Sigma\Delta H_f$(products) = 103 kcal/mol, see Table 1, footnote [f].

Figure 6-2. The UMP2(Full)/6-31G** optimized geometries for the HBRC 7 and its key isomers and transition states. The geometry for CT was calculated at the UHF/6-31G* level of theory, see text. Structures labelled with 'EF' were located with an eigenvalue-following routine, see theoretical section.

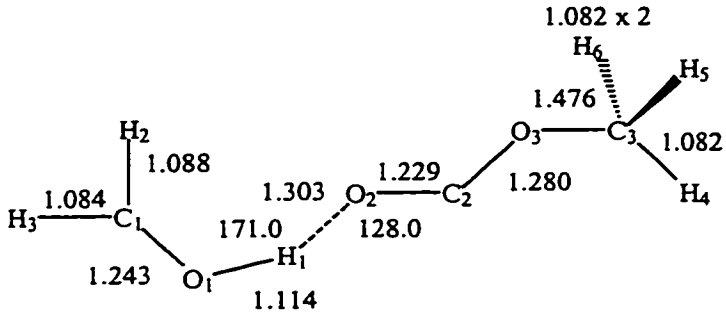

7

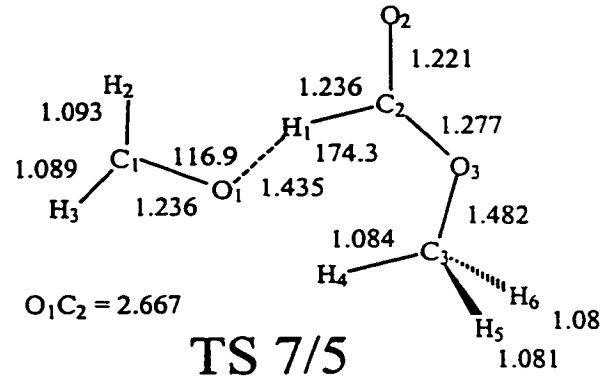

TS 7/5

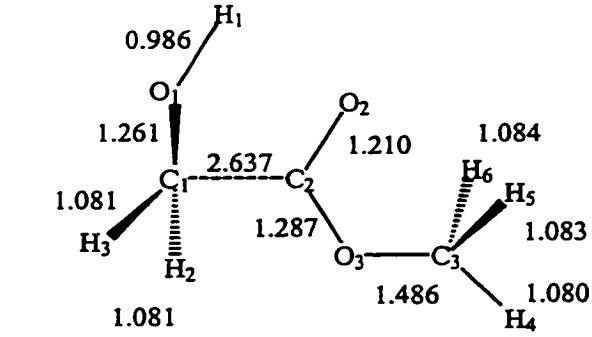

$O_1C_1C_2O_2 = -39.5$ TS 1'/7

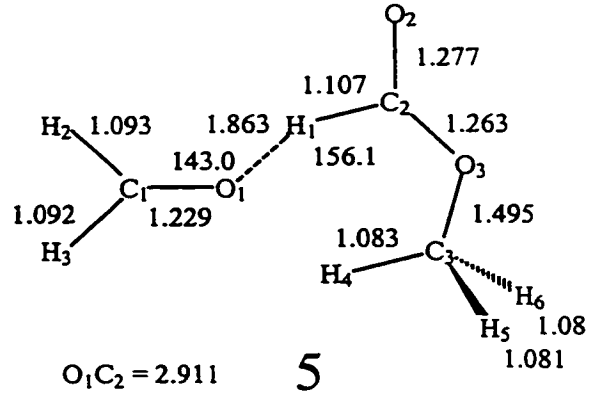

$O_1C_2 = 2.911$ 5

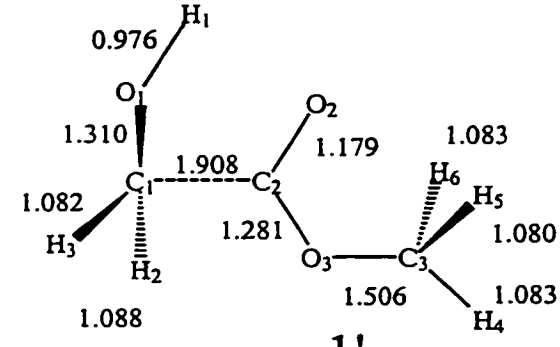

$O_1C_1C_2O_2 = -43.8$ 1'

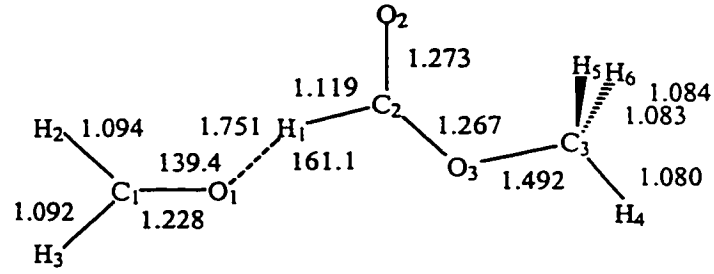

$O_1C_2 = 2.833$ 5'

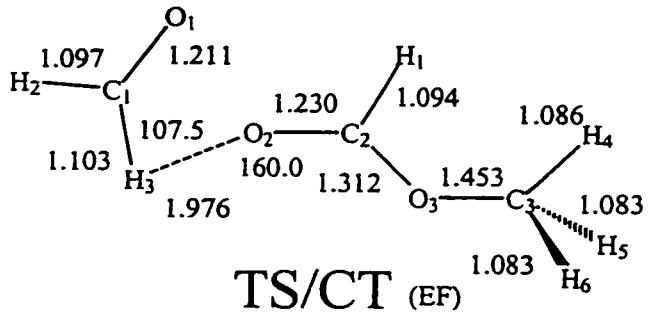

TS/CT (EF)

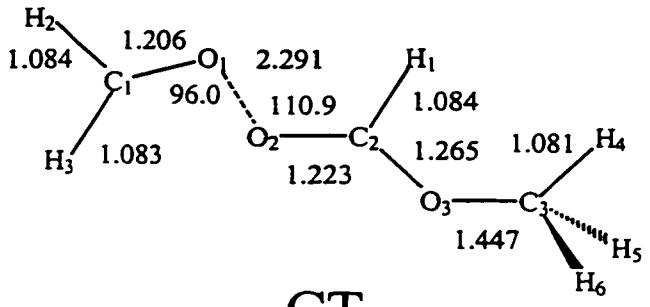

CT

1.077 x 2

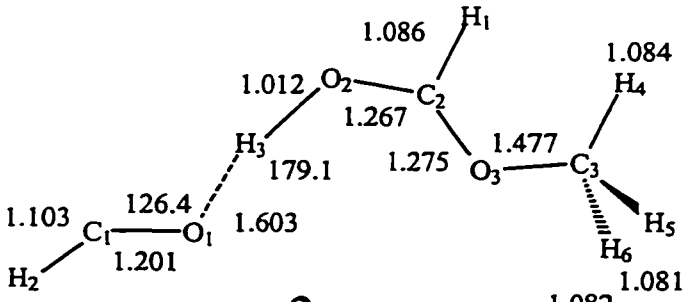

3

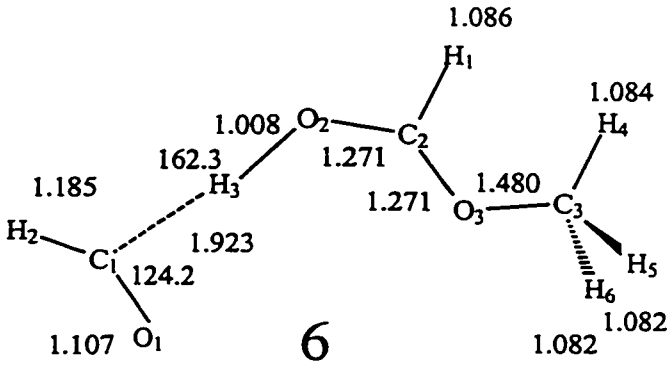

6

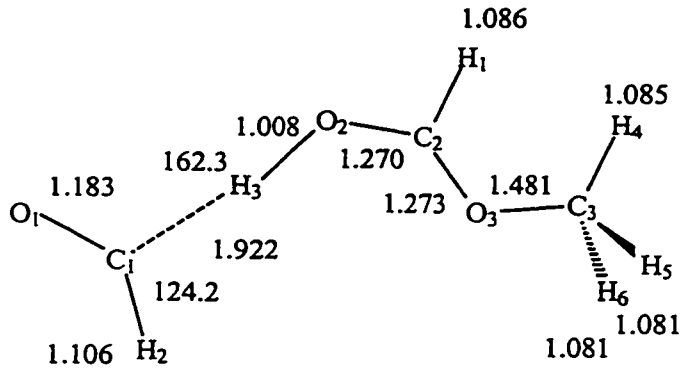

TS 6/3 (EF)

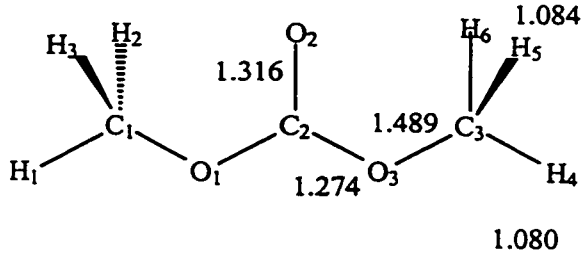

2

Table 6-1. The UMP2(Full)/6-31G(*d,p*) and CCSD(T)/cc-pVDZ//UMP2 energies (hartrees), scaled[a] zero-point vibrational energies (ZPVEs, kcal/mol) and relative energies, E_{rel} (kcal/mol) of the H-bridged ion $CH_2{=}O{\bullet\bullet\bullet}H{\bullet\bullet\bullet}O{=}C\text{-}OCH_3^{\bullet+}$ and its most important isomers and dissociation products.

Species		*ZPVE*	*MP2(Full) /6-31G(d,p)* -342.	E_{rel}	*CCSD(T) /cc-pVDZ* -342.	E_{rel}	E_{rel} *(+ ZPVE)*	E_{rel} *expt*
$HOCH_2C(=O)OCH_3^{\bullet+}$	**1′**	58.9	0.31134	-4.2	0.38616	-1.6	2.5	4[b]
$CH_3OC(=O)OCH_3^{\bullet+}$	**2**	58.7	0.29882	3.6	0.38165	1.2	5.1	3[c]
$HC{=}O{\bullet\bullet\bullet}H{\bullet\bullet\bullet}OC(H)OCH_3^{\bullet+}$	**3**	57.2	0.32994	-15.9	0.40854	-15.6	-15.1	
$CH_2{=}O{\bullet\bullet\bullet}H\text{-}C(=O)OCH_3^{\bullet+}$	**5**	55.9	0.27119	21.0	0.36131	14.0	15.1	
$CH_2{=}O{\bullet\bullet\bullet}H\text{-}C(=O)OCH_3^{\bullet+}$	**5′**	55.4	0.26988	21.8	0.36099	14.2	14.7	
$^{\bullet+}O{=}C(H)\text{-}H{\bullet\bullet\bullet}O{=}C(H)OCH_3$	**6**	56.4	0.32277	-11.4	0.40148	-11.2	-9.6	
$CH_2{=}O{\bullet\bullet\bullet}H{\bullet\bullet\bullet}O{=}C\text{-}OCH_3^{\bullet+}$	**7**	55.6	0.31280	-5.1	0.39068	-4.4	-3.6	
$CH_2{=}O^{\bullet+}{\bullet\bullet\bullet}O{=}C(H)OCH_3$	**CT-1**		0.26090	27.4	0.36266	13.2		
$CH_2{=}O{\bullet\bullet\bullet}^{\bullet+}O{=}C(H)OCH_3$	**CT-2**		0.26369	25.7	0.36298	13.0		
TS-CT-1 (see text)	**TS/CT**	55.3	0.26718	23.5	0.36305	12.9	13.4	
	TS 7/5	53.2	0.26515	24.8	0.36415	12.3	10.6	
	TS 1/7	57.2	0.28985	9.3	0.36823	9.7	12.1	
	TS 6/3[h]	56.4	0.31980	-9.5	0.39869	-9.4	-7.9	
$CH_2{=}O + HC(=O)OCH_3^{\bullet+}$	**A**	54.5	0.24273	38.8	0.33169	32.6	32.2	35[d]
$CH_2{=}O + HOCOCH_3^{\bullet+}$	**B**	54.6	0.26154	27.0	0.34006	27.4	27.2	29[e]
$^{+}CH_2OH + CH_3OC{=}O^{\bullet}$	**C**	55.8	0.25905	28.6	0.33886	28.1	29.1	25[f]
$HC{=}O^{\bullet} + HOC(H)OCH_3^{+}$	**D**	54.9	0.30463	0.0	0.38369	0.0	0.0	0[g]

[a] Scaled by a factor of 0.9646 (see ref. 9).
[b] Using ΔH_f (**1**) = 107 ± 2 kcal/mol, from ΔH_f (ester) = -133.1 ± 1.5 kcal/mol [8a] and IE(ester) = 10.42 ± 0.05 eV[2].
[c] ΔH_f (**2**) = 106 ± 2 kcal/mol, from Ref 2 but using a revised value for ΔH_f (ester) = -136.5 ± 1.5 kcal/mo l[8b].
[d] Using ΔH_f^{total} = 138.4 kcal/mol, from ΔH_f ($CH_2{=}O$) = -26.0 kcal/mol [5a] and ΔH_f ($CH_3OC(H){=}O^{\bullet+}$) = 164.4 kcal/mol [5a].
[e] Using ΔH_f^{total} = 132.0 kcal/mol, from ΔH_f ($CH_2{=}O$) = -26.0 kcal/mol [5a] and ΔH_f ($CH_3OCOH^{\bullet+}$) = 158 kcal/mol [5a].
[f] UsingΔH_f^{total} = 128 kcal/mol, from ΔH_f (CH_2OH^{+}) = 168 kcal/mol [5a] and ΔH_f ($CH_3OC{=}O^{\bullet}$) = -40 kcal/mol [7].
[g] Using ΔH_f^{total} = 103 kcal/mol, from ΔH_f ($HC{=}O^{\bullet}$) = 10 kcal/mol [5b] and ΔH_f ($CH_3OC(H)OH^{+}$) = 93 kcal/mol [5a].
[h] IRC for TS 6/3 not performed but imaginary vibrational frequency was geometrically analyzed

A 1,2-proton shift in HBRC **7** yields the C-H-O bridged ion **5** via **TS 7/5**, whose MP2 energy, see Table 6-1, lies only slightly above that of the connecting ion **5**. Note also that the optimized geometries for **5** and **TS 7/5** are closely similar: the only significant difference lies in the position of the bridging H relative to the connecting moieties. When single point calculations are performed to obtain better relative energies, both the energy of **5** and that of **TS 7/5** are significantly lowered, to such an extent that the resulting values (15 and 11 kcal/mol respectively, see Table 6-1) are now compatible with the ~ 12 kcal/mol derived from experiments for the highest point along the reaction coordinate. Unfortunately, in the single point calculations the energy of **TS 7/5** becomes lower than that of the connecting ion **5**. This is an imperfection in the methodology used which probably stems from the fact that the MP2 optimized geometries of the two closely similar species are not sufficiently refined. The problem could be remedied by performing the geometry optimizations (and frequency calculations) at a higher level of theory (e.g. CCSD(T)), but considering the size and complexity of the system, such calculations are not yet feasible.

Nevertheless, it is clear that starting from ion **5** - which can be viewed as an ion-dipole complex between $CH_3OC(=O)H^{\bullet+}$ and $CH_2=O$ - the 1,2-H transfer leading to **7** occurs with little or no activation energy. Viewing this reaction as the isomerization of $CH_3OC(=O)H^{\bullet+}$ into its more stable carbene isomer, $CH_3OCOH^{\bullet+}$, it follows that the $CH_2=O$ moiety in **5** is responsible for the effective removal of the high barrier associated with the unassisted isomerization. The ions $CH_3OC(=O)H^{\bullet+}$ [11a] and $CH_3OCOH^{\bullet+}$ [11b] have entirely different MI characteristics and from an analysis of their structure characteristic dissociation reactions it follows that the two isomers are separated by a 1,2-H shift barrier of at least 40 kcal/mol. For a closely related system, viz. $CH_3C(=O)H^{\bullet+}$ and $CH_3COH^{\bullet+}$, this 1,2-H shift isomerization barrier has been recently calculated at the G2 level of theory as 37 kcal/mol [11c]. However, high level computational studies by Radom et al. [12a-c] and elegant experimental studies by Bohme et al. [13a] and Audier et al. [13b-d] have shown that the prohibitively high 1,2-H shift barrier for the unassisted isomerization in systems like $HCO^+ \rightarrow {}^+COH$ and $CH_3OH^{\bullet+} \rightarrow CH_2OH_2^{\bullet+}$ could be drastically lowered by interaction with a neutral base (B). For the transformation, it was found that efficient catalysis will take place, see eq 1, when the PA of the base lies

between the PA of [X-Y] at X and Y. If the PA [B] is significantly lower than the PA [XY] at Y, the first step in eq 1 will not take place.

$$[H-X-Y]^{\bullet+} + B \rightarrow + B\bullet\bullet\bullet H^{+}\bullet\bullet\bullet[X-Y]^{\bullet} \rightarrow B\bullet\bullet\bullet H^{+}\bullet\bullet\bullet[Y-X]^{\bullet} \rightarrow B + [X-Y-H]^{\bullet+} \quad \textbf{(1)}$$

If, on the other hand, PA [B] is significantly larger than PA [XY] at X, then the intermediate complex $B\bullet\bullet\bullet H^{+}\bullet\bullet\bullet[X-Y]^{\bullet}$ will dissociate to $[X-Y]^{\bullet}$ and HB^{+} via a unidirectional proton-transfer. In effect, if PA[B] is intermediate, the barrier becomes negative relative to the separated reactants and products and the base successfully catalyzes the isomerization. In our case we are dealing with a base (CH_2=O) with a slightly higher PA than required for the catalysis : this, and the fact that it has a significant dipole moment, effects a facile catalysis but without separation of the base after the event.

Ion **5** (and its slightly more stable conformer **5'**) can indeed be viewed as a complex of the methylformate radical cation and a formaldehyde dipole. A standard population analysis indicates that the charge is largely located on the carbonyl moiety of the methylformate component of the optimized geometry shown in Fig. 6-2. It is further seen that the neutral formaldehyde is oriented towards the charge such that ion-dipole stabilization can occur. We further note from the computational results in Table 6-1, that **5** is stabilized relative to its components CH_2=O and $^{\bullet+}O$=C(H)OCH_3 (**A**) by ca 17 kcal/mol and that the stabilization energy calculated from the classic ion-dipole interaction formula, $SE = 68.8\mu \cos\theta/r^2$ ($\mu(CH_2=O) = 2.33$ D, and deriving $r \sim 3.5$ Å and $\theta = 23°$ from the geometry in Fig. 6-2) yields 13 kcal/mol. Thus, apart from a conventional H-bridge, there is indeed a sizable electrostatic interaction in this C-H-O bridged intermediate.

The next step in the dissociation mechanism involves a H transfer from the CH_2=O moiety to the O atom of the carbonyl group in methylformate. However, transfer of a $H^{\bullet}$ from the neutral CH_2=O molecule to the charged methylformate moiety in **5** is expected to be more energy demanding (see ref. 4a) than dissociation of the ion-dipole complex into its components $CH_3OC(H)=O^{\bullet+}$ and CH_2=O. One of the possibilities that we have entertained to locate the TS for such a transfer involved an a priori plausible conformer of **5** as the starting point, *viz.*

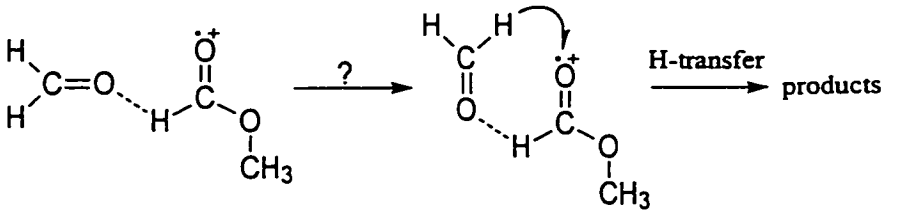

5" 5'''

However, neither **5"** nor **5'''** represent minima on the PES and geometry optimizations starting from these structures yielded the stable conformer **5** depicted in Fig. 6-2, in which the CH_2=O moiety has moved away from the ionized C=O moiety of the methylformate. That ion **5"** is not a stable minimum on the PES is not so surprising if one considers that a potentially favourable ion-dipole interaction is counteracted by a strong repulsion between the lone pair electrons of the two O atoms.

By analogy with previous computational studies on related systems (loss of HC=O$^{\bullet}$ from ionized acetol and ethylene glycol [4]) we therefore examined the possibility that the H is transfered as a proton, but this of course requires that the transfer is preceded by a charge transfer (CT) from the methylformate moiety to the formaldehyde molecule. Note that CT in this system may well be favourable because the components $CH_3OC(=O)H$ and CH_2=O have almost the same ionization energy (10.82 and 10.87 eV respectively [5a]) and substantial dipole moments as well (1.77 and 2.33 D respectively [2]). For reasons stated below, the feasibility of this charge transfer was first investigated at the HF level of theory. UHF/6-31G* calculations yielded a Minimum Energy Crossing Point whose optimized geometry is presented in Fig. 6-2 as **CT**. Its energy was derived from single point calculations on two electronic configurations, listed in Table 6-1 as **CT-1** and **CT-2**. **CT-1** represents an ion of fixed **CT** geometry where the charge is positioned on the methylformate moiety, whereas in **CT-2** the charge is positioned on the formaldehyde unit. The resulting E_{rel} value, 13 kcal/mol, is gratifyingly close to that for ion **5**, thus supporting the proposal that the charge transfer is energetically feasible. When, starting from the **CT** geometry with the charge located on the formaldehyde moiety, the UHF/6-31G* energy is optimized, a minimum is reached represented by the C-H•••O bridged ion $^{\bullet+}$O=C(H)-H•••O=C(H)OCH_3 , **6** and from which a facile proton transfer to the dissociation products, $CH_3OC(H)OH^+$ and HC=O$^{\bullet}$, may be expected to occur. [2] Starting from **CT-1** a connection with ion **5** was established, see

below, and thus at the HF level of theory the route **5** → **CT** → products appears to be feasible.

Reverting to the UMP2 methodology we are using to examine this PES, we find a transition state **TS/CT** whose geometry is closely similar to that of **CT** but with the charge situated on the formaldehyde component. A structure optimization starting from this **TS/CT** geometry yielded the very stable HBRC **3**, $HC{=}O{\bullet\bullet\bullet\bullet}HO{-}C(H)OCH_3^{\bullet+}$. This indicates that a facile proton transfer from the formaldehyde moiety in **TS/CT** to its methylformate component is feasible. Under the conditions imposed by the experiment, ion **3** generated upon charge transfer will only have a fleeting existence, since its internal energy is such, see Fig. 6-3, that a fast dissociation into $CH_3OC(H)OH^+$ and $HC{=}O^{\bullet}$ will occur by direct bond cleavage.

Although the optimization of **TS/CT** geometry spontaneously leads to ion **3**, we have also computationally identified the HBRC **6** as a low lying minimum on the PES. This HBRC, see Fig. 6-2, can be considered as a C-H-O bridged intermediate between the dissociation products **D**. Ion **6** can communicate with HBRC **3** via a low lying transition state, **TS 6/3**, and thus the exothermic dissociation step **CT** → **3** → products can also be envisaged as **CT** → **6** → products or **CT** → **6** → **3** → products. In fact, it is conceptually easier to picture the mechanism as **CT** → **6** → **3** → products but whether or not this sequence is preferred is not important here : at the elevated energies either **6** or **3** dissociates with little or no activation energy.

Establishing a connection between **TS/CT** and ion **5** appeared to be problematic. Structure optimizations starting from **TS/CT**-like geometries slightly distorted towards **5** were unsuccessful : the steps taken in this procedure tended to get smaller and smaller while the gradients remained sizable. The reason for this is that the Hessian becomes numerically unstable, leading to unreasonably large eigenvalues and therefore vanishingly small steps. This numerical instability may be caused by the fact that several UHF solutions coexist in this part of the PES. The wave function optimization uses the lowest possible UHF energy, but this does not always correspond to the lowest UMP2 energy. As a consequence it is difficult to find the minimum with the lowest UMP2 energy. If we start the UMP2 geometry optimization at the (UHF) **CT** geometry the calculation does not converge either, since here too the character of the UHF wave function changes all the time. However, optimizing the UHF/6-31G* energy starting

from the **CT** geometry with the charge located on the $CH_3OC(H)=O$ moiety yields **5**. This reaction path was checked by doing UMP2/6-31G** single point calculations for several of the geometries encountered in the UHF geometry optimization. Since the UMP2 energies found in this way were lower than the UMP2 energy for the **CT-2**, the rate-determining step in this reaction is the passage of the **CT/TS** region.

Thus, we have good computational evidence for the occurence of proton and electron transfers in this system and Figure 6-3 summarizes our computational results in an energy level diagram, which uses the dissociation level $CH_3OC(H)OH^+ + HC=O^\bullet$ as the anchor point. The hatched area in the Figure represents the energy range where the first proton transfer and the charge transfer occur. The dissociation level derived from experiment (12 kcal/mol relative to the anchor point, see Introduction) is also presented as a dashed line.

Figure 6-3. Energy level diagram describing the dissociation of the HBRC 7 and the methylglycolate ion 1 as derived from ab initio calculations. The hatched area represents the energy range where the first proton and the charge transfer occur.

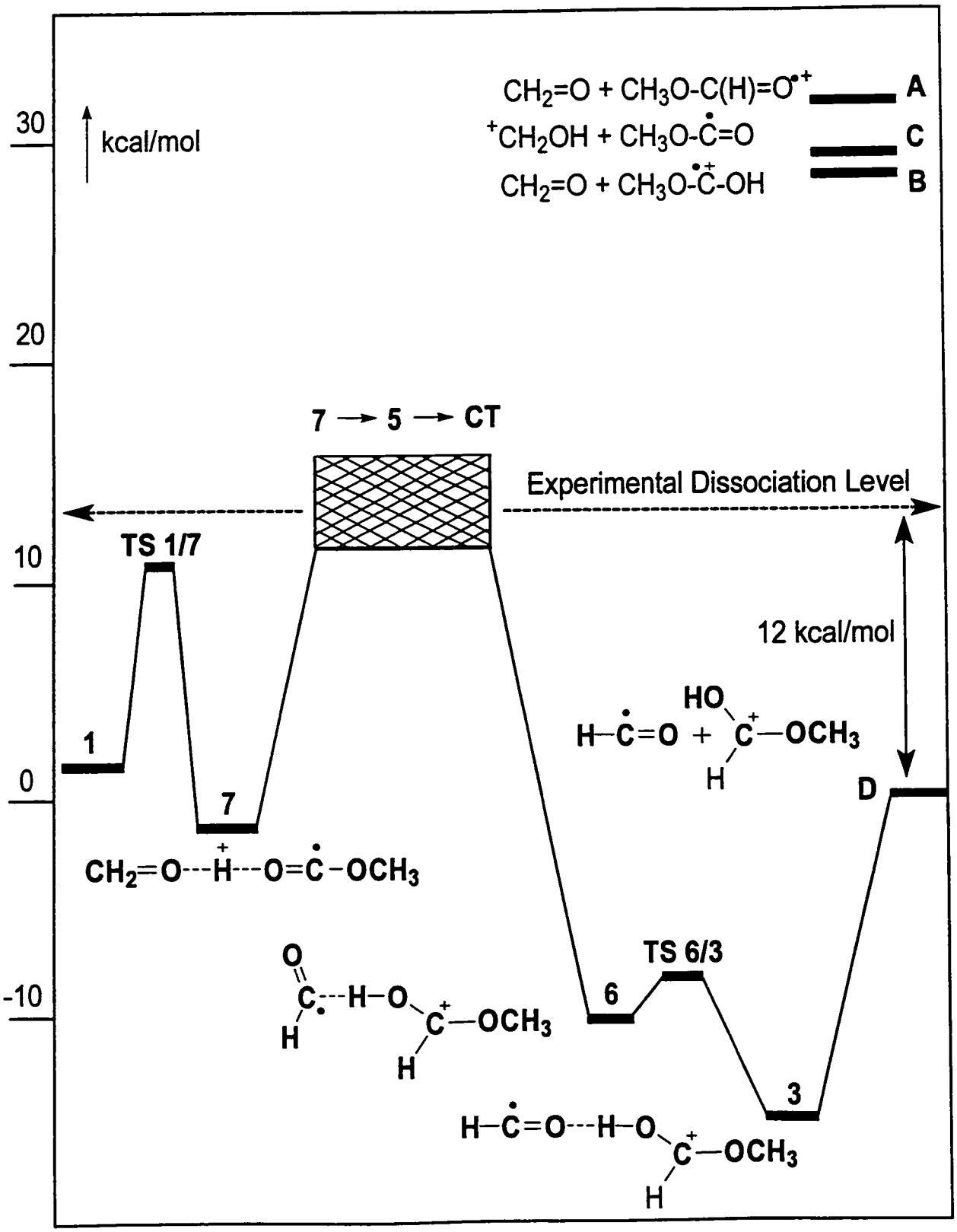

3. A new proposal for the isomerization 7→1 and the question of the communication between ions 1 and 2.

In the previous section it was proposed, on the basis of ab initio calculations, that the dissociation of low energy HBRC ions 7 occurs via a dipole catalyzed 1,2-H^+ shift and a charge transfer followed by a spontaneous proton transfer, i.e. the sequence **7** → **5** → **CT** (→ **6**) → **3** → products **D**.

The first question addressed in this section is whether the methylglycolate ions **1** can also follow this route, i.e. isomerize via the sequence **1** → **7** → **5** → **CT** (→ **6**) → **3** → **D** as suggested in the Introduction. As already mentioned, in the study of ref. 1 it was suggested that ion **7** cannot be generated directly from **1** because the (UHF) computations on the 1,4-H shift involved in this process all led to a facile isomerization into the stable but unreactive distonic ion **8**. There is little doubt that this simple 1,4-H shift requires little or no activation energy. In fact, computational studies on ionized ethylene glycol [4] and glycolic acid [1] showed that optimizing the geometry of an initial guess conformer of conventional C-C bond length which has the hydroxylic H pointing to the adjacent O atom yielded a distonic ion via a "spontaneous" 1,4-H transfer. However, it was also found in these studies (and also in computational studies on ionized acetol [4] and 1,2-propanediol [14]) that one of the conformers of the ionized precursor molecule existed as a stable long C-C bonded (non ion-dipole) species and that a 1,4-H shift starting from this conformer led to the formation of the O-H-O bridged ion. Five of the eight conformers of **1** were identified as stable minima in ref. 1 (q.v. structures **1b** - **1h** in Fig. 6-3) but they are all characterized by a C-C bond of conventional length (~ 1.52 Å) and a hydroxylic H that points away from the carbonyl O atom. This is not to say that a stable long-bonded conformer of **1** does not exist but one possibility is that the UHF level of theory employed in ref. 1 is not adequate to describe such a species as a stable minimum. In any case, we decided to search for such a species at the more advanced UMP2 level of theory and using an initial guess in which the distance between the central carbon atoms was large, ~ 2 Å, and which had the hydroxyl H pointing towards the keto oxygen. This geometry optimization led to the minimum **1′** in Fig. 6-2, which is characterized by both a long C-C bond (1.91 Å) and a hydroxylic H pointing to the carbonyl O atom.

Starting from this structure, it was fairly straightforward to find the elusive connection between ions **1** and **7** which is represented by **TS 1/7** in Fig. 6-2. This TS, see

Fig. 6-3, imposes a sizable energy barrier upon the isomerization **1** → **7** and since it also lies close to the dissociation threshold this may explain why the HBRC **7** does not significantly interconvert with **1** prior to dissociation. Thus we conclude that the dissociation route **1** → **7** → **D** is viable and Scheme 3 presents the new mechanism for the loss of $HC{=}O^{\bullet}$ from both ions **1** and **7**.

Scheme 3

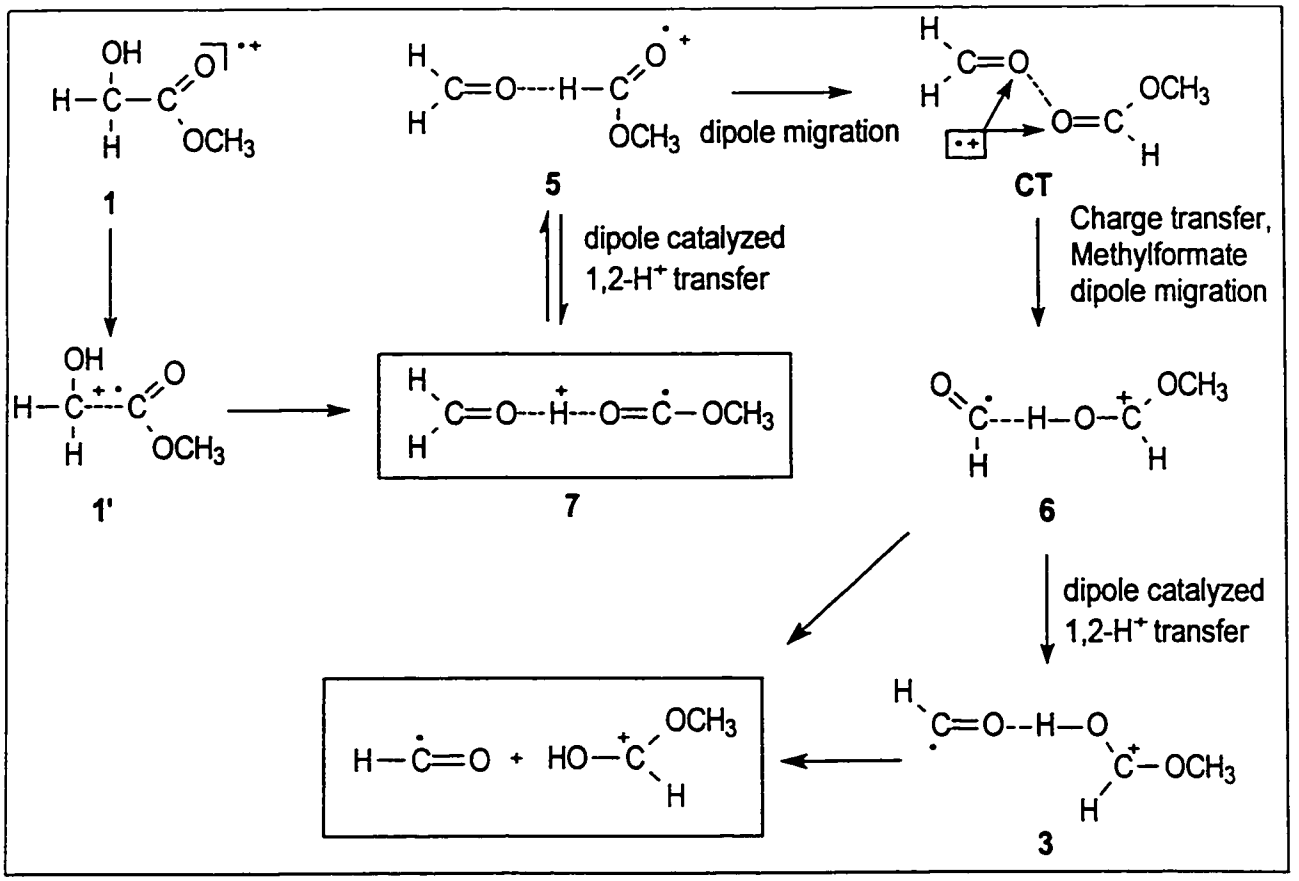

The second question involves the communication between the dimethylcarbonate ions **2** and the methylglycolate ions **1**. It is clear from the experimental observations on the labeled isotopomers that the original proposal from ref. 1, i.e. **2** → **7** → **1** cannot be valid and moreover the new mechanism derived from our computations cannot accommodate such a proposal either.

How then do ions **2** communicate with **1** prior to their dissociation into $CH_3OC(H)OH^+$ + $HC{=}O^{\bullet}$? We note that both **1** and **2** have a great many isomers and conformers whose relative energies lie below the c. 12 kcal/mol limit imposed by experiment and several of these have been reported in ref. 1. However, the presence of

such a large number of stable isomers and conformers makes the search for connecting transition states (TS) a truly formidable task. Moreover, as pointed out in the Introduction the elusive TS for **1** → **2** must be fairly high in energy (i.e. comparable to TS **1** → **7**) to accommodate the labeling results and this makes the search even more difficult.

One intuitive possibility is presented in the following scheme. It represents a connection of **1** (via **8**) with **2** (via **9**) via a ring closed oxirane-type ion. Exploratory calculations indicate this ion could be a fairly high lying TS but whether it does represent the elusive connection between **1** and **2** has to be further studied and results will be reported in a future publication.

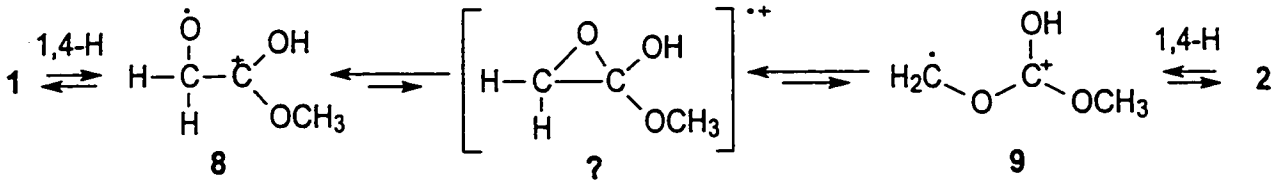

4. Theoretical Methods

The computational results reported in this study were obtained at the UCCSD(T)/cc-pVDZ//UMP2(Full)/6-31G** + ZPVE level of theory using the Gaussian-94 and GAMESS computational packages [15,16]. The coupled cluster approximation [17] utilizing singles, doubles and estimated triple excitations (CCSD(T)) was used to obtain our best relative energies on UMP2(Full)/6-31G** optimized structures. The CCSD(T) calculations used the double zeta correlation consistent basis set of Dunning, cc-pVDZ [18]. All transition states had the correct number of negative eigenvalues of the corresponding Hessian matrix. The spin contamination of the UHF wavefunctions was acceptable for all species investigated, i.e. less than 10 % of 0.75. The calculations are summarized in Table 6-1 and Figures 6-2 and 6-3. Table 6-1 presents the ZPVEs, theoretical relative energies and experimental relative energies for the isomers and some important dissociation products. All relative energies were calculated relative to the dissociation limit of the reaction studied, *viz.* $CH_3OC(H)OH^+$ + $HC{=}O^{\bullet}$ (**D**) for which reliable experimental energies are also available. Based on the results from the previous study we expect that the uncertainty in the relative energies derived from the computational procedure is about 3 kcal/mol [1]. Figure 6-2 presents the optimized

geometries of the minima, transition states and the charge transfer complex for the key isomers along the reaction path. The reaction pathways were verified with IRC calculations [15], and in regions of correct PES curvature, the eigenvalue-following [19] routine was used to find the stationary points, as indicated with (EF) in Figure 6-2. Figure 6-3 presents a combined experimental and theoretical energy level diagram for the loss of HC=O$^{\bullet}$ from both ions **1** and **7**.

5. Experimental Methods

The mass spectrometric experiments were performed with the McMaster University VG Analytical (Manchester, UK) ZAB-R instrument of BE_1E_2 geometry (B, magnet; E, electric sector) [20] using an accelerating voltage of 8 or 10 keV. Metastable ion (MI) mass spectra were recorded in the second field-free region (2ffr) ; Collision-induced dissociation (CID) mass spectra were recorded in the 2 and 3ffr using oxygen as collision gas (transmittance T = 70%). The CID mass spectra of the 2ffr metastable or CID peaks (MS/MS experiments) were obtained in the 3ffr using O_2 as the collision gas. All spectra were recorded using a small PC-based data system developed by Mommers Technologies Inc. (Ottawa). The DMO samples used in this study were obtained from Aldrich and used without further purification.

1. L.M. Fell, P.C. Burgers, P.J.A. Ruttink and J.K. Terlouw, Can. J. Chem., 76 (1998) 335.
2. D.Suh, C.A. Kingsmill, P.J.A. Ruttink, P.C. Burgers and J.K. Terlouw, Int. J.Mass Spectrom. Ion Processes, 146/147 (1995) 305.
3. D. Suh, P.C. Burgers and J.K. Terlouw. Rapid Commun. Mass Spectrom. 9 (1995) 862.
4. (a) P.J.A. Ruttink, P.C. Burgers and J.K. Terlouw. Can. J. Chem. 74 (1996) 1078 ; (b) P.J.A. Ruttink and P.C.Burgers. Org. Mass Spectrom. 28 (1993) 1087 ; (d) P.J.A. Ruttink, P.C. Burgers, L.M. Fell and J.K. Terlouw, J. Phys. Chem. A 102 (1998) 2976.
5. (a) S. Lias, J.E. Bartmess, J.F. Liebman, J.L. Holmes, R.D. Levin and W.G. Mallard. J. Phys. Chem. Ref. Data, 17 (1988) Supplement 1; E.P. Hunter and S.G. Lias, J. Phys. Chem. Ref. Data, to be published; See NIST Chemistry WebBook, http://webbook.nist.gov/chemistry/ ; (b) J.C. Traeger and B.M. Kompe, In *Energetics of Organic Free Radicals*; J.A.M. Simões, A. Greenberg and J.F. Liebman, Ed.; Blackie Academic & Professional, New York, 1996, Chapter 3 ; (c) L.M. Fell, P.C. Burgers, P.J.A. Ruttink and J.K. Terlouw, J. Phys. Chem. A 103 (1999) 1426 ; (d) J. E. Szulejko and T.B. McMahon, J. Am. Chem. Soc. 115 (1993) 7839.
6. M.A. Trikoupis, J.K. Terlouw, P.C. Burgers, M. Peres and C. Lifshitz, J. Am. Soc. Mass Spectrom., 1999, in press, and references cited therein.
7. J.L. Holmes, F.P. Lossing and P.M. Mayer, J. Am. Chem. Soc. 113 (1991) 9723.
8. (a) W.V. Steele, R.D. Chirico, S.E. Knipmeyer, A. Nguyen and N.K. Smith, J. Chem. Eng. Data 41 (1996) 1285 (b) W.V. Steele, R.D. Chirico, S.E. Knipmeyer, A. Nguyen and N.K. Smith, J. Chem. Eng. Data 42 (1997) 1037.
9. B.J. Smith and L. Radom, J. Phys. Chem. 99 (1995) 6468.

10. M. Meot-Ner (Mautner), J. Am. Chem. Soc. 106 (1984) 1257 and using the appropriate ΔH_f values from ref. 4.
11. (a) N. Heinrich, T. Drewello, P.C. Burgers, J.C. Morrow, J. Schmidt, W. Kulik, J.K. Terlouw and H. Schwarz, J. Am. Chem. Soc. 114 (1992) 3776 ; (b) J.K. Terlouw, J. Wezenberg, P.C. Burgers and J.L. Homes, Chem. Comm. (1983) 1121 ; (c) W. Bertrand and G. Bouchoux, Rapid Comm. Mass Spectrom. 12 (1998) 1697.
12. (a) A.J. Chalk and L. Radom, J. Am. Chem. Soc. 119 (1997) 7573 ; (b) J.W. Gauld, H. Audier, J. Fossey and L.Radom, J. Am. Chem. Soc. 118 (1996) 6299 ; (c) J.W. Gauld and L. Radom, J. Am. Chem. Soc. 119 (1997) 9831.
13. (a) D.K. Bohme, Int. J. Mass Spectrom. Ion Processes 115 (1992) 95 ; (b) P. Mourges, H.E. Audier, D. Leblanc and S. Hammerum, Org. Mass Spectrom. 28 (1993) 1098 ; (c) H.E. Audier, D. Leblanc, P. Mourges, T.B. McMahon and S. Hammerum, J. Chem. Soc. Chem. Commun. (1994) 2329; (d) H.E. Audier, J. Fossey, P. Mourgues, T.B. McMahon and S. Hammerum, J. Chem. Phys. 100 (1996) 18390.
14. P.C. Burgers, L.M. Fell, A. Milliet, M. Rempp, P.J.A. Ruttink and J.K. Terlouw, Int. J. Mass Spectrom. Ion Processes, 167/168 (1997) 291.
15. J.B. Foresman and A. Frisch, Exploring Chemistry with Electronic Structure Methods, Gaussian Inc., Pittsburgh, 1996.
16. (a) Gaussian-94, Revision B.3, M. J. Frisch, G.W. Trucks, H.B. Schlegel, P.M.W. Gill, B.G. Johnson, M.A. Robb, J.R. Cheeseman, T.A. Keith, G.A. Peterson, J.A. Montgomery, K. Raghavachari, M.A. Al-Laham, V.G. Zakrevski, J.V. Ortiz, J.B. Foresman, C.Y. Peng, P.Y. Ayala, W. Chen, M.W. Wong, J.L. Andres, E.S. Replogle, R. Gomperts, R.L. Martin, D.J. Fox, J.S. Binkley, D.J. de Frees, J. Baker, J.P. Stewart, M. Head-Gordon, C. Gonzales and J.A. Pople, Gaussian Inc., Pittsburgh PA, 1995. (b) M.F. Guest, J. Kendrick. GAMESS Users Manual, SERC Daresbury Laboratory, CCP/86/1, 1986 ; M. Dupuis, D. Spangler and J. Wendolowski. NRCC Software Catalog, Vol. 1, Program No. QG01 (GAMESS), 1980 ; M.F. Guest, R.J. Harrison, J.H. van Lenthe and L.C.H. van Corler, Theor. Chim. Acta ,71 (1987) 117.
17. (a) J. Cizek. Adv. Chem. Phys. **14**, 35 (1969) ; (b) J.A. Pople, R. Krishnan, H.B. Schlegel and J.S. Binkley. Int. J. Quant. Chem. **14**, 545 (1978) ; (c) R.J. Bartlett and G.D. Purvis. Int. J. Quant. Chem. **14**, 516 (1978).
18. (a) T.H. Dunning Jr., J. Chem. Phys. **90**, 1007 (1989) ; (b) R.A. Kendall,T.H. Dunning Jr and R.J. Harrison. J. Chem. Phys. **96**, 6796 (1992).
19. M.J. Frisch, AE.Frisch and J.B. Foresman, Gaussian 94 User's Reference, 2nd Ed. Pittsburg, PA USA, 1996.
20. H.F. van Garderen, P.J.A. Ruttink, P.C. Burgers, G.A. McGibbon and J.K. Terlouw, Int. J. Mass Spectrom. Ion Processes, 121 (1992) 159.

CHAPTER 7

G2 THEORY AND EXPERIMENT IN CONCERT: THE ENTHALPY OF FORMATION OF $CH_3O\text{-}C{=}O^+$ AND ITS ISOMERS REVISITED[1]

Abstract

Ab initio molecular orbital calculations at the Gaussian-2 level of theory on a set of isodesmic, atomization and substitution type reactions have been used to deduce the enthalpy of formation of the methoxycarbonyl ion as $\Delta H_{f,298}$ [$CH_3O\text{-}C{=}O^+$] = 130 ± 2 kcal/mol. From the G2 computed ionization energy (IE_a = 7.32 eV) and $\Delta H_{f,298}$ (-40 kcal/mol) of the parent radical, $CH_3O\text{-}C^{\bullet}{=}O$ we arrive at 129 kcal/mol for its ionic counterpart. Combining these theoretical findings with a re-evaluation of existing experimental data (appearance energy measurements) yields 129 ± 2 kcal/mol as our recommended value for $\Delta H_{f,298}$ [$CH_3O\text{-}C{=}O^+$], a large upward revision of the current literature value of 120 kcal/mol. Using the new value as the anchor point, G2 derived $\Delta H_{f,298}$ values for the isomers $H_2\overline{C\text{-}O\text{-}C}(H)OH^+$, $HOCH_2\text{-}C{=}O^+$, $^+CH_2\text{-}H{\bullet\bullet\bullet}O{=}C{=}O$, $^+CH(OH)\text{-}C(=O)H$, $^+CH_2\text{-}O\text{-}C(=O)H$, $\overline{CH_2\text{-}O\text{-}C(H)\text{-}O}^+$ and $^+CH_2O\text{-}C\text{-}OH$ have been calculated as 147, 131, 157, 144, 144, 140 and 177 kcal/mol respectively.

[1] This chapter has already appeared in print under the same title: P.J.A Ruttink, P.C. Burgers, L.M. Fell and J.K. Terlouw, *J. Phys. Chem. A*, **103** (1999) 1426-1431.

Introduction

The field of gas-phase ion chemistry has sparked the interest of physical chemists for a great many years. The determination of thermochemical quantities (such as enthalpy of formation, ΔH_f) of isomeric ions has been performed almost since the inception of computational chemistry. Computational thermochemistry has now reached a point where composite theoretical methods like G2 and CBS-Q can often reproduce ΔH_f of systems containing up to 10 heavy atoms to chemical accuracy, ± 1-2 kcal/mol [1]. The structural assignment of gas-phase ions via mass spectrometric experiments also has a long history, and its development has been greatly aided by the availability of such thermochemical information [2]. Indeed, this interplay between theory and experiment has had so much success that this partnership is becoming the norm. This paper uses this powerful combination with the emphasis on the computational aspects in a study of the methoxycarbonyl ion, (m/z 59) $CH_3OC{=}O^+$. This key fragment ion in the mass spectra of many methyl esters is of current interest, because of its methyl cation donor ability and its role in aromatic substitution reactions in the gas phase [3].

More than ten years ago, the structure and stability of the $CH_3OC{=}O^+$ ion, $\mathbf{6}^+$, and eleven of its isomers, see structures **1-11** in Scheme 1† , were investigated with the fruitful combination of (tandem) mass spectrometry and *ab initio* MO calculations [4]. The relative energies of the various isomers were calculated using a coupled electron pair approximation procedure (CEPA/6-31G*//6-31G*) which yielded $\Delta H_{f,298}$ [$\mathbf{6}^+$] = 120 ± 1 kcal/mol using the experimentally determined ΔH_f of the isomeric hydroxyoxiranyl cation, $\mathbf{2}^+$, as the anchor point.

In that study, results of appearance energy (AE) measurements on nine selected precursor molecules were also reported with the aim of obtaining an accurate experimental value for ΔH_f ($\mathbf{6}^+$). However, the resulting value, 131 ± 4 kcal/mol, was deemed to be too high because of competitive shifts in the measurements. In support of this, shortly after this work appeared, McMahon and co-workers [5] reported the methyl cation affinity (MCA) of carbon dioxide as 49.5 kcal/mol, and this translates into a low value, 118 ± 3 kcal/mol, for the methoxycarbonyl cation's heat of formation.

---

† Ions marked with an asterisk were computationally considered in reference 4 but not in this study.

Scheme 1

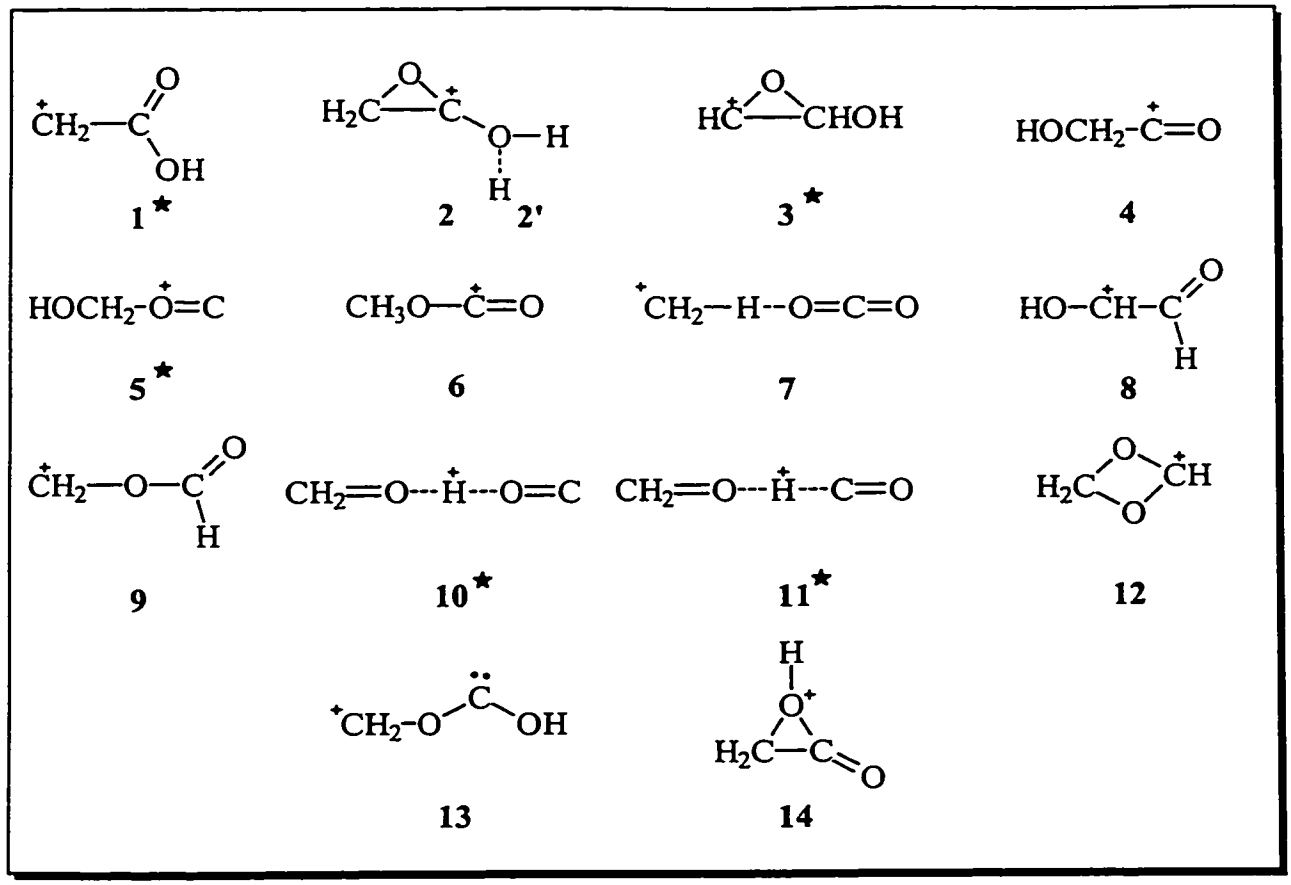

However, adopting the 120 kcal/mol value for ΔH_f [$CH_3OC{=}O^+$] makes it difficult to understand some aspects of the gas-phase ion chemistry of low energy (metastable) methyl pyruvate and methyl acetate radical cations. Using simple thermochemical arguments, we would expect the metastable ion (MI) spectrum of ionized methylpyruvate, $CH_3COCOOCH_3{\bullet}^+$, to display signals at both m/z 43 and m/z 59 for its competing dissociations into $CH_3C{=}O^+$ (m/z 43) + $CH_3OC{=}O\bullet$ and $CH_3OC{=}O^+$ (m/z 59) + $CH_3C{=}O\bullet$ because both sets of products have the same energy ($\sum\Delta H_{f,298}$ [products] = 116 and 117 kcal/mol respectively [6]). A similar situation obtains for ionized methylacetate, $CH_3COOCH_3{\bullet}^+$, where dissociation into $CH_3C{=}O^+$ + $CH_3O\bullet$ and $CH_3OC{=}O^+$ + $CH_3\bullet$ is also calculated to be competitive ($\sum\Delta H_{f,298}$ [products]= 160 and 155 kcal/mol respectively [6]). Nevertheless, a m/z 59 signal is absent in either MI spectrum. On the other hand, these observations are readily understood if ΔH_f [$CH_3OC{=}O^+$] were

several kcal/mol higher, i.e. in line with the results derived from the direct AE measurements mentioned above.

This prompted us to re-investigate this ion's enthalpy of formation by performing a G2 computational study on the series of reactions depicted in Scheme 2 :

Scheme 2

1.	$CH_3OC{=}O^+$	→	$C^+ + C + 2O + 3H$
2.	$CH_3OC{=}O^+$	→	$CH_3C{=}O^+ + O$
3.	$CH_3OC{=}O^+$	→	$CH_3^+ + CO_2$
4.	$CH_3OC{=}O^+ + CO$	→	$CH_3C{=}O^+ + CO_2$
5.	$CH_3OC{=}O^+ + H_2O$	→	$CH_3OH_2^+ + CO_2$
6.	$CH_3OC{=}O^+ + HCOOH$	→	$HOC{=}O^+ + CH_3OCH{=}O$
7.	$CH_3OC{=}O^+ + CH_3OH$	→	$CH_2OH^+ + CH_3OCH{=}O$
8.	$CH_3OC{=}O^+ + CH_3CH{=}O$	→	$CH_3C{=}O^+ + CH_3OCH{=}O$
9.	$CH_3OC{=}O^+ + CH_2{=}O$	→	$HOC{=}O^+ + CH_3CH{=}O$
10.	$CH_3OC{=}O^+ + N_2$	→	$CH_3N_2^+ + CO_2$

Currently many schemes are used to derive heat of formation values for ions and neutrals from *ab initio* calculations [7]. Most popular and accurate are : (i) the atomization procedure, where the *ab initio* atomization energy of the species is related to the experimental heats of formation of the constituent atoms and (ii) the use of isodesmic substitution reactions which combines the species of unknown ΔH_f with components of well established ΔH_f (typically at 298 K). The reaction energy is theoretically determined and the sought-after ΔH_f calculated.

In this study, we have used these procedures, see reactions **1** and **6-8** in Scheme 2, to determine the heat of formation of the methoxycarbonyl ion. The isodesmic reactions (**6-8**) involving the ion were designed along the lines of the bond separation scheme developed by Curtiss et al. for neutral species [7]. In addition, we have examined selected dissociation and non-isodesmic substitution reactions (reactions **2-5**, **9** and **10**) for which reliable experimental heat of formation data are available.

We have also used the G2 methodology to obtain an expectedly more reliable energy for the $CH_3OC{=}O^+$ ion and its key isomers vis-à-vis the hydroxyoxiranyl cation,

2^+, which was used as the anchor point in the determination of ΔH_f (6^+) in the previous CEPA *ab initio* study [4].

Finally, the previously reported appearance energy (AE) data on the methoxycarbonyl cation were combined, where appropriate, with recently revised ΔH_f values for the neutral species. The resulting experimental ΔH_f (6^+) was compared with the theoretical findings and the number obtained from the re-evaluated methyl cation affinity of CO_2.

Theoretical Method

Standard *ab initio* MO calculations were performed with the Gaussian 94 series of programs [8]. The G2 method approximates an energy at the QCISD(T)/6-311+G(*3df,2p*) level of theory based on MP2/6-31G(*d*) optimized geometries, incorporating scaled HF/6-31G(*d*) zero-point energies and an empirical higher level correction [1]. The G2 method was performed on all ions and molecules shown in Schemes 1 and 2 and the results of these calculations are summarized in Tables 7-1 and 7-2. Table 7-1 presents the G2 calculated ΔH_f for the $CH_3OC{=}O^+$ ion, 6^+, based on reactions **1** - **10**, whereas Table 7-2 gives the calculated (G2/atomization method) and experimental enthalpies of formation for the ionic and neutral components of reactions **1** - **10**. For most of the species examined in this study the available experimental enthalpy of formation refers to 298 K. These values were converted to 0 K using a correction term, ΔH_T in Table 7-2, based on standard thermodynamic formulae and scaled vibrational frequencies [1].

Table 7-3 presents ΔH_f (6^+) values derived from experiment (appearance energy measurements) and will be discussed in section 2 of "Results and Discussion". The relative energies, G2 total energies and derived ΔH_f values of selected $C_2H_3O_2^+$ isomers are presented in Table 7-4. Figure 7-1 presents the optimized geometries of the methoxycarbonyl cation and the various isomers. When not explicitly referenced, the experimental ΔH_f values have been taken from ref 6.

Apart from atomization and isodesmic reactions, Scheme 2 also lists some other reactions. These had to be chosen carefully to avoid significant systematic errors: for instance, if the reaction $CH_3^+ + CO \rightarrow CH_3C{=}O^+$, were chosen to calculate ΔH_f [$CH_3C{=}O^+$], then from ΔH_{rxn} (G2, 0 K) = 74 kcal/mol, $\Delta H_{f,0}$ [CO] = -27 kcal/mol and Δ

$H_{f,0}$ [CH_3^+] = 262 kcal/mol, one obtains $\Delta H_{f,0}$ [$CH_3C{=}O^+$] = 161 kcal/mol. This value compares poorly with the expected 157 kcal/mol derived from the well established experimental $\Delta H_{f,298}$ value and the ΔH_T correction mentioned above (see Table 7-2). Such errors stem from differences between the G2 calculated and experimental ΔH_f values of the various components of a given reaction. For the components of the reactions that we have selected, the differences are listed as Δ^{298} in the final column of Table 7-2. To minimize the overall error, we have chosen reactions $CH_3OC{=}O^+ + A \rightarrow B + C$, where A, B and C are species with established experimental ΔH_f and where the errors in the G2 calculation of ΔH_f compensate, i.e. $\Delta A^{298} \cong \Delta B^{298} + \Delta C^{298}$.

Results and Discussion

ΔH_f[CH_3O-C=O^+] derived from G2 calculations on the reactions depicted in Scheme 2.

In Table 7-1 we present the results of the G2 calculations of $\Delta H_f(\mathbf{6}^+)$ on reactions **1** through **10**. We have performed two different comparisons with two different sets of independent references. The first set of ΔH_f reference compounds uses experimental values for all the molecules and carbocations in reactions **1-10**; the results of these calculations are presented in the first column of Table 7-1. The second set of reference values is a "pure G2" set where the independent references are the heats of formation of the atoms only, that is the enthalpies of formation used are calculated with the G2 atomization method. Hence these values are more self consistent and have a lower standard deviation. Combining these results, we obtain $\Delta H_{f,298}$ ($\mathbf{6}^+$) = 130 ± 2 kcal/mol which includes a -2.4 kcal/mol temperature correction, see Table 7-2. Reactions **3** and **10** refer to methyl cation affinities and this point will be discussed in section 4.

Figure 7-1. The MP2(full)/6-31G(*d*) optimized geometries of selected $C_2H_3O_2^+$ isomers, bond lengths in Angstrom, bond angles in degrees.

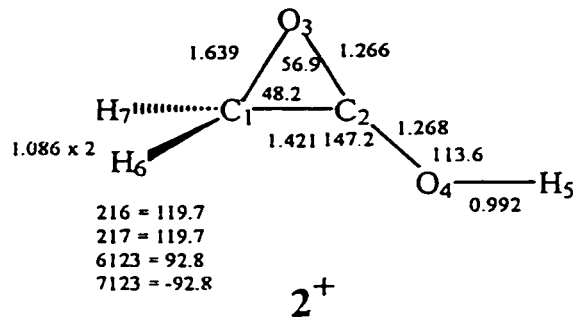

2^+

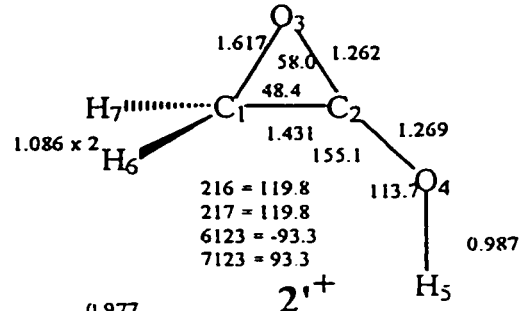

$2'^+$

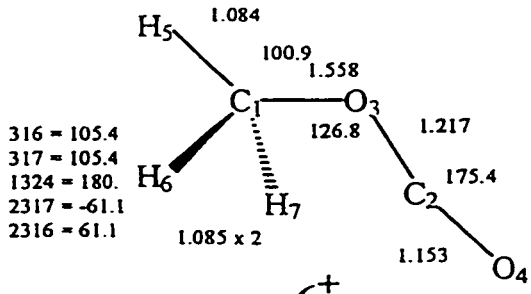

6^+

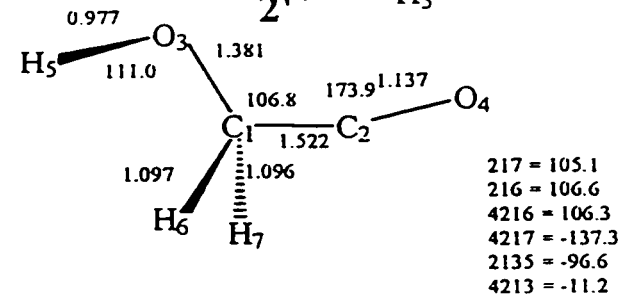

4^+

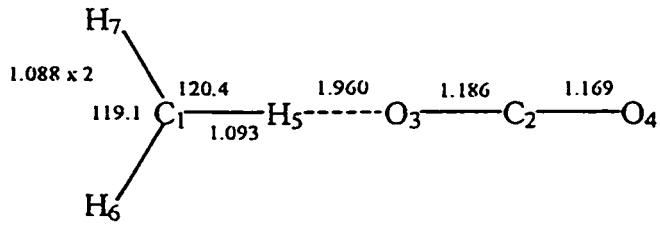

7^+

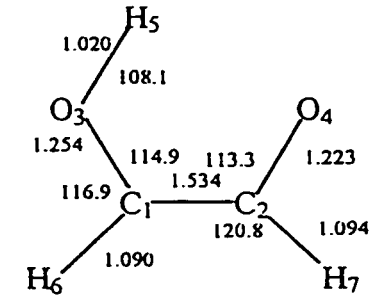

8^+

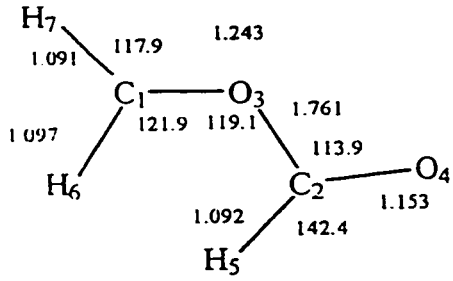

9^+

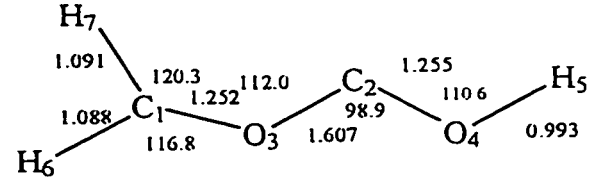

13^+

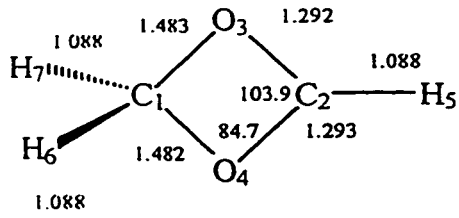

12^+

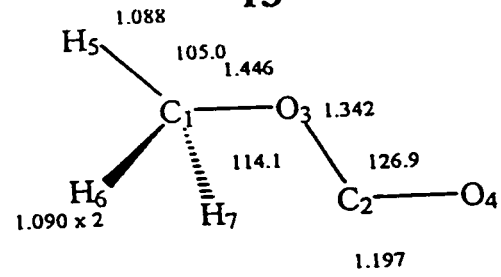

$6^{\bullet}$

316 = 110.4
317 = 110.4
1324 = 180.
2317 = -61.1
2316 = 61.1

Table 7-1. $\Delta H_{f,0}[CH_3OC{=}O^+]$ values (kcal/mol) calculated by the G2 method on the basis of reactions **1-10** in Scheme 2.

Reaction	G2 (0 K) expt[a]	G2 (0 K) theory[b]
1	132.2	132.2
2	131.3	132.2
3	133.9	132.2
4	132.1	132.2
5	133.3	131.3
6	134.5	132.2
7	133.9	130.5
8	133.5	132.2
9	132.0	132.2
10	129.3	131.7
Average	132.6 ± 1.6	131.9 ± 0.6

[a] Using the G2 $\Delta H_{reaction}$ and experimental $\Delta H_{f,0}$; [b] Using the G2 $\Delta H_{reaction}$ and theoretical $\Delta H_{f,0}$.

Table 7-2. G2 calculated and experimental enthalpies of formation (kcal/mol) for the species in Scheme 2.

Species	$\Delta H_{f,0}$ G2	$\Delta H_{f,298}$ G2	$\Delta H_{f,0}$ expt[d]	$\Delta H_{f,298}$ expt	ΔH_T[a] calculate	ΔH_T[b] expt	Δ 298[c] G2-expt
CO_2	-96.67	-96.80	-93.96	-94.05	-0.16	-0.09	2.8
H_2O	-57.39	-58.10	-57.10	-57.80	-0.72	-0.7	0.3
HCOOH	-90.78	-92.50	-88.8	-90.5	-1.73		2.0
$CH_3OC(H){=}O$	-85.68	-88.67	-82.0	-85.0	-3.01		3.7
CH_3OH	-46.79	-49.46	-45.6	-48.2	-2.68	-2.6	1.3
$CH_3C(H){=}O$	-38.49	-41.09	-37.0	-39.6	-2.62	-2.6	1.5
CO	-29.04	-28.60	-27.20	-26.42	0.42	0.78	2.2
$CH_2{=}O$	-27.06	-28.31	-25.0	-26.0	-1.25	-1.0	2.3
CH_3CO^+	159.92	158.74	157	156	-1.18		-2.7
CH_3^+	263.02	261.76	262.0	261.3	-1.26	-0.7	-0.5
CH_2OH^+	169.62	167.50	170	168	-2.12		0.5
$HOC{=}O^+$	142.60	141.96	143	142	-0.63		-1.0
$CH_3OC{=}O^+$	132.20	129.79	-	-	-2.41		-
$HC{=}O^+$	197.74	197.38	197.7	197.3	-0.36		-0.1
$CH_3OH_2^+$	141.26	138.67	139	136	-2.59		-2.7
$CH_3N_2^+$	222.81	223.45	218	217	-1.42		-4.4
N_2	1.19	1.21	0	0	0.02		-1.2

[a] From scaled vibrational frequencies, see text; [b] $\Delta H_{f,298}$ (exp) - $\Delta H_{f,0}$ (exp) ; [c] Δ 298 = Δ $H_{f,298}$(expt) - $\Delta H_{f,298}$ (theory) ; [d] Experimental values used when available, otherwise derived from Δ $H_{f,298}$(expt) using ΔH_T (calc).

The agreement between the two approaches is satisfactory but the resulting $\Delta H_{f,298}$ ($\mathbf{6}^+$) value is 10 kcal/mol higher than the current literature value. However, our re-evaluation of the experimental AE data, see section 2, also points to a much higher value, 129 kcal/mol. It is known that the G2 atomization procedure sometimes fails to reproduce ΔH_f of C=O containing molecules with chemical accuracy [7]. Thus, one may argue that the value derived from reaction **1** could be in error by several kcal/mol. However, the excellent agreement with the numbers derived from the isodesmic substitution reactions (where errors in the description of certain bonds are expected to cancel) and the consistency with the data for the other reactions clearly lends credence to the derived value.

Two further approaches based on theory support the above value. First, we derived ΔH_f ($\mathbf{6}^+$) from G2 calculations of the heat of formation and ionization energy of the methoxycarbonyl radical, **6**•, whose optimized geometry is presented in Figure 7-1. The heat of formation was calculated as $\Delta H_{f,298}$ (**6**•) = -40.1 kcal/mol using the atomization procedure, in excellent agreement with the experimental value [6b]. The IE obtained from G2 calculations at 0 K is 7.32 eV (169 kcal/mol) and this yields $\Delta H_{f,298}$ ($\mathbf{6}^+$) = 129 kcal/mol.

Secondly, we calculated the G2 and G2MP2 energy difference between ionized methyl acetate and its direct bond cleavage dissociation products $CH_3OC{=}O^+$ and CH_3•. The result, 25.4 and 24.9 kcal/mol, combined with experimental $\Delta H_{f,298}$ values for the ionized ester (139 kcal/mol [6a]) and the methyl radical (35.0 kcal/mol [6a]), yields $\Delta H_{f,298}$ ($\mathbf{6}^+$) = 129 and 128 kcal/mol, respectively. The resulting value is the same as that derived from the appearance energy measurement tabulated in Table 7-3 and this indicates that this reaction does not suffer from a competitive shift.

$\Delta H_f[CH_3O\text{-}C{=}O^+]$ derived from direct AE measurements.

Table 7-3 reproduces the previously published [4] AE measurements and combines these with the partially revised thermochemical data on the precursor molecules and neutral reaction products required to derive $\Delta H_{f,298}$ ($\mathbf{6}^+$). One precursor molecule from the

Table 7-3. $\Delta H_{f,298}[CH_3OC{=}O^+]$ values derived from appearance energy measurements.[a]

Precursor molecule (M)	ΔH_f(M) kcal/mol	AE m/z 59 ± 0.05 eV	Neutral product and ΔH_f values kcal/mol		ΔH_f (CH_3OCO^+) kcal/mol
$(CH_3O)_2CO$	-137[b]	11.50	$CH_3O\cdot$ ($CH_2OH\cdot$)	4.1 (-4.0[e])	124 (132)
$BrCH_2COOCH_3$	-89	11.16	$CH_2Br\cdot$	42.0	126
$ClCH_2COOCH_3$	-99	11.10	$CH_2Cl\cdot$	28.3	129
$ClCOOCH_3$	-104	11.24	$Cl\cdot$	29.0	126
CH_3COOCH_3	-98.0	11.32	$CH_3\cdot$	35.0	128
cy-$C_3H_5COOCH_3$	-72.4	10.56	$CH_2CHCH_2\cdot$	40.9	130
			cy-$CH_2CHCH_2\cdot$	39.5	132
$CH_3CH_2COOCH_3$	-103.8	11.42	$CH_3CH_2\cdot$	29.4	130
$HOCH_2COOCH_3$	-133	11.38	$CH_2OH\cdot$	-4.0[e]	133
FCH_2COOCH_3	-139[c]	11.16[d]	$FCH_2\cdot$	-8[f]	126

[a] Unless indicated otherwise, data obtained from reference 4 ; [b] Reference 9; [c] Estimate, based on G2 $\Delta H_{f,298}$ [FCH_2COOH] = -144 kcal/mol, adding 5.3 kcal/mol for CH_3 substitution (methyl substitution effect based on $\Delta H_f[CH_3COOCH_3] - \Delta H_f[CH_3COOH]$ = 5.3 kcal/mol [6a]) ; [d] Reference 10 ; [e] Reference 11 ; [f] Reference 12.

original study, methyl pyruvate, is not listed because the generation of $\mathbf{6}^+$ therefrom is not a simple direct bond cleavage reaction [4]. Instead, we have included an as yet unpublished AE measurement on methyl fluoroacetate as the last entry in the Table. The derived enthalpy of formation of ion $\mathbf{6}^+$ for the reactions listed in the Table range from 124 to 133 kcal/mol, with an average value of 129 kcal/mol. The average value (and also the range) is smaller than that previously reported. Nevertheless it is still 9 kcal/mol higher than the preferred value in ref 4, but in excellent agreement with the G2 result proposed above. This agreement indicates that very little, if any, competitive shift is present in the AE measurements. Hence, a value of 129 ± 2 kcal/mol becomes our preferred value for $\Delta H_f[CH_3OC{=}O^+]$.

$\Delta H_f[CH_3O\text{-}C{=}O^+]$ derived from the G2 calculated energy difference with other isomers.

Another established procedure to derive an ion's heat of formation involves the calculation of its relative energy vis-à-vis that of an isomeric reference ion whose enthalpy of formation is experimentally well established. This procedure was followed in ref 4, that is $\Delta H_{f,298}$ ($\mathbf{6}^+$) was derived from the computed energy difference with the ionic isomer $\mathbf{2}^+$ whose $\Delta H_{f,298}$ was experimentally determined, from an AE measurement on the loss of iodine from iodoacetic acid, as 141 ± 1 kcal/mol. This procedure yielded the 120 kcal/mol value which we now question. The discrepancy with the newly proposed value could *a priori* originate from an inaccuracy in either (i) the computationally derived energy difference or (ii) the heat of formation of the anchor point or (iii) the structure assigned to the anchor point ion is incorrect. In this section we address these three questions.

The first question is dealt with in Table 7-4, which lists the CEPA relative energies from ref 4 and compares these with the G2 results. It appears that the G2 energy difference between ions $\mathbf{6}^+$ and $\mathbf{2}^+$ is somewhat lower than the original CEPA value but the derived $\Delta H_{f,298}$ ($\mathbf{6}^+$) = 123 kcal/mol still falls short of the recommended value by 6 kcal/mol.

In this context, we verified that ion $\mathbf{2}^+$'s rotamer, $\mathbf{2'}^+$, is a species of higher energy and also that its ring opened isomer, $\mathbf{1}^+$, remained a saddle point on the potential energy surface (see ref 4) when electron correlation was included in the geometry optimizations.

Table 7-4. G2 total energies (hartrees), relative energies E_{rel} (kcal/mol), and ΔH_f values for selected $C_2H_3O_2^+$ isomers based on the recommended $\Delta H_{f,298}$ [$CH_3OC{=}O^+$] (**6**$^+$) = 129 kcal/mol.

Ion	G2 (0 K)	G2 (298 K)	E_{rel} (0 K)	E_{rel} (298 K)	E_{rel} (CEPA)[a]	$\Delta H_{f,0}$[b]	$\Delta H_{f,298}$[b]
2$^+$	-227.77141	-227.76752	18.8	18.1	20.5	150	147
2'$^+$	-227.76979	-227.76594	19.8	19.1		151	148
4$^+$	-227.79854	-227.79391	1.7	1.6	3.6	133	131
6$^+$	-227.80131	-227.79639	0.0	0.0	0.0	131	129
7$^+$	-227.75859	-227.75173	26.8	28.0	27.2	158	157
8$^+$	-227.77680	-227.77263	15.4	14.9	11.3	146	144
9$^+$	-227.77783	-227.77308	14.3	14.6	9.4	145	144
12$^+$	-227.78224	-227.77871	12.0	11.1		143	140
13$^+$	-227.72440	-227.71981	48.3	48.1		179	177

[a] Reference 4; [b] Recommended values ± 2 kcal/mol; see text.

As for the second question, we will first consider an alternative anchor point *viz.* the $C_2H_3O_2^+$ ion generated by loss of CH_3• from ionized ethyl formate, CH_3CH_2O-C(=O)H•$^+$. Ion **9**$^+$ in Scheme 1, $^+CH_2O$-C(=O)H, has been proposed to be the product ion structure. Its appearance energy from the ester, AE = 11.60 ± 0.16 (268 ± 4 kcal/mol), was determined using the sophisticated threshold photoelectron photoion coincidence (TPEPICO) technique [13]. Using $\Delta H_{f,298}$ [CH_3CH_2O-C(=O)H] = -93.5 kcal/mol [4] we then arrive at $\Delta H_{f,298}$ (**9**$^+$) = 139 ± 4 kcal/mol, not inconsistent with the 144 ± 2 kcal/mol proposed in Table 7-4. However, when it is postulated that the CH_3• loss from the ester does not yield ion **9**$^+$ (by direct bond cleavage) but rather its ring closed isomer **12**$^+$ (via anchimeric assistance) the agreement becomes much better: $\Delta H_{f,298}$ (**12**$^+$) as proposed in Table 7-4 is 140 ± 2 kcal/mol. Unfortunately, this proposal cannot be substantiated since the reported CID spectrum (ref 4) is clearly compatible with either of the proposed ion structures.

As far as the original experimental anchor point is concerned, we note that ΔH_f (**2**$^+$) = 141 ± 1 kcal/mol, is based on AE(m/z 59) = 10.86 ± 0.05 eV, ΔH_f[I•] = 25.5 kcal/mol[6] and ΔH_f[ICH_2COOH] = -84 ± 1 kcal/mol [4]. The latter heat of formation may

be less certain than originally proposed and could be revised to -83.2 ± 2.5 kcal/mol [14] but this does not substantially reduce the discrepancy noted above.

The discrepancy would disappear if the ions generated by loss of I• from $ICH_2COOH^{\bullet+}$ would not have structure $\mathbf{2}^+$ but rather that of an isomeric ion of slightly lower energy, such as ions $\mathbf{8}^+$, $\mathbf{9}^+$ or $\mathbf{12}^+$ in Scheme 1, see Table 7-4. However, there is little evidence that the original assignment of the ion structure is incorrect. In the previous study, the collision induced dissociation (CID) mass spectrum of *source* generated ions was analyzed and on the basis of the observed dissociation reactions structure $\mathbf{2}^+$ was assigned to the ions. We have repeated this measurement, found an identical spectrum, and agree with this assignment. Nevertheless, it is not inconceivable that the *low energy* product ions have a different structure (see ref 15 for a classical example involving CH_3-S^+=O vs. CH_2=S=OH^+). Since it is these low energy species that are sampled in the AE experiment, we have obtained a CID spectrum of the metastably generated m/z 59 ions from $ICH_2COOH^{\bullet+}$. The resulting spectrum, see Figure 7-2, is essentially the same as that of the source generated ions (obtained at the same translational energy) and this leaves little doubt that the original assignment was correct.

To reinforce this conclusion, we also verified that the isomeric ions $\mathbf{13}^+$ and $\mathbf{14}^+$ could be eliminated as potential product ions generated in the loss of I• from $ICH_2COOH^{\bullet+}$. The carbene type ion $\mathbf{13}^+$ represents the C-C ring-opened form of ion $\mathbf{2}^+$, but, not unexpectedly, this isomer lies very high in energy, at 177 kcal/mol (Table 7-4). The carbonyl protonated acetolactone ion $\mathbf{14}^+$ plays no role in this dissociation either: upon geometry optimization it collapses to the hydroxyacetylium ion, $\mathbf{4}^+$, whose CID spectrum is entirely different from that assigned to ion $\mathbf{2}^+$.

Thus, combining G2 relative energies with ion $\mathbf{2}^+$ as the anchor point yields ΔH_f ($\mathbf{6}^+$) = 124 ± 3 kcal/mol, whereas ion $\mathbf{9}^+/\mathbf{12}^+$ as the anchor point gives ΔH_f ($\mathbf{6}^+$) = 125/129 ± 4 kcal/mol. The numbers resulting from this approach are somewhat lower than the recommended value but their uncertainties are such that consistency is still maintained.

Figure 7-2. The CID (3ffr, O_2) mass spectrum of the $C_2H_3O_2^+$ ions generated from low energy (metastable) iodoacetic acid ions.

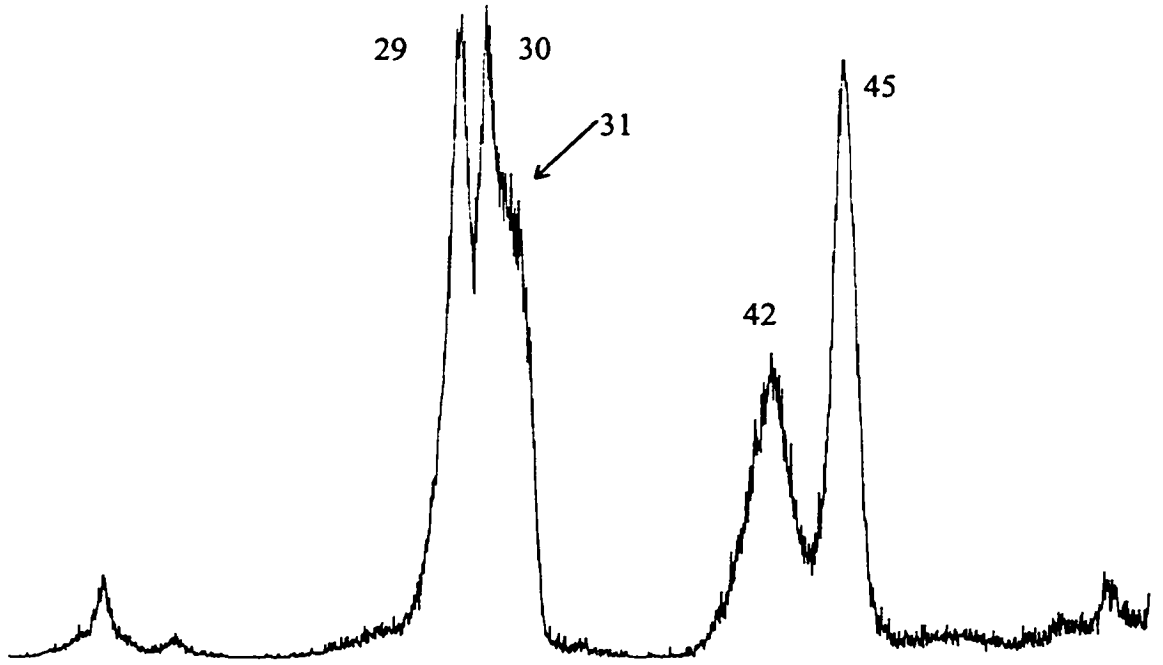

Methyl Cation Affinity of Carbon Dioxide

Finally, one more important experimental finding remains to be addressed, i.e. the heat of formation of $CH_3OC{=}O^+$ derived from the Methyl Cation Affinity (MCA) of CO_2, defined as the negative enthalpy change for the reaction $CH_3^+ + CO_2 \rightarrow CH_3OC{=}O^+$. As stated in the introduction, the literature value, 49.5 ± 3 kcal/mol [5], supports the originally proposed low enthalpy value for ion **6**$^+$. In sharp contrast, a much lower value, 38.3 ± 2.0 kcal/mol, follows from our G2 calculations on reaction **3** in Scheme 2, see Table 7-1/Column 3, using $\Delta H_{f,298}$ (**6**$^+$) = 129 kcal/mol in combination with experimental enthalpy data for CO_2 and CH_3^+. In 1994 the MCA of N_2 was re-evaluated [16] using high-pressure mass spectrometry based experiments and G2 theory and this transforms the MCA (CO_2) reported in ref 5 to 46.2 and 44.7 kcal/mol, respectively [17]. From these values one derives $\Delta H_{f,298}$ (**6**$^+$) = 121 - 123 kcal/mol, some 7 kcal/mol below our

recommended value. Considering the evidence presented in sections 1-3, we feel that a reexamination of the experimentally determined MCA of CO_2 would appear appropriate.

Concluding Remarks

Evidence has been presented that the enthalpy of formation of the methoxycarbonyl cation, $\mathbf{6}^+$, and some of its key isomers should be revised. The revision is based on : (i) a G2 study on a series of different reactions producing $\Delta H_{f,298}$ ($\mathbf{6}^+$) = 130 ± 2 kcal/mol, (ii) the AE of $CH_3OC{=}O^+$ from 10 different precursor molecules yielding an average value of 129 kcal/mol and (iii) G2 calculated energy differences with two isomeric ions used as the anchor point. We recommend $\Delta H_{f,298}$ [$CH_3OC{=}O^+$] = 129 ± 2 kcal/mol. Using this value as the anchor point, G2 derived $\Delta H_{f,298}$ values for the isomers $H_2\overline{C\text{-}O\text{-}C}(H)OH^+$ ($\mathbf{2}^+$), $HOCH_2\text{-}C{=}O^+$ ($\mathbf{4}^+$), $^+CH_2\text{-}H{\bullet\bullet\bullet}O{=}C{=}O$ ($\mathbf{7}^+$), $^+CH(OH)\text{-}C(=O)H$ ($\mathbf{8}^+$), $^+CH_2\text{-}O\text{-}C(=O)H$ ($\mathbf{9}^+$), $\overline{CH_2\text{-}O\text{-}C(H)\text{-}O}^+$ ($\mathbf{12}^+$) and $^+CH_2O\text{-}C\text{-}OH$ ($\mathbf{13}^+$), have been calculated as 147, 131, 157, 144, 144, 140 and 177 kcal/mol respectively.

The revised heat of formation of the methoxycarbonyl cation also provides a rationale for the absence of these ions in the MI spectra of ionized methyl pyruvate and methyl acetate.

Finally, we note that our revised $CH_3\text{-}O\text{-}C^+{=}O$ enthalpy value leads to a 13 kcal/mol stabilization brought about by methyl substitution in $H\text{-}O\text{-}C^+{=}O$ ($\Delta H_{f,298}$ = 142 kcal/mol [18]). This stabilization energy is virtually identical with that established by the late Dr Lossing [19] for the analogous substitution on the non-charge bearing O atom in $H\text{-}O\text{-}CH_2^+$.

References

1. (a) Foresman, J.B.; Frisch, A. *Exploring Chemistry with Electronic Structure Methods*, Gaussian Inc: Pittsburgh, 1996 and references cited therein. (b) Curtiss L.A.; Raghavachari K.; Trucks, G.W.; Pople J.A. *J. Chem. Phys.*, **1991**, *94*, 7221.
2. (a) Burgers, P.C.; Terlouw, J.K. In *Specialist Periodical Reports : Mass Spectrometry*; Rose, M.E., Ed.; London, The Royal Society of Chemistry, Vol. 10, Chapter 2, 1989. (b) Holmes, J.L. *Org. Mass Spectrom.* **1985**, *20* 169. (c) Radom, L. *Int. J. Mass Spectrom. Ion Processes* **1992**, *118/119*, 339.
3. (a) Sekiguichi,O.; Aoyagi, K.; Tajima, S.; Nibbering, N.M.M. *J. Mass Spectrom.*, **1997**, *32*, 755. (b) J. Chamot-Rooke, B. Amekaz, J. Tortajada, P. Mourgues and H.E. Audier, *J. Mass Spectrom.*, **1997**, *32*, 779. (c) Giacomello, P.; Pepi, F. *J. Phys. Chem.* **1993**, *97*, 4421.
4. Blanchette M.C.; Holmes J.L.; Hop C.E.C.A.; Lossing F.P.; Postma R.; Ruttink P.J.A.; Terlouw J.K. *J. Am. Chem. Soc.*, **1986**, *108*, 7589.
5. (a) Hovey,J.K.; McMahon, T.B. *J. Phys. Chem.* **1987**, *91*, 4560. (b) McMahon,T.B.; Heinis, T.;

Nicol, G.; Hovey, J.K.; Kebarle, P. *J. Am. Chem. Soc.*, **1988**, *110*, 7591.
6. (a) Lias, S.; Bartmess, J.E.; Liebman, J.F.; Holmes, J.L.; Levin, R.D.; Mallard, W.G.; *J. Phys. Chem. Ref. Data*, **1988**, *17*, Supplement 1. (b) Holmes, J.L.; Lossing, F.P.; Mayer, P.M. *J. Am. Chem. Soc.* **1991**, *113*, 9723.
7. (a) Nicolaides, A.; Rauk, A.; Glukhovstev, M.N.; Radom, L. *J. Phys. Chem.* **1996**, *100*, 17460. (b) Ochterski, J.W.; Petersson, G.A.; Wiberg, K.B. *J. Am. Chem. Soc.* **1995**, *117*, 11299. (c) Raghavachari, K.; Stefanov, B.B.; Curtiss, L.A. *J. Chem. Phys.* **1997**, *106*, 6764. (d) S. Hammerum, *Int. J. Mass Spectrom. Ion Processes* **1997**, *165/166*, 63. (e) Nicolaides, A.; Radom, L. *Mol. Phys.* **1996**, *88*, 759. (f) Curtiss, L.A.; Raghavachari, K.; Redfern, P.C.; Stefanov, B.B. *J. Chem. Phys.* **1998**, *108*, 692. (g) Raghavachari, K.; Stefanov, B.B.; Curtiss, L.A. *Mol. Phys.* **1997**, *91*, 555. (h) Mayer, P.M.; Glukhovstev, M.N.; Gauld, J.W.; Radom, L. *J. Am. Chem. Soc.* **1997**, *119*, 12889. (i) Wiberg, K.B.; Ochterski, J.W.; *J. Comp. Chem.* **1997**, *18*, 108. (j) Andersen, P.E.; Hammerum, S. *Eur. Mass Spectrom.* **1995**, *1*, 499.
8. Gaussian 94, Revision B.3, M. J. Frisch, G.W. Trucks, H.B. Schlegel, P.M.W. Gill, B.G. Johnson, M.A. Robb, J.R. Cheeseman, T.A. Keith, G.A. Peterson, J.A. Montgomery, K. Raghavachari, M.A. Al-Laham, V.G. Zakrevski, J.V. Ortiz, J.B. Foresman, C.Y. Peng, P.Y. Ayala, W. Chen, M.W. Wong, J.L. Andres, E.S. Replogle, R. Gomperts, R.L. Martin, D.J. Fox, J.S. Binkley, D.J. de Frees, J. Baker, J.P. Stewart, M. Head-Gordon, C. Gonzales and J.A. Pople, Gaussian Inc., Pittsburgh PA, 1995.
9. Steele, W.V.; Chirico, R.D.; Knipmeyer, S.E.; Nguyen, A.; Smith, N.K. *J. Chem. Eng. Data*, **1997**, *42*, 1037.
10. J.L. Holmes and F.P. Lossing, unpublished results.
11. (a) Traeger, J.C.; Kompe, B.M. In *Energetics of Organic Free Radicals*; Simões, J.A.M.; Greenberg, A.; Liebman, J.F., Ed.; Blackie Academic & Professional, New York, 1996, Chapter 3. (b) Bauschlicher, Jr., C.W.; Partridge, H. *J. Phys. Chem* **1994**, *98*, 1826.
12. J.L. Holmes, unpublished results.
13. Zha, Q.; Nishimura, T.; Meisels, G.G. *Int. J. Mass Spectom.Ion Processes*, **1992**, *120*, 85.
14. (a) Holmes, J.L.; Dakubu, M. *Org. Mass Spectrom.*, **1989**, *24*, 461. (b) Benson, S.W. *Chem. Rev.*, **1993** *93*, 2419.
15. McGibbon, G.A.; Burgers, P.C.; Terlouw, J.K. *Chem. Phys. Lett.*, **1994**, *218*, 499.
16. Glukhovtsev, M.N.; Szulejko, J.E.; McMahon, T.B.; Gauld, J.W.; Scott, A.P.; Smith, B.J.; Pross, A.; Radom, L. *J. Phys. Chem.*, **1994**, *98*, 13099.
17. G2 calculated MCAs have been found to be systematically lower than the experimental values, by ca 1 kcal/mol, because of a slight discrepancy between theory and experiment in the heat of formation of CH_3^+, see ref 16.
18. Ruttink, P.J.A.; Burgers, P.C.; Terlouw, J.K. *Int. J. Mass Spectrom.* in press.
19. Lossing, F.P. *J. Am. Chem. Soc.* **1977**, *99*, 7526.

SUMMARY

This thesis presents several studies on a unified mass spectrometric and computational chemistry approach to problems of gas-phase ion chemistry. Attention is focussed on the structure, stability and isomerization behaviour of intermediates in dissociative rearrangement reactions which include ion-dipole complexes, distonic ions and hydrogen-bridged radical cations. Hydrogen-bridged radical cations have played an increasing and pivotal role in the description of ionic rearrangements. Particularly, their application in the concept of "proton transport catalysis" have provided answers to some gas-phase ion chemistry problems.

The first chapter introduces the combined approach by describing tandem mass spectrometry, general mechanistic aspects and computational chemistry. Some examples are given to show how these elements can be combined to solve mechanistic problems in gas-phase ion chemistry.

Chapters 2 and 3 discuss the unimolecular chemistry of the ionized diols 1,2-ethanediol and 1,2-propanediol studied with the above approach. In 1,2-ethanediol, proton transport catalysis occurs through hydrogen-bridged species and is a key step in the production of $HCO^{\bullet}$ + $CH_3OH_2^+$. For the higher homologue, ionized 1,2-propanediol, the calculations and experiments showed that although the presence of an extra methyl group allows several new dissociation reactions to occur, the prominent loss of $CH_3CO^{\bullet}$ occurs in an analogous way to that of $HCO^{\bullet}$ from 1,2-ethanediol. That is, the dissociation again, occurs by sequential transfers of a proton, electron and another proton.

Chapter 4 describes the ion chemistry of oxalacetic acid. One important conclusion is that the commercial available compound does not have the proposed keto acid structure but rather is the Z-enol isomer, hydroxyfumaric acid. The (E)-enol is not present in the solid, nor is its ion generated in the gas phase via isomerization of the ionized (Z)-enol form. However, even under gentle sample introduction conditions, a partial ketonization of the neutral (Z)-enol takes place. The resulting keto OAA molecules are either ionized intact or decarboxylate to yield a mixture of α-hydroxyacrylic acid, CH_2=C(OH)COOH, and its keto isomer pyruvic acid, $CH_3C(=O)COOH$.

From experiment and theory, ionic enthalpies of formation of 95 and 109 kcal/mol were derived for CH_2=C(OH)COOH$^{\bullet}$ and $CH_3C(=O)COOH^{\bullet+}$ respectively.

Chapter 5 discusses the intriguing ion chemistry of β-hydroxypyruvic acid whose dissociative rearrangement ion at m/z 76 (loss of CO) was examined in two different energy regimes : the high internal energy species are hydrogen-bridged radical cations, CH_2=O•••H•••O=C-OH$^{\bullet+}$ while the low energy (metastable) ions are ion-dipole complexes of ionized hydroxyketene and water, HOC(H)=C=O$^{\bullet+}$/H_2O. The high energy hydrogen-bridged radical cations show an intriguing dissociative rearrangement into $CH_2OH_2^{\bullet+}$, whose mechanistic pathway was examined in depth with computational chemistry. Decarboxylation into the ylidion $CH_2OH_2^{\bullet+}$ characterizes the dissociation chemistry of both the H-bridged ion and its glycolic acid isomer $HOCH_2COOH^{\bullet+}$. A computational analysis of this reaction leads to the proposal that the decarboxylation occurs via a H-bridged ion CH_2-O(H)•••H•••O=C=O$^{\bullet+}$ as the key intermediate.

Chapter 6 investigates the methyl ester of β-hydroxypyruvic acid, which also decarbonylates to produce the H-bridged ion CH_2=O•••H•••O=C-$OCH_3^{\bullet+}$ as identified by experiment. This H-bridged radical cation also shows an interesting rearrangement reaction yielding protonated methylformate, $CH_3OC(H)OH^+$ and the formyl radical, HC=O$^{\bullet}$. This dissociation occurs via sequential transfers of a proton, electron and another proton within ion-dipole complexes, akin to the diols mentioned above. The first step in this rearrangement process is a 1,2-proton shift catalyzed by a formaldehyde dipole. This yields an ion/dipole complex, CH_2=O•••H-C(=O)$OCH_3^{\bullet+}$, which is in the correct configuration for electron transfer to occur at the energetic threshold dictated by experiment. The resulting intermediate triggers the transfer of yet another *proton* from the formaldehyde unit thereby generating another stable H-bridged radical cation *viz.* HC=O•••H•••OC(H)$OCH_3^{\bullet+}$. This final intermediate dissociates with little or no activation energy into $HOC(H)OCH_3^+$ and HC=O$^{\bullet}$.

Chapter 7 describes an investigation of the heat of formation ΔH_f of the methoxycarbonyl cation, $CH_3OC{=}O^+$. Ab initio calculations at the G2 level of theory on a set of isodesmic, atomization and substitution reactions combined with a reevaluation of existing appearance energy measurements yields ΔH_f^{298} = 129 kcal/mol as the recommended value, a large upwards revision of the current literature value of 120

kcal/mol. This work formed the basis of a subsequent study (M.A. Trikoupis, J.K. Terlouw, P.C. Burgers, M. Peres and C. Lifshitz, J. Am. Soc. Mass Spectrom., **10**, 1999, 869) on the dissociation of dimethyloxalate ions, where it was found that the ions do *not* break in half, to form $CH_3OC{=}O^+$ + $CH_3OC{=}O^{\bullet}$, but fragment in a step-wise manner losing CO_2 then $CH_3^{\bullet}$ to produce $CH_3OC{=}O^+$.